BIOGENESIS OF LYSOSOMES IN MACROPHAGES: INTRACELLULAR PATHWAY OF LYSOSOMAL MEMBRANE PROTEIN TO LYSOSOMES.

Roshan Ebrahim

Thesis Presented for the Degree of

DOCTOR OF PHILOSOPHY

in the

Division of Medical Biochemistry

Department of Clinical Laboratory Sciences

Faculty of Health Sciences

UNIVERSITY OF CAPE TOWN

Supervisor: Prof. L. Thilo

February 2008

DECLARATION

I **Roshan Ebrahim** hereby grant the University of Cape Town free licence to reproduce this thesis in whole or in part, for the purpose of research and declare that this thesis is my own unaided work, both in concept and execution. I have received no assistance apart from the normal guidance from my supervisor. Neither the substance nor any part of this thesis has been submitted in the past, or is being, or is to be submitted for a degree at this University or any other university.

SIGNED: _____

DATE : _____

ACKNOWLEDGMENTS

THANKYOU,

MOM & DAD, for enduring years of intense labour to afford all your children a tertiary education. I will be forever grateful. Your quiet, but stable presence has always been a source of comfort and strength that gave me the freedom to explore my full potential. I am sorry that I have not paid more attention to you in recent times due to my intense efforts to speed up the completion of my thesis.

my brothers and sisters, for having been responsible for most of the challenges during my growing-up years and thus for having contributed greatly to who I am today, for having encouraged me to 'get on with it' and for having stepped in to help when it was needed, especially Muzafarh for the shopping.

my families and friends, for your encouragement and understanding when my social visits became few and far between.

my teachers throughout my primary and tertiary education, for all your effort and contribution to my learning curve, your motivational talks and the faith you had in my ability to achieve.

my supervisor, for your patience during painstaking sessions heavily laden with conceptual clarification of scientific thought, the constructive criticism during the analyses of my results and the writing of my thesis, the stimulating in-depth discussions and deliberations that moulded a mentorship that extended beyond the academic arena. Despite our differences on a range of issues, we have managed to nurture a special relationship that I am indeed grateful for.

my fellow laboratory colleagues, the late Thomas Haylett for technical expertise inside as well as outside the laboratory, Bienyameen Baker, Raydean Pietersen, Maurice Itoe, Alon Gordon for stimulating conversations and debates on scientific as well as soul-searching issues.

the staff of the Division of Medical Biochemistry, for all your support that ranged from administrative aspects, the provision of clean glassware to warm friendships.

the staff of the Lipid Clinic, for extending your hospitality by providing our laboratory group with work-space. Thankyou for the warm and pleasant working environment that we have.

Mike Begg from the LDL laboratory, for technical advice during the initial stages of my project.

Nancy Dahms from the Medical College of Wisconsin, USA, for the serum against the CD-MPR.

the Katz laboratory group, for your companionship during the writing-up phase of my thesis and Michael Madziva for having read my thesis and providing helpful discussions on it.

CONTENT

1 ABSTRACT

Lysosomal constituents are synthesised in the endoplasmic reticulum (ER), processed in the Golgi cisternae and transported to the trans-Golgi network (TGN), from where they are sorted for delivery to lysosomes. It is not known whether newly-synthesised lysosomal constituents are targeted directly to lysosomes, or whether they are first delivered into preceding stages of the endocytic pathway, in particular early endosomes. Horse-radish peroxidase (HRP) can be endocytosed by cells and delivered to successive stages of the endocytic pathway. It thus serves as a marker along the endocytic pathway. HRP catalyses the cross-linking of membrane-permeable diaminobenzidine (DAB). This renders HRP-containing organelles detergent insoluble. The fraction of lysosomal constituents which colocalise with HRP in the endocytic pathway can thus be determined experimentally. The present study examines the kinetics that describe where and when newly-synthesised (metabolically labelled) lysosome-associated membrane protein-1 (LAMP-1) colocalises with HRP in different organelles of the endocytic pathway. The results show a transient presence of newly-synthesised LAMP-1 in early endosomes and suggest that the bulk of newly-synthesised LAMP-1 enters the endocytic pathway via early endosomes prior to its delivery to lysosomes. This study was extended to include the cation-dependent mannose 6-phosphate receptor (CD-MPR) to serve as a control protein that behaves differently to LAMP-1. Results for the CD-MPR are compatible with a transient presence of the CD-MPR in lysosomes, to which the bulk of newly-synthesised CD-MPR is transported before transport to late endosomes. Due to low expression levels of total cellular CD-MPR, and especially endocytic CD-MPR, the CD-MPR pathway has not been resolved clearly. Nevertheless, since different results have been obtained for the two membrane proteins of this study, the present approach can be considered to provide specific information on their different entry routes into the endocytic pathway.

2 PREFACE

The intracellular millieu of the cell can communicate with its environment through the exchange of materials via the endocytic system (reviewed in Mukherjee *et al.*, 1997). The processing of extracellular nutrients, regulation of cell-surface receptors, maintenance of membrane homeostasis and defence against extracellular pathogens occur via the endocytic and/or exocytic process. Extracellular and cell surface-derived materials are internalised (internalisation being synonymous with endocytosis) through the invagination of the cell membrane and the subsequent formation of vesicles, as shown in figure 2.1. These vesicles fuse together and form what are known as early endosomes, from where molecules are sorted. Re-usable molecules are recycled to the plasma membrane or the Golgi, while those destined for degradation are retained in carrier vesicles. There are two models for the transfer of early endosomal content to late endosomes. In the vesicular model, the carrier vesicles fuse with already existing late endosomes. In the maturation model, the carrier vesicles mature into late endosomes through the exchange of resident proteins.

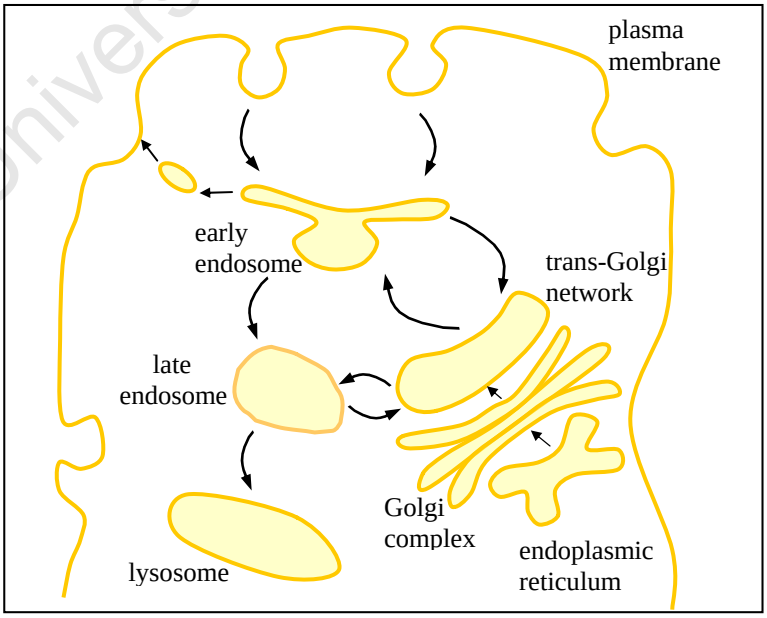

Figure 2.1 Intracellular trafficking pathways. Main routes employed by eukaryotic cells.

Late endosomes deliver their contents to lysosomes, the end station of the endocytic pathway, by two mechanisms that occur concurrently. Using time-lapse confocal microscopy, these have been identified as the 'kiss-and-run' and the 'fusion-fission' mechanisms. The 'kiss-and-run' mechanism involves transient fusion of late endosomes and lysosomes to exchange contents, followed by rapid dissociation. In the 'fusion-fission' mechanism, late endosomes fuse fully with lysosomes to form hybrid organelles from which lysosomes are reformed by fission events (Bright *et al.*, 2005; reviewed in Luzio *et al.*, 2007).

Lysosomes are single-membrane-bound organelles that are the main site of degradation in the endosomal pathway of multicellular organisms. The membrane is enriched in a group of highly glycosylated trans-membrane proteins (LAMPs, LIMPs or LGPs) and sequesters a large variety of acid hydrolases. The hydrolases digest the substances acquired via endocytosis (for example, phagocytosis and pinocytosis) and autophagy. The digestive products are translocated across the lysosomal membrane for use in the cytoplasm or transported to other cellular compartments. The carbohydrates of the glycosylated membrane proteins form a dense glycocalyx on the lumenal surface, as if to shield themselves and the membrane from the hydrolytic enzymes (Neiss, 1984). Protease resistance has been observed for glycoproteins in general (Yeo *et al.*, 1985). Some lysosomal membrane proteins (LAMP-1, LAMP-2, LIMPs) have been shown to be protected from the proteolytic environment of the lysosomal lumen by the asparagine-linked oligosaccharides (Barriocanal *et al.*, 1986; Kundra and Kornfeld, 1999), in particular those containing poly-N-acetyllactosamines (Lee *et al.*, 1990). These proteins may serve to protect the membrane from the hydrolytic action of the diverse complement of hydrolases and thus preserve the integrity of the lysosome. Although the role of lysosomal membrane proteins have not been clearly determined (reviewed in Eskelinen et al., 2003), they may be involved in more specific functions. For example, the transport of protons to maintain the acidic pH in lysosomes (Ohkuma and Poole, 1978), the specific interaction and fusion of

lysosomes with other organelles (Steinman *et al.*, 1983), and the transport of amino acids and carbohydrates resulting from the hydrolytic degradation (Cohn and Ehrenreich, 1969; Ehrenreich and Cohn, 1969). The lamp family has been implicated in melanogenesis (Jimbow *et al.*, 1994). Levels of LAMP-2A in the lysosomal membrane have been correlated with chaperone-mediated autophagic activity (Cuervo and Dice, 1996; Majeski and Dice, 2004) and LAMP-2A has also been shown to promote MHC class II presentation of cytoplasmic antigens (Zhou *et al.*, 2005). In human peripheral blood mononuclear cells LAMP-1 and LAMP-2 are activation-dependent cell-surface glycoproteins that mediate cell adhesion to the vascular endothelium (Kannan *et al.*, 1996). LAMP-2 and LAMP-3 might be indicators of platelet activation (Kannan *et al.*, 1995). LAMP-1 and LAMP-2 have been shown to play a role in phagosome maturation (Huynh *et al.*, 2007).

Cellular processes in which lysosomes function include protein turnover, cholesterol homeostasis (Brown and Goldstein, 1976; Eskelinen *et al.*, 2004), recycling of endocytic nutrients, down-regulation of cell-surface receptors (Beguinot *et al.*, 1984; Kasuga *et al.*, 1981; Mellman *et al.*, 1983; Mellman and Plutner, 1984), defence against pathogens (Silverstein, 1977) and loading of processed antigens onto MHC class II molecules (Harding and Geuze, 1993). Lysosomes have also been implicated in regulated secretion (Peters *et al.*, 1991), repair of damaged plasma membrane (McNeil, 2002), and formation of an osteoclast's ruffled border (Stenbeck, 2002). Lysosomes are considered to be part of a family of lysosome-related organelles with cell-specific functions, for example melanosomes (Raposo *et al.*, 2001), lytic granules, MHC class II compartments, platelet dense granules, basophil granules, azurophil granules and Drosophila pigment granules (reviewed in Dell'Angelica *et al.*, 2000). The crucial role that lysosomes play in cellular metabolism is evident from the many diseases associated with lysosomal malfunctioning.

Lysosomal storage diseases include at least 40 enzymopathies where indigestible molecules accumulate in lysosomes. The homeostasis of the cell is altered, thus leading to a diseased state. Deficiency of LIMP-2 in mice results in ureteric pelvic junction obstruction, deafness and peripheral neuropathy (Gamp *et al.*, 2003). Lysosomes have been implicated in Danon's disease (LAMP-2) (Nishino *et al.*, 2000; Tanaka *et al.*, 2000), Niemann-Pick type C1 (NPC1) (Chang *et al.*, 2005; Zhang *et al.*, 2001), cystinosis (cystinosin) (Jonas *et al.*, 1982), Salla disease (sialin) (Renlund *et al.*, 1983), Alzheimer's disease (Tagawa *et al.*, 1992), and more generally, auto-immune diseases, resistance to drugs, cancer and infectious diseases. LAMP-1 plays a role in auto-immune disease (type 1 diabetes) progression (Bittencourt *et al.*, 2005). Lysosomal membrane proteins have been shown to be upregulated in tumour cells, mediating adhesion of tumour cells to vascular endothelial cells and the extracellular matrix, and promoting tumour progression (Furuta *et al.*, 2001; Kanao *et al.*, 2005; Kunzli *et al.*, 2001; Saitoh *et al.*, 1992; Sarafian *et al.*, 1998). In tuberculosis, phagosomes harbour virulent bacteria and do not mature (Clemens and Horwitz, 1995; Thilo and de Chastellier, 1995), and thus do not fuse with lysosomes. This has been considered as a main strategy for intracellular survival of mycobacteria in that it avoids their exposure to the harsh hydrolytic environment in phago-lysosomes. In spite of this non-fusion with lysosomes, these mycobacteria-containing phagosomes, nevertheless, contain lysosomal enzymes and membrane constituents. This apparent anomaly may find an explanation in the biogenesis of lysosomes (see Discussion). Abnormal expression of lysosomes and lysosome-related organelles are characteristic of human genetic diseases such as Chediak-Higashi and Hermansky-Pudlak syndromes (Dell'Angelica *et al.*, 1999; reviewed in Starcevic *et al.*, 2002). The discovery of mutant genes linked to these diseases is only beginning to reveal the molecular mechanisms implicated in the biogenesis of lysosomes and lysosome-related organelles.

The role of lysosomes in the above-mentioned diseases and the molecular processes underlying lysosomal biogenesis (reviewed in Mullins and Bonifacino, 2001) remain poorly defined. A thorough knowledge of how lysosomes are synthesised and maintained would contribute to a better understanding of lysosome-related diseases. Unravelling lysosomal biogenesis requires a complete elucidation of the dynamics of membrane and protein transport to and from the lysosome, and the molecular machineries that govern these events. This would include characterisation of the pathways along which newly-synthesised lysosomal membrane proteins and lumenal enzymes are transported for delivery to lysosomes.

The sorting of enzymes and membrane proteins for delivery to lysosomes occurs in the TGN. Lysosomal enzymes are sorted from other proteins by mannose 6-phosphate receptors (MPRs) that bind the enzymes through a mannose 6-phosphate (man-6-P) recognition moiety on the surface of the enzymes. A number of sorting signals in the MPR are then responsible for ensuring delivery of lysosomal enzymes to lysosomes. The exact pathway for the delivery of enzymes by MPRs has not been resolved. MPR-enzyme complexes are transported to an endocytic organelle where the low pH causes the enzymes to dissociate. MPRs have predominantly been localised to late endosomes at steady state. Late endosomes have thus been presumed to be the endocytic organelle into which MPR-enzyme complexes are delivered and where the dissociation of MPRs and enzymes occurs. MPRs are recycled to the TGN while the enzymes are delivered to lysosomes. MPRs could deliver their cargo directly to late endosome or indirectly via another endocytic organelle, for example early endosomes. Lysosomal enzyme targeting is reviewed in (Dahms *et al.*, 1989). The lysosomal membrane proteins do not have the man-6-P recognition moiety (Barriocanal *et al.*, 1986; Waheed *et al.*, 1988). Their delivery to lysosomes is therefore not mediated by MPRs (Croze *et al.*, 1989). Instead, a tyrosine (tyr) or a di-leucine (di-leu) motif in their cytoplasmic tails and the position of the motif relative to

the membrane are critical for lysosomal sorting. This signal is similar to that for receptor-mediated endocytosis (Chen *et al.*, 1990; Jadot *et al.*, 1992; Jing *et al.*, 1990).

The similarity in the signals for lysosomal targeting and endocytosis prompted the much debated and studied questions in the literature: Are lysosomal membrane proteins delivered to lysosomes indirectly, that is, first to the cell surface via the secretory pathway and then to lysosomes by endocytosis. Or, are they delivered to lysosomes directly? Since the plasma membrane and early endosomes are in rapid dynamic equilibrium, these two compartments are kinetically unresolved. The presence of a particular lysosomal membrane protein in the early endosomal/plasma-membrane compartment could thus be due to delivery to the plasma membrane via the secretory pathway or to early endosomes intracellularly from the TGN. During initial studies, however, the presence on, or movement through, the plasma membrane was generally interpreted to be as a result of delivery via the secretory pathway. Only gradually did delivery via early endosomes through an intracellular pathway from the TGN find its way into experimental design and interpretations.

The goal of this project was to use a kinetic approach to characterise the pathway of newly-synthesised LAMP-1, to serve as a marker for delivery of lysosomal membrane proteins from the TGN. More specifically, the question asked was: Is LAMP-1 delivered to lysosomes directly or via early endosomes, as shown in figure 2.2.

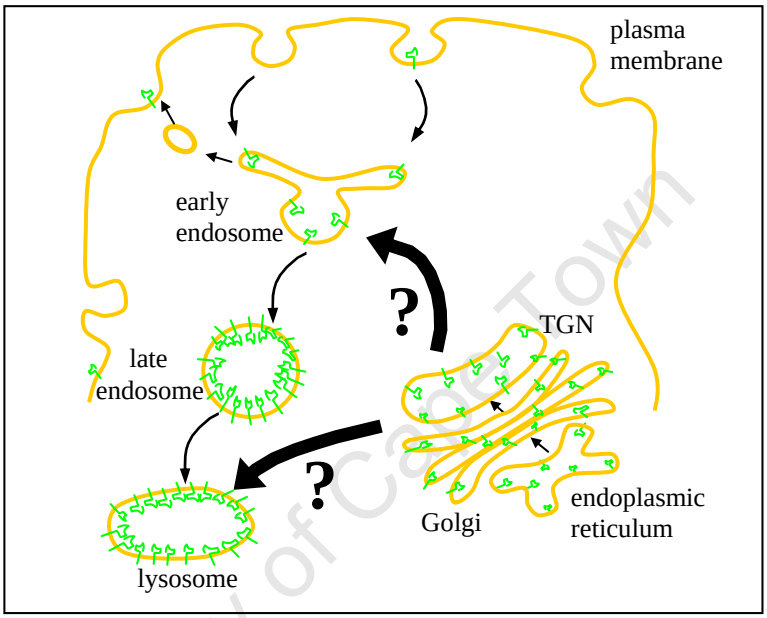

: LAMP-1 (Lysosome-associated membrane protein-1)

Figure 2.2 Pathways to be considered for the lysosomal delivery of LAMP-1. LAMP-1 is predominantly localised to the late endosomes and lysosomes. Since LAMP-1 has also been detected on the plasma membrane and in early endosomes, albeit at low concentrations, this project specifically addressed the question whether LAMP-1 is transported from the TGN directly to lysosomes or via early endosomes.

As an example of a protein that behaves differently to LAMP-1, the study was extended to include the CD-MPR, figure 2.3.

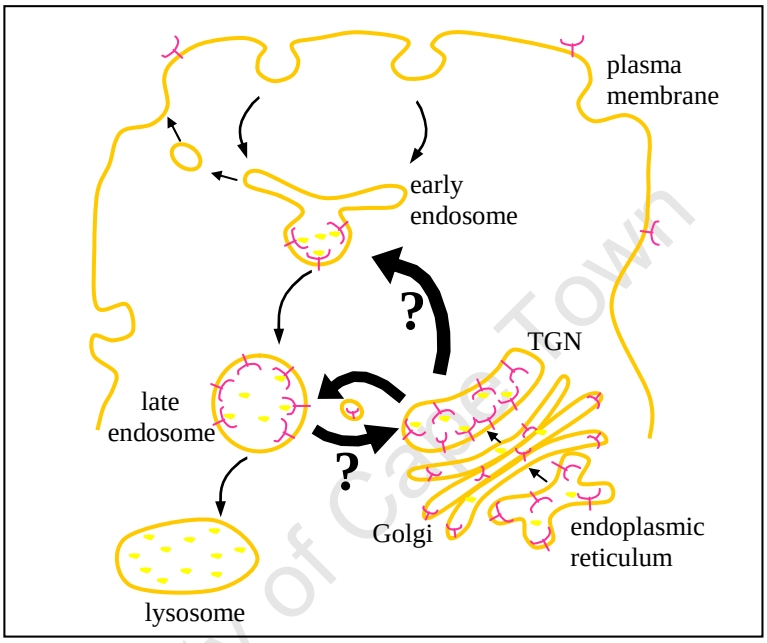

Figure 2.3 Pathways to be considered for the delivery of the CD-MPR into the endocytic pathway. The CD-MPR is predominantly localised to the TGN and endosomes, especially the late endosomes. There is also evidence for its presence on the cell surface in low concentrations. Based on its steady-state distribution, it is presumed to cycle between the TGN and late endosomes. However, the possibility that it is first transported to early endosomes can not be excluded. This project addressed the question whether the CD-MPR is transported from the TGN to early endosomes.

3 INTRODUCTION

This section consists of two parts; the lysosomal membrane proteins and the MPRs. First, background information about the different types and structures of lysosomal membrane proteins or MPRs, their targeting signals and molecular machinery involved in targeting are summarised. This is followed by a critical analysis of the studies performed to characterise the targeting pathways of the respective proteins in the context of the main goal of this project.

3.1 LYSOSOMAL MEMBRANE PROTEINS

3.1.1 Types and structures

Lysosomal membrane proteins are known as lysosome-associated membrane proteins (LAMPs), lysosomal membrane glycoproteins (LGPs) or lysosomal integral membrane proteins (LIMPs) (reviewed in Eskelinen *et al.*, 2003; Fukuda, 1990; Fukuda, 1991; Hunziker and Geuze, 1996; Peters and von Figura, 1994). These proteins are richly glycosylated with complex carbohydrates such as poly-N-acetyl-lactosamines, comprising 25 – 50% of their total molecular weight. They are often terminally sialylated and thus have very acidic iso-electric points (pIs between 2 and 4). They can be placed into three groups, based on their molecular weights: 90 – 120; 60 – 85 and 30 – 55 kDa, or six groups, based on their protein chemistry and amino acid sequence: LAMP-1, LAMP-2, LAMP-3/LIMP-I, LIMP-II, lysosomal acid phosphatase (LAP) and endolyn. Table 3.1.1 is a summary of the nomenclature and some properties of the major lysosomal membrane proteins.

Nomenclature	**LAMP-1**	**LAMP-2**	**LAMP-3**	**LIMP-II**
Human	hlamp-1/ lamp-A CD107a	hlamp-2 lamp-B CD107b	CD63 antigen ME491	CD36L2
Rat	LIMP-III lgp-A lgp120 lgp107	LIMP-IV lgp-B lgp110 lgp96 lgp95	LIMP-I AD1-antigen	lgp85
Mouse	mLAMP-1 P2B	mLAMP-2 mouse lgp110		
Chicken	LEP100			
Others	GpIIa SGM110	AC17 antigen		
Properties				
Molecular mass (kDa)	90 – 120	95 – 120	30 – 55	60 – 85
Copies/cell (X 10^{-4})	30 – 60	20 – 60	<20	<20
Polypeptide chain (residues)	382 – 396	380 – 389	238	478
No. of N-glycans	17 – 20	16 – 17	3	up to 11
No. of O-glycans	+	+	?	?
Carbohydrate content (%)	55 – 65	55 – 65	25 – 55	20 – 45
Targeting signal	gly-tyr	gly-tyr	gly-tyr	di-leu

Table 3.1.1 Nomenclature and properties of the major lysosomal membrane glycoproteins. This table was adapted from Eskelinen *et al.* (2003) and Fukuda (1991). LAMPs have been spelled in various ways in the literature: for example, LAMP-1/LAMP1/Lamp-1/Lamp1/lamp-1/lamp1 and LAMP-2/LAMP2/Lamp-2/Lamp2/lamp-2/lamp2. LAMP-1 and LAMP-2 are the most widely used according to Eskelinen *et al.* (2005), and have been applied in the writing of this thesis.

3.1.1.1 LAMP-1 and LAMP-2

LAMP-1 (Chen *et al.*, 1985; Howe *et al.*, 1988; Lewis *et al.*, 1985) and LAMP-2 (Granger *et al.*, 1990) are the most abundant glycoproteins in the lysosomal membrane (Marsh *et al.*, 1987). cDNAs from human, mouse, rat and chicken cells have been cloned. Their primary sequences are strikingly conserved, with higher sequence similarity among LAMP-1 or LAMP-2 genes across species than between LAMP-1 and LAMP-2 genes from the same species (Fukuda *et al.*, 1988; Sawada *et al.*, 1993). LAMP-1 and LAMP-2 are encoded by separate genes on chromosomes 13q34 and Xq24-25, respectively (Mattei *et al.*, 1990). Taken together, these observations imply that LAMP-1 and LAMP-2 diverged from a single gene very early on in evolution, but the individual LAMP-1 and LAMP-2 genes have been conserved during evolution. Although LAMP-1 and LAMP-2 are highly homologous, they are immunogenically distinct.

They are both type-1 integral membrane proteins, figure 3.1.1. Both have three domains; a large N-terminal ectodomain, a single transmembrane domain and a short C-terminal tail. The lumenal domain consists of two domains. The two domains of LAMP-1 on either side of the proline and serine-rich hinge region are homologous, whereas no such homology has been detected for the two domains of LAMP-2 on either side of the proline and threonine-rich hinge region (Fukuda *et al.*, 1988). Each of the two ectodomains has two loops generated by disulphide bonding between neighbouring cysteines. The 40 kDa protein core has 16 to 20 sites for potential N-linked glycosylation, most of which are found to be glycosylated in the isolated protein. Human LAMP-1 has been estimated to have 18, and human LAMP-2 16, N-linked carbohydrate chains (Carlsson *et al.*, 1988; Fukuda *et al.*, 1988). The mature protein is thus heterogeneous with molecular weights ranging between 90 to 120 kDa. O-linked oligosaccharides are also attached to the hinge region (Carlsson *et al.*, 1993). Some of the glycans are modified by poly-N-acetyl-lactosamines (Carlsson and Fukuda, 1990) and are

often terminally sialylated, thus accounting for the low pIs (2 − 4). The cytoplasmic domain of 10 – 11 amino acid residues displays a higher degree of diversity for LAMP-2 than for LAMP-1. Due to differential splicing, LAMP-2 has three isoforms. LAMP-2A, LAMP-2B and LAMP-2C have distinct transmembrane domains and cytosolic tails (Hatem *et al.*, 1995). At the C-terminal end of the cytosolic tail of both LAMP-1 and LAMP-2 is a highly conserved gly-tyr motif which interacts with the μ-subunit of four hetero-tetrameric adaptor protein (AP, defined in section 3.1.3) complexes. The interaction of the gly-tyr motif with one or more of these AP complexes leads to incorporation of LAMPs into coated vesicles that mediate selective protein transport to lysosomes.

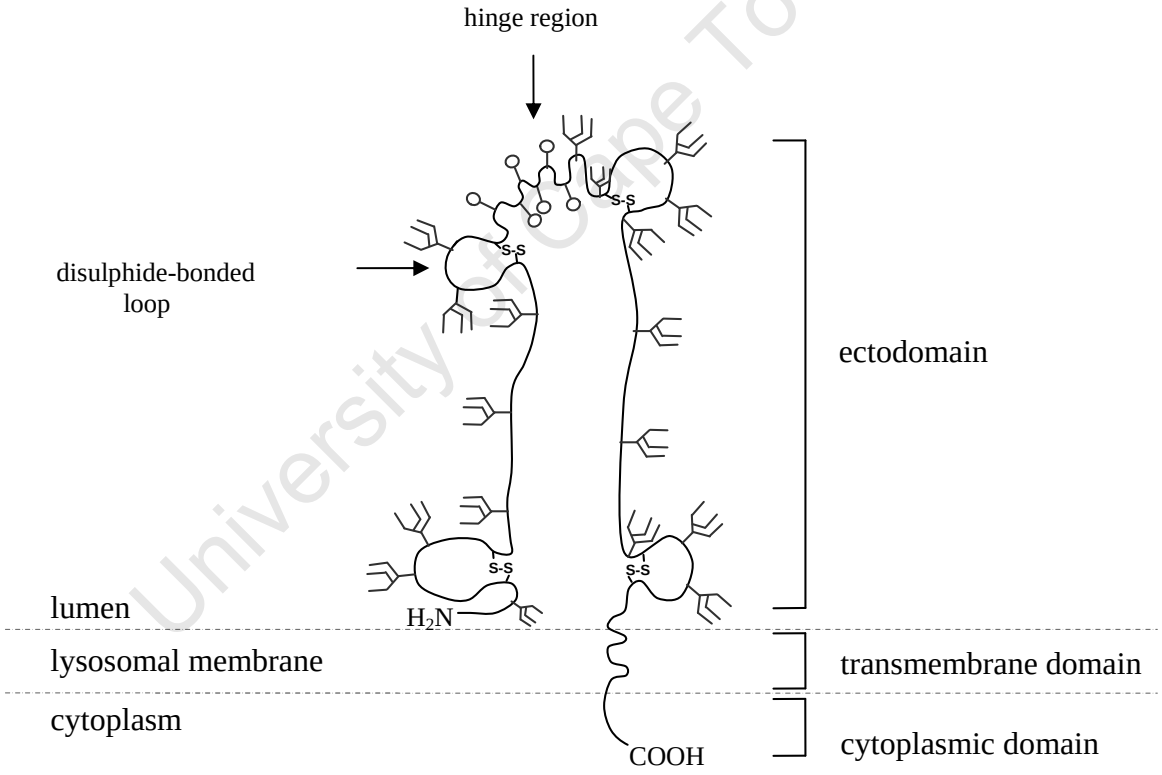

: N-linked poly-lactosaminoglycans and complex N-linked oligosaccharides

: O-linked carbohydrates are almost exclusively located at the flexible hinge region

Figure 3.1.1 The structure of LAMP-1 and LAMP-2. Loops are formed by disulphide bonds. The hinge region is flexible. This figure was adapted from Fukuda (1991) and Hunziker and Geuze (1996).

3.1.1.2 LAMP-3

The cDNA of LIMP-I, also known as LAMP-3 or CD63, has been isolated from human, mouse and rat cells. It is a type III integral membrane protein that traverses the membrane four times, as shown in figure 3.1.2. The core protein of 25 kDa has three N-glycosylation sites in the lumenal domain close to the lipid bilayer. The poly-N-acetyl-lactosamine glycosyl moieties added, yields a heterogeneous population of mature proteins with molecular weights from 30 to 54 kDa (Barriocanal *et al.*, 1986). While there is no overall homology with either LAMP-1 or LAMP-2, its 10-amino acid cytoplasmic tail contains the gly-tyr motif. Hence it has been renamed LAMP-3.

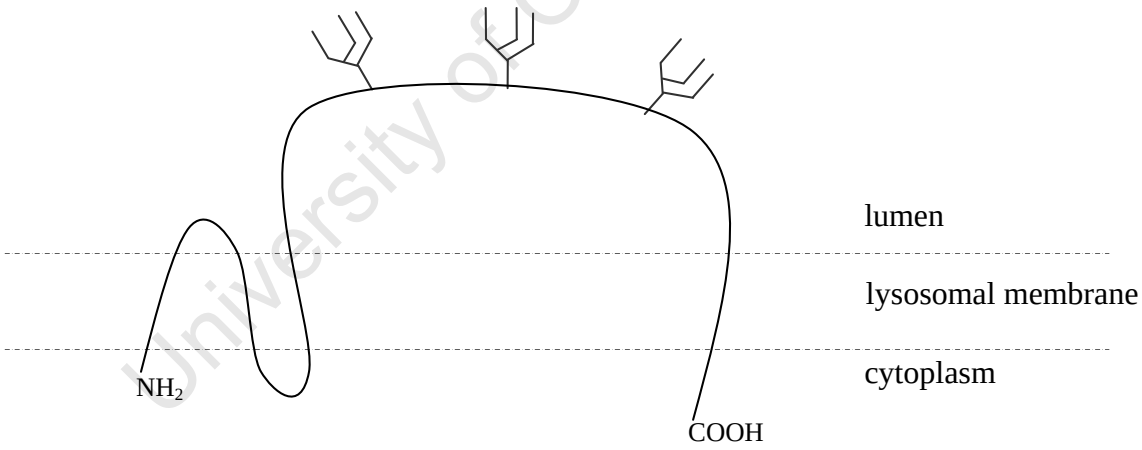

: N-linked poly-lactosaminoglycans and complex N-linked oligosaccharides.

Figure 3.1.2 The structure of LIMP-I (LAMP-3). This figure was adapted from Hunziker and Geuze (1996).

3.1.1.3 Limp-II

Limp-II cDNA has been cloned from rat cells. It is a type III integral membrane protein that traverses the membrane twice, as depicted in figure 3.1.3. The ectodomain is the greater part of the protein and the N-terminal and C-terminal cytoplasmic tails are 2 – 4 and 20 amino acids, respectively. The protein core of 50 kDa has 11 potential N-glycosylation sites on the ectodomain, thus yielding a 74 to 85 kDa mature product (Barriocanal *et al.*, 1986). The ectodomain also has 5 cysteine (cys) residues which may form disulphide bonds. Limp-II is not homologous to any of the LAMPs, a fact emphasised by limp-II utilising a completely different lysosomal targeting signal, a di-leu-type signal.

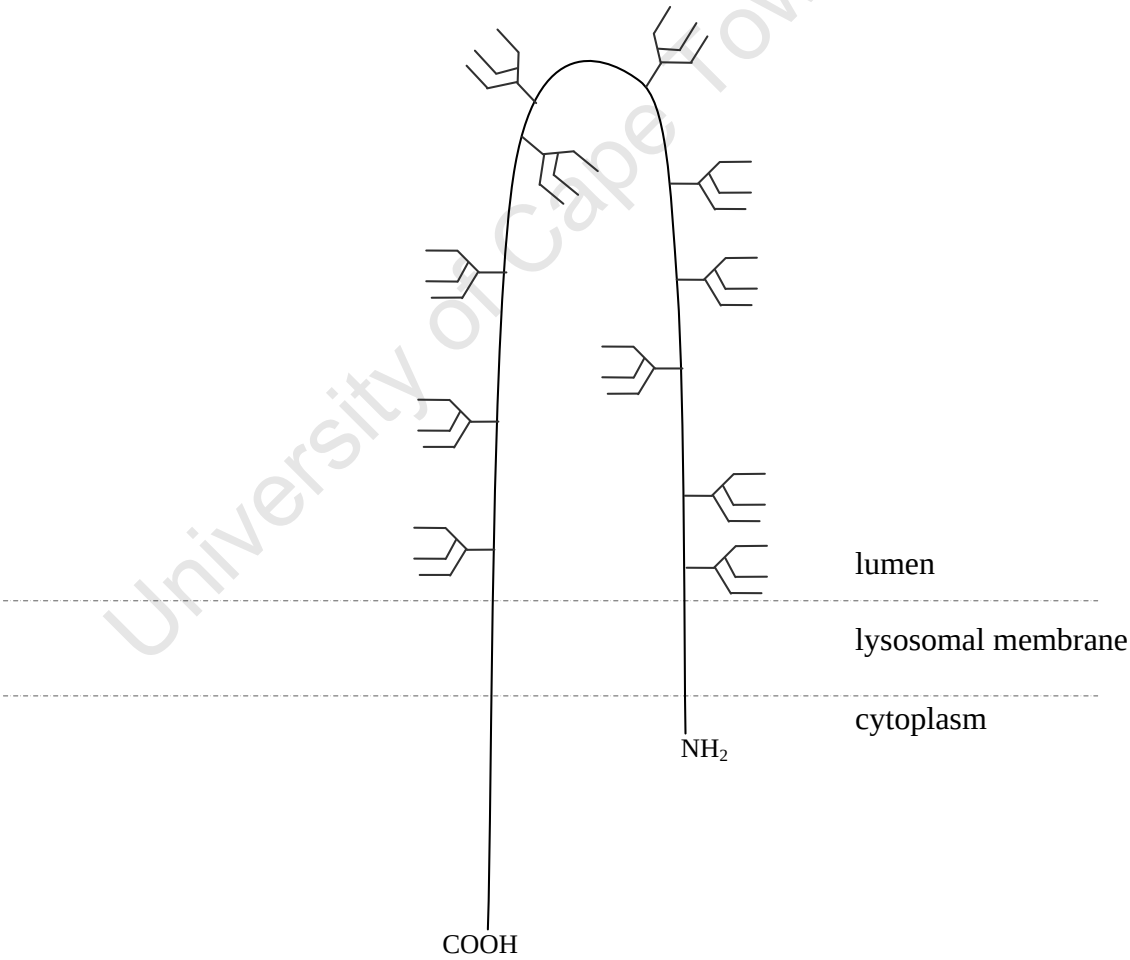

: N-linked poly-lactosaminoglycans and complex N-linked oligosaccharides.

Figure 3.1.3 The structure of limp-II. This figure was adapted from Hunziker and Geuze (1996).

3.1.1.4 Lysosomal acid phosphatase (LAP)

The LAP precursor is transiently associated with the membrane as an integral membrane protein that is proteolytically processed into the mature soluble enzyme upon arrival in late endosomes or lysosomes (Tanaka *et al.*, 1990a; Waheed *et al.*, 1988). It is a type I integral membrane glycoprotein with a large N-terminal domain, a single transmembrane domain and a cytoplasmic tail of 19 amino acids (figure 3.1.4.). The eight N-glycosylation sites on the lumenal domain are used by complex-type oligosaccharides, in part substituted by sialic acid residues, generating a membrane-associated LAP precursor of 63 kDa. The mature soluble LAP is 52 kDa. A gly-tyr motif, similar to that found in LAMP-1, –2 and –3, is encoded by the cytoplasmic tail.

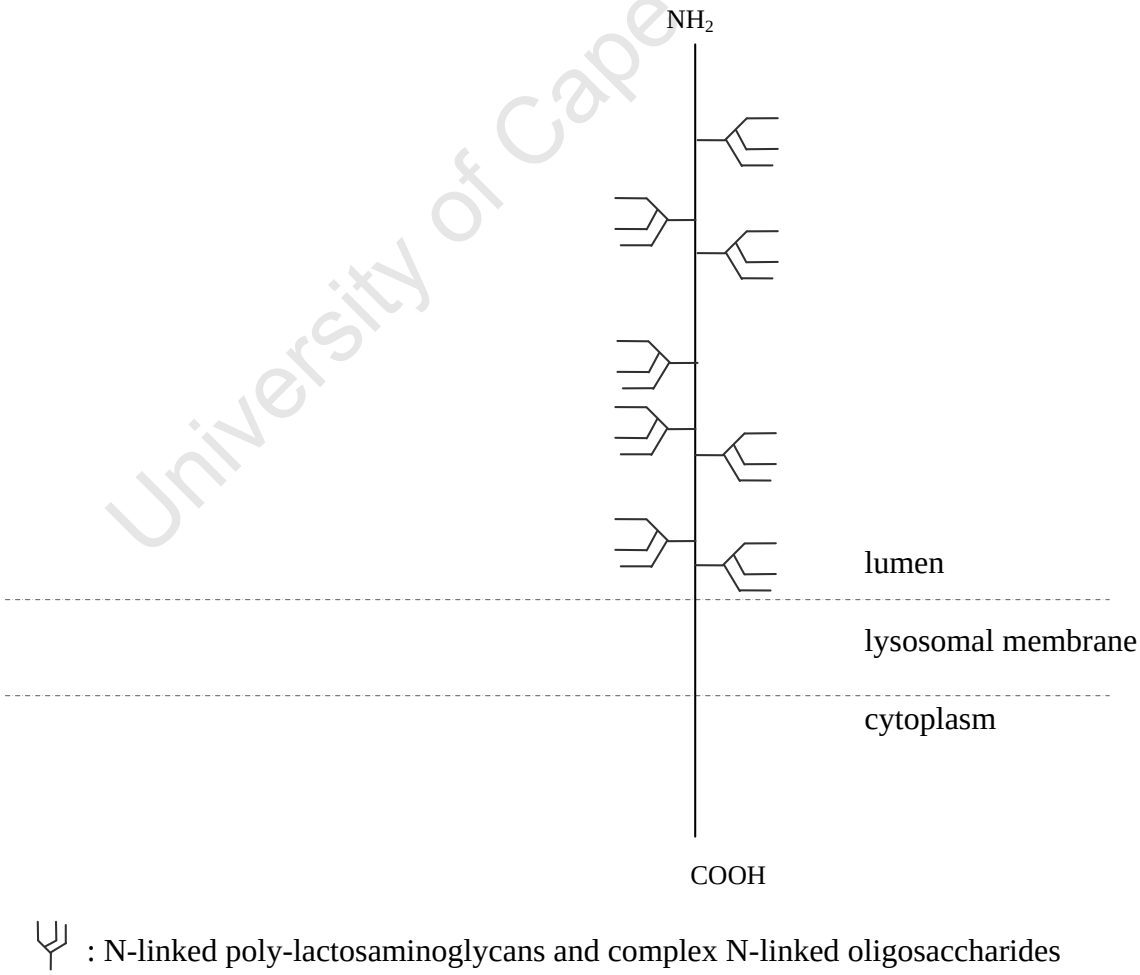

Figure 3.1.4 The structure of LAP. This figure was adapted from Hunziker and Geuze (1996).

3.1.1.5 Endolyn

This protein is predominantly localised to lysosomes, but a substantial fraction also occurs in endosomes, hence the name endolyn. cDNA of rat endolyn encodes a type I integral membrane protein with a 13 amino acid cytoplasmic tail and many potential N– and O-linked glycosylation sites in the predicted lumenal domain, as shown in figure 3.1.5. Mature endolyn has been observed as a heterogeneous population with molecular weights from 60 to 80 kDa. It is mucin-like and shares 52% similarity with two mucins, Muc5C and Muc2. Endolyn may also be distantly related to the lamp family. Two of the cysteines align with the conserved cys-3 and cys-4 in domain 1 of LAMP-1 and LAMP-2. The transmembrane and cytoplasmic domain of endolyn shares 35% similarity with those of the LAMPs. A tyr motif is encoded by its cytoplasmic tail, but with no gly preceding it (Ihrke *et al.*, 2000).

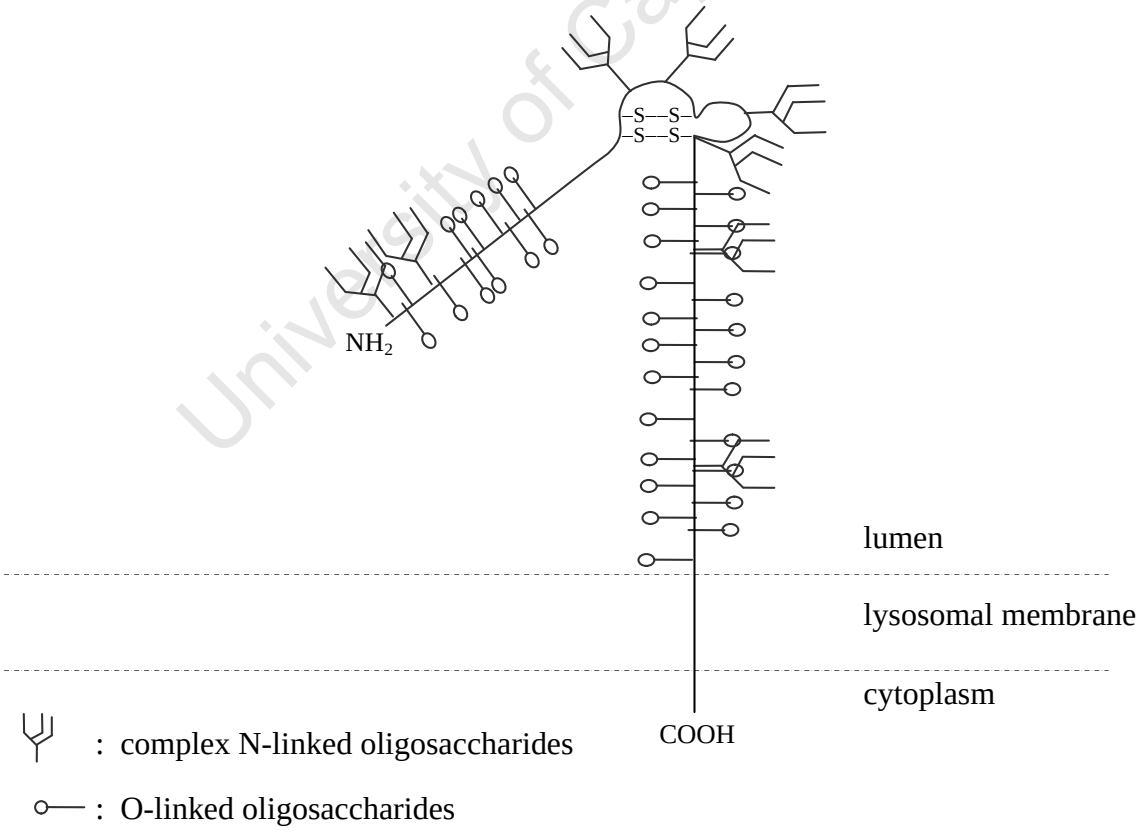

Figure 3.1.5 The structure of endolyn. The possible topology and structure of endolyn has been predicted from the primary sequence. The position of the N-terminal O-glycosylated domain relative to the membrane is not known. This figure was adapted from Ihrke *et al.* (2000).

3.1.2 Targeting signals

Two types of signals in the cytosolic tails of lysosomal membrane proteins are implicated in lysosomal targeting: a tyr-containing signal in LAMP-1, LAMP-2, LAMP-3, LAP and endolyn, and a di-leu type signal in LIMP-II. The tyr signal in LAMP-1, LAMP-2, LAMP-3 and LAP has a gly preceding the tyr. Mutations in these determinants result in lysosomal mistargeting and cell-surface accumulation. These signals are thus important in targeting lysosomal membrane proteins to lysosomes and in endocytosing cell-surface–expressed lysosomal membrane proteins for delivery to lysosomes. However, their role in sorting newly-synthesised proteins into specific pathways at the TGN is still largely undefined. The position of both motifs relative to the membrane is important for their proper function (Fukuda, 1990; Ogata and Fukuda, 1994; Rohrer *et al.*, 1996; Williams and Fukuda, 1990). The gly-tyr motif for LAMP-1, –2 and –3 occurs at the end of the cytoplasmic tail, while that for LAP occurs seven amino acids away from the end. Overexpression of chimeras with different cytoplasmic domains and/or targeting signals in HeLa cells (immortal cell-line derived from human cervical cancer cells) by transient transfection shows that both the tyr– and di-leu signal-dependent targeting components are saturable. Overexpression of proteins containing these signals results in cell-surface accumulation and interferes with targeting to the correct destinations (for example, lysosomes). This is probably due to the saturation of specific components (presumably specific receptors) of the targeting machinery operating in the sorting of proteins at the TGN, early endosomes or plasma membrane. The evidence suggests that proteins with tyr-based sorting signals share saturable components, irrespective of the targeted destination, whereas tyr– and di-leu-mediated targeting use distinct saturable components (Marks *et al.*, 1996).

3.1.2.1 Tyrosine-containing signal

This signal consists of four amino acids, YXXϕ, where Y is tyr, X is any amino acid, ϕ is a bulky, hydrophobic amino acid that varies for the different lysosomal proteins (reviewed in Bonifacino and Dell'Angelica, 1999).

3.1.2.1.1 LAMPs

LAMP-1, –2, and –3 have an 11 amino-acid cytoplasmic tail. The tyr motif occurs at the end of the tail with seven residues separating it from the membrane. The tyr is preceded by a gly, hence the signal is $G^{7}Y^{8}XX\phi^{11}$, where 7, 8, and 11 refer to the positions of the amino acids in the 11 amino-acid cytoplasmic tail (Honing and Hunziker, 1995). For LAMP-1, ϕ is isoleucine (ile); LAMP-2A, phenylalanine (phe); LAMP-2B, valine (val); LAMP-2C, leu and LAMP-3, methionine (met) (Gough and Fambrough, 1997).

The cytoplasmic tail of human LAMP-1 fused to a cell-surface–reporter glycoprotein in transformed African Green Monkey kidney fibroblasts (COS-1 cells) causes the chimera to be delivered to lysosomes instead of the plasma membrane, whereas substitution of the tyr^{8} with an alanine (ala) results in surface accumulation of the chimera (Williams and Fukuda, 1990). These results implicate the requirement for a tyr-containing signal in the cytoplasmic tail for lysosomal sorting. A similar tyr-containing signal mediates cell-surface internalisation, thus potentially mediating sorting at both the TGN and the cell surface.

Mutagenesis and transfection of murine-LAMP-1 cDNA into human embryonic kidney fibroblasts have revealed the three amino acids distal to the tyr residue to be X-X-ϕ. The tyr-containing signal in the cytoplasmic tail was thus characterised to contain the amino-acid sequence, Y-X-X-ϕ (Guarnieri *et al.*, 1993).

In cases where LAMP-1 is not normally detected on the cell surface (for example, Chinese Hamster Ovary (CHO) and Madin-Darby Canine Kidney (MDCK) cells) substitution of gly^{7}, tyr^{8} or ile^{11} by ala results in LAMP-1 detection on the cell surface. The tyr^{8}ala and ile^{11}ala mutants accumulate on the cell surface and abolish lysosomal delivery, whereas the gly^{7}ala mutant is internalised from the cell surface and delivered to lysosomes with the same kinetics as the wild-type (Harter and Mellman, 1992; Honing and Hunziker, 1995). Using the yeast two-hybrid approach, tyr-based sorting signals, in general, have been shown to bind the μ_1 and μ_2 subunits of AP-1 and AP-2 (defined in section 3.1.3), respectively, *in vitro*. Mutation of the tyr residue abolishes interaction with the μ_2 subunit (Ohno *et al.*, 1995). A possible role for the gly^{7}, tyr^{8} and ile^{11} in sorting at the TGN is suggested by the different affinities of the mutants for the intact Golgi-restricted AP-1 adaptor protein *in vitro*. Binding of tyr^{8}ala and ile^{11}ala mutants is virtually abolished when compared to the wild-type, while the gly^{7}ala mutant binds, but with reduced efficiency. Both wild-type LAMP-1 and the gly^{7}ala mutant bind the plasma membrane adaptor protein, AP-2, whereas the tyr^{8} and ile^{11} mutants' binding is only slightly better than for the AP-1. This is consistent with the endocytosis of LAMP-1 being unaffected for the gly^{7}ala mutant and practically non-existent for the tyr^{8} and ile^{11} mutants (Honing *et al.*, 1996). Taken together, these results therefore suggest that gly^{7} is important for efficient lysosomal sorting at an intracellular sorting site such that LAMP-1 is not detected on the cell surface, but is not critical for internalisation of cell-surface LAMP-1. In contrast, tyr^{8} and ile^{11} are critical for efficient intracellular lysosomal sorting, as well as sorting at the plasma membrane and subsequent internalisation. In addition to ile, the second last amino acid, threonine (thr), has also been shown to be important for binding of AP-1 and for lysosomal delivery without detection on the cell surface (Obermuller *et al.*, 2002). It can be concluded that the LAMP-1 tyr motif is GYXTI.

In mouse L cells transfected with chimeras composed of the lumenal domain of chicken LAMP-1 (LEP100) and the transmembrane and cytosolic domains of the LAMP-2 isoforms, it has been shown that the targeting signal in the cytosolic tail of each of the LAMP-2 isoforms (a, b and c) is sufficient for lysosomal delivery of chimeric LAMP proteins (Hatem *et al.*, 1995). The three isoforms differ in the hydrophobic amino acid (ϕ) at the end of the tail and are differentially expressed on the cell surface at steady state. Site-directed mutagenesis identified the terminal residue as critical in determining steady-state distributions of LAMP-2A, –B and –C (Gough and Fambrough, 1997). The tyr motif for LAMP-2A is GYXXF, LAMP-2B, GYXXV and LAMP-2C, GYXXL. At steady state LAMP-2C is predominantly localised to lysosomes, whereas higher levels of LAMP-2A and –B occur at the cell surface.

The C-terminal sequence in the cytoplasmic tail of human CD63 (LAMP-3) has the lysosomal targeting motif, GYEVM. In normal rat kidney (NRK) cells transfected with a chimera composed of the lumenal and transmembrane domains of human T-cell surface marker (CD8) and the cytoplasmic tail of CD63, the CD8-CD63 chimera colocalise with endogenous LAMP-2 and CD63. The GYEVM targeting motif in the cytoplasmic tail is thus sufficient to target CD8 to lysosomes. Alanine-scanning mutagenesis of this motif in human CD63 has shown increased cell-surface expression of the mutants in stably transfected NRK cells by immuno-fluorescence microscopy. The order of cell-surface expression is: GAEVM > GYEVA > GYAVM > AYEVM > GYEAM = GYEVM (wild-type) (Rous *et al.*, 2002). The tyr is thus more important than gly in preventing cell-surface expression. This is consistent with that which has been observed for LAMP-1. The terminal amino acid, met, is also relatively important in determining cell-surface expression, as has been observed for LAMP-1 and –2.

3.1.2.1.2 LAP

The tyr-containing signal in the 19 amino-acid cytoplamic tail of LAP is necessary and sufficient for endocytosis and lysosomal targeting of LAP (Peters *et al.*, 1990). Mutation of the tyr in the cytoplasmic tail to phe and deletion of the cytoplasmic tail have resulted in cell-surface accumulation. A chimera composed of the lumenal and transmembrane domains of hemagglutinin (a cell-surface glycoprotein) and the cytoplasmic tail of LAP is rapidly internalised. A chimera composed of the lumenal domain of the CD-MPR and the transmembrane domain and cytoplasmic tail of LAP is delivered to lysosomes. Differential internalisation of LAP cytoplasmic-tail truncation and substitution mutants has identified $PG^{8}Y^{9}RHV^{12}$ as the tyr motif, where P is proline (pro), G is gly, Y is tyr, R is arginine (arg), H is histidine (his) and V is val. This motif is positioned six residues from the membrane and seven residues from the end of the cytoplasmic tail (Lehmann *et al.*, 1992; Obermuller *et al.*, 2002). Interestingly, substitution or truncation of amino acids in the C-terminal end of the tail has the potential to inactivate this internalisation signal.

3.1.2.1.3 Endolyn

The last 10 amino acids of the cytoplasmic tail of endolyn are sufficient to re-direct CD8 to endosomes and lysosomes. A chimera composed of the lumenal and transmembrane domain of CD8 and the cytoplasmic tail of endolyn (CD8-endolyn) colocalises with endogenous endolyn in stably transfected NRK cells, as was measured by double immuno-fluorescence confocal microscopy (Ihrke *et al.*, 2000). The cytoplasmic tail of endolyn contains the tyr motif, NYHTL, at the C-terminus with no gly preceding the tyr, where N is asparagine (asp), Y is tyr, H is his, T is thr and L is leu. The gly that precedes the tyr in other lysosomal membrane proteins is absent. A chimera in which the tyr or the leu of the NYHTL motif is mutated to an ala redistributes to the cell surface. The relatively higher expression of wild-type endolyn on the cell surface and in endosomes when compared with lysosomal membrane proteins that have

the GYXXϕ motif suggests that the gly confers greater efficiency in lysosomal sorting at an intracellular sorting site such that appearance on the cell surface is reduced. This has been confirmed when a mutant CD8-endolyn chimera that contained a GYHTL motif resulted in less anti-CD8 antibody internalisation than a chimera with the wild-type NYHTL (Ihrke *et al.*, 2004). These observations correlate with what has been observed for LAMP-1 and LAMP-3 when the gly of the GYXXϕ motif was mutated to alanine.

When the above results are taken together, one can conclude that tyr in the GYXXϕ motif is more important than gly and ϕ in maximising lysosomal sorting and minimising cell-surface expression, but tyr, gly and ϕ together determine the efficiency of lysosomal sorting. The second last amino acid has also been shown to play a role. Gly is implicated to function at an intracellular sorting site while tyr probably functions at an intracellular sorting site, as well as on the cell surface.

3.1.2.2 di-leucine type signal

This signal is designated $L^{17}I^{18}$, where L is leu, I is ile and 17 and 18 refer to the positions of the amino acids in the 20 amino-acid cytoplasmic tail of LIMP-II. In COS-1 cells, the cytoplasmic tail is sufficient to ensure efficient lysosomal targeting of transfected LIMP-II without its detection on the cell surface (Vega *et al.*, 1991). In two parallel studies, it has been shown that the $L^{17}I^{18}$ motif in the carboxyl terminal four amino-acid sequence, $leu^{17}Ile^{18}ala^{19}thr^{20}$, is critical to the targeting signal. Substitution or deletion of leu^{17} or ile^{18} of LIMP-II leads to accumulation of the mutant protein on the cell surface with concomitant reduced efficiency in or complete inhibition of lysosomal targeting. Ile^{18} has a greater tolerance to substitution than leu^{17}. Substitution of ile^{18} by leu causes no loss in targeting efficiency (Ogata and Fukuda, 1994; Sandoval *et al.*, 1994). The addition of three amino acids to the C-terminus does not interfere with lysosomal sorting (Sandoval *et al.*, 1994), while a deletion of

nine amino acids next to the transmembrane domain abolishes the sorting function (Ogata and Fukuda, 1994). The position of the sorting motif relative to the C-terminus is thus not important, while its position relative to the transmembrane domain is essential in both lysosomal targeting and internalisation from the cell surface.

3.1.3 Sorting machinery involved in targeting

Targeting signals specify the location to which lysosomal membrane glycoproteins are destined. A mechanism has to exist whereby these glycoproteins are shuttled from the sites of synthesis to lysosomes. This trafficking function involves the packaging of lysosomal membrane glycoproteins into vesicles, a process facilitated by the sorting machinery of the cell.

Generally, vesicle formation from the membrane is a multi-step process. Cargo proteins are sorted into specific vesicles through the recognition of the sorting signals in their cytoplasmic tails by coat proteins (sorting machinery). The coat is the structural anchor through which vesicles can form. Coat proteins such as adaptor proteins (APs) bind cargo to structural protein, mostly clathrin. Clathrin forms the shell that surrounds vesicles. It is not clear whether the cargo proteins first concentrate in budding vesicles, with the binding of the coat proteins being a subsequent event or whether the coat proteins bind to cargo proteins first, resulting in the recruitment of cargo proteins into the budding vesicle. Once cargo proteins have been concentrated in certain areas, membrane curvature follows. This results in the formation of pits which are then pinched off from the membrane leading to fully-formed vesicles. The vesicles are then sorted to their intracellular destination because of the presence of accessory proteins that have been recruited during the vesicle formation step.

The tyr- or di-leu-based signals in the cytoplasmic tails of cargo proteins interact with AP complexes: AP-1, AP-2, AP-3 or AP-4. These are hetero-tetrameric complexes, consisting of 2 large subunits (~100 kDa), namely β and either γ, α, δ or ε, as is in AP-1, AP-2, AP-3 or AP-4, respectively, a medium μ subunit (50 kDa) and a small σ subunit (20 kDa). AP-1, AP-2 and AP-3 form part of a clathrin-coat, whereas AP-4 forms part of a non-clathrin-coat. The lysosomal targeting signals interact with the μ subunit (Gough *et al.*, 1999; Ohno *et al.*, 1995; Ohno *et al.*, 1996; Rous *et al.*, 2002). However, exactly where and to what extent these adaptors mediate the transport of lysosomal membrane protein is still unknown.

3.1.3.1 Adaptor protein-1

AP-1 forms part of the clathrin lattice that is known to mediate sorting at the TGN, although AP-1 and clathrin have also been observed on early endosomes (Le Borgne *et al.*, 1996; Mauxion *et al.*, 1996; Waguri *et al.*, 2003). LAMP-1 cytosolic tails bind the μ subunit of AP-1 (Ohno *et al.*, 1995) and intact AP-1 (Honing *et al.*, 1996) *in vitro*. The residues, thr (T) and ile (I), in the GYQTI motif of LAMP-1 are critical for AP-1 binding, as well as lysosomal targeting without cell-surface detection (Obermuller *et al.*, 2002). Using immuno-gold electron microscopy in MDCK cells stably transfected with the wild-type and tyr^{8}ala LAMP-1, the wild-type has been observed to colocalise with AP-1–coated vesicles and tubules in the trans-region of the Golgi complex, but not the tyr^{8}ala mutant (Honing *et al.*, 1996). This is evidence for AP-1–mediated sorting of LAMP-1 at the TGN. However, overexpression of chimeric proteins (the cytoplasmic tail of LAMP-1, LIMP-I and LAP fused to the lumenal and transmembrane domains of the Varicellar-zoster virus (VZV) envelope glycoprotein) in HeLa cells does not cause recruitment of AP-1 onto membranes (Le Borgne *et al.*, 1998). TGN-derived transport vesicles containing LAMPs or γ-adaptin (AP-1 subunit) together with MPRs, generated *in vitro*, migrate to different positions on nycodenz gradients (Karlsson and Carlsson, 1998). Also, in μ1A-deficient mouse fibroblasts there is no change in the steady-state

distribution of LAMP-1 and no missorting of LAMP-1 via the cell surface, as was measured by anti-LAMP-1 antibody uptake experiments. In contrast, the steady-state distribution of the MPRs is shifted toward the endosomes (Meyer *et al.*, 2000). These observations suggest that LAMPs and MPRs are sorted at the TGN into different vesicles; the lamp-containing vesicles being AP-1 negative and the MPR-containing vesicles, AP-1 positive. However, depletion of AP-1 by ribonucleic-acid (RNA) interference did increase cell-surface expression (less than two fold) of LAMPs, although the effects were much lower than for other adaptors (Janvier and Bonifacino, 2005).

3.1.3.2 Adaptor protein-2

AP-2 is exclusively associated with plasma-membrane clathrin coats. A high-affinity interaction has been observed between the cytoplasmic domain of LAP and adaptors from plasma-membrane–coated vesicles *in vitro* (Sosa *et al.*, 1993). Depletion of clathrin and AP complexes using RNA interference suggests that AP-2 and clathrin play the most important role in targeting LAMPs to lysosomes. Clathrin depletion results in a three to four-fold increase in cell-surface expression of LAMPs and AP-2 depletion, a five to ten-fold increase. Depletion of AP-1, AP-3 or non-clathrin associated AP-4, singly or in combinations, had relatively lower effects on cell-surface expression (less than two-fold increase) and on the steady-state intracellular distribution (Janvier and Bonifacino, 2005).

3.1.3.3 Adaptor protein-3

AP-3 has been implicated in the sorting of lysosomal membrane glycoproteins to lysosomes because depletion of AP-3 using anti-sense oligonucleotides in HeLa, NRK cells and mouse fibroblasts causes selective misrouting of LAMP-1 and LIMP-II to the plasma membrane, as was determined by antibody internalisation. However, the overall steady-state distributions of LAMP-1 and LIMP-II remain unchanged (Le Borgne *et al.*, 1998). This study implicates AP-3

at an intracellular sorting site. The di-leu-based motif in the cytoplasmic tail of LIMP-II has been shown to selectively bind AP-3 (Diment *et al.*, 1998; Honing *et al.*, 1998). Also, Hermansky Pudlock syndrome patients who have a defect in the β3A subunit of AP-3 exhibit increased cell-surface expression of LAMP-1, LAMP-2 and CD63 in fibroblasts (Dell'Angelica *et al.*, 1999; Starcevic *et al.*, 2002). Using a yeast two-hybrid system, differential interaction has been observed between the μ3 subunit of AP-3 and the wild-type and alanine mutants of the CD63 cytoplasmic tail. The strength of the interaction (GYEVM (wild-type) = GYEAM > AYEVM > GYAVM >> GYEVA >> GAEVM) correlated with the extent of lysosomal localisation of similarly mutated human CD63 expressed in stably transfected NRK cells (Rous *et al.*, 2002). Tyr is thus more important than gly in determining the strength of the interaction with the μ3 subunit of AP-3, but both tyr and gly are necessary for optimal binding. Similar experiments have shown that the wild-type endolyn cytoplasmic tail with a NYHTL motif also bound the μ3 subunit of AP-3, but with lower affinity than a mutated cytoplasmic tail with a GYHTL motif. A role for AP-3 in endolyn traffic has been confirmed by the mislocalisation of wild-type rat endolyn to the cell surface in AP-3–deficient *pearl* mouse cells. More efficient lysosomal sorting of endolyn was restored upon transient transfection of these cells with wild-type β3A cDNA (Ihrke *et al.*, 2004). Endolyn is a lysosomal membrane glycoprotein that has a higher cell-surface and early endosomal expression than those with a GYXXϕ motif in their cytoplasmic tails. Taken together, these results suggest that AP-3 functions at an intracellular sorting site where lysosomal sorting efficiency (minimising cell-surface or early endosomal expression) is determined by the presence of both tyr and gly in the tyr motif. Immunofluorescence in mammalian cells has localised AP-3 to perinuclear buds or vesicles, where it has partially colocalised with TGN markers, as well as buds or vesicles in the cell periphery, where it has partially colocalised with endocytic tracers (Dell'Angelica *et al.*, 1997; Dell'Angelica *et al.*, 1998; Simpson *et al.*, 1996; Simpson *et al.*, 1997). Using immuno-electron

microscopy, AP-3 has been localised to a novel tubular sorting endosome. Resolution at this level enhances the identification of micro-domains involved in protein sorting and other colocalised proteins, such as AP-1, transferrin, transferrin receptor, asialoglycoprotein receptor, low amounts of cation-independent mannose 6-phosphate receptor (CI-MPR) and LAMPs. LAMPs concentrate in the AP-3 positive membranes of the tubular sorting endosomes, unlike AP-3 mutant cells that exhibit enhanced recycling of lysosomal membrane proteins to the plasma membrane. This tubular endosome is thus considered to be a site where lysosomal membrane proteins are sorted from recycling membrane proteins destined for the plasma membrane or TGN for lysosomal delivery (Peden *et al.*, 2004). AP-3 may thus function at both the TGN and early endosomes.

The exact molecular mechanisms employed by the various adaptor proteins to regulate lysosomal membrane protein trafficking still need to be clearly defined. The results for AP-1 are contradictory and might imply that it plays a minor role in LAMP trafficking. The involvement of AP-2 at the plasma membrane and AP-3 in peripheral sorting endosomes in LAMP trafficking, as discussed above, have implications for transport of LAMPs via the plasma membrane and/or early endosomes (see Discussion).

3.1.4 Targeting pathways

Current studies suggest that some lysosomal membrane proteins are delivered directly to lysosomes, others via the plasma membrane and/or early endosomes and still others via both pathways. These apparent contradictory results could be due to lack of kinetic information, with most studies having been done at steady state. Generally, the relative amounts of lysosomal membrane proteins localised to a particular organelle at steady state has been interpreted as a measure of the fraction of total protein delivered to lysosomes via this compartment. However, steady-state observations contain no information on dynamic membrane flow rates and the absence or very low levels of lysosomal membrane proteins in a particular compartment could be a reflection of rapid movement through this compartment. Furthermore, the presence of lysosomal membrane protein in a particular compartment could be due to recycling and not because they are delivered there *en route* to lysosomes. Here follows a critical analysis of these studies and their interpretations that support either direct delivery to lysosomes or indirect delivery via the plasma membrane and/or early endosomes, or both pathways.

3.1.4.1 Direct delivery to lysosomes

Suggestions for the direct pathway to lysosomes are based on observations that lysosomal membrane proteins are preferentially localised to lysosomes (Barriocanal *et al.*, 1986; D'Souza and August, 1986; Lewis *et al.*, 1985). Generally, the absence of lysosomal membrane proteins on the plasma membrane or the lack of movement of lysosomal membrane proteins through the plasma membrane has been interpreted to imply that lysosomal membrane proteins are delivered directly to lysosomes.

In NRK cells and murine macrophages (J774 cells), the kinetics have been compared for the appearance of newly-synthesised, pulse-labelled lysosomal proteins and plasma-membrane

proteins in lysosomes and on the plasma membrane, respectively. Lysosomal proteins were immunoprecipitated from Percoll density-gradient fractions and the accessibility of plasma-membrane proteins to trypsinisation of intact cells was measured. Lysosomal membrane glycoproteins and enzymes were delivered to lysosomes with the same lag and with similar kinetics as plasma-membrane proteins were delivered to the plasma membrane (Green *et al.*, 1987). The authors have argued that if lysosomal membrane proteins are delivered via the plasma membrane and endocytosis, they would have to be delivered to lysosomes with an additional lag and with slower kinetics as has been observed for the delivery of membrane-bound endocytic markers from the cell surface to lysosomes. The kinetics of this study have been determined in terms of the half-times ($t_{½}$[time]) of appearance of the various proteins at their final destinations. However, the half-time of appearance of a specific protein in a particular compartment is not a direct measure for the flux of a protein into a compartment. Only when the half-time is related to the respective compartment's pool size (m[molecules]) at steady state, can information on membrane flux ($f \alpha m/t_{½}$ [molecules per time]) be obtained. A comparison of the half-times of appearance of proteins at their final destinations is thus not a meaningful assessment of the rate of their transport.

Further support for the direct pathway came in 1992 and 1995 with immuno-fluorescence and antibody-internalisation studies. In NRK and transfected CHO cell lines that expressed low levels of rat lgp120, this protein was not detected on the cell surface at steady state, by immuno-fluorescence microscopy. This has been interpreted to imply that lgp120 is delivered to lysosomes without appearance on the cell surface (Harter and Mellman, 1992). The same has been observed in MDCK cells that stably expressed a chimeric protein, a fusion product of the lumenal and transmembrane domain of a murine cell-surface protein (IgG FcRII-B2 receptor) and the cytoplasmic domain of lgp120, FcR-lgp120. Neither wild-type lgp120 nor the chimera was detected on the cell surface at steady state. Both were localised to lysosomes. The

possibility that lgp120 is transported to the cell surface, but rapidly endocytosed for delivery to lysosomes, was tested by incubating MDCK cells for 60 min at 37ºC in the presence of antiserum against lgp120 or FcR-lgp120. No antibodies were internalised and this has implied no movement of lgp120 or the chimera through the plasma membrane (Honing and Hunziker, 1995). This interpretation, however, has been based on the assumption that the antiserum to lgp 120 or FcR-lgp120 had a high affinity for the specific antigen, so that lgp120 or lgp120-FcR would have been bound even at very low concentrations, before these proteins could have left the plasma membrane. In fact, MDCK cells that overexpressed the corresponding proteins did internalise antibodies. Similarly, in CHO cells that overexpressed lgp120, this protein was detected on the cell surface by immuno-fluorescence microscopy. The same has been observed for an endogenous lysosomal glycoprotein that was not detected on the cell surface of low-expressing CHO cells. This suggests that surface expression results from the saturation of a sorting site involved in the delivery of lysosomal membrane proteins from the TGN to lysosomes (Harter and Mellman, 1992). A saturable sorting site could occur at the TGN or plasma-membrane/early endosomal compartment (see Discussion). Evidence that this sorting site is also very specific comes from cell-surface detection of lgp120 mutants in which the gly^{7}, tyr^{8} and ile^{11} residues of the tyr-sorting signal in the cytoplasmic tail were mutated (Harter and Mellman, 1992; Honing and Hunziker, 1995; Williams and Fukuda, 1990). In the case of overexpression of lgp120 or the expression of its mutants, the sorting site is possibly saturated or less efficient, respectively, and thus misrouting of lgp120 or its mutants via the plasma membrane occurs (as is popularly thought), or movement through the plasma-membrane/early endosomal compartment is slower and thus more easily detectable.

Kinetics and cell-fractionation studies in NIH Swiss transformed mouse embryonic fibroblasts (mouse HaNIH 3T3 cells) have suggested intracellular delivery of LAMP-1 to lysosomes (D'Souza and August, 1986). The processing and delivery of newly-synthesised pulse-labelled

LAMP-1 to lysosomes were followed by the immunoprecipitation of LAMP-1 from sucrose density-gradient fractions. Newly-synthesised LAMP-1 was detected in fractions that were coincident with the rough endoplasmic reticulum (after 15 min), Golgi (after 30 min) and lysosomal markers (after 1h), but not in fractions positive for plasma-membrane markers. These observations have been interpreted to imply that LAMP-1 is delivered intracellularly to endosomes or lysosomes. Cell fractionation is generally not a quantitative technique. Newly-synthesised LAMP-1 was chased for relatively long time intervals. If LAMP-1 moves rapidly through the plasma membrane, it may not have been detected. Also, early endosomes were not distinguished from lysosomes with early endosomal markers. Passage through early endosomes could also have implied indirect delivery to lysosomes.

From similar studies in the human promyelocytic leukaemia cell line (HL60 cells) it has been suggested that the majority of LAMP-1 is delivered directly to lysosomes and a minor fraction is delivered to lysosomes via the plasma membrane (Carlsson and Fukuda, 1992). Pulse-chase labelling, cell-surface biotinylation, fractionation of Percoll density-gradients and immunoprecipitation were used to measure the kinetics of appearance of newly-synthesised LAMP-1 on the plasma membrane and in lysosomes. Newly-synthesised LAMP-1 accumulated in lysosomes with biphasic kinetics and moved through the cell surface transiently. The appearance of LAMP-1 on the cell surface was concurrent with its appearance in dense lysosomes. At the time when the plateau (70% of total LAMP-1) of the first wave was reached in dense lysosomes, LAMP-1 on the cell surface was at its maximum of only 2% of total LAMP-1. The authors have argued that this excludes the possibility that the majority of LAMP-1 first transits the cell surface before delivery to lysosomes. Newly-synthesised cell-surface–derived LAMP-1 accumulated in lysosomes with slow kinetics, as for the second phase of total LAMP-1 delivery to lysosomes. This has been interpreted to suggest that the fraction of LAMP-1 transported to the cell surface is delivered to lysosomes during this second

phase. After granulocytic differentiation of HL60 cells, the fraction of LAMP-1 that travelled via the cell surface was reduced 10-fold even though the LAMP-1 expression levels increased two-fold. A reduction of cell-surface–expressed LAMPs in HL60 cells, upon differentiation of these cells to granulocytic precursors, has also been observed by (Mane et al., 1989). This is in contrast to what has been observed by Harter (1992) and Honing (1995) for overexpressing CHO cells, mentioned above. It suggests, however, that the sorting machinery in differentiated cells is more efficient and that passage through the cell surface is due to inefficient sorting (Carlsson and Fukuda, 1992).

Reservations about the reliability of the above results stem from the fact that cell fractionation is generally not a quantitative technique. In Percoll density-gradients the lysosomal fraction can be split between a low-density and a high-density fraction (Courtoy, 1993; Haylett and Thilo, 1986). In the above study only the high-density fraction was used to measure the appearance of LAMP-1 in lysosomes. The fact that LAMP-1 appearance on the cell surface was co-incident with its appearance in lysosomes and that LAMP-1 was still at its maximum of 2% on the cell surface when the plateau of the first wave was reached in lysosomes are not sufficient reasons to argue that the majority of LAMP-1 is not delivered to lysosomes via the cell surface. An observed increase of molecules in a specific compartment is the net movement of those molecules moving into and out of that compartment. So an observed increase does not imply that no molecules are moving out of the compartment. This is an assumption that is made by the authors. Molecules could thus be moving out of the plasma membrane compartment and into lysosomes before the plateau is reached in the plasma-membrane compartment. The kinetics produced in the above study are thus not sufficient to resolve this question.

Further support for the direct route has been taken from observed interactions between the LAMP-1 cytosolic tail and AP-1. The cytosolic tail of LAMP-1 binds the μ subunit of AP-1 *in vitro* (Ohno *et al.*, 1995), as well as intact AP-1 (Honing *et al.*, 1996). The tyr motif in the cytoplasmic tail is necessary and sufficient to target LAMP-1 to lysosomes (Williams and Fukuda, 1990). The residues, thr (T) and ile (I), in the GYQTI motif of LAMP-1 are critical for AP-1 binding, as well as lysosomal targeting without cell-surface detection (Obermuller *et al.*, 2002). Immunogold-labelling of MDCK cells transfected with LAMP-1 has shown that AP-1 positive membranes (Golgi-derived) are positive for LAMP-1 (Honing *et al.*, 1996). Since AP-1 is the adaptor protein on clathrin-coated vesicles (CCVs) at the TGN, and CCVs do not transport their cargo along the secretory route (Urbe *et al.*, 1997), these observations have been interpreted to support the direct route. However, CCVs could deliver their contents intracellularly to early endosomes. The observation that *in vitro*-generated TGN-derived transport vesicles that contain either LAMPs or γ-adaptin (AP-1 subunit) together with MPRs migrate to different positions on nycodenz gradients (Karlsson and Carlsson, 1998) suggests that LAMPs and MPRs are sorted at the TGN into different vesicles and that AP-1 might not play such an important role in LAMP sorting. In fact, sorting of LAMP-1 is not affected in μ1A-deficient fibroblasts, whereas the sorting of MPRs is affected (Meyer *et al.*, 2000). Also, GGAs (see 3.2.5.4 for definition) have been shown to play a role in MPR sorting at the TGN, but not in LAMP-1 delivery to lysosomes (Puertollano *et al.*, 2001). However, in this regard it is worthwhile to note that lysosomal-associated multispanning membrane protein 5 (LAPTM5) has been shown to be delivered to lysosomes by a pathway that involves ubiquitin-ligase Nedd4 and ubiquitinated GGA3 (Pak *et al.*, 2006).

The differential steady-state distributions of the three LAMP-2 isoforms that vary in their cytoplasmic recognition signal have prompted the suggestion that the usage of the direct or indirect (via the secretory pathway and plasma membrane) pathway is determined by the

cytoplasmic targeting signal. The different LAMP-2 isoforms (A, B, & C) (Fambrough, 1995; Hatem *et al.*, 1995) have a similar tyr motif as LAMP-1 and would therefore probably be gathered into similar CCVs at the TGN. However, transfection of mouse L cells with chimeras consisting of the lumenal domain of avian LAMP-1 (LEP100) and the transmembrane and cytosolic domains of avian LAMP-2 has shown that the various isoforms have different steady-state distributions. Chimeras with the LAMP-2C cytosolic domain are predominantly localised in lysosomes. Higher levels of the chimeras with the LAMP-2A or –B cytosolic domain occur on the cell surface. This increase is not due to saturation of the sorting machinery, but due to the differences in the recognition of the targeting signals. Site-directed mutagenesis identified the hydrophobic amino acid (ϕ) to be critical in determining the different steady-state distributions. Based on the steady-state distribution of the various isoforms, Gough *et al.* (1999) have argued that a particular LAMP-2 isoform may reach the endosomal system via the direct or the indirect pathway (via the secretory pathway and plasma membrane), depending on the signal in the cytoplasmic tail. However, it is also possible that all LAMP-2 isoforms are delivered intracellularly via early endosomes. LAMP-2 isoforms with high affinity for sorting sites in the early endosome/plasma-membrane compartment will result in efficient sorting to lysosomes and therefore rapid movement through this compartment with limited cell-surface expression at steady state. Alternately, LAMP-2 isoforms with low affinity for these sorting sites will result in inefficient sorting, slower movement through this compartment and increased cell-surface expression at steady state (see Discussion). Steady-state distributions do not give any information about the possible movement of molecules through compartments.

Evidence for the direct delivery of LIMPs to lysosomes has been obtained from pulse-chase experiments that were combined with immunoprecipitation of LIMPs in lysosomal fractions obtained from Percoll density-gradients in NRK cells. The incorporation of newly-synthesised LIMPs into the plasma membrane was determined by incubating the cells with anti-LIMP

antibodies and then immunoprecipitating the LIMP-antibody complexes. None was detected on the cell surface. Immunoprecipitation of LIMPs in fractions from Percoll density-gradients of proteinase K treated cells confirmed that LIMPs in the fraction that colocalised with Golgi and plasma-membrane markers did not originate from the cell surface. These data have been interpreted to imply that LIMPs are delivered to lysosomes without appearance on the cell surface (Barriocanal *et al.*, 1986). In addition to Percoll density-gradient fractionation not being quantitative, these observations also do not rule out the possibility that LIMPs are delivered to lysosomes via early endosomes which migrate to the same position as the plasma membrane and Golgi on Percoll density-gradients. The cytoplasmic tail of LIMP-II, which has been shown to be sufficient for lysosomal sorting (Vega *et al.*, 1991), contains a di-leu-based motif (Sandoval *et al.*, 1994) and selectively binds AP-3 (Diment *et al.*, 1998; Honing *et al.*, 1998), an adaptor protein that has been colocalised with TGN markers in the perinuclear region as well as with endocytic tracers in the cell periphery (Dell'Angelica *et al.*, 1997; Dell'Angelica *et al.*, 1998; Simpson *et al.*, 1996; Simpson *et al.*, 1997). Since AP-3 forms part of a clathrin-coat, it could mediate sorting of LIMP-II at the TGN along an intracellular route (either directly to lysosomes or toward early endosomes), as well as at the early endosomes where it could be prevented from recycling to the plasma membrane.

Further support for the direct pathway for LAMP-1 and LIMP-II has come from neuraminidase treatment and biotinylation of cell-surface chimeras expressed in BHK-21 cells. Chimeras were constructed of the lumenal and transmembrane domains of LAP (a lysosomal protein that normally cycles between the plasma membrane and endosomes) and the cytoplasmic tails of LAMP-1 or LIMP-II. The appearance of chimeras on the cell surface and their ability to cycle between the plasma membrane and endosomes, as was determined from the extent of desialylation of cell-surface chimera in response to neuraminidase treatment at 4ºC or 37ºC, or protection of biotinylated cell-surface chimera from biotin stripping due to internalisation, were

greatly reduced or abolished (Obermuller *et al.*, 2002). These observations are, however, a reflection of the steady-state distribution of these chimeras and do not give any information with regard to the fluxes of movement of these proteins.

The above studies have been interpreted to imply that lysosomal proteins LAMP-1, LAMP-2C, and LIMPs are not transported to lysosomes via the secretory pathway and the plasma membrane. Instead, they are potentially sorted at the TGN into clathrin-coated vesicles and directly delivered to lysosomes. Surface detection of these lysosomal membrane proteins as a result of overexpression or mutations in the sorting motif (GYXXϕ) of the cytoplasmic tail has been interpreted to be due to saturation of or inefficient binding to an intracellular sorting site (presumably the TGN) and thus misrouting to the plasma membrane via the secretory route. However, it is also possible that these lysosomal membrane proteins are sorted at the TGN into CCVs for transport to early endosomes. A second level of sorting could then occur in early endosomes for transport of lysosomal membrane proteins to lysosomes via the endocytic pathway. Early endosomes and the plasma membrane are in dynamic equilibrium. Saturation of sorting sites or inefficient sorting could result in slower removal from the early endosomal/plasma membrane compartment relative to the exchange of contents between these compartments and thus surface detection.

Rous *et al.* (2002) have suggested, however, that a major fraction of CD63 (LAMP-3) is delivered directly to lysosomes by a pathway that bypasses early endosomes. When NRK cells stably transfected with wild-type human CD63 (LAMP-3) were treated with chloroquine, CD63 was predominantly localised to lysosomes and only a small fraction occurred in early endosomes, as was shown by indirect immunofluorescence. Chloroquine (a lysosomotropic agent) is a weak base that increases the pH of endosomal compartments. Alkalinisation of endosomes and lysosomes disrupts normal intracellular trafficking by inhibiting transport from

early endosomes to lysosomes without affecting initial internalisation significantly (Clague *et al.*, 1994). A protein that cycles between early endosomes and the TGN (TGN38) was used as an early endosomal marker. A chimera that consisted of the lumenal and transmembrane domain of CD63 and the cytoplasmic tail of TGN38 (CD63-TGN38) colocalised with endogenous TGN38 and served as a control of a protein that trafficks via early endosomes. The rationale is that if CD63 is delivered to lysosomes via early endosomes, the CD63 would accumulate in TGN38-positive early endosomes. CD63 was, however, mainly observed in TGN38-negative structures while some colocalised with TGN38. These results have been interpreted to imply that CD63 is mainly delivered to lysosomes by a pathway that bypasses early endosomes while a small fraction is delivered via early endosomes.

Reservations about the implications of the above observations stem from the following technical limitations: Immunofluorescence is generally not a quantitative technique. Results are based on the assumption that upon treatment of cells with chloroquine, transport from early endosomes to lysosomes is completely inhibited before newly-synthesised protein enters the endocytic pathway. Hence, the appearance of the control CD63-TGN38 chimera in TGN38-negative structures has been interpreted to be as a result of CD63-TGN38 delivered to late endosomes and lysosomes before chloroquine was added. But according the methods, the synthesis of protein was induced at the same time when chloroquine was added. So it is possible that the full effect of chloroquine is not felt immediately upon administration and that newly-synthesised proteins might enter the endocytic pathway before early endosome-lysosome transport is completely inhibited, hence the appearance in lysosomes. No controls are in place to label TGN38-negative structures as late endosomes or lysosomes. Also, chloroquine treatment results in an abnormal cellular state. Intracellular trafficking might be affected at other as yet unknown levels that are not controlled for here.

3.1.4.2 Indirect delivery to lysosomes

The appearance of lysosomal membrane proteins (albeit at low concentrations) on the cell surface, in early endosomes or both compartments at steady state or movement through these compartments have generally been interpreted to imply that they are delivered to lysosomes via the secretory pathway, plasma membrane and endocytosis. However, they could also be delivered to early endosomes intracellularly and then reach the plasma membrane by recycling. The plasma membrane and early endosomes are in dynamic equilibrium and cannot be kinetically resolved.

3.1.4.2.1 Delivery via the secretory pathway, plasma membrane and endocytosis

Lysosomal membrane proteins have been observed on either the plasma membrane or on the plasma membrane and in early endosomes of rat hepatoma and kidney cells (endolyn-78) (Croze *et al.*, 1989), chicken fibroblasts (LEP100) (Lippencott-Schwartz and Fambrough, 1986), rat hepatocytes (LAMP-2, LAP, LGP85, LGP107) (Akasaki *et al.*, 1993; Akasaki *et al.*, 1994; Furuno *et al.*, 1989a; Furuno *et al.*, 1989b), BHK cells (LAP) (Braun *et al.*, 1989; Obermuller *et al.*, 2002), mouse L-cells transfected with avian LAMP-1 (Mathews *et al.*, 1992), MDCK cells (endogenous AC17 antigen) (Nabi *et al.*, 1991) and MDCK cells transfected with endolyn (Ihrke *et al.*, 2001), NRK cells (CD8-endolyn chimera) (Ihrke *et al.*, 2004), human leukaemia cells (LAMP-1 and LAMP-2) (Mane et al., 1989).

In rat hepatoma (Fu5C8) and NRK cells, immuno-cytochemical experiments have shown that a 78 kDa lysosomal membrane protein is present at low levels on the plasma membrane and peripheral tubular endosomes. It is more concentrated on vacuoles, such as multivesicular bodies (late endosomes), filled with endocytic tracers at 18.5ºC and positive for the MPR, as well as on secondary lysosomes that contain hydrolases, but no MPRs or endocytic tracers at

18.5 ºC. Since this protein is present in endosomes and lysosomes, it is termed endolyn-78 (Croze *et al.*, 1989).

Using antibody internalisation at 37ºC, cell-surface (~2%) LAMP-1 (LEP100) in chicken fibroblasts has been observed to be continually internalised and replenished, even in the presence of cycloheximide, a molecule which inhibits protein synthesis. Cell-surface LAMP-1 is thus in continuous exchange with the intracellular pool (Lippencott-Schwartz and Fambrough, 1986). Lysosomotropic agents result in LAMP-1 depletion from lysosomes and augmentation in early endosomes. This has been interpreted to be due to a block in the flow of LAMP-1 from endosomes to lysosomes and continuous recycling from lysosomes to the plasma membrane. The exchange of cell-surface LAMP-1 with the intracellular pool is thus probably a cycling between lysosomes and the plasma membrane via endosomes (Lippencott-Schwartz and Fambrough, 1987).

Similar studies have been done in rat hepatocytes. Lysosomal glycoproteins of 107 kDa (LAMP-1), 96 kDa (LAMP-2), 85 kDa and LAP have been shown to cycle between the cell surface and the endocytic vacuolar system using antibody internalisation assays in the absence or presence of cycloheximide. HRP linked to the Fab fragment of the antibody against either one of the previously mentioned lysosomal proteins was internalised and accumulated in lysosomes as has been observed by morphological studies or biochemical assays on Percoll density-gradient fractions. The accumulation continued in the presence of cycloheximide. This implied that dissociation of antibody from these lysosomal membrane proteins occurred in the endocytic pathway (lysosomes) and that these lysosomal membrane proteins cycle between the plasma membrane and the endocytic system (Akasaki *et al.*, 1993; Akasaki *et al.*, 1994; Furuno *et al.*, 1989a; Furuno *et al.*, 1989b).

LAP is synthesised as a membrane-bound precursor which is processed into the soluble mature form in lysosomes. In transfected, LAP-overexpressing BHK cells, 17% of total LAP precursor was accessible to neuraminidase treatment at 4ºC and therefore has been localised to the cell surface. Newly-synthesised LAP (metabolically labelled for 30 min) appeared at the cell surface with a half-time of 45 min, as was measured by antibody binding at 4ºC. The fraction of LAP (labelled for 2 h) on the cell surface remained constant during a chase of up to 14 h, as was measured by the response to neuraminidase treatment at 4ºC. During the 14th chase hour LAP disappeared from the cell surface. LAP that was labelled for 2 h and chased for 2 h cycled (a cycling time of 3 to 20 min has been estimated) between the plasma membrane and the intracellular pool, based on its response to neuraminidase treatment. When cells were incubated at 37ºC between neuraminidase treatments at 4ºC, intracellular LAP precursors became susceptible to the removal of sialic acid residues. Braun *et al.* (1989) have interpreted these results to imply that the LAP precursor is delivered to the cell surface where it cycles between the plasma membrane and the endosomal pool for a considerable length of time before delivery to lysosomes. In BHK-21 cells, the appearance on the cell surface and recycling between the plasma membrane and the endosomes of chimera consisting of the lumenal and transmembrane domain of LAMP-1 or LIMP-II (proteins which normally occur at very low levels on the cell surface) and the cytoplasmic domain of LAP were greatly enhanced (Obermuller *et al.*, 2002).

The above studies have shown that certain lysosomal membrane proteins continually cycle between the plasma membrane and the intracellular pool (early endosomes and lysosomes) at steady state. Kinetic studies have involved long labelling times of 30 min and 2 h and thus do not provide sufficient kinetic data to make any definitive conclusions about the directional movement of the lysosomal proteins.

Using immunofluorescence in mouse-L cells, the plasma membrane has been implicated as a site lying *en route* to lysosomes (Mathews *et al.*, 1992). Mouse-L cells were transfected with the chimera of the lumenal domain of the vesicular stomatitus virus G-protein and the transmembrane domain and cytoplasmic tail of LEP100. Transient expression of the chimera was visualised on the cell surface by immuno-fluorescence microscopy. The surface population disappeared after protein synthesis inhibition by cycloheximide, and appeared and accumulated in lysosomes when lysosome proteolysis was inhibited.

Indirect delivery via the plasma membrane or early endosomal compartment has been suggested for the AC17 antigen in MDCK cells. Nabi *et al.* (1991) have observed a steady-state expression of endogenous lysosomal membrane glycoprotein, AC17 antigen, and transfected LEP100 on both apical (0.8%) and basolateral (2.1%) membranes of MDCK cells, using periodate oxidation of cell-surface carbohydrates and reaction with biotin-X-hydrazide followed by immunoprecipitation and ^{125}I-streptavidin blotting. The passage of newly-synthesised AC17 antigen through the basolateral membrane and early endosomes, but not the apical membrane, has been observed from pulse-chase experiments in which antibodies to the AC17 antigen were internalised during the last 15 min of the chase. According to the authors, late endosomes in MDCK cells would be reached only after 15 min of fluid-phase endocytosis. Non-immune antibodies were not noticeably internalised and therefore antibodies were presumably not taken up by fluid-phase endocytosis. Newly-synthesised AC17 antigen appeared at the basolateral membrane with a half-time of 35 min and disappeared with a half-time of 35 min. The authors have argued that since the AC17 antigen moved through the Golgi with a half-time of 25 min (based on Endo H resistance), the appearance on the basolateral membrane ($t_{1/2}$ = 35 min) was too rapid for prior delivery to lysosomes. The fraction of newly-synthesised protein delivered via the basolateral membrane was determined to be 74% by incubating the cells with anti-AC17 antigen antibody for 90 min, the time

required for a 20 min pulse of AC17 antigen to move through the basolateral membrane/early endosomal compartment. Movement of the AC17 antigen through the apical membrane was measurable only after chloroquine treatment. The results have been interpreted to imply that the AC17 antigen is targeted basolaterally before delivery to lysosomes and that apical appearance is as a result of recycling from lysosomes (Nabi *et al.*, 1991). While the above study shows transient presence of newly-synthesised AC17 antigen through the basolateral membrane and early endosomes, sufficient kinetic data is not available to conclude that 74% of total newly-synthesised AC17 antigen is delivered via the basolateral membrane/early endosomal compartment. Firstly, a 20 min ^{35}S-methionine pulse is relatively long and would thus contribute to a lack in kinetic resolution. Secondly, no kinetic information about the appearance of newly-synthesised AC17 antigen in lysosomes is available to compare with its appearance in the basolateral membrane/early endosomal compartment so as to draw conclusions about the delivery path followed. As mentioned before, since the half-time of appearance of a protein in a particular compartment is dependent on both its flux and pool size, it cannot be used as a direct measure of the rate of transport into the compartment. Also, nothing precludes the possibility that apical appearance of the AC17 antigen after chloroquine treatment is due to newly-synthesised protein from the biosynthetic pathway that has become detectable as a result of accumulation in the apical membrane/early endosomal compartment.

In a separate study in 2001, antibodies to endolyn have been shown to be preferentially internalised from the apical domain and efficiently delivered to lysosomes in transfected polarised MDCK cells. To distinguish between polarised sorting of newly-synthesised endolyn at the TGN and redistribution to the cell surface after delivery to lysosomes, newly-synthesised proteins were radiolabelled for 15 min and captured as they appeared on the apical or basolateral membrane by chasing in the presence of antibodies to endolyn for 1 hour. However, redistribution/recycling during this 1 hour chase cannot be ruled out. An analysis of CD8-

endolyn chimeras in which the lumenal and transmembrane domain or just the lumenal domain of endolyn is replaced by that of CD8 (a plasma-membrane protein) has revealed apical targeting information in the lumenal domain of endolyn that predominated over basolateral information in its cytoplasmic tail (Ihrke *et al.*, 2001).

Endolyn has been shown to traffic via the cell surface by antibody-internalisation assays and immunofluorescence in NRK cells expressing a chimera composed of the lumenal and transmembrane domain of CD8 and the cytoplasmic tail of rat endolyn (CD8-endolyn) (Ihrke *et al.*, 2004). When AP-2–mediated endocytosis was inhibited in 3T3 cells, lysosomal delivery of endolyn was virtually abolished and cell-surface appearance increased. When transport from early endosomes to lysosomes was inhibited by chloroquine treatment of NRK cells stably transfected with the CD8-endolyn chimera, there was no colocalisation of the newly-synthesised chimera with the lysosomal marker, lgp120. Although no early endosomal marker was present, these results have been interpreted to imply that the CD8-endolyn chimera accumulated in early endosomes. These results suggest that endolyn is delivered to lysosomes almost exclusively along the indirect pathway, either via the secretory route, the plasma membrane and endocytosis or intracellularly via early endosomes.

3.1.4.2.2 Intracellular delivery via early endosomes

Newly-synthesised ^{35}S-labelled LAP has been observed in endosomes of rat liver cells. Its presence in endosomes containing asialofetuin conjugated-HRP, a fluid-phase marker endocytosed for 10 min, was measured as a loss of ^{35}S-LAP due to the formation of insoluble polymers, a reaction catalysed by HRP in the presence of DAB and hydrogen peroxide (Tanaka *et al.*, 1990b). The authors have interpreted this to be an indication of LAP present in early endosomes. This introduces the possibility that newly-synthesised LAP is delivered to lysosomes via early endosomes and is transported to the plasma membrane due to recycling.

(Since the LAP cytoplasmic tail does not bind AP-1 *in vitro* (Obermuller *et al.*, 2002), it is possible that LAP might be sorted into Golgi-derived CCV's that involve other adaptors.) However, it is important to note that relatively long ^{35}S-methionine pulses (30 and 60 min) were used. This makes it difficult to clearly resolve where or when on the delivery path of LAP the early endosomes are located.

Akasaki and co-workers (Akasaki *et al.*, 1995; Akasaki *et al.*, 1996) have examined the transport of newly-synthesised lysosomal membrane proteins to early and late endosomes, in addition to the cell surface and lysosomes. They performed kinetic studies on rat hepatocytes using pulse-chase experiments, Percoll density-gradient fractionation, antibody binding and internalisation and immunoprecipitation. The accumulation of labelled newly-synthesised lysosomal membrane proteins on the plasma membrane, early endosomes, cell periphery, late endosomes and lysosomes was measured. They have interpreted their kinetic curves to suggest the following: LAMP-1 is delivered to lysosomes via the plasma membrane, early endosomes and late endosomes, LAMP-1 being delivered to the plasma membrane with a slight delay. LAMP-2 is delivered to lysosomes via early endosomes and late endosomes, with a small amount reaching the plasma membrane via recycling. In addition to the LAMPs being delivered to early endosomes directly from the TGN, a second wave is delivered from the late endosomes due to recycling (and in the case of LAMP-1, also from the plasma membrane due to endocytosis). A greater fraction of LAMP-2 is delivered via the cell peripheral compartments than is the case for LAMP-1. They have suggested that this difference could be due to the differences in the tyr motif in the cytoplasmic tail, resulting in differences in binding affinities for the AP proteins and thus differences in the efficiencies with which they are concentrated into CCVs.

The conclusions of the above study remain limited because of technical and kinetic uncertainties: Percoll density-gradient fractionation is not ideal for quantitative measurements and may not clearly resolve endosomes from the TGN. Antibody binding to the cell surface at 4ºC was used to determine the amount of newly-synthesised protein that moved through the plasma membrane. Proper quantification of LAMP on the cell-surface requires that the antibody be added in excess, a detail the authors failed to address. Also, after the unbound antibody was washed away and the cells were lysed so that the immunocomplexes could be removed with Sepharose beads, it was assumed that the bound antibody would not dissociate to establish a new equilibrium. The interpretation of the kinetic curves in the above experiments is purely arbitrary. For example, it is an assumption that an increase of LAMP in a particular compartment is as a result of newly-synthesised LAMP arriving from the TGN. It could be due to recycling from another endocytic compartment. Also, the conclusion about the compartments from which recycling of LAMP occurs is presumptive. There are no controls in place to substantiate these interpretations. The delay (20 min) that has been observed in the delivery of LAMP-1 to the plasma membrane is based on one experimental point. Relatively long radio-active pulses of 20 min contribute to a lack in kinetic resolution. The rate-limiting step in the trafficking of most proteins is export from the ER (Lodish *et al.*, 1983). Subsequent movement from the Golgi and TGN to the final destination occurs rapidly. Newly-synthesised molecules would thus accumulate transiently in intermediate compartments. Unless very short labelling periods are used, it is very difficult to determine when a labelled protein has exited the TGN and kinetic resolution is compromised.

In an attempt to overcome this obstacle, Cook *et al.* (2004) have designed a LAMP-1 chimera with a heterologous lumenal domain containing a motif that allows for tyr sulfation, a post-translational modification restricted to the TGN, and the core sequence of avidin (Av) allowing high-affinity interaction with biotinylated probes introduced into the endocytic pathway. The

chimera could thus be radio-actively labelled with high specific-activity to serve as a marker for exiting the TGN. The radio-actively labelled, newly-synthesised LAMP-1 chimera (YAL) could then be captured as they entered endocytic vesicles by interaction with endocytosed biotinylated IgG (BIG). YAL molecules were degraded in lysosomes after a lag of 15-20 min, but entered the endocytic pathway within 5 min of chase. They have interpreted this to imply that YAL does not enter lysosomes directly. This, however, assumes that YAL is degraded immediately upon entering lysosomes. Pulse-chase experiments in which BIG was internalised during the last 5 min of the chase have shown that YAL transits early endosomes. The authors have suggested that YAL is delivered into the endocytic pathway only via early endosomes on the basis of *in vitro* acceptor-donor fusion assays: 5 min acceptors-containing BIG produced the same fusion activity as 60 min acceptors, or acceptor membranes prepared from cells pulsed for 5 min with BIG and then chased for 30 min, when incubated with radio-actively labelled TGN-derived YAL. Under conditions where the 5 min BIG pulse was chased for 45 min, they have shown with Percoll density-gradient fractionation that even though most BIG was in late endosomes, the fusion activity was higher in early endosomes. Since rab5 (marker for early endosomes) was also detected in late endosomal fractions, they have concluded that the residual fusion activity in the late endosomal fractions was a result of contaminating early endosomes (Cook *et al.*, 2004).

Reservations about the above results stem from the following technical limitations: The authors were unable to measure directly what fraction of the total newly-synthesised LAMP-1 chimera was delivered via early endosomes. They did this indirectly with *in vitro* fusion assays. While limiting donor membrane could be a reason for not having observed an increase in fusion activity for the 60 min acceptors, the fusion product could also have been degraded in the lysosomes. A contamination of late endosomal fractions with early endosomes does not

necessarily imply that fusion seen in these fractions was a result of early endosomes only. The behaviour of the chimera could be different to endogenous LAMP-1.

3.1.4.3 Summary

Arguments for direct delivery to lysosomes have been based on the absence of lysosomal membrane proteins on the cell surface at steady state, no movement (or movement of only a very small fraction) of newly-synthesised lysosomal membrane protein through the cell surface, the fact that newly-synthesised proteins are delivered to the plasma membrane with the same half-time as they are delivered to lysosomes, the colocalisation of lysosomal membrane proteins and AP-1 in Golgi-derived membranes and the failure of newly-synthesised lysosomal membrane proteins to accumulate in early endosomes upon chloroquine treatment of cells.

Arguments in favour of the indirect pathway via the secretory pathway and plasma membrane have been based on the presence of lysosomal membrane proteins on the plasma membrane and in early endosomes at steady state, albeit at low concentrations, an exchange of lysosomal membrane proteins on the cell surface with an intracellular pool and the movement of newly-synthesised lysosomal membrane proteins through the plasma membrane. Delivery of lysosomal membrane proteins to lysosomes intracellularly via early endosomes has been suggested by the observation of the movement of newly-synthesised lysosomal membrane protein through early endosomes. The plasma membrane and early endosomes are in rapid dynamic equilibrium and can not be kinetically resolved. Movement of newly-synthesised lysosomal membrane protein through the plasma membrane or early endosomes could thus either be due to delivery via the secretory pathway, the plasma membrane and endocytosis or intracellularly via early endosomes, the plasma membrane being reached due to rapid exchange with early endosomes.

These apparent contradictory results and interpretations could be due to different cell types, different lysosomal membrane proteins following different delivery paths, limitations of experimental techniques and the lack of efficient kinetic resolution. Generally, experiments have been performed at steady state. Even when pulse-chase experiments have been performed, the relatively long labelling pulse limited detailed kinetic resolution.

To circumvent some of these problems, my approach allowed observation of the path of newly-synthesised endogenous LAMP-1 in mouse $P388D_1$ macrophages, labelled for a very short period (5 min) at a very high specific-activity of ^{35}S-methionine. The kinetics of ^{35}S-labelled-LAMP-1 entry into early endosomes or lysosomes were measured. As a reference, the kinetics of LAMP-1 entry into the endocytic pathway (includes early endosomes and lysosomes) were also measured. Results showed that the bulk of newly-synthesised LAMP-1 that entered the endocytic pathway, entered via early endosomes and remained in early endosomes transiently. I suggest that newly-synthesised LAMP-1 entered lysosomes only after it had left early endosomes.

3.2 MANNOSE 6-PHOSPHATE RECEPTORS

3.2.1 Types and structure

There are two types of MPRs, namely the cation-independent MPR (CI-MPR) and the cation-dependent MPR (CD-MPR). The MPRs are type I integral membrane proteins. Their structures are depicted in figure 3.2.1.

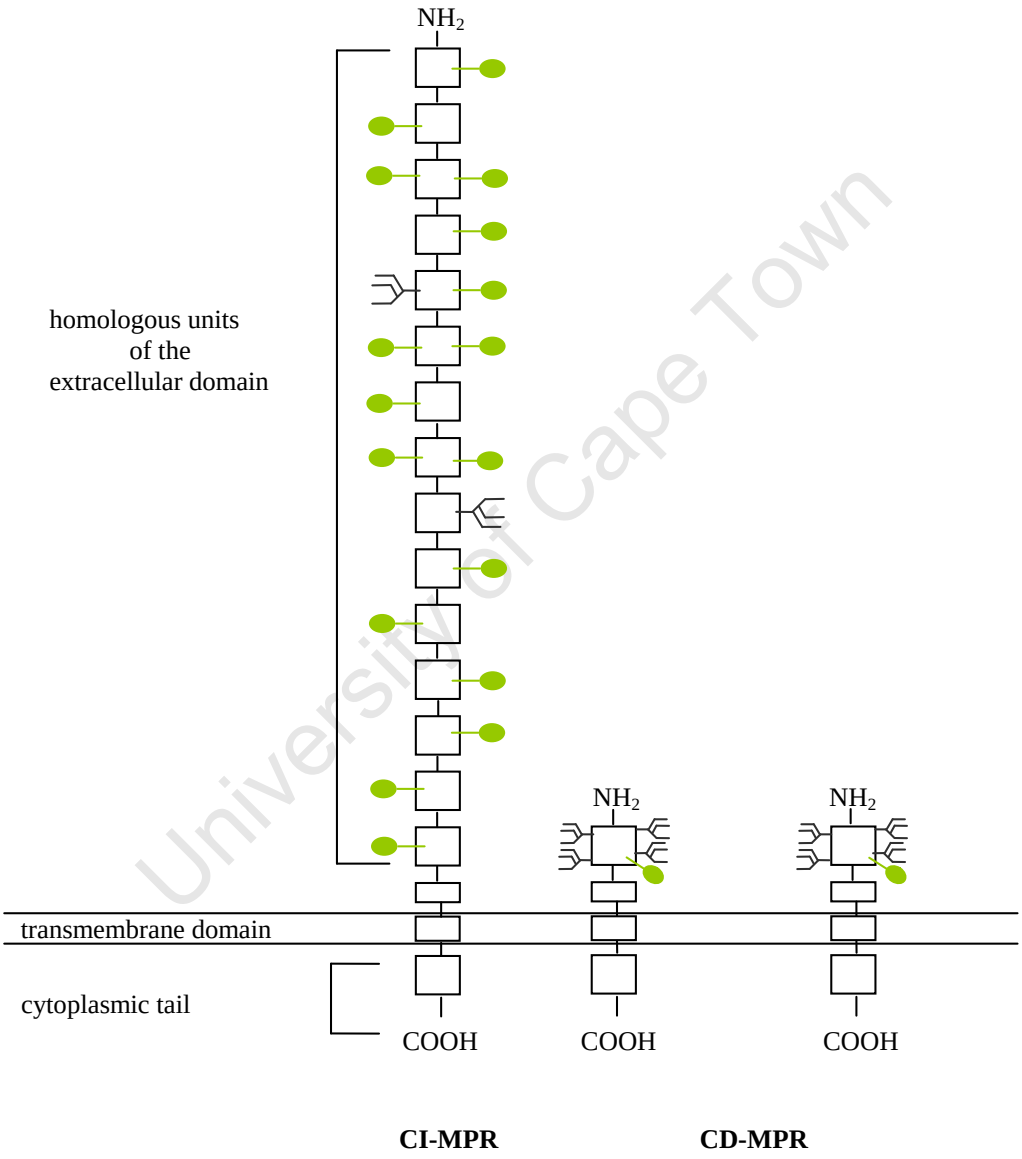

Figure 3.2.1 A schematic diagram of the CI-MPR and the CD-MPR

●—: potential glycosylation sites

⋔ : known, used glycosylation sites

This figure was adapted from (Dahms and Kornfeld, 1987; Dahms *et al.*, 1989).

3.2.1.1 Cation-independent mannose 6-phosphate receptor (CI-MPR)

The CI-MPR was first purified from bovine liver membranes using immunoprecipitation succeeded by lysosomal β-galactosidase−Sepharose 4B affinity chromatography (Sahagian *et al.*, 1981). This receptor does not require cations for binding to its ligands, hence the name cation-independent MPR. It consists of an N-terminal extracytoplasmic domain, a transmembrane domain and a C-terminal cytoplasmic tail. The lumenal domain consists of 15 units with sequence identity to each other (16 − 38%) and to the extracytoplasmic domain of the CD-MPR (14 − 28%) (Lobel *et al.*, 1988). Two of the 19 potential glycosylation sites on the lumenal domain are utilised. The oligosaccharides are asparagine-linked. It contains fucose and terminal sialic acid residues. High-mannose residues are converted to complex-type oligosaccharides, as determined by acquisition of resistance to Endo H in CHO cells (Pryor *et al.*, 1983; Sahagian and Neufeld, 1983). Phosphorylation of serine residues on the mature protein occurs when this protein is in the TGN or just after it has exited from the TGN (Meresse and Hoflack, 1993). Under reducing conditions the apparent molecular weight is 215 kDa. Under non-reducing conditions it migrates faster and can be resolved into two bands of apparent molecular weights 180 and 168 kDa, suggesting the presence of intrachain disulphide bonds (Sahagian and Neufeld, 1983). The calculated molecular weight of the CI-MPR's protein component is 270 kDa. The actual molecular weight probably ranges between 275 − 300 kDa as a result of glycosylation (Oshima *et al.*, 1988). The CI-MPR is often referred to as the MPR300. Two high-affinity man-6-P binding sites have been localised to domains 1 – 3 and 9 and one low-affinity site to domain 5 of the extracytoplasmic region. Domain 1 and 2 are required for optimal binding by domain 3 (Hancock *et al.*, 2002b; Reddy *et al.*, 2004). Single amino-acid substitutions in constructs that encoded either of the two man-6-P binding sites of the CI-MPR and that were expressed in COS-1 cells, have identified four amino acids (gln^{392}, ser^{431}, glu^{460}, tyr^{465}) in domain 3 and four (gln^{1292}, his^{1329}, glu^{1354}, tyr^{1360}) in domain 9 as critical for man-6-P binding (Hancock *et al.*, 2002a). A similar set four amino acids (gln^{644}, arg^{687},

glu[709], tyr[714]) is also critical for carbohydrate recognition by domain 5 which has a higher affinity for phosphodiesters than phophomonoesters (Chavez *et al.*, 2007).

3.2.1.2 Cation-dependent mannose 6-phosphate receptor (CD-MPR)

This receptor has been first identified in $P388D_1$ macrophages which fail to synthesise detectable CI-MPR (Gabel *et al.*, 1983; Pryor *et al.*, 1983). My project is based on studies with $P388D_1$ macrophages and the CD-MPR. Therefore, I deal with this receptor here in more detail than the CI-MPR. Cations are required for the binding of ligands, hence the name cation-dependent MPR (Hoflack and Kornfeld, 1985a; Hoflack and Kornfeld, 1985b). The effect of divalent cations on the binding efficiency of the CD-MPR is mediated by Asp[103] (Sun *et al.*, 2005). The CD-MPR consists of an N-terminal extracytoplasmic domain, a hydrophobic transmembrane domain and a C-terminal cytoplasmic tail. The lumenal domain is homologous to the repeating units of the 215 kDa CI-MPR (Dahms and Kornfeld, 1987). This suggests that both receptor types arose from a single ancestral gene. In BW5147 lymphoma and MOPC 315 plasmacytomal cells, the CD-MPR is synthesised as a 40 kDa glycoprotein that is processed to a mature 43 kDa due to conversion of high-mannose residues to complex-type oligosaccharides (Kornfeld, 1987b). It is also 43 kDa in human fibroblasts, but 46 kDa in human HepG2 cells, U937 monocytes, blood-derived macrophages, rat Morris hepatoma 7777 cells (Stein *et al.*, 1987a) and mouse $P388D_1$ macrophages (Hoflack and Kornfeld, 1985b). Hence the CD-MPR is often referred to as the MPR46. It has been reported to have 7-8 asparagine-linked oligosaccharides, of which 5 are converted to Endo H resistant types (Stein *et al.*, 1987a), or 5 potential asparagine-linked glycosylation sites of which 4 are utilised (Dahms *et al.*, 1989). N-glycosylation assists the nascent CD-MPR to fold into a conformation that enhances ligand binding and promotes efficient intracellular transport (Zhang and Dahms, 1993). The receptor has potential serine phosphorylation sites and clusters of acidic residues. Ser[56] is phosphorylated, but is not essential for the stability, cell-surface expression or transport

function of the receptor (Hemer *et al.*, 1993). It has been shown to be palmitoylated at two cysteines in its cytoplasmic tail (Reddy *et al.*, 2003). Chemical cross-linking studies on affinity-purified CD-MPR and solubilised membranes containing CD-MPR have indicated that the mature protein exists as a homo-dimer. Similar studies on mutant CD-MPR have shown that the transmembrane domain is important for dimer formation, but that a single lumenal domain is necessary and sufficient for binding and release of ligand (Dahms and Kornfeld, 1989). Site-directed mutagenesis of the binding site of bovine CD-MPR, expressed transiently in COS-1 cells, has revealed four amino acids (gln^{66}, arg^{111}, glu^{133}, tyr^{143}) which are essential for ligand binding (Olson *et al.*, 1999; Sun *et al.*, 2005). This set of amino acids (gln, arg, glu, tyr) is similar to that which is critical for binding in the binding sites of the CI-MPR. The three-dimensional structure of the MPRs in complex with bound man-6-P confirms the mutagenesis studies.

3.2.2 Steady-state distribution

Immuno-cytochemical data on the intracellular distribution of the CI-MPR have on occasion been contradictory. In general, using immuno-fluorescence and immuno-electron microscopy, it has been observed in the endoplasmic reticulum, throughout the Golgi, in the TGN, coated buds and coated vesicles arising from the TGN, in the plasma membrane, coated pits and endosomes which include organelles that have been defined as CURL (compartment of uncoupling of receptor and ligand) (Geuze *et al.*, 1983; Geuze *et al.*, 1984; Geuze *et al.*, 1985), figure 2.3. The bulk is localised to the TGN and endosomes (Geuze *et al.*, 1984; Geuze *et al.*, 1985; Stein *et al.*, 1987a; Willingham *et al.*, 1983), predominantly late endosomes (Geuze *et al.*, 1988; Griffiths *et al.*, 1988). MPRs are either present at very low levels, as in rat parenchymal liver cells (Geuze *et al.*, 1984) and in CHO cells (Willingham *et al.*, 1983), or not detected at all in lysosomes, as in human fibroblasts (Stein *et al.*, 1987a; von Figura *et al.*, 1984), CHO cells (Sahagian and Neufeld, 1983) and rat hepatoma cells (Geuze *et al.*, 1988). Morphological studies on the CD-MPR are not as extensive, but evidence suggests that both receptors exhibit a similar qualitative distribution (Bleekemolen *et al.*, 1988). Using immuno-labelling and semi-quantitative analyses, however, the CI-MPR has been observed to be enriched in multi-vesicular endosomes while the CD-MPR is enriched in the associated tubules and vesicles (ATV) which are different to those destined for the plasma membrane (Klumperman *et al.*, 1993). It has been suggested that this difference could be due to the CD-MPR recycling much more rapidly to the TGN.

3.2.3 MPR Function

The MPRs bind lysosomal enzymes in the TGN for delivery to lysosomes. The CI-MPR also recognises and binds the insulin-growth factor (II) (IGF-II).

3.2.3.1 Biosynthesis of lysosomal enzymes

Lysosomal enzymes are co-translationally glycosylated in the rough endoplasmic reticulum (RER). High-mannose residues are added at specific asparagine residues. The enzymes are translocated into the ER with cleavage of the signal peptide and transported to the Golgi where they are post-translationally modified. Specific determinants on lysosomal enzymes are identified as signals for phosphorylation of mannose (Hasilik and Neufeld, 1980a) by enzymes, N-acetylglucosaminyl-1-phosphotransferases and α-N-acetylglucosaminyl phosphodiesterases, localised in *cis*-Golgi cisternae (Pohlman *et al.*, 1982).

3.2.3.2 Binding of lysosomal enzymes

Phopho-mannosyl residues on lysosomal enzymes are recognised by MPRs in the Golgi (Hickman *et al.*, 1974; Hieber *et al.*, 1976). While the terminal man-6-P on lysosomal enzymes is the critical determinant, inhibition binding studies have indicated that high-affinity binding is attained through the recognition of an extended oligosaccharide structure, which probably includes the manα1,2man linkage (Olson *et al.*, 1999; Reddy *et al.*, 2003). MPRs bind the lysosomal enzymes in the Golgi at a pH close to neutral. Optimal binding of lysosomal enzymes by CD-MPR occurs at pH 6.3, as determined by affinity-chromatography. At neutral pH some lysosomal enzymes could be oriented such that the phosphorylated oligosaccharides are not accessible to the CD-MPR binding site (Kornfeld, 1987a). Comparison of ligand-bound versus ligand-free structures of the CD-MPR has revealed a significant change in the quartenary structure. The binding pocket is re-organised by the relocation of a loop (glu^{134}-cys^{141}). Olson *et al.* (2002) have proposed that the pKa of the sugar phosphate and his^{105} in the

binding pocket could be responsible for its inability to bind ligand at the cell surface (pH 7.4), and the pKa of glu^{133} could determine ligand release in the acidic environment of late endosomes. The CI-MPR, on the other hand, is able to bind lysosomal enzymes on the cell surface. Small changes in pH in the Golgi could result in differential binding by the two receptors in the TGN (Kornfeld, 1987a).

3.2.3.3 Delivery of lysosomal enzymes to lysosomes

By binding to MPRs, lysosomal enzymes are sorted from the rest of the proteins in the TGN (Duncan and Kornfeld, 1988; Griffiths and Simons, 1986; Willingham *et al.*, 1983) and packaged into CCVs. MPR-enzyme complexes are delivered into an acidic endocytic organelle where the enzymes dissociate from the receptor due to the low pH (Dahms and Kornfeld, 1989; Hoflack and Kornfeld, 1985a). The pKa of glu^{133} in the binding site could be responsible for ligand release in the acidic environment (Olson *et al.*, 2002). The requirement of an acidic environment for the dissociation of enzymes from receptors is consistent with the depletion of unoccupied receptors and the enhanced secretion of newly-synthesised acid hydrolases upon chloroquine treatment of fibroblasts (Gonzalez-Noriega *et al.*, 1980). (Chloroquine raises the pH of acidic organelles above 6 and subsequently inhibits the dissociation of receptor-ligand complexes. The depletion of unoccupied receptors results in missorting of lysosomal enzymes and the blocking of endocytosis of exogenous lysosomal enzymes, hence the enhanced secretion of enzymes.) Once the enzymes have dissociated from MPRs, phosphatases remove the phosphates from the enzymes to prevent rebinding to receptors. If the acidic endocytic organelle is a pre-lysosomal organelle, the enzymes are delivered to lysosomes along the endocytic pathway. The receptors are sorted into tubular membrane elements and recycled to the TGN for re-use (Duncan and Kornfeld, 1988). The recycling of the receptors to the Golgi is triggered by the dissociation of the enzymes (Brown *et al.*, 1986).

3.2.4 Targeting signals

A series of sorting signals that ensure correct sorting of the MPRs at the plasma membrane, TGN and endosomes has been identified (reviewed in Hille-Rehfeld, 1995).

3.2.4.1 Plasma membrane sorting

Internalisation of the CI-MPR at the cell surface is mediated by a tyr-based sorting signal, $Y^{24}KYSKV^{29}$ (tyr^{24}-lys-tyr-ser-lys-val^{29}), in the 163-residue cytoplasmic tail (Canfield *et al.*, 1991; Jadot *et al.*, 1992; Lobel *et al.*, 1989). Three signals in the 67-residue cytoplasmic tail of the CD-MPR mediate its internalisation: a signal that includes phe^{13} and phe^{18}, $F^{13}PHLAF^{18}$ (phe^{13}-pro-his-leu-ala-phe^{18}), with phe^{18} being more important; a signal that involves tyr^{45}, $Y^{45}RGV^{48}$ (tyr^{45}-arg-gly-val^{48}) and a di-leu motif (L^{64}-L^{65}) at the C-terminal (Denzer *et al.*, 1997; Johnson *et al.*, 1990).

3.2.4.2 Trans-Golgi Network sorting

Efficient sorting of the MPR at the TGN has been concluded from the characteristic steady-state distribution of the MPR and efficient lysosomal enzyme sorting. The CI-MPR has two signals in the cytoplasmic domain, a di-leu-based sorting signal, LLHV (leu-leu-his-val), and a tyr-based endocytosis motif, $Y^{24}KY^{26}SKV^{29}$, for efficient lysosomal enzyme sorting in the Golgi. Deletion of LLHV partially impaired sorting. Mutation of YKYSKV does not affect sorting, but in combination with the LLHV deletion disrupts enzyme sorting completely (Johnson and Kornfeld, 1992a). There is evidence, however, that the cytoplasmic tail of the CI-MPR is not sufficient to ensure the characteristic intracellular steady-state distribution of the CI-MPR. In mouse 3T3 cells stably transfected with chimera composed of the lumenal and transmembrane domains of the human epidermal growth factor (EGF) receptor and the cytoplasmic tail of the CI-MPR (EEM) the EEM's failed to localise to the TGN and the endosomes. They predominantly localised to the cell surface and cycled efficiently between the

cell surface and early endosomes (Dintzis and Pfeffer, 1990). However, chimeras composed of the lumenal and transmembrane domains of the CI-MPR and the cytoplasmic tail of the human EGF receptor (MME) or the lumenal domain of the CI-MPR and the transmembrane domain and cytoplasmic tail of the EGF receptor (MEE) expressed transiently in CHO cells, localised predominantly to a perinuclear structure, similar to the endogenous CI-MPR. These observations have implicated determinants in the lumenal domain of the CI-MPR as being involved in the targeting of the CI-MPR (Dintzis *et al.*, 1994).

A di-leu-based sorting signal, HLL (his-leu-leu), in the cytoplasmic tail of the CD-MPR in mouse L cells has been implicated in efficient intracellular sorting of cathepsin D (a lysosomal enzyme). Mutation of the last five amino-acids (his-leu-leu-pro-met) to alanines resulted in decreased efficiency of cathepsin D sorting. Mutation of the last two amino acids (pro-met) had no effect, thus implicating only HLL. Ligand binding and receptor recycling from the cell surface were unaffected. Hence, sorting at the level of the TGN was probably the step that was affected (Johnson and Kornfeld, 1992b).

3.2.4.3 Endosomal sorting

Efficient sorting of the MPR in endosomes has been deduced from proper lysosomal enzyme sorting and protection of the receptor from lysosomal delivery and subsequent degradation. The effect of cytoplasmic tail truncation mutants and ala-scanning mutants (short stretches of alanines were created using PCR mutagenesis) of bovine CD-MPR, expressed in mouse L cells, on the recycling of the receptor to the TGN has been analysed using Percoll density-gradient fractionation. Amino-acids 34-39 in the cytoplasmic tail are critical in preventing lysosomal delivery and degradation of the receptor. The transmembrane domain contributes to this function (Rohrer *et al.*, 1995). Substitution of cys^{34} to ala caused lysosomal delivery of the receptor and total loss of cathepsin D sorting. Cys^{34} is reversibly palmitoylated by membrane-

bound palmitoyl-transferase that cycles between the plasma membrane and endosomes (Stockli and Rohrer, 2004). This palmitoylation is impaired when amino-acids 34-39 are substituted by alanines, thus causing abnormal receptor trafficking and missorting of cathepsin D (Schweizer *et al.*, 1996). A di-aromatic amino-acid motif, $F^{18}W^{19}$ (phe^{18}-trp^{19}), in the cytoplasmic tail of the CD-MPR at a specific position relative to the transmembrane domain also determines efficient sorting of the CD-MPR and avoids lysosomal delivery. Trp^{19} plays the main role, while phe^{18}, phe^{13} and neighbouring residues have a contributory role. According to Schweizer *et al.* (1997), the substitution of phe^{18} and trp^{19} with other hydrophobic residues has no effect. However, Nair *et al.* (2003) have reported that substitution with more bulky hydrophobic amino acids decreased binding to Tip47 (a protein involved in this sorting step (Orsel *et al.*, 2000)) and resulted in delivery of receptor to lysosomes. Substitution with less hydrophobic amino acids decreased binding to Tip47 further and increased receptor delivery to lysosomes (Nair *et al.*, 2003). *In vitro* transport from endosomal membranes to the TGN has also been shown to be inhibited by a peptide that contains the acidic cluster di-leu motif of the CD-MPR tail, thus implicating the di-leu motif (Medigeshi and Schu, 2003).

The CI-MPR, on the other hand, depends on a $P^{49}PAPRPG^{55}$ (pro^{49}-pro-ala-pro-arg-pro-gly^{55}) loop and other hydrophobic amino acids in the cytoplasmic tail for efficient endosomal sorting. The membrane-proximal residues, $P^{49}PAPRPG^{55}$ loop and $V^{69}A^{71}$ (val^{69}-ala^{71}), are important for direct interaction with Tip47 and the membrane-distal residues are important for proper folding and correct presentation (hydrophobic interphase) of the membrane-proximal sequences (Orsel *et al.*, 2000).

3.2.5 Sorting machinery involved in targeting

The targeting signals specify the location to which MPRs must be transported. Presumably MPRs carry lysosomal enzymes to endosomes from where MPRs are recycled to the TGN for re-use, while the enzymes are delivered to lysosomes. A similar trafficking mechanism as explained for LAMPs in section 3.1.3 shuttles MPRs between the TGN and endosomes. Different sorting machineries are responsible for sorting MPRs into vesicles at the different sites.

Adaptor proteins have been implicated in sorting at the TGN, plasma membrane and endosomes. Clathrin-coat adaptor proteins such as AP-1, AP-2 and Golgi-localizing, γ-ear-containing, ARF-binding protein (GGA's) and AP-3 (can bind clathrin, but has been shown to function without clathrin) are implicated in MPR trafficking. AP-1, GGA and AP-3 binding to the membrane are regulated by ADP-ribosylation factor-1 (ARF-1), a small GTP-binding protein. AP-1 and AP-2 mediate the binding between receptors and clathrin during the formation of clathrin-coated vesicles at the TGN and the cell surface, respectively (Ahle *et al.*, 1988). Plasma-membrane-derived adaptor proteins (AP-2) and Golgi-derived adaptor proteins (AP-1) bind to different signals in the cytoplasmic tail of the CI-MPR and CD-MPR (Glickman *et al.*, 1989; Honing *et al.*, 1997; Pearse, 1988). Other proteins that have been implicated in MPR recycling to the TGN and efficient lysosomal enzyme delivery are: dynamin (Nicoziani *et al.*, 2000), rab9 GTPase (Pryor *et al.*, 2000), rab7 GTPase (Hoflack, 1998), phosphatidylinositol 3-kinase (PI3-K) (Davidson, 1995; Reaves *et al.*, 1996), Tip47 (Krise *et al.*, 2000; Orsel *et al.*, 2000) and the mammalian retromer complex (Bonifacino, 2004).

3.2.5.1 Adaptor protein-1

AP-1, also named the HAI-adaptor, colocalises with both the CI-MPR and the CD-MPR at the trans-Golgi reticulum (TGR) (Klumperman *et al.*, 1993). Both the MPR and the ARF-1 play a role in CCV formation, which involves the recruitment of AP-1 to the TGN membranes and subsequent clathrin-coat assembly. The exact sequence of how these molecular events unfold has not been resolved. It has, however, been suggested that ARF-1 is responsible for creating the initial high-affinity binding sites for AP-1 on the TGN membrane and that the MPRs regulate ARF-GTP hydrolysis (Le Borgne *et al.*, 1993; Le Borgne *et al.*, 1996; Le Borgne and Hoflack, 1997; Zhu *et al.*, 1998; Zhu *et al.*, 1999).

Two determinants in the cytoplamic tail of the MPRs are implicated in high-affinity binding of AP-1 to TGN membranes: the casein kinase II phosphorylation site and a sequence that includes the reversibly palmitoylated cys[34], which is critical in preventing lysosomal delivery of the receptor (discussed in 3.2.4.3). There is evidence that the phosphorylation of the casein kinase II site is not a prerequisite for AP-1 binding, but this is still controversial. The importance of the palmitoylation in AP-1-binding is not known (Honing *et al.*, 1997; Le Borgne *et al.*, 1993; Mauxion *et al.*, 1996). Glutathione-S-transferase (GST) pull-down assays have shown that AP-1 does not bind the acidic-cluster-dileucine signal in the cytoplasmic tail of the MPR (Puertollano *et al.*, 2001).

Immunostaining for the γ-adaptin subunit of AP-1 in µ1A-adaptin-deficient mouse fibroblasts has shown no labelling on TGN membranes (Meyer *et al.*, 2000). The µ1A subunit thus probably mediates binding of AP-1 to TGN membranes. Using quantitative immuno-electron microscopy in secretory cells, it has been shown that MPRs and AP-1 colocalise on clathrin-coated buds of immature secretory granules arising from the TGN. During maturation of the secretory granules the MPRs and AP-1 are sorted out of the granules (Klumperman *et al.*,

1998). This is evidence for AP-1 being involved in sorting the MPRs away from the secretory pathway, and probably toward the endocytic pathway.

Evidence that AP-1 may also be involved in sorting at the endosomes has come to light. In μ1A-deficient mouse fibroblasts, the steady state of both MPRs is shifted from the TGN to the endosomes. Recycling of the MPR46 to the TGN is impaired (Meyer *et al.*, 2000). *In vitro* transport from μ1A-deficient endosomal membranes to the TGN is also severely hampered (Medigeshi and Schu, 2003).

In HeLa cells, two-colour time-lapse video microscopy has shown colocalisation of chimera consisting of a cyan fluorescent protein (CFP), the transmembrane domain and the cytoplasmic tail of the CI-MPR (CFP-CI-MPR) and chimera consisting of a yellow fluorescent protein (YFP) and the γ-subunit of AP-1 (YFP-AP-1) at the TGN, TGN-derived tubules and peripheral structures (Waguri *et al.*, 2003). This supports the notion that AP-1 may mediate sorting of the MPR at the TGN and endosomes.

AP-1 binds both phosphofurin acidic cluster sorting protein 1 (PACS-1) (Wan *et al.*, 1998, Crump *et al.*, 2001) and GGA (Doray *et al.*, 2002a). Both proteins are involved in TGN-endosome trafficking. AP-1 has been shown to colocalise with GGAs in clathrin-coated buds at the TGN. It is possible that AP-1 mediates both retrograde and anterograde trafficking between the TGN and endosomes. Interaction with either PACS-1 or GGA could determine the active pathway.

3.2.5.2 Adaptor protein-2

Tyrosine residues in positions 24 and 26 in the cytoplasmic tail of the CI-MPR are critical for the binding of AP-2 at the plasma membrane. It has been suggested that this binding process selects specific receptors for incorporation into CCVs and subsequent internalisation (Glickman *et al.*, 1989; Lobel *et al.*, 1989; Pearse, 1988).

Studies on the binding of determinants in the cytoplasmic tail of the CD-MPR have been inconsistent. Plasmon surface resonance has shown AP-2 binding to the phenylalanine determinant, $F^{13}PHLAF^{18}$, and not the tyr motif (Honing *et al.*, 1997). Yeast two-hybrid system and mutational analyses, on the other hand, have shown binding of the medium subunit of AP-2 (μ2) to the tyr-based signal and not the phenylalanine motif (Storch and Braulke, 2001). Both studies, however, have shown AP-2 binding to a distal sequence rich in acidic amino acids (casein kinase 2 site) and no binding to the di-leu motif (Puertollano *et al.*, 2001).

3.2.5.3 Adaptor protein-3

AP-3 is localised to the TGN and endosomes and its association to the membrane is regulated by ARF-1 (Ooi *et al.*, 1998). Multiple, partially overlapping C-terminal signals, comprising a di-leu motif, tyr motif and clusters of acidic residues in the cytoplasmic tail of the CD-MPR have been shown to be involved in μ3A binding. The cytoplasmic tail of the CI-MPR, however, fails to bind μ3A (Storch and Braulke, 2001). Cytosolic AP-3 inhibits *in vitro* transport from endosomal membranes to the TGN (Medigeshi and Schu, 2003). This and the fact that AP-3 binds PACS-1 (Crump *et al.*, 2001) implicate AP-3 in endosome to TGN transport.

3.2.5.4 Golgi-localising, γ-ear-containing, ARF-binding proteins (GGA's)

This is a monomeric, multidomain family of proteins that facilitates trafficking from the TGN to the endosomes. Three of the four domains are homologous to other proteins according to which the domains have been named. GGAs consist of an amino-terminal VHS (for **V**ps27, **H**rs and **S**TAM homology) domain, a GAT (for **G**GA and **T**OM homology) domain, a non-conserved linker region and a carboxy-terminal GAE (for **γ-a**daptin **e**ar homology) domain (Mullins, 2005). ARF-1 facilitates the association of GGAs to the TGN membrane (Black and Pelham, H. R. B., 2000; Dell'Angelica *et al.*, 2000; Zhdankina *et al.*, 2001) and then regulates the binding of GGAs with MPRs (Hirsch *et al.*, 2003). Yeast two-hybrid systems, GST pull-down assays and plasman resonance spectroscopy have shown that GGAs bind to the CI-MPR and the CD-MPR (Puertollano *et al.*, 2001; Zhu *et al.*, 2001). The acidic cluster di-leu motif in the cytoplasmic tail of MPRs interacts with the N-terminal (VHS) domain of the GGAs. The spacing of the di-leu motif relative to the membrane is important for optimal GGA binding. Specific amino acids in the cytoplasmic tail of the CI-MPR are responsible for the higher affinity-binding of the CI-MPR compared to the CD-MPR (Doray *et al.*, 2002b). GGAs have been colocalised with MPRs at the TGN and peripheral vesicles. Tubulo-vesicular structures were shown to bud from the TGN and move toward the cell periphery using immunofluorescence and time-lapse, confocal microscopy in MDCK cells (Puertollano *et al.*, 2001). This is evidence that GGAs might mediate movement from the TGN to early endosomes.

3.2.6 Targeting pathways

Limited studies have been directed at determining the pathway along which MPRs transport lysosomal hydrolases to lysosomes. Suggestions about its possible route have mostly been based on steady-state observations. Here follows a critical account of the development of these suggestions and interpretations.

3.2.6.1 Direct delivery of lysosomal enzymes by MPRs to lysosomes

In hepatocytes, exocrine pancreatic and epididymal epithelial cells, MPRs have been observed in the *cis*-Golgi cisternae, coated vesicles, endosomes and lysosomes by electron microscopy (Brown and Farquhar, 1984b). Since MPRs are limited to the *cis* side of the Golgi in these cells, Brown *et al.* (1984) have suggested that MPR-enzyme complexes are packaged into CCVs from the *cis*-Golgi cisternae. This does not, however, explain the presence of phosphorylated, sialylated hybrid and complex type oligosaccharides in lysosomal enzymes in lysosomes. These modifications can only occur in the *trans*-Golgi cisternae where the necessary enzymes (for example, terminal glycosyltransferases) are localised. In normal fibroblasts, MPRs have been observed in the Golgi, coated vesicles, lysosomes and endosomes by immunocytochemistry. In mucolipidosis II (I-cell) disease fibroblasts, in which the lysosomal enzymes lack man-6-P, the MPRs accumulate in one or two Golgi cisternae (has been assumed to be the putative *cis*-Golgi sorting site) and coated vesicles concentrated on the side of the presumed *cis*-Golgi sorting site. These vesicles were initially thought of as primary lysosomes via which MPRs delivered lysosomal enzymes directly to secondary lysosomes (Brown and Farquhar, 1984a). However, treatment of cultured clone 9 hepatocytes with NH_4Cl or chloroquine resulted in depletion of CI-MPRs from the Golgi and accumulation in dilated vacuoles which were endosomes on the basis of the presence of endocytic tracers and absence of lgp120 (Brown *et al.*, 1984; Brown *et al.*, 1986).

3.2.6.2 Indirect delivery of lysosomal enzymes by MPRs to lysosomes

It is possible for MPR-enzyme complexes to be delivered into any one of the organelles along the endocytic pathway. The enzymes would dissociate from the receptors because of the acidic environment of endosomes and be delivered to lysosomes via the endocytic process, while the receptors would recycle to the TGN.

Studies that involved the inhibition of intra-organellar acidification have suggested that MPR-enzyme complexes are transported to a pre-lysosomal acidified organelle. A decrease in the uptake of lysosomal enzymes by MPRs has been observed in CHO mutants defective in ATP-dependent acidification of endosomes (Merion *et al.*, 1983; Robbins et al., 1983; Robbins *et al.*, 1984). This is probably due to the inhibition of MPR-enzyme dissociation and a resultant depletion of unoccupied receptors. Since the acidification of lysosomes is not defective in these mutants, these observations have implied that MPR-enzyme complexes are delivered to an acidic pre-lysosomal endosome. This view has been supported by observations from immuno-cytochemical and biochemical experiments that have indicated that MPRs are generally either present at very low levels or not detected at all in lysosomes (see section 3.2.2). Palmitoylation of cys^{34} in the cytoplasmic tail of the CD-MPR has been shown to prevent lysosomal delivery of the receptor (Schweizer *et al.*, 1996). Localisation of the relevant palmitoyltransferase in the plasma membrane and endosomes supports the view that CD-MPRs transport enzymes indirectly to lysosomes (Stockli and Rohrer, 2004).

MPRs could transport lysosomal enzymes into the endocytic pathway via the secretory route, to the plasma membrane from where the MPR-enzyme complexes would then be endocytosed. Alternately, the enzymes are transported intracellularly via early endosomes or late endosomes from where they would reach the cell surface by recycling.

3.2.6.2.1 Delivery via the secretory route, plasma membrane and endocytosis

MPRs and lysosomal enzymes occur in coated pits of the plasma membrane and colocalise with albumin in Golgi secretory vesicles, as observed by immuno-gold double-labelling. Treatment of cells with lysosomotropic agents resulted in accumulation of MPRs in the TGR and coated buds. Since these buds also contained albumin, a marker of the secretory pathway, the data have been interpreted as suggesting that the MPR-lysosomal enzyme complexes are transported in coated vesicles along the secretory route to the cell surface and endocytosed for delivery of lysosomal enzymes to lysosomes (Geuze *et al.*, 1984; Geuze *et al.*, 1985).

Secreted lysosomal enzymes are often interpreted as a measure of the indirect pathway via the secretory route to the plasma membrane. Secreted enzymes could reach the cell surface via secretory vesicles in an unbound form or they could be bound to MPRs and then be released into the extracellular medium by dissociation from the receptors. In non-transfected Baby Hamster Kidney (BHK) and mouse L cells, antibodies to the binding site of the CD-MPR reduce secretion of lysosomal enzymes. Endogenous CD-MPRs therefore contribute somewhat to basal secretion (Chao *et al.*, 1990). Since basal levels of secreted enzymes are low in cells expressing both MPRs, it has been interpreted to imply that the indirect pathway via the secretory route is only a minor pathway. This is supported by the fact that when cells were incubated in media containing man-6-P or any other compounds that interfere with MPR-dependent uptake of lysosomal enzymes, lysosomal enzymes were not depleted from the cells and little, if any, extracellular accumulation occured (Hasilik and Neufeld, 1980b; Kasper *et al.*, 1996; Vladutiu and Rattazzi, 1978; von Figura and Weber, 1978). However, if binding between enzyme and receptor is avid, very little, if any, enzyme would be released into the extracellular medium. Low levels of secreted enzyme therefore do not necessarily exclude the possibility for transport via the cell surface to be a major pathway.

The CD-MPR has been shown to mediate both secretion and transport to lysosomes of lysosomal enzymes. In BHK and mouse L cells that overexpressed CD-MPRs, secretion of enzymes was induced. Incubation of these cells with antibodies against CD-MPRs reduced their secretion (Chao *et al.*, 1990). In mouse embryonic fibroblasts (MEFs) deficient in both MPRs, overexpression of CD-MPRs has, however, been shown to reduce secretion and mediate sorting of lysosomal enzymes to lysosomes (Kasper *et al.*, 1996). The addition of antibodies to the medium of Morris hepatoma 7777 cells, that only expressed CD-MPRs, increased secretion of newly-synthesised lysosomal enzymes (Stein *et al.*, 1987b). The ability of the CD-MPR to mediate both secretion and transport of enzymes to lysosomes is best explained by the fact that CD-MPR-enzyme complexes pass through a site from which ligands can access the medium *en route* to lysosomes. The plasma membrane and early endosomes have been proposed as candidates for this site (Chao *et al.*, 1990). CD-MPRs can internalise antibodies but do not endocytose exogenous lysosomal enzymes (Stein *et al.*, 1987b). These observations suggest that CD-MPRs do not bind lysosomal enzymes on the cell surface where the pH is 7.4 (see section 3.2.3.2). It is therefore possible that as CD-MPR-enzyme complexes move through the plasma membrane, the enzymes dissociate from the receptors. Since the plasma membrane is in rapid equilibrium with early endosomes, it is possible for the CD-MPR-enzyme complexes to evade this dissociation process on the cell surface and thus be internalised. Alternately, CD-MPR-enzyme complexes could be delivered to early endosomes where dissociation might not take place to the same extent as on the cell surface. Secretion or delivery to lysosomes of enzymes will therefore depend on the affinity of the ligands for the receptors.

3.2.6.2.2 Intracellular delivery via endosomes

Several observations have indicated that MPR-enzyme complexes leave the TGN in CCVs which deliver their cargo to the endocytic pathway without reaching the plasma membrane (Le Borgne and Hoflack, 1998). MPRs and AP-1 are sorted out of maturing secretory granules (Klumperman *et al.*, 1998) probably toward the endocytic pathway. The identification of CURL, where enzymes occur in the lumina of smooth vesicles while the MPRs are present on the tubules (Geuze *et al.*, 1984; Geuze *et al.*, 1985), has suggested an endosomal site for the delivery and dissociation of MPR-enzyme complexes. Also, immature lysosomal enzymes, such as pro-cathepsin D, were detected in endosomes, labelled with early or late endocytic tracers (Rijnboutt, 1992), and in CI-MPR positive membranes (von Figura and Hille-Rehfeld, 1994). Further evidence for delivery to endosomes came from treatment of cultured clone 9 hepatocytes with lysosomotropic agents (NH_4Cl or chloroquine). The CI-MPR was depleted from the Golgi and accumulated in dilated vacuoles which were endosomes, based on the presence of endocytic tracers and absence of lgp120 (Brown *et al.*, 1986).

Delivery via early endosomes

The secretion of lysosomal enzymes has often been interpreted in the literature to be as a result of indirect delivery via the secretory route to the plasma membrane (Chao *et al.*, 1990; Kasper *et al.*, 1996). However, this could also be an indication of MPR-enzyme complexes delivered to early endosomes. The early endosomes are in dynamic equilibrium with the cell surface. Any dissociation of enzymes from receptors in early endosomes could thus result in secretion.

Using quantitative immunocytochemistry, four categories of vacuoles have been identified in rat hepatoma cells: $MPR^+/lgp120^-$, $MPR^+/lgp120^+$, $MPR^-/lgp120^+$ and $MPR^-/lgp120^-$, where '+' and '–' indicate the presence and absence of the specific protein, respectively. The kinetics of

appearance of endocytic tracers (HRP) in these vacuoles have been determined indirectly through the removal of MPR and lgp120 (detected via western blotting) from cell homogenates, after these were subjected to HRP–DAB cross-linking. Endocytic tracers appeared in $MPR^{+}/lgp120^{-}$ vacuoles almost immediately after endocytosis. Only after much longer incubation periods did they appear in $lgp120^{+}$ vacuoles (Geuze *et al.*, 1988). $MPR^{+}/lgp120^{-}$ vacuoles could thus most likely be early endosomes into which MPR-enzyme complexes are delivered. $MPR^{+}/lgp120^{+}$ vacuoles could most likely be late endosomes where MPRs are sorted from lgp120 and recycled to the TGN.

Further evidence for the presence of the CI-MPR, as well as lysosomal enzymes, in early endosomes came from determining their concentrations in early and late endosomes, using immunoblotting and/or enzymatic assays in rat hepatocytes. The concentrations of the CI-MPR as well as those of five lysosomal acid hydrolases were determined to be similar in early and late endosomes separated on a discontinuous sucrose gradient (Runquist and Havel, 1991). The CI-MPR was enriched in membranes corresponding to the receptor recycling compartment whereas the acid hydrolases were reduced. In addition to mature cathepsin D, procathepsin D was also detected in the endosome fractions, as if to suggest that processing of enzymes occurs in endosomes.

The above observations reflect the steady-state distribution of the MPRs and lysosomal enzymes and thus only provide circumstantial evidence for possible delivery via early endosomes. Some kinetic information has become available with the work of Ludwig *et al.* (1991). Using pulse-labelling, internalisation of antibody against cathepsin D (5 min) at the end of every chase period and subsequent immunoprecipitation in the presence of excess unlabelled cathepsin D, newly-synthesised cathepsin D has been shown to be a transient component of early endosomes in NRK cells. The same amount of enzyme was observed in early endosomes

in the presence of man-6-P in the medium. Man-6-P in the medium prevents possible uptake of secreted enzymes. This suggests intracellular delivery to early endosomes, either directly from the TGN or via recycling from late endosomes. The latter has been thought to be unlikely because no evidence had existed for recycling from late endosomes. Due to the inability to immunoprecipitate cathepsin D quantitatively, the authors have acknowledged that they were unable to determine whether the early endosome is a major delivery site or whether what they have observed is missorting of the enzymes destined to late endosomes (Ludwig *et al.*, 1991).

Shifts in the steady-state distribution of the CI-MPR and an immature form of cathepsin D toward early endosomes have also suggested delivery via early endosomes. Transport from early to late endosomes was blocked in BHK cells that inducibly expressed dominant-negative mutant forms of rab7 GTPase. Using pulse-labelling, gradient fractionation, HRP–DAB cross-linking and immunoprecipitation, the CI-MPR and an immature form of cathepsin D were shown to accumulate in early endosomes. The increase in the early endosomal pool of hydrolases was not due to secreted hydrolases because the experiments were performed in the presence of man-6-P in the media. There was thus a delay in the processing of cathepsin D (Hoflack, 1998). These observations are in favour of newly-synthesised cathepsin D and MPR delivery via early endosomes.

Umeda *et al.* (2003) have shown that in normal and Niemann-Pick Type C (NPC) fibroblasts the CI-MPR is preferentially localised to the TGN, positive for AP-1 and syntaxin 6, thus indicating efficient recycling of the receptor from the endosomes to the TGN. This is in contrast to what has previously been observed by Kobayashi *et al.* (1999), according to whom the CI-MPR redistribute to late endosomes, positive for CD 63, in NPC fibroblasts. In NPC fibroblasts cholesterol accumulates in late endosomes and late endocytic trafficking is impaired. The fact that the CI-MPR does not accumulate in late endosomes and receptor

recycling is not impaired in NPC fibroblasts (Umeda *et al.*, 2003) imply that the late endosome is not the site from where recycling occurs. When normal and NPC fibroblasts were treated with chloroquine, an inhibitor of membrane flow from early endosomes, the CI-MPR accumulated in early recycling endosomes, positive for early endosomal antigen 1 (EEA1) and transferrin. Since the same was observed for TGN38 (a protein that normally recycles between the TGN and the cell surface via early endosomes), the authors have interpreted these observations to imply that the CI-MPR is delivered to early endosomes from the TGN and recycled from early endosomes to the TGN (Umeda *et al.*, 2003).

In HeLa cells, time-lapse video microscopy studies have shown movement and fusion of TGN-derived tubules containing green fluorescent protein (GFP)–CI-MPR (fluorescent chimera) to and with the peripheral tubular network which is in dynamic equilibrium with early endosomes (Waguri *et al.*, 2003), thus supporting delivery to early endosomes.

Delivery via late endosomes

An 'acidic reticular-vesicular structure', where the bulk of the MPR is localised, has been identified in normal rat kidney cells (Griffiths *et al.*, 1988). This structure is positive for lysosomal enzymes and the lysosomal membrane protein, lgp120. It can be loaded with endocytic markers at 37ºC, but not at 20ºC. It is thus a late endocytic structure, but not a lysosome which is generally devoid of MPRs. Griffiths *et al.* (1988) have proposed that MPR-enzyme complexes are delivered into this MPR/LGP-enriched late endosome where lysosomal enzymes dissociate from MPRs and, together with LGPs, are packaged for delivery to lysosomes, while MPRs are recycled to the TGN.

Work by (Kasper *et al.*, 1996) has been interpreted to imply that CI-MPRs transport newly-synthesised lysosomal enzymes along an intracellular route via late endosomes, and that

lysosomal enzymes transported via the cell surface are missorted enzymes that have been recaptured by CI-MPRs. In MEFs deficient in both MPRs, overexpression of CI-MPRs completely restores lysosomal enzyme sorting. However, 25% of lysosomal enzymes are transported via a man-6-P–sensitive pathway. Since lysosomal enzyme transport is insensitive to man-6-P in the medium in control MEFs that express both receptors or overexpress the CI-MPR in addition to expressing the CD-MPR, the authors have suggested that this fraction of enzymes binds CD-MPRs in the TGN, but not CI-MPRs. In the absence of CD-MPRs these enzymes could be secreted. These missorted enzymes are recaptured probably because they can bind CI-MPR on the cell surface. The authors have indirectly suggested that the remaining 75% lysosomal enzymes are transported via an intracellular man-6-P–insensitive pathway. Since early endosomes are in dynamic equilibrium with the cell surface, it has been considered sensitive to man-6-P in the medium. The man-6-P–insensitive pathway would thus probably be via late endosomes. Another explanation for the above observations is that CI-MPRs transport all enzymes via the man-6-P–sensitive plasma membrane/early endosomal compartment; the 75% of enzymes just bind to CI-MPRs with a very high affinity such that they do not dissociate, whereas the 25% of lysosomal enzymes binds with a lower affinity to CI-MPRs and more tightly to CD-MPRs.

3.2.6.3 Summary

From the above account it is clear that there is a substantial amount of circumstantial evidence to suggest that delivery of MPR-enzyme complexes into the endocytic pathway could occur via early endosomes. However, there is very limited kinetic information available to make any conclusive arguments. Work presented here on the CD-MPR was aimed at providing a control for the kinetic behaviour of a protein that has a different steady-state distribution to LAMP-1.

My approach was designed to allow direct observation of the pathway followed by newly-synthesised endogenous CD-MPR in mouse $P388D_1$ macrophages, labelled for a very short period (5 min) at a very high specific activity of ^{35}S-methionine. The kinetics of ^{35}S-labelled-CD-MPR entry into early endosomes or lysosomes were measured. As a control for total endocytic CD-MPR along the time course, the kinetics of ^{35}S-CD-MPR entry into the endocytic pathway were also measured. Results suggested that the bulk of newly-synthesised CD-MPR was delivered into the endocytic pathway via lysosomes from where they were transported to late endosomes for recycling to the TGN. Due to relatively low CD-MPR expression levels, however, results were not sufficiently reproducible to make any definite conclusions.

3.3 APPROACH OF THIS STUDY

To determine whether LAMP-1 or CD-MPR are delivered directly to lysosomes or via early endosomes, the kinetics by which newly-synthesised ^{35}S-LAMP-1/^{35}S-CD-MPR entered into either early endosomes or lysosomes were compared with the kinetics of entry into the endocytic pathway.

3.3.1 Formation of newly-synthesised ^{35}S-LAMP-1/^{35}S-CD-MPR

Newly-synthesised LAMP1/CD-MPR was metabolically labelled by the incubation of P388D$_1$ cells in medium containing ^{35}S-methionine for 5 min at 37ºC. The pulse was then chased as a function of time in medium with unlabelled methionine.

3.3.2 Capturing ^{35}S-LAMP-1/^{35}S-CD-MPR in the different organelles

The localisation of chased ^{35}S-LAMP-1/S^{35}-CD-MPR in the endocytic pathway, early endosomes or lysosomes was determined by trapping it in the respective organelles. This trapping was attained due to colocalisation with HRP that catalyses the cross-linking of DAB in the presence of hydrogen peroxide (H_2O_2). HRP could be positioned in the respective compartment by endocytic uptake for various times. All proteins in the specific organelle, including the ^{35}S-LAMP-1/^{35}S-CD-MPR were then trapped in the resultant meshwork (Courtoy *et al.*, 1984; Stoorvogel, 1998).

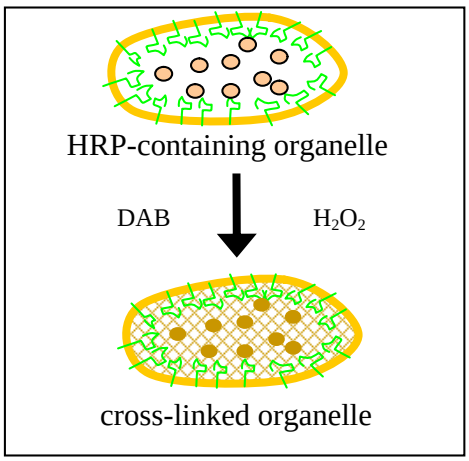

Figure 3.3.1 HRP–DAB cross-linking

3.3.3 The colocalisation of ^{35}S-LAMP-1/^{35}S-CD-MPR with HRP along the endocytic pathway

HRP is a fluid-phase endocytic marker that can be administered to the cells such that it is present along the entire endocytic pathway, early endosomes or lysosomes. To determine the localisation of ^{35}S-LAMP-1/^{35}S-CD-MPR along the **endocytic pathway,** the endocytic pathway was loaded with HRP by incubating the cells in medium that contained HRP before labelling the cells with ^{35}S-methionine. HRP was continually present during the labelling and chase periods. To determine the localisation of ^{35}S-LAMP-1/^{35}S-CD-MPR in **early endosomes,** the early endosomes were loaded with HRP by incubating the cells with HRP during the last 5 min of every chase period. This was based on the finding that early endosomes mature with a half-life of 3 min in P388D$_1$ cells (Thilo *et al.*, 1995). To determine the localisation of ^{35}S-LAMP-1/^{35}S-CD-MPR in **lysosomes,** lysosomes were first loaded with HRP before the pulse-labelling and chase procedures. The HRP internalisation periods that would ensure optimal cross-linking of proteins in the endocytic pathway and lysosomes were optimised as described in Results 4.1.3.2.

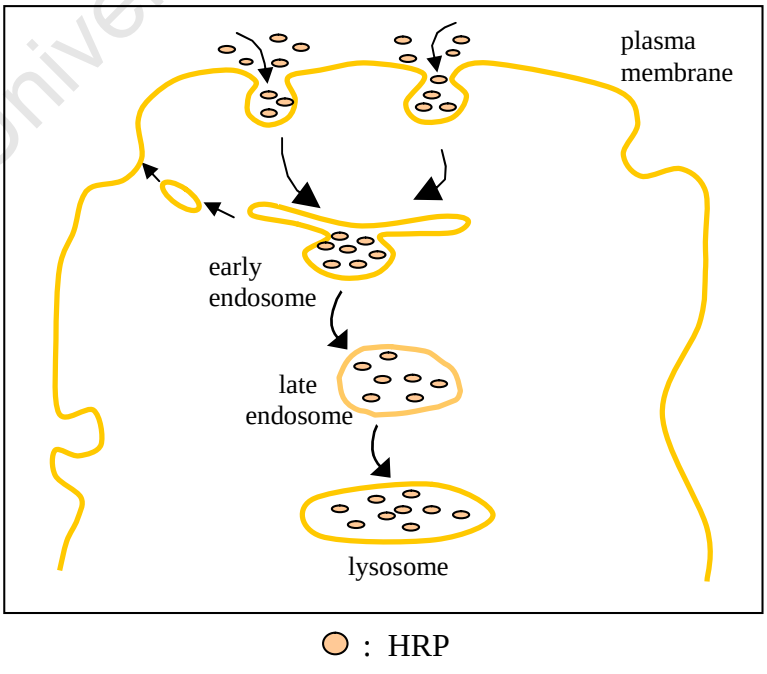

Figure 3.3.2 HRP Internalisation. HRP can be internalised by endocytosis and restricted to specific organelles along the endocytic pathway depending on the period of incubation.

3.3.4 Detection and quantitation of ^{35}S-LAMP-1/^{35}S-CD-MPR

Metabolically labelled cells in which HRP was localised to specific organelles were split into two fractions. One fraction was subjected to HRP–DAB cross-linking and the other served as a control. The cells were lysed and the insoluble and cross-linked material was removed by centrifugation. Antibodies against LAMP-1 or CD-MPR were used to immunoprecipitate LAMP-1/CD-MPR from the detergent-soluble fraction of the lysate. The immunoprecipitant was resolved using sodium dodecyl sulphate-polyacrylamide gel electrophoresis (SDS-PAGE). The gel was dried and exposed using the InstantImager or Optiquant digital analysis program. The position of the visible ^{35}S-LAMP-1/^{35}S-CD-MPR band was determined relative to molecular-weight markers that were marked with ^{14}C. Based on this pre-determined position, the invisible LAMP-1/CD-MPR band was subsequently excised from wet gels relative to silver-stained molecular-weight markers. The gel was solubilised in hydrogen peroxide and subjected to scintillation counting for detection of ^{35}S-LAMP-1/^{35}S-CD-MPR. Since both total and non-cross-linked ^{35}S-LAMP-1/^{35}S-CD-MPR were measured, the fraction of cross-linked ^{35}S-LAMP-1/^{35}S-CD-MPR was calculated using the equation discussed in Results 4.1.4.6.

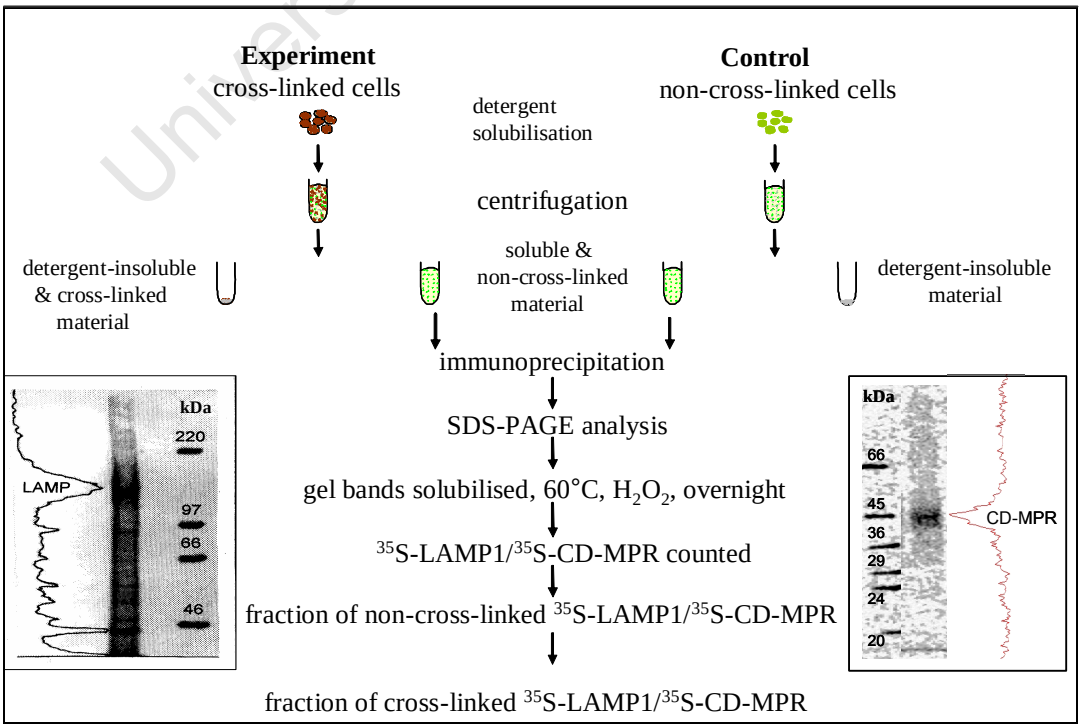

Figure 3.3.3 Sample processing and analyses

3.4 PREDICTIONS

The outcome of such experiments can be predicted by compartmental modelling. New lysosomal membrane protein is synthesised at rate dS/dt [mole/time] and enters the endocytic pathway either via early endosomes or directly into lysosomes, followed by equilibration to steady state as illustrated in the diagram below. Due to rapid equilibration between the plasma membrane and early endosomes, these organelles are considered as a single, well-mixed compartment. A second compartment consists of lysosomes and interacts with the first via late endosomes.

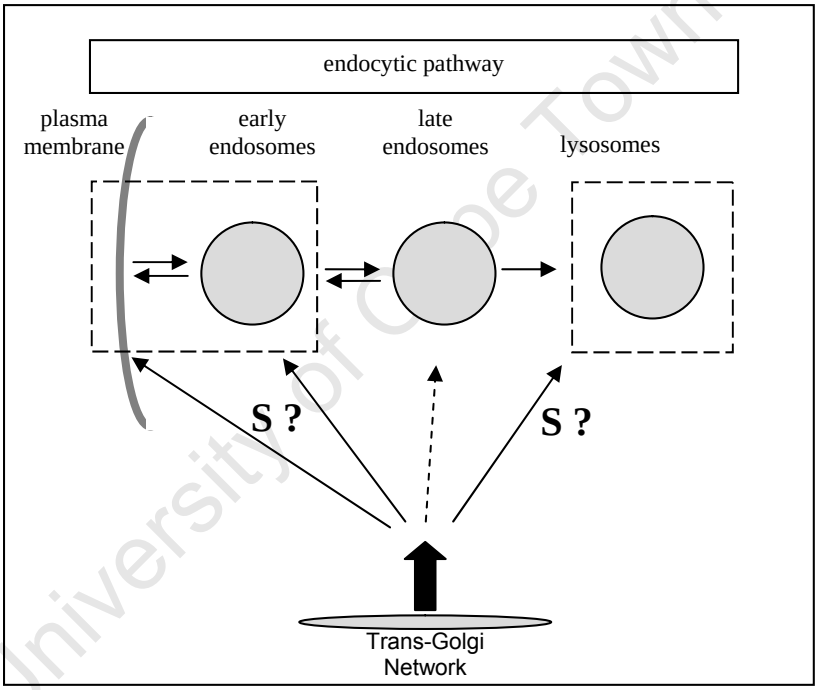

In general, this biological process can be modelled as follows, where S enters the endocytic pathway via one of the compartments, n_1 or n_2.

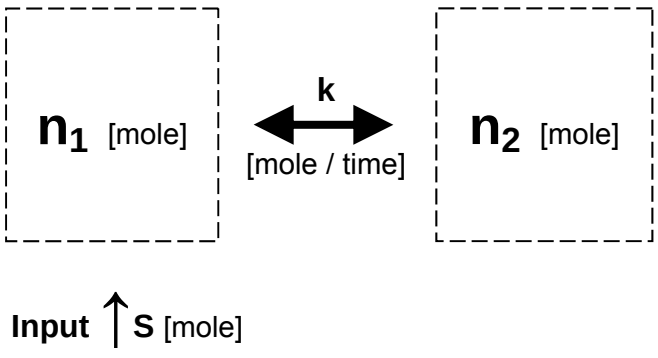

When $(n')_1$ designates the amount of newly-synthesised protein in pool n_1, the differential increase of $(n')_1$ is given by

$$d(n')_1/dt + k*(1/n_1 + 1/n_2)*(n')_1 = dS/dt + k*S/n_2 \quad \ldots\ldots\ldots\ldots\ldots\ldots\ldots\ldots\ldots\ldots \quad [1]$$

where entry of newly-synthesised protein [n'] is via compartment n_1. Interchanging the indexes describes entry via n_2.

Because the bulk of LAMP-1 resides in lysosomes at steady state, the two options for input are not symmetric. As an example, a steady state is assumed where 90% of LAMP-1 is in lysosomes and 10% in early endosomes [$n_1 = 0.1$ and $n_2 = 0.9$]. For simplicity of modelling, it is considered that LAMP-1 enters the endocytic pathway with first-order kinetics, as this allows for an algebraic solution of equation 1. Zero-order input will result in a sigmoidal increase of S and this would require numerical integration of equation 1.

Integration of equation 1 yields the kinetics that will be observed for the two scenarios of entry, with LAMP-1 cross-linked in (1) the entire endocytic pathway, (2) lysosomes or (3) early endosomes.

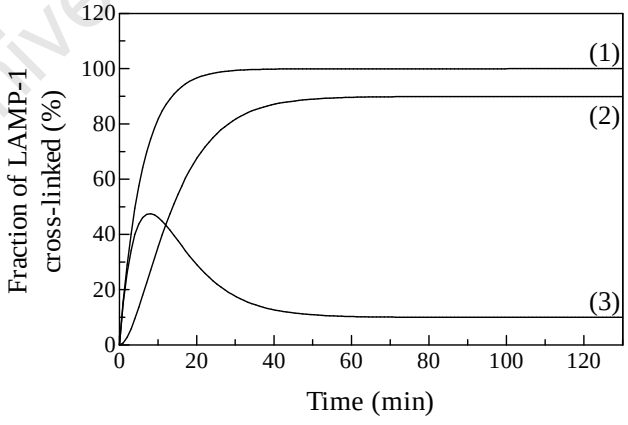

Figure 3.4.1 Scenario 1 with LAMP-1 entering via early endosomes. In this case n_1 = early endosomes and n_2 = lysosomes.

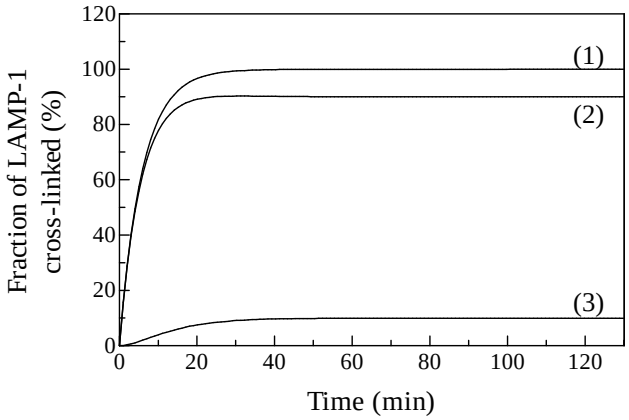

Figure 3.4.2 Scenario 2 with LAMP-1 entering via lysosomes. In this case n_1 = lysosomes and n_2 = early endosomes.

The different levels of steady-state abundance of LAMP-1 in early endosomes and lysosomes result in clearly distinct outcomes for the two different routes of entry. This clear difference in the pattern of the two sets of simulated curves makes it possible to unambiguously decide the pathway followed by LAMP-1.

4 RESULTS

In this section an account is first given of the optimisation of methods required to quantitate soluble LAMP-1/CD-MPR and trap (cross-link) LAMP-1/CD-MPR in specific organelles along the endocytic pathway. (Details of the optimised methods have been summarised in Methods, section 6. Detailed methods as they apply to individual figures only, are indicated under Methods in the figure legends.). I then show how these optimised methods were used to measure the kinetics of ^{35}S-LAMP-1/^{35}S-CD-MPR delivery into the respective endocytic organelles.

4.1 LAMP-1

The movement of newly-synthesised LAMP-1 through the cell was observed by using a short pulse of metabolically labelled LAMP-1. Newly-synthesised, ^{35}S-methionine-labelled LAMP-1 was chased for various periods and trapped by HRP–DAB cross-linking in early endosomes, lysosomes or the endocytic pathway. A rat antibody (ID4B) against mouse-LAMP-1 was used to immunoprecipitate LAMP-1 from solution to quantitate the fraction of ^{35}S-LAMP-1 that became trapped. In order to quantitate the relative amounts of LAMP-1 that remained soluble (in HRP-free compartments), the optimal conditions for quantitative detection of LAMP-1 had to be established.

4.1.1 Purification of anti-LAMP-1 antibodies and evidence for their functional activity

ID4B antibodies were first tested for their functional activity. Rat hybridomas, which secrete ID4B antibodies, were grown in tissue-culture and the antibody-containing tissue-culture medium (ab-TCM) was collected, see Methods 6.3.1. To confirm that anti-LAMP-1 antibodies were secreted into the TCM, the ID4B antibodies were purified from the TCM and tested for functional activity. Antibodies were then initially used in the purified form, but later the TCM was used as a direct source of antibodies. Two methods were tested for the purification of ID4B; first, caprylic-acid precipitation followed by Amicon filtration (figure 4.1.1, panel A) and second, protein-G affinity chromatography (figure 4.1.1, panel B, see Methods 6.4). The first method did not yield an antibody band at the expected 160 kDa position (arrows). Protein-G affinity chromatography yielded a protein that was observed as a 160 kDa band under non-reducing SDS-PAGE conditions and as 50 and 25 kDa bands under reducing SDS-PAGE conditions. This is characteristic of antibodies (Pain, 1963; Williamson and Askonas, 1968), as was observed for the control antibodies against the low-density lipoprotein (LDL) receptor. These observations implied that protein-G affinity chromatography was a much more efficient method for purifying ID4B antibodies than caprylic-acid precipitation followed by Amicon filtration. To determine whether the hybridomas were the only source of antibodies, protein-G beads were incubated in TCM that had not been exposed to hybridomas. A protein in the same position as the ID4B antibody was observed in figure 4.1.2, lane 1 (arrow). This was assumed to represent antibody from foetal-calf serum in the TCM. The presence of secreted ID4B in medium that had been exposed to hybridomas was confirmed by measuring its ability to bind LAMP-1 via Western blotting and immunoprecipitation. To show that the ID4B identified a protein that was localised to the lysosomal membranes, lysosomal membranes were used as an antigen source, figures 4.1.3 and 4.1.4.

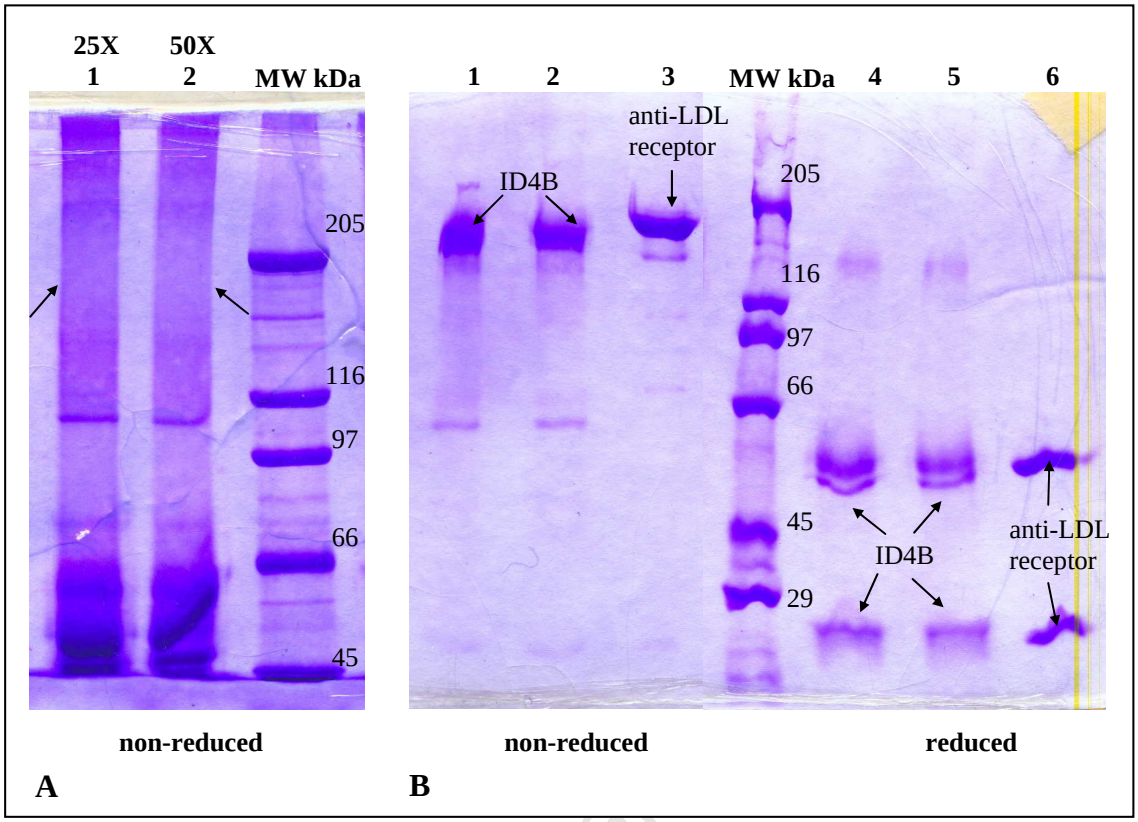

Figure 4.1.1 Purification of ID4B from TCM using, (A) caprylic-acid precipitation and Amicon filtration or, (B) protein-G affinity chromatography. A: ID4B was partially cleared of non-specific proteins by caprylic-acid precipitation as outlined in, "Antibodies - A Laboratory Manual" (Harlow and Lane, 1988). Non-specific proteins were removed by centrifugation and filtration. The partially purified ID4B antibodies were concentrated by Amicon filtration and analysed by SDS-PAGE, as indicated in lanes 1 and 2 in panel A. No band was observed in the expected position of 160 kDa (arrows). **B:** ID4B was purified by protein-G affinity chromatography (Methods 6.4.2). The purified antibody was analysed by SDS-PAGE, as in panel B. 160 kDa bands (arrows, lanes 1 and 2, duplicates) were observed under non-reducing conditions. These bands were converted to 50 and 25 kDa bands under reducing conditions (lanes 4 and 5, duplicates). This is characteristic for antibodies, as can be seen for the control antibody against the low-density lipoprotein (LDL) receptor (arrows, lanes 3 and 6). These observations indicated that protein-G affinity chromatography is a much more efficient method for purifying ID4B than caprylic-acid precipitation and Amicon filtration. **Method:** Caprylic-acid precipitation and Amicon filtration: Two volumes of 60 mM Na-acetate (pH 4) were added to one volume of ab-TCM while continuously stirring the mixture. If necessary, the pH was adjusted to 4.8. Caprylic-acid (0.4 ml per 10 ml of original volume of ab-TCM) was added drop-wise. The mixture was stirred for 30 min at room temperature. The precipitated non-specific protein was pelleted by centrifugation, thrice at 9 000 g for 10 min, once at 18 000 g for 2 h and once at 18 000 g for 1 h, and discarded. Since not all non-specific, precipitated protein could be removed by centrifugation, the supernatant was filtered through a filter paper. The filtrate was then dialysed against water and concentrated 5–, 25– or 50-fold by filtration through an X100 Amicon membrane. The 25– and 50-fold concentrated fractions were analysed by SDS-PAGE.

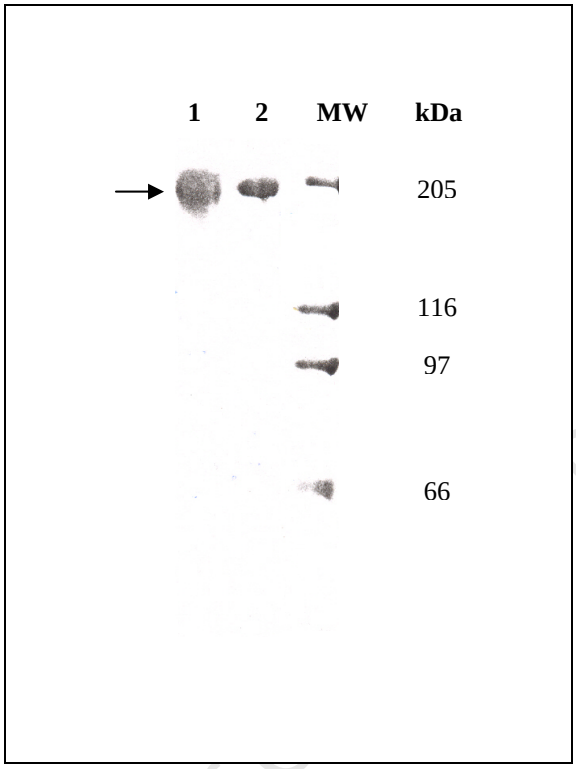

Figure 4.1.2 Binding of antibody from foetal-calf serum to protein-G beads. Protein-G beads were incubated with either neat TCM (lane 1) or TCM collected from a culture of ID4B antibody-secreting hybridomas (lane 2). The bound proteins were eluted as in Methods 6.14 and separated using non-reducing SDS-PAGE. A band (arrow) in the position of non-reduced antibody was observed in both lanes. The result indicated that protein-G beads also bound protein other than ID4B. This protein was assumed to be antibody present in foetal-calf serum.

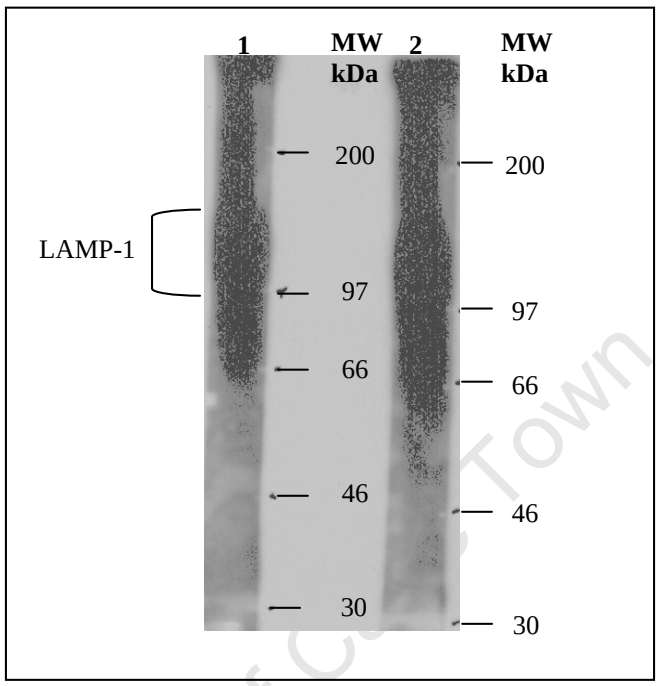

Figure 4.1.3 Western blot of LAMP-1 from lysosomal membrane fractions. Lysosomal membranes, collected as a high-density fraction on a 27% Percoll gradient, were prepared as in Methods 6.5.2, subjected to non-reducing SDS-PAGE and Western blotting. The nitrocellulose membrane was either incubated with commercially purchased partially purified ID4B-containing TCM, (lane 2-control) or with ID4B-containing TCM collected in the laboratory, (lane 1). The ID4B antibodies were detected using peroxidase-linked antibodies and the enhanced-chemiluminescence (ECL) detection system (see Methods, 6.7.1). The broad band (bracket) observed for both control (lane-2) and ID4B (lane-1) is mature LAMP-1.

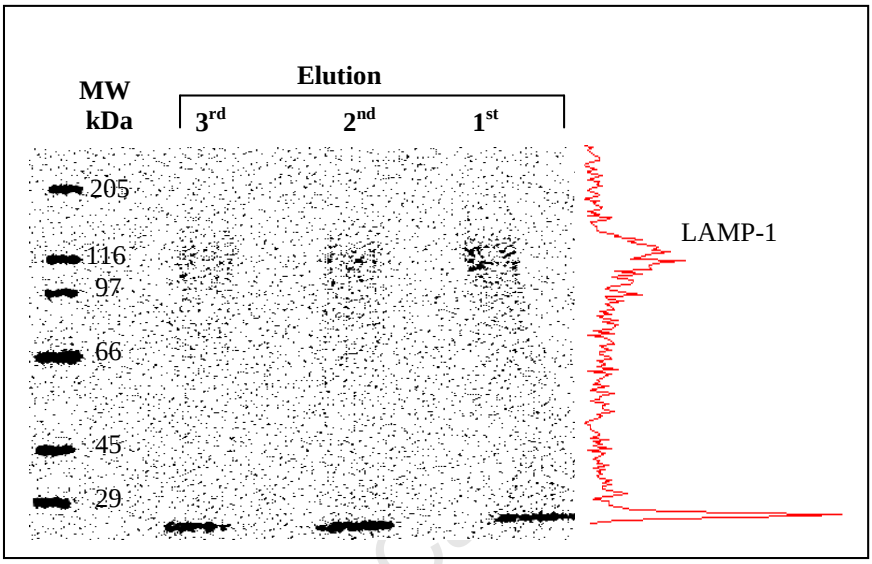

Figure 4.1.4 Immunoprecipitation of LAMP-1 from ^{35}S-labelled lysosomal membrane. LAMP-1 was immunoprecipitated from soluble ^{35}S-labelled lysosomal membranes by incubation with protein-G–ID4B complexed beads and subjected to reducing–SDS-PAGE, followed by autoradiography for 20 h. The lane profile, for the 1st elution round, was obtained through InstantImager scanning software and aligned to the lane by eye. LAMP-1 is indicated by the profile peak. **Method:** To purify ^{35}S-labelled lysosomal membrane, cells ($88 \cdot 10^6$) were incubated at $10 \cdot 10^6$ cells/ml, for 2 h at 37°C in medium, with a methionine concentration of $2 \cdot 10^{-6}$ M at a specific activity of 20 Ci/mmol. The lysosomal membrane was collected as a high-density fraction on a 27% Percoll gradient and was lysed in 100 µl lysis buffer (see Methods: 6.5). An arbitrarily chosen amount of protein-G beads (0.1 ml) was incubated with 60 µg purified ID4B antibody (90 µl antibody at 0.7 µg/µl made up to 200 µl with lysis buffer) for 2 h at 4°C. The beads were washed 6 times with 1.0 ml lysis buffer. The soluble lysosomal membrane was diluted to a final volume of 200 µl with lysis buffer and immunoprecipitated with the protein-G–ID4B complexed beads, overnight at 4°C. The beads were washed as above. The bound LAMP-1 was eluted from the beads through 3 rounds of 60 µl elution buffer (Gly/HCl, pH 2.65) for 5 min at room temperature.

Lysosomal membranes were collected as the high-density fractions on a 27% Percoll gradient as characterised by the lumenal lysosomal enzyme, N-acetyl glucosaminidase (NAGA), that is predominantly localised to lysosomes (De Duve, 1983; Vaes, 1966; Haylett and Thilo, 1986).

A broad band which ranges from 90 kDa to 120 kDa is expected for LAMP-1 due to the heterogeneity in its glycosylation. This can be observed in the Western blot, figure 4.1.3. The smear below 90 kDa and above 120 kDa is probably due to non-specific binding and overexposure. Since the control (lane 2) yielded the same result as the experiment (lane 1) and the functional activity for ID4B observed here was confirmed with immunoprecipitation (figure 4.1.4), it was not deemed necessary to further optimise the above result.

The heterogeneous band observed for the immunoprecipitation (figure 4.1.4) was also in the expected molecular-weight (MW) range of 90 kDa – 120 kDa that is indicative of mature LAMP-1. Because lysosomal membrane was used as an antigen source, the detected glycoprotein must have been of lysosomal origin. The antibodies secreted into the TCM thus appeared specific for LAMP-1.

The experimental design of our kinetic experiments required the quantification of LAMP-1 from soluble cell extracts. The Western blot and immunoprecipitation were thus repeated using soluble cell extract as an antigen source, figures 4.1.5 and 4.1.6.

A similar heterogeneous protein band in the molecular-weight range of 90 kDa to 120 kDa was observed when soluble cell extract was used as an antigen source. These experiments further confirmed the functional activity of the ID4B antibodies secreted into the TCM and also set the stage for further optimisation of conditions for the quantitation of ^{35}S-LAMP-1 in soluble cell extracts.

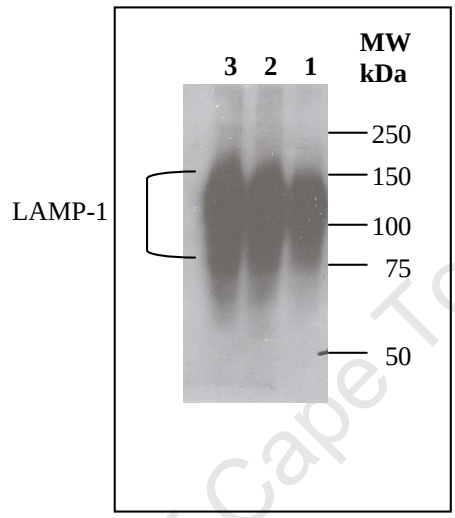

Figure 4.1.5 Western blot of LAMP-1 from detergent-soluble cell extract. Proteins from soluble cell lysate were separated on an 8% polyacrylamide gel, lane 1 − $250{\cdot}10^6$ cells, lane 2 − $500{\cdot}10^6$ cells, lane 3 − $750{\cdot}10^6$ cells, and subjected to Western blotting, see Methods 6.7.2. Blots were incubated with anti-LAMP-1 antibody (22-fold concentrated ID4B-TCM as prepared in Methods 6.4.3) diluted 5000-fold with Tris buffered saline-Tween 20 (TBS-T, see Reagents 7.5), 0.5% fat-free milk powder. The primary antibody was detected with HRP-linked goat anti-rat secondary antibody (cat. no. NA935, Amersham) diluted 2000-fold. The blot was developed with KPL luminoglo. **Method:** Preparation of soluble cell lysate: Cells were lysed at $50{\cdot}10^6$ cells/ml in LAMP-1 lysis buffer (see Reagents 7.5), 0.02% NaN_3. Lysate was incubated on a roller overnight at 4ºC. The following day the insoluble material was removed by centrifugation, once at 8 000 g for 30 min and once at 100 000 g for 30 min at 4ºC.

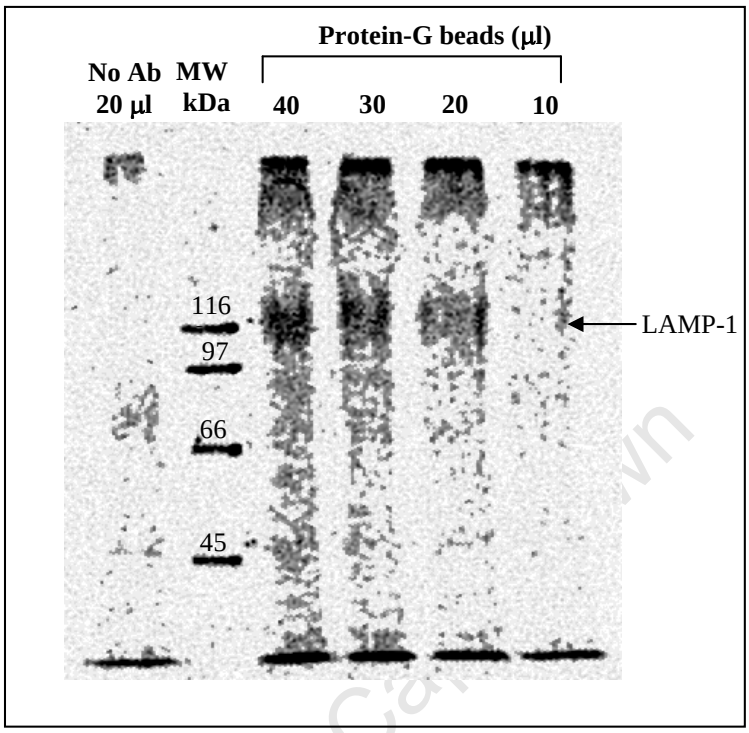

Figure 4.1.6 Immunoprecipitation of LAMP-1 from ^{35}S-labelled, detergent-soluble cell extract. LAMP-1 was immunoprecipitated from soluble cell extract by increasing amounts of protein-G–ID4B complexed beads and processed for the quantitation of LAMP-1, as in figure 4.1.4. In lane 1, 20 µl beads were incubated with soluble cell extract in the absence of antibody as a control. **Method:** To prepare ^{35}S-labelled, soluble cell extract, cells ($100 \cdot 10^6$) were incubated at $10 \cdot 10^6$ cells/ml, for 2 h at 37°C in medium, with a methionine concentration of $2 \cdot 10^{-6}$ M at a specific-activity of 40 Ci/mmol. Cells were washed extensively with Hepes-saline–bovine serum albumen (HeSBSA, see Reagents 7.5), once with 50 ml and 5 times with 10 ml and then lysed at $100 \cdot 10^6$ cells/ml LAMP-1 lysis buffer (Reagents 7.5). The lysate was incubated on ice for 30 min, freeze-thawed thrice and clarified by centrifugation at 100 000 g for 1 h at 4°C in a fix angle rotor, 40 Ti. Protein-G beads were saturated with ID4B antibody (ab) according to the maximal capacity of the beads (11 mg/ml) as per manufacturer's instructions: 200 µl beads were incubated with 2 mg ab in 2.07 ml phosphate-buffered saline (PBS, see Reagents 7.5), pH 7.4 (0.971 mg/ml), for 2 h at 4°C. The beads were washed 7 times with LAMP-1 lysis buffer, resuspended in 600 µl LAMP-1 lysis buffer and aliqouted as indicated above the lanes. These increasing amounts of protein-G–ID4B complexed beads were used to immunoprecipitate LAMP-1 from 100 µl ($10 \cdot 10^6$ cells) samples of soluble cell extract, overnight at 4°C. The beads were washed 6 times with 1.0 ml LAMP-1 lysis buffer and once with 1.0 ml dH_2O. The bound LAMP-1 was eluted from the beads through two rounds of 50 µl non-reducing sample buffer, at 95°C for 5 min. The two 50 µl eluted fractions were then pooled.

4.1.2 Development of methods for quantification of ^{35}S-LAMP-1

Immunoprecipitation served to remove total LAMP-1 (labelled and unlabelled) from cell lysates. Proteins were separated using SDS-PAGE and the newly-synthesised ^{35}S-LAMP-1 was then detected and quantitated. In order to select conditions for optimal binding of the antibody (ab) to antigen (ag) and solid phase, various aspects of the immunoprecipitation assay were considered. This included the type of solid phase, binding buffer, incubation period, incubation temperature and the immunoprecipitation approach (direct versus indirect, explained below). For the efficient detection and quantitation of ^{35}S-LAMP-1, digital analyses using InstantImager software and scintillation counting were compared. In order to ensure the quantitative immunoprecipitation of LAMP-1, conditions for a linear dose-response were determined.

4.1.2.1 Selection of the solid phase

A protein can be removed from solution by an antibody in two ways. In the earlier methods the primary antibody against the target protein was first added to the solution. The antibody-antigen complexes were then precipitated by adding a secondary antibody at a critical concentration, hence the term immunoprecipitation. A method developed later entails removing the antigen-antibody complexes from solution with a solid phase. This method is also referred to as an immunoprecipitation, although technically ag-ab complexes are not precipitated but immobilised. Immobilisation of antigen-antibody (ag-ab) complexes was compared for three solid phase systems: protein-G beads, Dynabeads and cyanogen-bromide(CN-Br)–activated beads. Protein-G beads bind directly to primary rat antibodies. Dynabeads and CN-Br–activated beads can be coupled to secondary anti-rat antibodies via which the beads then bind primary rat antibodies. Dynabeads, coupled to secondary anti-rat-Fc antibodies, were commercially purchased. Secondary anti-rat-Fc antibodies (AAR-02) were covalently linked to CN-Br–activated Sepharose beads in the laboratory (see Methods 6.8). These will henceforth

be termed AAR-02 beads. Protein-G beads were compared with Dynabeads for the binding of two primary antibodies that were secreted into TCM by hybridomas, namely anti-LAMP-1 antibody (ID4B) and anti-LAMP-2 antibody (ABL93), figure 4.1.7. Protein-G beads were compared with AAR-02 beads for the binding of one primary antibody, ABL93, figure 4.1.8. It was observed that protein-G beads bound much more ab than Dynabeads or AAR-02 beads. Dynabeads or AAR-02 beads were, however, more specific. Hence, to compare the binding of LAMP to these antibody-linked beads, both sets of beads were subsequently used to immunoprecipitate ^{35}S-labelled LAMP-2, figures 4.1.9 and 4.1.10. Protein-G beads yielded a more intense LAMP signal than either Dynabeads or AAR-02 beads. Even though Dynabeads were more specific for the binding of antibody, protein-G beads were chosen because these yielded a greater LAMP signal.

4.1.2.2 Selection of buffer, temperature and period of immunoprecipitation

In an immunoprecipitation assay, antibody binding to the beads is pH, temperature and time dependent. A sodium-acetate, pH 5 buffer was recommended for binding antibodies to protein-G beads (Pierce). However, cells were lysed in a Tris/HCl, pH 7.5 buffer (D'Souza and August, 1986) to generate and maintain a physiological environment. The efficiency of ID4B binding to protein-G beads in the two buffer systems was thus compared in table 4.1.1.

To establish the effect of time and temperature on the binding efficiency, ID4B was incubated with protein-G beads under different time and temperature conditions (table 4.1.2.). Although the overnight incubation at 4ºC was observed to be optimal, incubation conditions of 2 h at 4ºC were considered sufficient, and chosen for practical reasons and to eliminate the possibility of extensive protein degradation over a longer time frame.

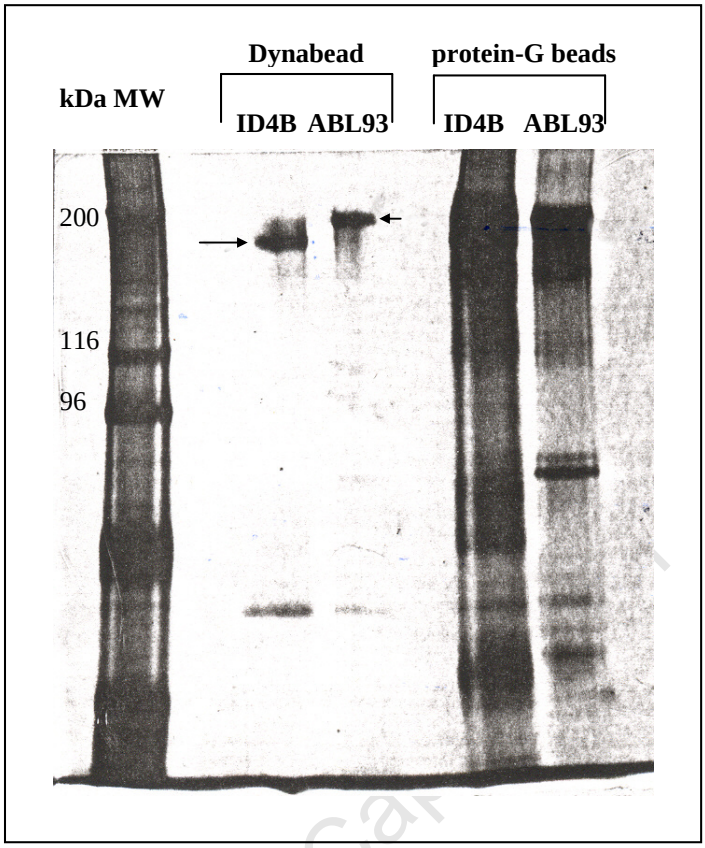

Figure 4.1.7 Comparison of the binding efficiencies of protein-G beads versus Dynabeads. Either ID4B or ABL93 ab-TCM was incubated with equal volumes of protein-G beads or Dynabeads. Bound antibody was eluted from the beads as in Methods 6.14 and separated on a non-reducing gel. The gel was silver-stained (Methods 6.16.2). Arrows indicate antibodies. The protein-G beads bound much more antibody. (In order to visualise the Dynabead bands, the gel had to be overexposed and thus the protein-G bands appear to be overstained.)

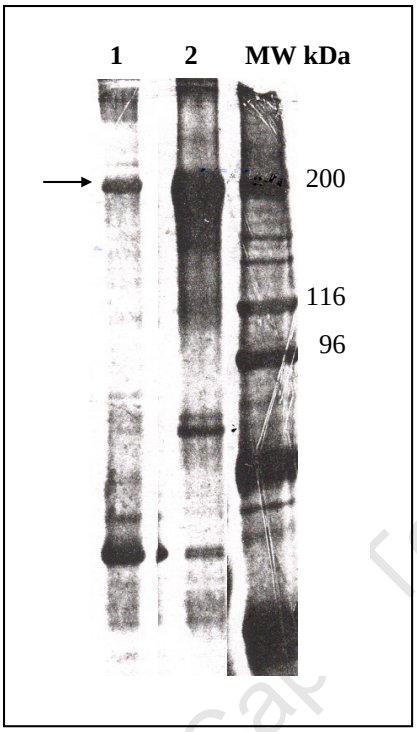

Figure 4.1.8 Comparison of the binding efficiencies of protein-G beads and AAR-02 beads. Anti-rat-Fc antibody (AAR-02) was covalently linked to cyanogen-bromide(CN-Br)–activated Sepharose beads (see Methods 6.8). ABL93-containing TCM was incubated with either AAR-02 beads (lane 1) or protein-G beads (lane 2). The bound protein was eluted (as in figure 4.1.7) from the beads and analysed on a non-reducing gel. The gel was coomassie-stained (Methods 6.16.1). Arrow indicates antibody. Protein-G beads bound much more antibody. (In order to visualise the AAR-02 bands, the gel had to be overexposed and thus the protein-G bands appear to be overstained. Lanes, not necessary for the present illustration, were eliminated by cropping.)

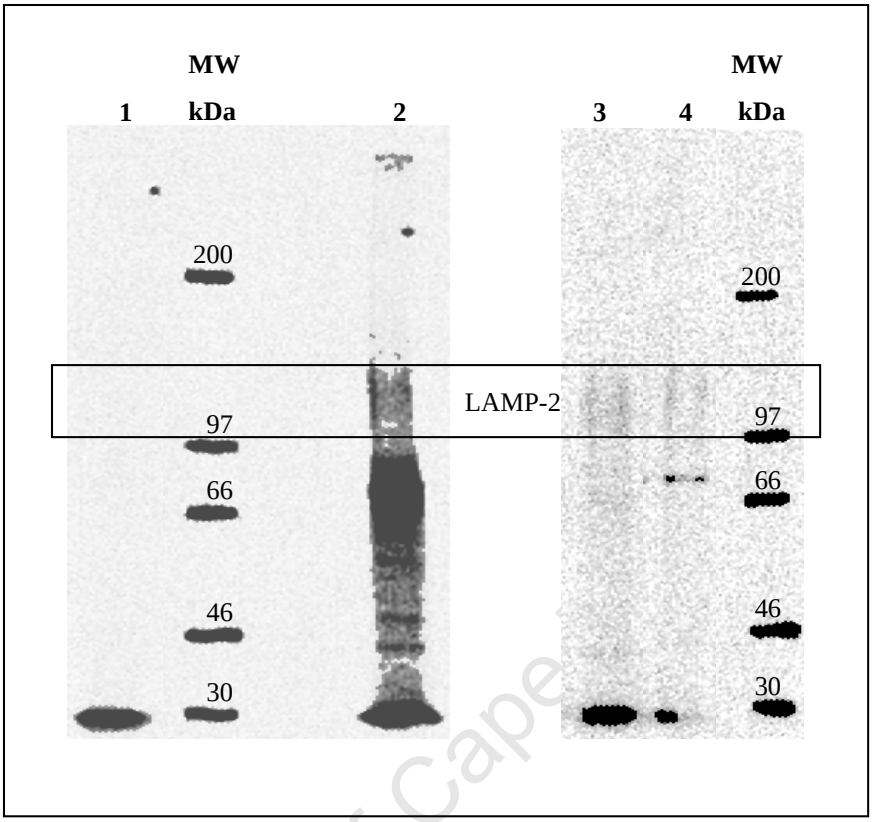

Figure 4.1.9 Comparison of LAMP-2 immunoprecipitation by Dynabeads versus protein-G beads. ^{35}S-labelled LAMP-2 was immunoprecipitated with 50 µl ABL93–Dynabeads (lane 1) versus 20 µl ABL93–protein-G beads (lane 2). Antigen-antibody (ag-ab) complexes were eluted with SDS-reducing sample buffer and separated by SDS-PAGE. No LAMP-2 signal (box) was visible for the Dynabead sample (lane 1). LAMP-2 was faintly visible when 250 µl Dynabeads (lane 4) was compared with 20 µl ABL93–protein-G beads (lane 3) under milder elution conditions (Gly/HCl, pH 2.5). Protein-G beads were thus more effective. (The two panels are excerpts from two different gels.)

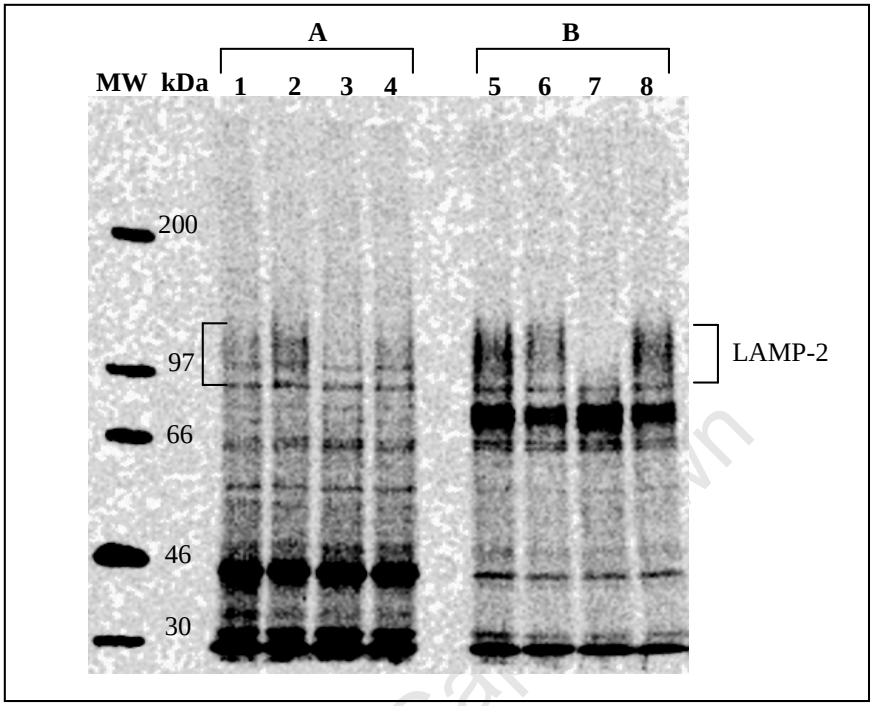

Figure 4.1.10 Comparison of LAMP-2 immunoprecipitation by protein-G beads versus AAR-02 beads. ^{35}S-labelled LAMP-2 was immunoprecipitated with AAR-02 beads (A) or ABL93–protein-G beads (B) through two rounds of immunoprecipitations (lanes 1 & 5: 1st round, lanes 2 & 6: 2nd round). Lanes 3 & 7 served as a control where lysate was incubated with beads without antibody. This precleared lysate was re-incubated with ab-linked beads in lanes 4 & 8. Ag-ab complexes were eluted from the beads with SDS-reducing sample buffer and analysed by SDS-PAGE. The LAMP-2 signal (brackets) obtained using protein-G beads (B) was more intense than the signal obtained using AAR-02 beads (A). Lanes 1 & 2 also indicate that immunoprecipitation with AAR-02 beads was not reproducible, since a more intense signal was expected in lane 1 than in 2. Lane 3 shows more background for the AAR-02 beads when compared to lane 7 for the protein-G beads. These results thus indicated that ABL93–protein-G beads bound LAMP-2 more efficiently.

	Fraction of ID4B eluted from protein-G beads (%)	
Sample	Na-acetate, pH 5	Tris/HCl, pH 7.5
1.	80	100
2.	95	82
3.	85	79
4.	71	89
5.	77	106
Average	82 ± 8	91 ± 10

Table 4.1.1 The effect of buffer conditions on the efficiency of ID4B binding to protein-G beads, in two different binding buffers. Varying amounts (ranging from 23 to 48 µg) of protein-G–affinity-purified ID4B were incubated with protein-G beads (0.1 ml), either in Na-acetate buffer, pH 5 or in Tris/HCl buffer, pH 7.5 for 2 h at room temperature. The beads were washed 6 times with 0.5 ml of the respective immunoprecipitation buffer. The bound antibody was then eluted from the beads through 2 rounds of 300 µl elution buffer (Gly/HCl, pH 2.5) for 5 min at room temperature. The protein concentration was determined by the Lowry protein assay (see Methods 6.9.1). The eluted antibody was expressed as a fraction of the total amount added to the beads. The data indicated that protein-G beads bound ID4B with similar efficiencies in both buffers, with Tris/HCl, pH 7.5 being slightly favoured.

Incubation conditions	Fraction of ID4B eluted from protein-G beads (%)
1 h, room temperature	72 ± 4.5
1 h, 4ºC	79 ± 2.9
2 h, room temperature	80 ± 4.0
overnight, 4ºC	111 ± 6.8

Table 4.1.2 The effect of time and temperature on the efficiency of ID4B binding to protein-G beads. ID4B was incubated with protein-G beads in Tris/HCl, pH 7.5 buffer for 1 h or 2 h at room temperature and 1 h or overnight at 4ºC. The bound antibody was eluted from the beads and the concentration determined by the Lowry protein assay (see Methods 6.9.1). The eluted antibody was expressed as a fraction of the total amount added to the beads. Experiments were done in triplicate. The overnight incubation at 4ºC was observed to be optimal.

4.1.2.3 Selection of the elution buffer.

During the immunoprecipitation incubation the beads bind ab-ag complexes and potentially non-specific proteins as well. The beads were washed extensively in an attempt to remove non-specific proteins that may have been bound. However, tightly-bound non-specific proteins would not be removed by the washing procedure. An elution buffer functions to release the ag-ab complexes back into solution. It can potentially release some of these tightly-bound non-specific proteins.

An elution buffer had to be chosen on the basis that it allowed for maximal LAMP-1 elution, but minimal elution of non-specific protein. The efficiency of two elution buffers, reducing sample buffer versus a low pH buffer, Gly/HCl, pH 2.65, was compared (figure 4.1.11). Although the reducing sample buffer eluted a greater fraction of the total radioactivity that was bound to the beads, the Gly/HCl, pH 2.65 was more specific, in that it eluted less of a non-specific protein that was positioned just below the LAMP-2 band. Since this band could potentially contaminate the LAMP band, the low pH buffer was chosen as the elution buffer.

To determine the number of elution rounds that would remove the maximum amount of LAMP-1–ID4B complexes from the beads, ^{35}S-LAMP-1 was eluted from the beads through three rounds of 60 µl elution buffer as described in figure 4.1.4 and analysed as shown in figure 4.1.12. The equation used in the figure is explained as follows: If f denotes the fraction of LAMP-1 eluted with each elution round and L denotes the total bead load, then the first elution round will elute f·L, leaving (1-f)·L. Every elution round (n) will elute $f \cdot L \cdot (1-f)^{(n-1)}$. It was observed that when 60 µl elution buffer was used to elute ag-ab complexes from 100 µl of beads loaded at 0.6 µg antibody/µl beads, one third of the bead load was eluted with every elution round. This implied that 33% of the total bead load was eluted during the first elution round, 55% after the second round and 70% after the third elution round.

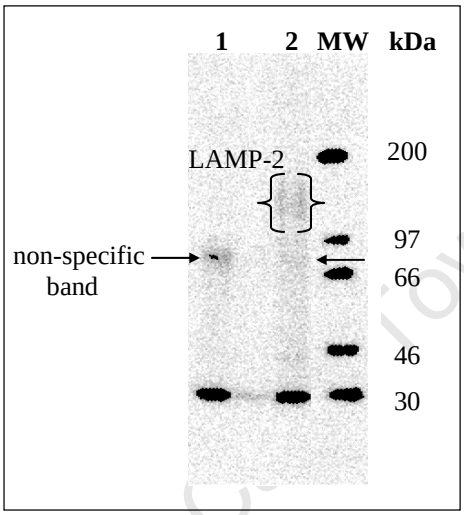

Figure 4.1.11 Comparison of the efficiencies of two elution buffers. Immunoprecipitation was performed in duplicate with ABL-93–protein-G beads and ^{35}S-methionine-labelled LAMP-2–containing lysate. Ag-ab complexes were eluted with SDS-reducing sample buffer (lane 1) or Gly/HCl, pH 2.65 (lane 2). Equal amounts (in dpm) of eluted products were loaded onto the gel. Only a fraction (6%) of the SDS-sample buffer–eluted product was loaded, whereas all Gly/HCl−eluted product was loaded. The Gly/HCl buffer eluted more of the LAMP-2 signal (brackets) relative to a non-specific signal just below the LAMP band (arrows). The sample buffer eluted 17-fold more total label (dpm), but only twice as much of the LAMP-2 signal, determined on a gel not shown here. Therefore, the Gly/HCl buffer was more efficient.

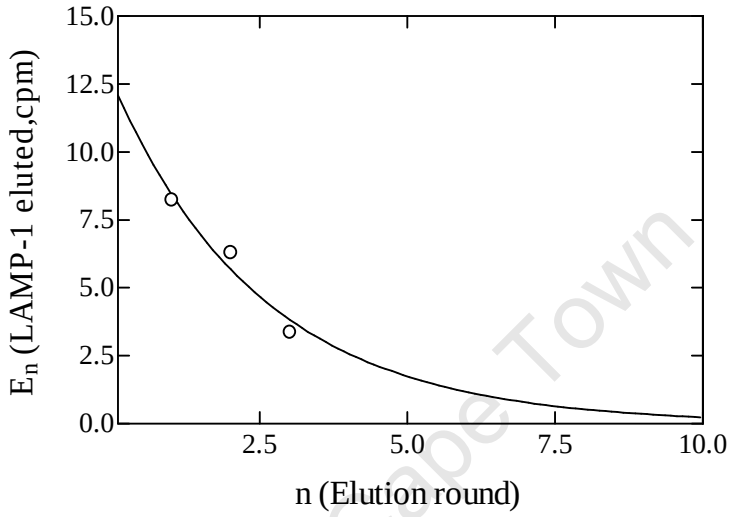

Figure 4.1.12 Determination of the number of elution rounds required to remove the maximum amount of LAMP-1−ID4B complexes from the beads. ^{35}S-LAMP-1 immunoprecipitated and processed in figure 4.1.4, was quantified as the area under the profile peak. The amount of LAMP-1 eluted from the beads decreased with each successive elution round. The indicated curve is described by the equation, $E_n = f \cdot L \cdot (1-f)^{(n-1)}$, where f is the fraction of LAMP-1 eluted with each elution round, L is the total bead load and E_n is the amount of LAMP-1 eluted at round n. The values L = 26 cpm, f = 0.33 were obtained from the best-fitted curve. One third of the bead load was thus eluted with every elution round.

The fraction (f) of ab-ag complexes eluted from the beads could be improved by increasing the ratio of elution-buffer volume to antibody (µg) bound to the beads. However, 100% of the bead load is unlikely to be removed in one elution round. The volume of elution buffer and number of elution rounds were limited by the maximum volume of sample that could be loaded onto a gel lane. The amount of antibody (µg) used, was determined by the linear dose-response characteristics of the immunoprecipitation assay (established below).

4.1.2.4 Selection of the LAMP-1 detection method

The immunoprecipitation products eluted from the beads contained both unlabelled and newly-synthesised ^{35}S-labelled-LAMP-1. To quantitate the newly-synthesised LAMP-1, the ^{35}S-LAMP-1 had to be detected and quantified. The efficiency of detection of ^{35}S-LAMP-1 relative to background was critical in view of very short pulses of metabolic labelling required for optimal kinetic resolution. Autoradiographic detection by the InstantImager system was compared with scintillation counting of solubilised gel pieces, figure 4.1.13. The two detection methods were reproducible as can be seen from the linear relationship between the data obtained from the respective methods. The scintillation counter yielded 270-fold higher counts per min than the InstantImager as determined from the slope of the graph. The excision of LAMP-1 gel bands and scintillation counting was chosen as the method for ^{35}S-LAMP-1 quantification because of its 270-fold higher detection sensitivity that would yield better experimental resolution.

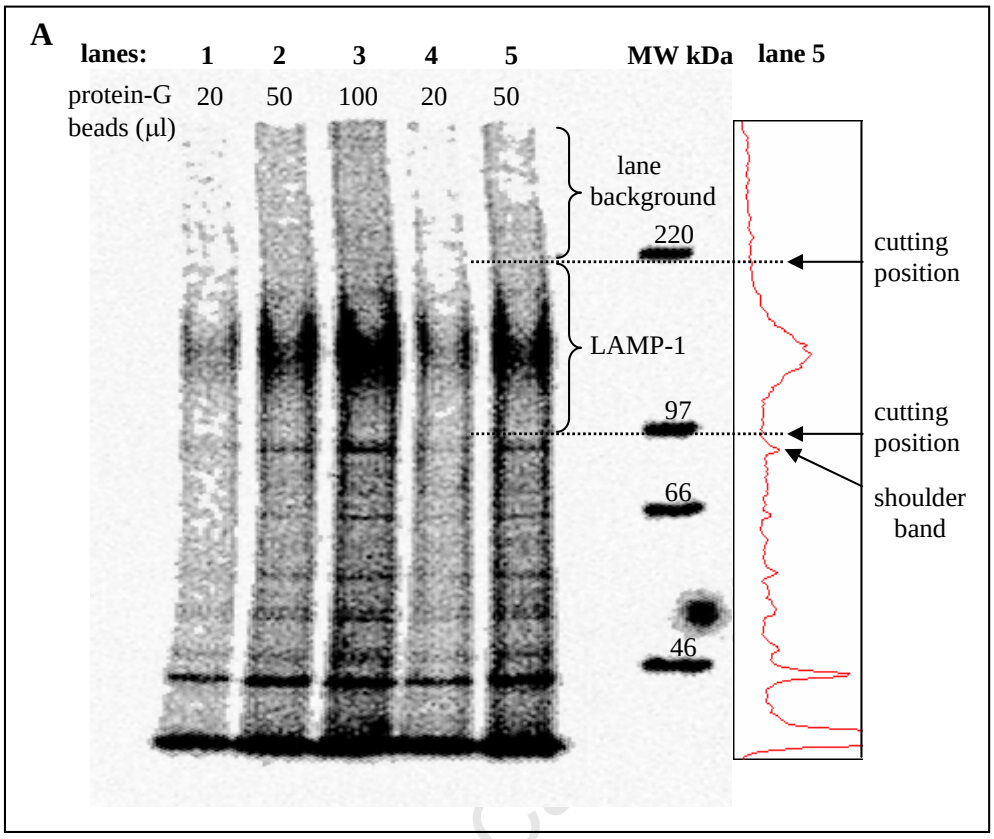

Figure 4.1.13 (see legend on next page)

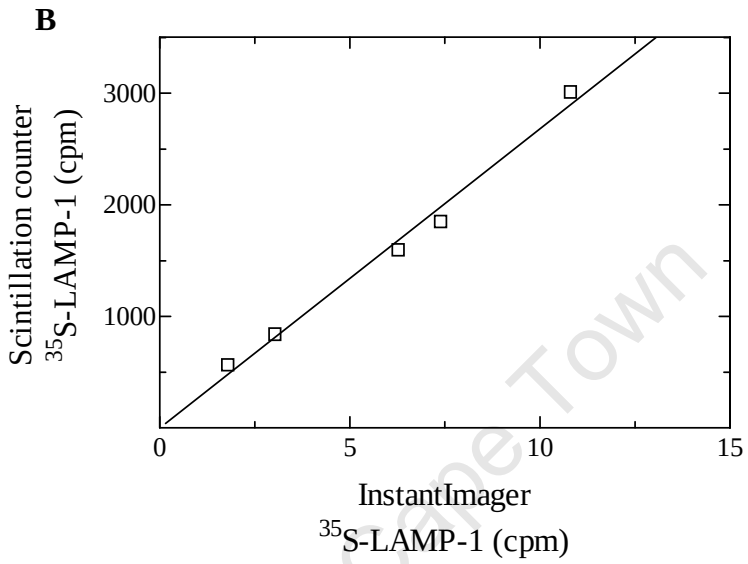

Figure 4.1.13 Quantitation of immunoprecipitated ^{35}S-LAMP-1 using Instant Imager scanning software versus liquid scintillation counting. A: ^{35}S-LAMP-1 was immunoprecipitated from soluble cell extract with ID4B antibodies and protein-G beads, eluted from the beads and subjected to SDS-PAGE, followed by autoradiography. The immunoprecipitated ^{35}S-LAMP-1 was quantified by digital analysis using InstantImager software. The lane profile for lane 5, also obtained through InstantImager scanning software, was aligned to the lane by eye. **B:** The LAMP-1 band was subsequently excised relative to molecular-weight markers, as indicated, dissolved in 2 ml 30% H_2O_2 overnight at 60°C and then quantified by scintillation counting in a scintillation counter. The counts obtained from the scintillation counter were then plotted against the counts obtained from the InstantImager. Results reflected a linear relationship with a slope of 268.1±7.8. **Method:** P388D$_1$ cells were metabolically labelled for 2 h, at 37°C with ^{35}S-methionine at 10^{-7} M (specific-activity = 1175 Ci/mmol). Soluble cell extract ($50 \cdot 10^6$ cells/ml) was prepared as in figure 4.1.6. Soluble ^{35}S-LAMP-1 was immunoprecipitated from 200 µl soluble cell extract ($10 \cdot 10^{-6}$ cells) by incubation with 10 µl ID4B-containing, 50-fold concentrated TCM (Methods 6.4.3) overnight at 4°C, followed by incubation with protein-G beads at the indicated volumes for 2 h at 4°C (lanes 1 − 3); Alternatively, the antibody was first bound to protein-G beads and then the detergent-soluble lysate was added to the antibody-bound beads (lanes 4 & 5). The bound LAMP-1 was eluted from the beads through 2 rounds (65 µl and then 55 µl) of 0.1 M Gly/HCl, pH 2.65 for 5 min at room temperature and subjected to SDS-PAGE, followed by autoradiography for 64 h.

4.1.2.5 The direct versus the indirect approach to immunoprecipitation

The immunoprecipitation could be performed in one of two ways. In the direct approach antibody was added directly to the antigen. The ag-ab mixture was then added to the beads, see lanes 1 − 3, figure 4.1.13 A. In the indirect approach antibody was first bound to the beads. The ab-beads were then incubated with the antigen, see lanes 4 and 5, figure 4.1.13 A. Using the scintillation counter results, the two methods did not yield significantly different results. Since the direct approach required less hands-on manipulation and would thus probably result in less experimental variation, it was henceforth selected as the method of choice.

4.1.2.6 Maximisation of specific signal relative to noise and non-specific proteins

The position of the LAMP-1 band relative to molecular-weight markers was determined using lane profiles obtained from two gels through InstantImager software. The average of these positions, dotted lines indicated in figure 4.1.13 A, was used to excise the LAMP-1 band relative to molecular-weight markers from silver-stained wet gels. The LAMP-1 profile peak was shouldered by a protein band just below the 97 kDa molecular-weight marker, see figure 4.1.13 A. This could have been the LAMP-1 precursor which is approximately 90 kDa. However, it was also observed in the absence of antibody. This implied that a non-specific protein that could potentially contaminate the LAMP-1 band was also located at this position. The 7% SDS-polyacrylamide gel was already at the recommended concentration for optimal resolution of proteins in the 100 kDa range. In an attempt to further improve the separation of the proteins, gels were run for 40 min longer after the gel-front had run off. This was the maximum amount of extra run-time that could be allowed for, without risking the loss of the LAMP-1 band. During the electrophoretic separation of the proteins, labelled particles in the protein mixture could have adhered to the gel non-specifically. This would have contributed to lane background. To quantitate the counts due to specific signal, the counts due to lane background had to be eliminated. The position of a region allocated as lane background,

chosen on the basis that the radioactivity in this region was consistently lower than the rest of the lane, was determined relative to molecular-weight markers, as indicated in figure 4.1.13 A. A non-specific band was sometimes observed in the 205 kDa position as in figure 4.1.14. In the presence of this non-specific signal, the area that could be allocated to lane background would have been too small relative to the area of the specific LAMP-1 signal. The optimal reduction of this non-specific signal to lane background levels was thus essential. Toward this end a centrifugation step was introduced after the ag-ab incubation, figure 4.1.14. Using InstantImager software analyses, it was determined that the centrifugation step removed 86% of the non-specific signal while the LAMP-1 signal was not significantly affected. It was thus decided to introduce this centrifugation step in all future immunoprecipitations.

4.1.2.7 Quantitative immunoprecipitation of LAMP-1

In an attempt to establish conditions for a linear dose-response of LAMP-1, I first set out to determine the *optimal ID4B/protein-G bead ratio* (the minimum amount of protein-G beads required to bind the maximum amount of antibody). The detergent-soluble fraction of a ^{35}S-LAMP-1–containing cell lysate ($10 \cdot 10^{-6}$ cells at $50 \cdot 10^{-6}$ cells/ml) was incubated with 10 µl of ID4B-containing, 50-fold concentrated TCM, followed by incubation with increasing volumes of protein-G beads, see figure 4.1.13 A, lanes 1-3. As shown in figure 4.1.15 A, the amount of ^{35}S-LAMP-1–ID4B complexes bound, increased linearly with protein-G bead volume. This implied that the amount of protein-G beads was the limiting factor and that the ^{35}S-LAMP-1–ID4B complexes were not depleted from solution in the range of protein-G bead volumes used. The ag-ab complexes were not depleted even when 5-fold less ag-ab complexes were present in the incubation mixture, see figure 4.1.15 B. Either the protein-G bead volume had to be increased or the ab concentration had to be decreased. The protein-G bead volume was arbitrarily fixed at 50 µl, as this resulted in a sufficient yield being obtained.

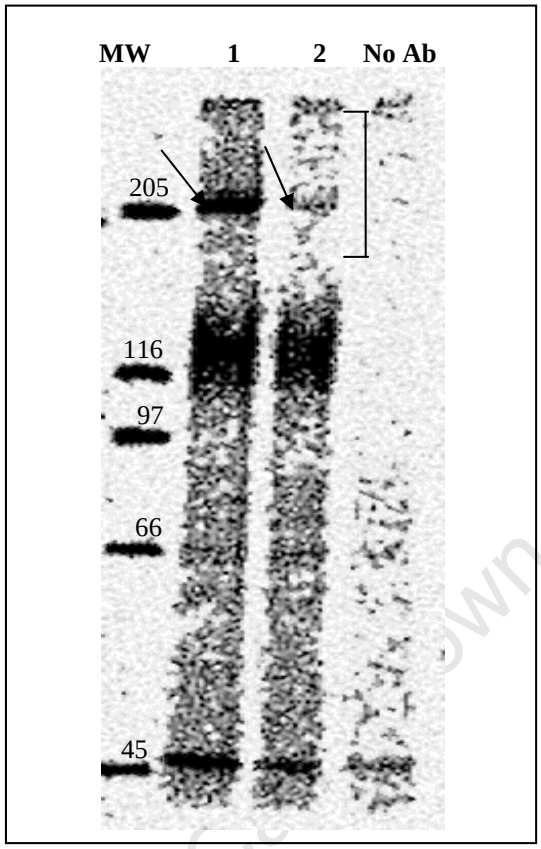

Figure 4.1.14 The elimination of a non-specific signal by centrifugation after the antigen-antibody incubation step in the immunoprecipitation assay. $P388D_1$ cells were metabolically labelled with ^{35}S-methionine. ^{35}S-LAMP-1 from the detergent-soluble fraction of the cell lysate was incubated with ID4B antibody, followed by centrifugation in a microfuge at 8 000 g for 10 min before incubation with protein-G beads (lane 2). As a control, the centrifugation step was excluded (lane 1). ^{35}S-LAMP-1 was eluted from the beads, subjected to SDS-PAGE and processed using InstantImager software. The centrifugation step reduced the non-specific band (indicated by the arrow) to background levels.

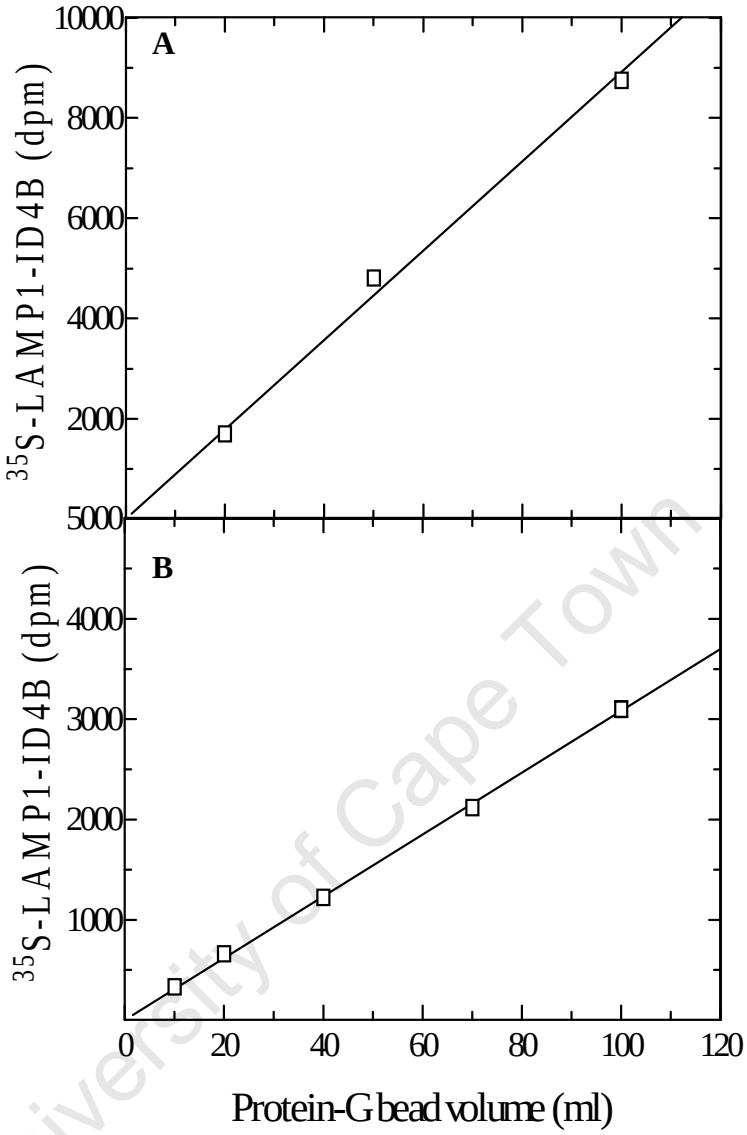

Figure 4.1.15 The binding capacity of protein-G beads. (A) The amount of ^{35}S-LAMP-1 (dpm for lanes 1-3 in figure 4.1.13) increased linearly with protein-G bead volume. **(B)** This linearity was also observed when a 5-fold dilution of ag-ab complex was used: 40 µl of the detergent-soluble fraction of a cell lysate ($2 \cdot 10^6$ cells at $50 \cdot 10^6$cells/ml) that contained ^{35}S-LAMP-1 and 2 µl ID4B antibody. [variation between duplicates was smaller than symbol]

Before the ab concentration could be reduced, it had to be ensured that the specific ab concentration used, would generate a linear-dose response in an ag concentration range that would yield experimentally reproducible results. The relationship between ab and ag concentrations was thus first explored.

In order to determine the antigen concentration range for *linearity of signal*, fixed amounts of protein-G beads (50 µl) and ID4B antibodies (2 µl of ab-containing, 50-fold concentrated TCM) were used to precipitate LAMP-1 from increasingly higher concentrations of this antigen, figure 4.1.16. A curve representing Michaelis-Menton kinetics was fitted to the data and generated a K_m of 10.63 units/ml. The response could be considered approximately linear up to an antigen concentration of ~10 units/ml. This concentration of antigen is equivalent to the concentration of LAMP-1 in the detergent-soluble fraction of a cell lysate prepared at a concentration of $10 \cdot 10^6$ cells/ml. Pulse-chase experiments were designed such that the maximal concentration at which cells could possibly be lysed in the final sample, was $10 \cdot 10^6$ cells/ml. When cell loss due to washes in between experimental steps was factored in, the working cell lysate concentration range was most likely less than $10 \cdot 10^6$ cells/ml, within the linear dose-response range.

I can conclude that 2 µl of ID4B from 50-fold concentrated ID4B-TCM was sufficient to generate a linear dose-response from LAMP-1 samples prepared from cell lysates below $10 \cdot 10^6$ cells/ml. This corresponds to the amount of ab that was used to optimise the amount of protein-G beads in figure 4.1.15 B. In order to further optimise the ab to protein-G bead ratio, the antibody concentration had to be reduced, as discussed above. To determine the minimal ab concentration that would effect maximal precipitation of LAMP-1 at a concentration in the linear dose-response range, increasing amounts of antibody were used to immunoprecipitate LAMP-1 at $6.25 \cdot 10^6$ units/ml (figure 4.1.17).

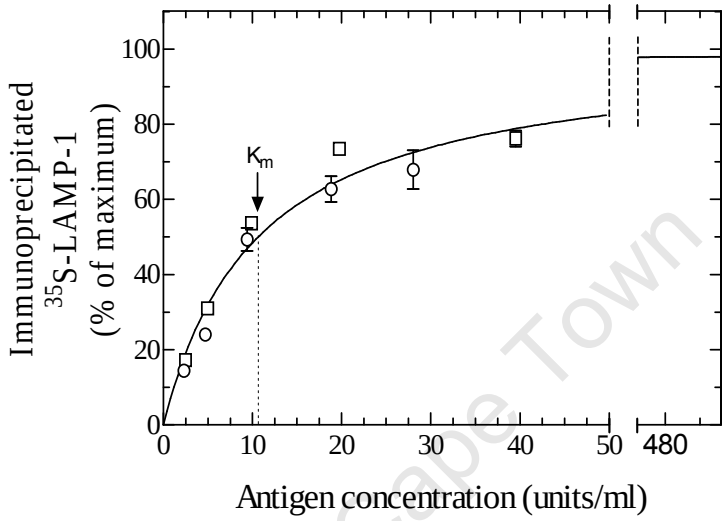

Figure 4.1.16 Optimisation of the cell-concentration range to be used for the quantitative immunoprecipitation of ^{35}S-LAMP-1. P388D$_1$ cells were metabolically labelled with ^{35}S-methionine and lysed to prepare ^{35}S-LAMP-1. Increasing amounts of the detergent-soluble fraction of the cell lysate were added to the immunoprecipitation assay in order to apply an increasing concentration of ^{35}S-LAMP-1 (indicated as the antigen concentration, where 1 unit of antigen is that amount of ^{35}S-LAMP-1 obtained from 10^6 cells). ^{35}S-LAMP-1 was immunoprecipitated with a constant amount of ID4B and protein-G beads. Error bars (where larger than symbol) indicate variation between duplicates. Different symbols refer to independent experiments. The curve shows Michaelis-Menton kinetics with a K_m = 10.63 units/ml. Values obtained for maximal binding (under present assay conditions) were used to normalise the dpm values of the two experiments. **Method:** P388D$_1$ cells were metabolically labelled with ^{35}S-methionine at $1.16 \cdot 10^{-7}$ M (specific-activity = 1175 Ci/mmol) for 2.5 h. Cells were lysed at $50 \cdot 10^6$ cells/ml (Methods 6.12.1). The detergent-soluble fraction of the cell lysate was aliqouted as explained above. ^{35}S-LAMP-1 was immunoprecipitated with 2 µl ID4B-containing, 50-fold concentrated TCM in a final volume of 162 µl, overnight at 4°C, followed by incubation with 50 µl protein-G beads for 2 h at 4°C. ^{35}S-LAMP-1−ID4B complexes were eluted with Gly/HCl, pH 2.65, subjected to SDS-PAGE, followed by solubilisation of LAMP-1−containing gel pieces and quantitation by scintillation counting.

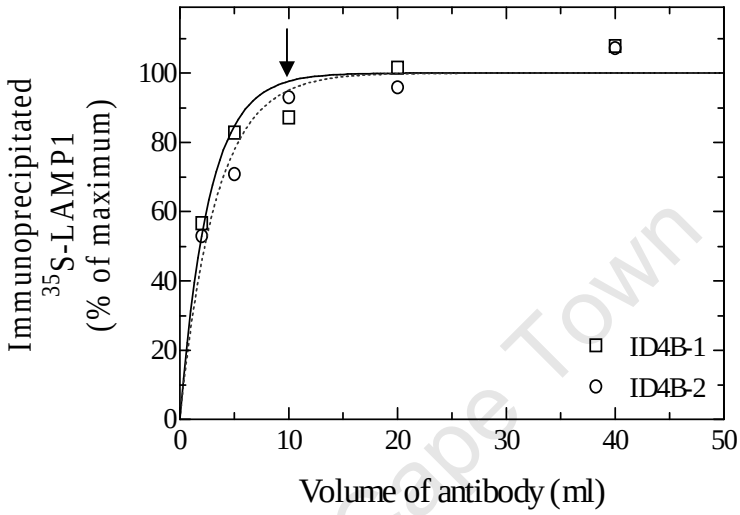

Figure 4.1.17 Optimisation of the antibody volume required for the quantitative immunoprecipitation of LAMP-1. P388D$_1$ cells were metabolically labelled with ^{35}S-methionine and lysed to prepare ^{35}S-LAMP-1. Increasing amounts of ID4B were used to immunoprecipitate ^{35}S-LAMP-1 at a concentration of 6.25 units/ml. Approximately 10 µl of either ID4B-1 or ID4B-2 (two separate batches of ID4B-containing TCM, concentrated 10-fold) was sufficient to bind close to the maximum amount of LAMP-1 at this ag concentration. Values obtained for maximal binding (under present assay conditions) were used to normalise the dpm values of the two experiments. **Method:** P388D$_1$ cells were starved in methionine-free medium (30 min) and metabolically labelled (1 h) with ^{35}S-methionine at 10^{-7} M. Labelled proteins were chased for 1 h. Cells were lysed as in figure 4.1.16. A constant amount of the detergent-soluble fraction of the cell lysate (20 µl) was added to the immunoprecipitation assay at a final volume of 160 µl to prepare an antigen concentration of 6.25 units/ml. ^{35}S-LAMP-1 was immunoprecipitated with the indicated volumes of either ID4B-1 or ID4B-2 (concentrated 10-fold). Samples were processed as explained in figure 4.1.16.

An amount of ~10 µl ID4B and above from a 10-fold concentrated ID4B-TCM was required to ensure maximal precipitation of LAMP-1 at a concentration in the mid-point of the linear dose-response range. I could thus conclude that 10 µl ID4B from 10-fold concentrated ID4B-TCM (2 µl of ID4B from 50-fold concentrated ID4B-TCM) was the minimal amount of antibody required to generate a linear dose-response from LAMP-1 samples prepared from cell lysates at the mid-point of the linear dose-response range. The latter corresponds to the amount of antibody that was used to optimise the amount of protein-G bead volume in figure 4.1.15 B. If the ab concentration was to be reduced, to further optimise the ab to protein-G bead volume ratio, the corresponding optimal cell concentration range to achieve a linear dose-response would have been lower. This would have implied working at very low cell concentrations that could potentially have resulted in increased fractional cell loss and thus increased experimental variation. It was thus decided to maintain the ID4B concentration at 10 µl of a 10-fold concentrated (2 µl of a 50-fold concentrated) ID4B-TCM.

A linear response was important in order to detect quantitative differences in LAMP-1 abundance in two samples prepared from the same cell concentration when LAMP-1 abundance in one of the samples was reduced by the removal of LAMP-1 by HRP–DAB cross-linking, see Methods 6.11.4. At very high LAMP-1 concentrations the antibodies become saturated and the LAMP-1 binding responses are non-linear. Measurements would then no longer reflect the difference in LAMP-1 abundance. This was illustrated in figure 4.1.18 where an expected constant difference in LAMP-1 abundance decreased in samples prepared from cell lysates at concentrations above $10 \cdot 10^6$ cells /ml.

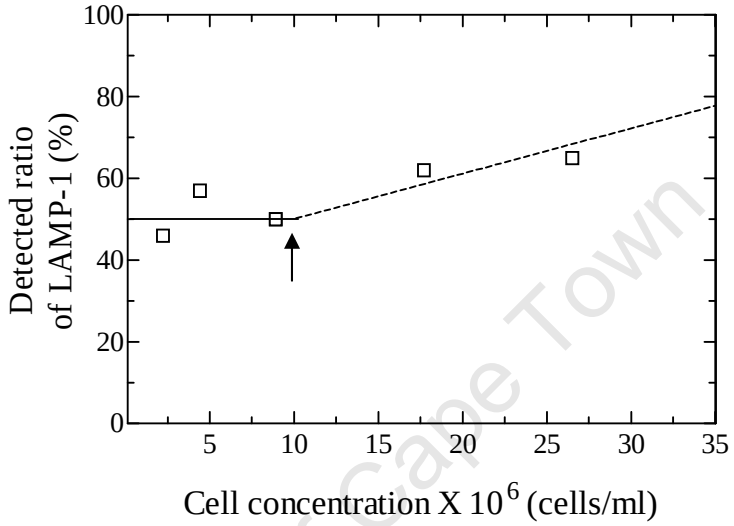

Figure 4.1.18 The effect of high LAMP-1 concentrations in the immunoprecipitation assay on detecting differences of LAMP-1 abundance. Using immunoprecipitation, the ratio of LAMP-1 abundance in two samples with different LAMP-1 concentrations (LAMP-1 was removed from one of the samples by HRP–DAB cross-linking, see Methods 6.11.4), prepared from the same cell concentration, was determined for samples of increasing overall LAMP-1 concentrations (indicated as increasing cell concentrations). Due to non-linear LAMP-1−binding responses at high LAMP-1 concentrations (see figure 4.1.16), the deviation from an expected constant ratio (~50%) was observed to become higher at cell concentrations above $10 \cdot 10^6$ cells/ml (arrow). (100% corresponds to no difference in LAMP-1 abundance.)

4.1.2.8 Reproducibility of the immunoprecipitation assay

In view of the many steps involved in the processing of experimental samples, it was important to assess, where possible, the reproducibility of measurements along the way. To determine the extent to which the immunoprecipitation assay was reproducible, it was performed in quadruplicate on the same day, using the same reagents and equipment (figure 4.1.19). It can be concluded that within a single experiment the excision of protein bands from gel lanes was reproducible with a variation that ranged from ±1.9% to ±3.8% and that the immunoprecipitation assay was reproducible with a variation of ±3.6%.

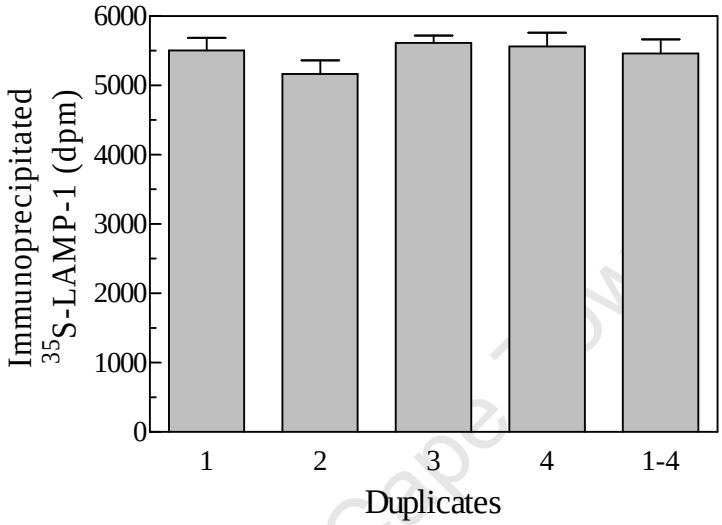

Figure 4.1.19 Reproducibility of immunoprecipitation of ^{35}S-LAMP-1. P388D$_1$ cells were metabolically labelled with ^{35}S-methionine. ^{35}S-LAMP-1 was immunoprecipitated, eluted from the beads and processed for quantitation by scintillation counting. The immunoprecipitation assay was performed in quadruplicate, as indicated by bar graphs labelled 1, 2, 3 and 4. The product of each assay was run on duplicate gel lanes. The error bars in bar graphs 1, 2, 3 and 4 refer to variation between duplicate gel lanes and range from ±1.9% to ±3.8%. The bar graph labelled 1-4 refers to the average from the four assays and the error bar shows a variation of ±3.6% among assays. **Method:** P388D$_1$ cells were metabolically labelled with ^{35}S-methionine at $2.8 \cdot 10^{-7}$ M (specific activity = 588 Ci/mmol) for 3 h. Cells were lysed as in figure 4.1.16 and immunoprecipitation was performed as in figure 4.1.17 with 4 µl ID4B from 25-fold concentrated ID4B-TCM.

4.1.3 Optimisation of conditions for kinetic experiments

Kinetic experiments entailed following the movement of newly-synthesised LAMP-1 into specific organelles of the endocytic pathway, as mentioned in Introduction 3.3. To distinguish newly-synthesised LAMP-1 from already existing LAMP-1 molecules, the former was labelled with ^{35}S-methionine as this label is incorporated into newly-synthesised proteins. To differentiate between ^{35}S-labelled-LAMP-1 that had entered specific endocytic organelles and that which was present in the rest of the cell, the former was trapped in the respective organelles by HRP–DAB cross-linking. Conditions for optimal metabolic labelling of LAMP-1 with ^{35}S-methionine and trapping of LAMP-1 in the specific endocytic organelles were established, as follows.

4.1.3.1 Metabolic labelling

The **period of metabolic labelling** had to be as short as possible to maximise kinetic resolution. The period over which the total pulse of newly-synthesised ^{35}S-LAMP-1 entered the endocytic pathway had to be short in comparison to its trafficking towards its final destination. In order to generate a short pulse with a ^{35}S-LAMP-1 signal that had sufficient intensity, it was important to ensure that the amount of ^{35}S-LAMP-1 produced over such a short pulse was optimal. The amount of ^{35}S-LAMP-1 produced is determined by the rate of protein synthesis, which in turn is proportional to the amino acid concentration available in the medium. The intensity of the signal of one molecule of ^{35}S-LAMP-1 is determined by the number of ^{35}S-methionine residues incorporated into that molecule. This in turn is dependent on the specific activity of ^{35}S-methionine in the medium. The **minimum methionine concentration range** that would ensure optimal rates of protein synthesis and efficient incorporation of ^{35}S-methionine was determined, see figure 4.1.20.

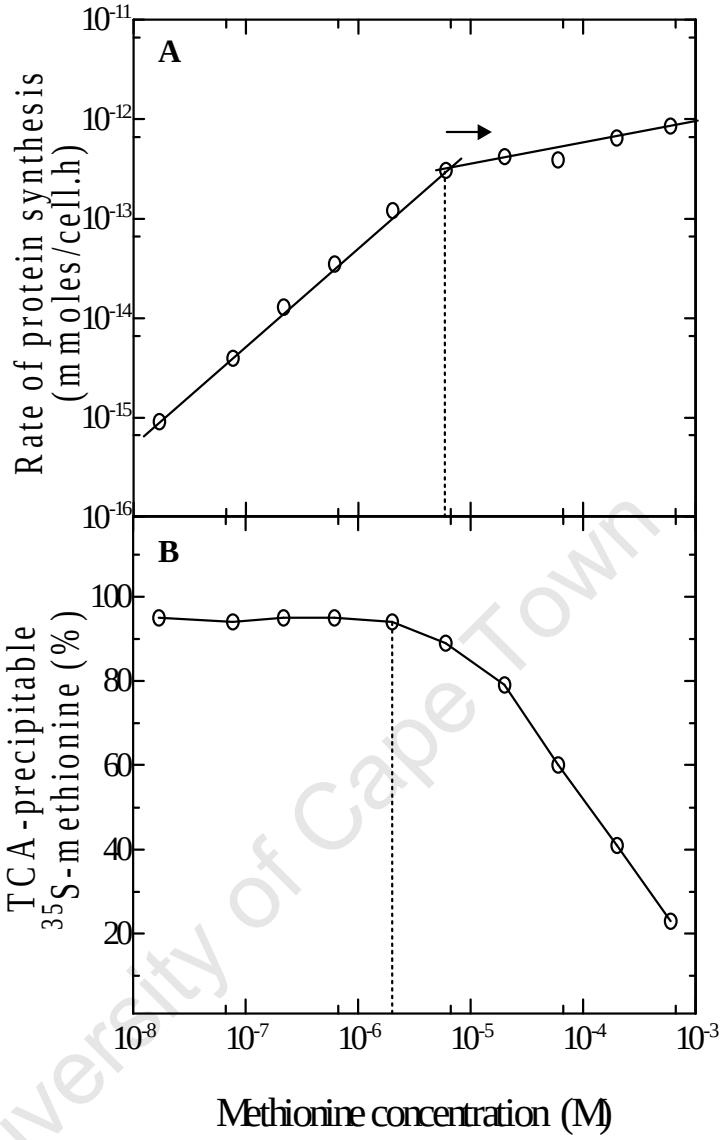

Figure 4.1.20 Determination of the methionine concentration in the medium required for optimal rates of protein synthesis and efficient incorporation of ^{35}S-methionine. P388D$_1$ macrophages were starved for 2 h at 37°C in methionine-free medium. Cells were incubated in TCM ($5 \cdot 10^6$ cells/ml) with increasing methionine concentrations, corresponding to decreasing ^{35}S-methionine specific-activities. After 2 h incubation at 37°C, cellular protein was precipitated with trichloro-acetic acid (TCA), see Methods 6.9.3. In **A**, the total amount of methionine (mmole) incorporated into protein was calculated on the basis of the effective specific-activity of methionine in the medium (Equations 7.4). This served as a measure of the total amount of protein synthesised by the cell over a 2 h period. As indicated by the arrow, the availability of methionine was no longer a rate limiting factor above ~$5 \cdot 10^{-6}$ M. In **B**, the fraction of TCA-precipitable ^{35}S-methionine (^{35}S-methionine incorporated into protein) was calculated and plotted against methionine concentration. Efficient incorporation of ^{35}S-methionine occurred below ~$2 \cdot 10^{-6}$ M, above which decreasing specific-activity was no longer compensated by increasing rates of protein synthesis (compare (cf.) with **A**).

A minimum methionine concentration of ~$2 \cdot 10^{-6}$ to $5 \cdot 10^{-6}$ M was established as required for optimal rates of protein synthesis and efficient incorporation of ^{35}S-methionine over a 2 h period. A ^{35}S-methionine concentration at 10^{-7} M was chosen for short labelling periods, such as 5 min and further explored for its feasibility.

The general procedure was as follows: Cells were incubated in methionine-free medium for 30 min at 37°C to ensure the depletion of unlabelled methionine. At time zero, ^{35}S-methionine was added to the warm medium (37°C) to ensure maximum uptake of ^{35}S-methionine and incorporation into protein. The cells were incubated for 5 min in the medium containing ^{35}S-methionine, after which the labelling was stopped by rapid cooling in a mixture of ice and water. The labelling medium was removed after the cells were pelleted. To ensure the maximal removal of residual ^{35}S-methionine, cells were washed with medium containing unlabelled methionine. The ^{35}S-protein was then chased through the endoplasmic reticulum, Golgi, TGN and into the endocytic pathway by incubating the cells in medium with unlabelled methionine at 37°C. Samples were processed by using the optimised conditions for immunoprecipitation and detection of ^{35}S-LAMP-1, as discussed in 4.1.2. A labelling pulse of 5 min was found to give enough signal intensity for satisfactory quantification of ^{35}S-LAMP-1. Lane background varied from 20% of the specific signal at early time-points to 5% at later time-points.

4.1.3.2 HRP internalisation

HRP catalyses the cross-linking of DAB. When this occurs in an organelle, the resultant meshwork traps the proteins in the organelle, see Introduction 3.3.2 and 3.3.3. Three cross-linking situations were envisaged: the early endosomes, lysosomes and the entire endocytic pathway.

To cross-link newly-synthesised ^{35}S-LAMP-1 in early endosomes, ^{35}S-LAMP-1 was first chased and then HRP was endocytosed for 5 min at the end of every chase period. A 5 min HRP internalisation period to fill early endosomes was chosen, based on the fact that early endosomes in P388D$_1$ cells mature with a half-life of 3 min (Thilo *et al.*, 1995). These 5 min endosomes were indeed characteristic of early endosomes, since they were positive for the early endosomal markers, EEA1 (Mu *et al.*, 1995) and Rab 5b (Chavrier *et al.*, 1990), see figure 4.1.21. Some limited staining for EEA1 and Rab 5b was also observed for lysosomes. This was probably due to contamination of the lysosomal fraction on the 27% Percoll gradient with early endosomes. (No surface label has previously been detected in the lysosomal fraction (Haylett and Thilo, 1986).) Accordingly, limited Rab 5b was also observed in non-cross-linked lysosomes.

To cross-link newly-synthesised ^{35}S-LAMP-1 in the endocytic pathway, the entire endocytic pathway was loaded with HRP before and during the entry of ^{35}S-LAMP-1. To cross-link newly-synthesised ^{35}S-LAMP-1 in lysosomes, a pulse of HRP was chased to lysosomes before the entry of ^{35}S-LAMP-1. The period of HRP internalisation required to fill the endocytic pathway and the length of the HRP pulse to be chased to lysosomes were determined, as shown below in figures 4.1.22 to 4.1.26.

For my quantitative assays, it was important to ensure maximal cross-linking of the proteins in the organelle. The concentration of HRP in an organelle would determine the efficiency of cross-linking. This in turn is dependent on the concentration of HRP in the medium in which the cells are incubated and the period over which HRP is internalised. The lumenal lysosomal protein, NAGA, can easily be measured and was used for optimising the conditions for HRP-catalysed DAB cross-linking. The assay for measuring NAGA was developed from Hall *et al.* (1978) by Thomas Haylett, see Methods 6.9.4.

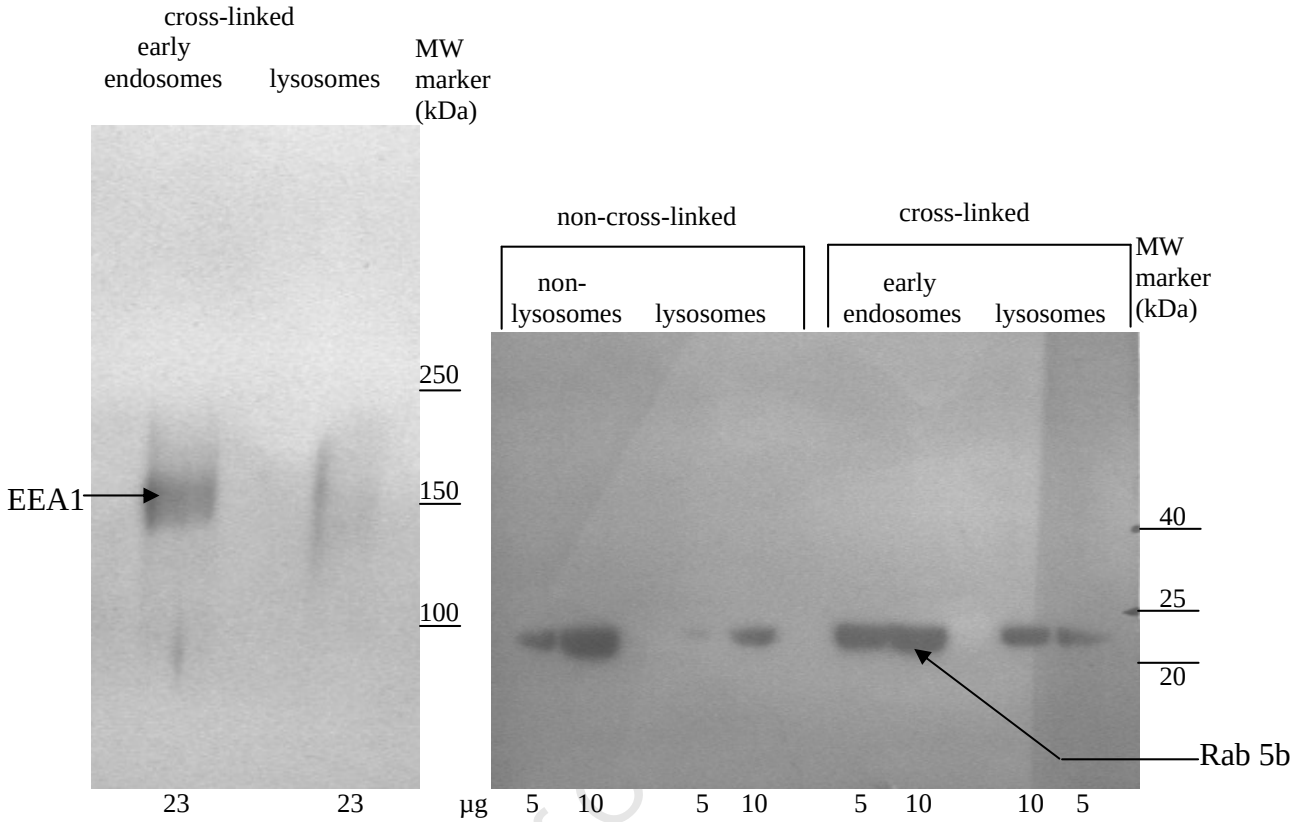

Figure 4.1.21 Characterisation of early endosomes by EEA1 and Rab 5b. Early endosomes (5 min HRP pulse) or lysosomes (30 min HRP pulse, 70 min chase) were filled with HRP, cross-linked and separated on a 27% Percoll gradient (see Methods 6.5.3). Peripheral proteins on early endosomes or lysosomes were solubilised, subjected to SDS-PAGE and Western blotting (see Methods 6.7.2). The transfer was performed for 3 h. To detect the EEA1, proteins were separated on a 7% gel and rabbit polyclonal primary antibody against mouse EEA1 (1 mg/ml, diluted 500-fold) was used. To detect Rab 5b, proteins were separated on a 13% gel and a rabbit polyclonal anti-human Rab 5b (200 µg/ml, diluted 100-fold) primary antibody was used. A peroxidise-labelled anti-rabbit antibody (Amersham, cat.no. NIF824, diluted 1000-fold) was used as a secondary antibody. The blots were developed with the KPL luminoglo. The EEA1 blot was exposed for 10 min and the Rab 5b blot for 5 min. Early endosomes were positive for EEA1 and Rab 5b (arrows). (Non-lysosomes include plasma membrane and early endosomal components.)

The **cross-linking of NAGA** was dependent on *HRP concentration in the medium* when only a 5 min pulse of HRP was chased to lysosomes (figure 4.1.22). When HRP was endocytosed for 30 min, cross-linking was independent of HRP concentrations at 1 mg/ml and above in the medium (figure 4.1.23). A pulse of 30 min was thus chosen to ensure that cross-linking of NAGA in lysosomes was independent of HRP concentration in the medium. The *period of HRP internalisation* to fill the entire endocytic pathway for maximal cross-linking of NAGA (77%) was observed to be 100 min (figure 4.1.24). To ensure maximal cross-linking of NAGA in lysosomes in the case of a 30 min pulse of HRP (1 mg/ml), a chase period of about 70 min was necessary to make up for a total delivery time of 100 min. Since NAGA is a lumenal lysosomal protein, as opposed to LAMP-1 which is an integral lysosomal membrane protein, the above conditions were tested to confirm whether these would be directly applicable to the cross-linking of LAMP-1.

To measure the **cross-linking of LAMP-1**, LAMP-1 was first labelled with ^{35}S-methionine. The labelled proteins were then equilibrated to steady state. The effect of *HRP concentration* in a 30 min pulse chased to lysosomes on cross-linking was measured, as shown in figure 4.1.25. The fraction of cross-linked LAMP-1 remained constant (40%) and independent of HRP concentration below 3 mg/ml, but decreased and showed greater experimental variation at concentrations higher than 3 mg/ml.

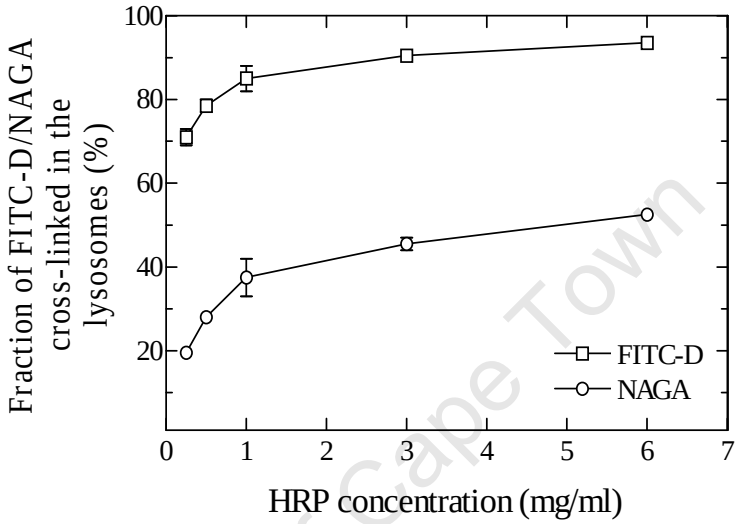

Figure 4.1.22 The effect of concentration in a 5 min pulse of HRP uptake on the cross-linking of NAGA. FITC-D (Fluorescein isothiocyanate-dextran) was internalised by $P388D_1$ cells and chased to lysosomes to serve as a marker for intra-lysosomal cross-linking. $P388D_1$ cells were incubated in medium containing HRP at one of the indicated concentrations. HRP was endocytosed for 5 min and chased to lysosomes. Half of each sample was treated for HRP–DAB cross-linking and the other half served as a measure of the total NAGA/FITC-D. Cross-linked NAGA/FITC-D was expressed as a percentage of the total NAGA/FITC-D in each sample. The cross-linking of both FITC-D and NAGA was dependent on the concentration of HRP in the medium when only a 5 min pulse of HRP was chased to lysosomes. Error bars indicate variation (standard error of the mean, SEM) between duplicate determinations of the fraction of cross-linked FITC-D or NAGA from the same sample. **Method**: $P388D_1$ cells were subjected to a 5 min pulse of FITC-D (6 mg/ml), which was then chased for 30 min to lysosomes at 37°C. Cells were split into 5 batches, each of which was suspended in medium containing HRP at one of the indicated concentrations. HRP was endocytosed for 5 min and chased to lysosomes for 40 min at 37°C. Half of each sample was treated for HRP–DAB cross-linking, see Methods 6.11.4. The other half served as a measure of total NAGA/FITC-D in the sample. In both cases, soluble NAGA was quantified by measuring the product of an enzymatic reaction spectrophotometrically, see Methods 6.9.4. FITC-D was measured spectrophotometrically.

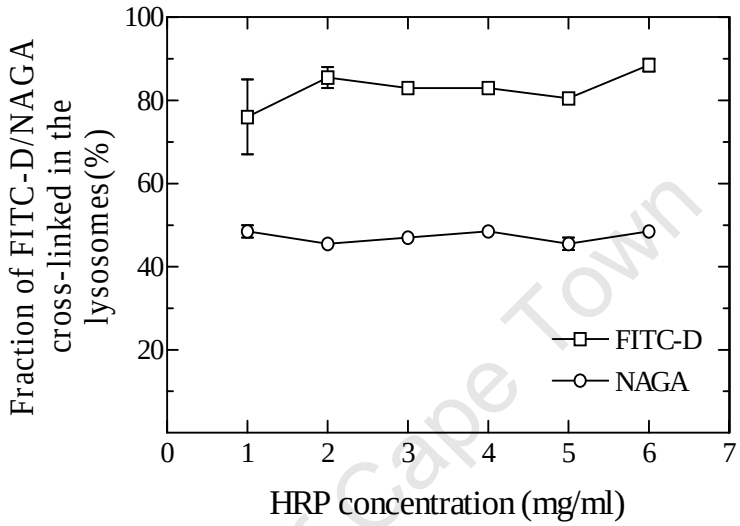

Figure 4.1.23 The effect of concentration in a 30 min pulse of HRP uptake on the cross-linking of lysosomal FITC-D and NAGA. P388D$_1$ cells were subjected to a 5 min pulse of FITC (6 mg/ml), which was then chased for 30 min to lysosomes at 37°C. Cells were split into 6 batches, each of which was suspended in medium containing HRP at one of the indicated concentrations. HRP was endocytosed for 30 min at 37°C. Samples were analysed as described in figure 4.1.22. Concentration of HRP in the medium did not affect the cross-linking efficiency of both FITC-D and NAGA after a 30 min pulse of HRP. Error bars indicate variation (SEM) between duplicate determinations of the fraction of cross-linked FITC-D or NAGA from the same sample.

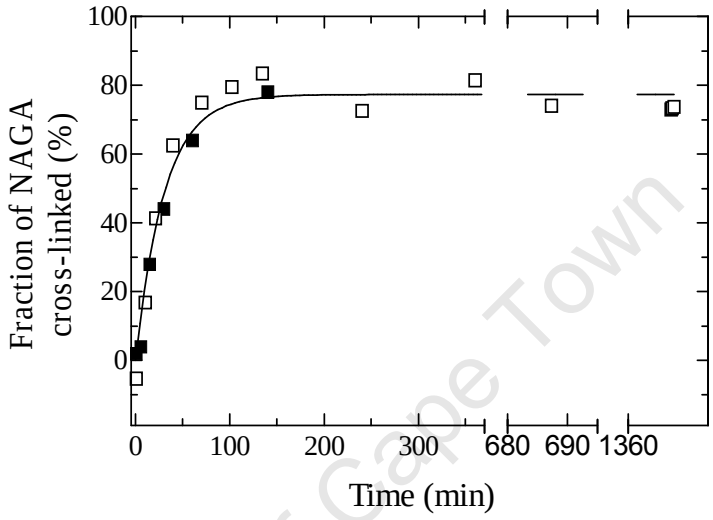

Figure 4.1.24 Time required for HRP to fill the endocytic pathway, and thus also for HRP delivery to lysosomes, to effect maximal cross-linking of NAGA. $P388D_1$ cells were incubated at 37ºC in the presence of HRP (1 mg/ml) for the indicated times. Samples were analysed as described in figure 4.1.22. A curve was fitted manually and indicated a maximal cross-linking of 77% after about 100 min of HRP uptake. Different symbols refer to independent experiments.

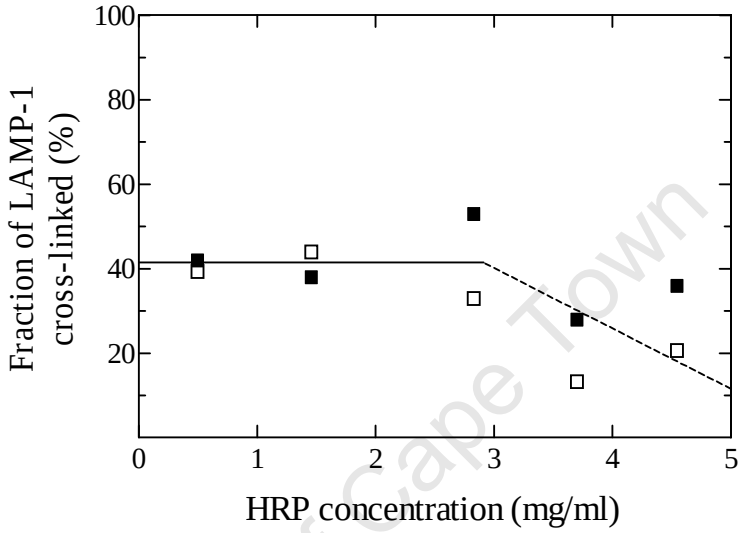

Figure 4.1.25 The effect of HRP concentration in a 30 min pulse on the cross-linking of LAMP-1 in lysosomes. P388D$_1$ cells were metabolically labelled with ^{35}S-methionine to produce ^{35}S-LAMP-1. HRP was internalised at the indicated concentrations during the last 30 min of the labelling period. The internalised HRP was chased to lysosomes for a further 2.5 h (total duration of the chase period of an HRP pulse in a cross-linking experiment was ~3 h). Samples at the indicated HRP concentrations were split into two fractions, one of which was treated for HRP–DAB cross-linking. The other fraction served as a measure for total ^{35}S-LAMP-1. In both fractions, the soluble (non-cross-linked) ^{35}S-LAMP-1 was quantified by scintillation counting of the appropriate band after SDS-PAGE of the immunoprecipitated soluble LAMP-1. The amount of cross-linked ^{35}S-LAMP-1 was expressed as a fraction of the total ^{35}S-LAMP-1 in each sample. Different symbols refer to duplicate immunoprecipitations of individual samples. **Labelling method:** P388D$_1$ cells were starved for 15 min in methionine-free medium. ^{35}S-methionine was added, the cell suspension split into 5 aliquots and cells were metabolically labelled at 37°C for 1.5 h.

To determine the *period of HRP internalisation* that would ensure maximum LAMP-1 cross-linking in the entire endocytic pathway, HRP was endocytosed continuously for the indicated times and the fraction of cross-linked ^{35}S-LAMP-1 was determined (figure 4.1.26). Although a maximum of 76% cross-linking was achieved after about 150 min HRP internalisation, 100 min (as determined for NAGA) was considered acceptable because cross-linking increased by only 6% in the extra 50 min period.

From the above experiments it could be concluded that the conditions established for the efficient cross-linking of NAGA as a lysosomal marker were also applicable to cross-linking of LAMP-1. These conditions were then used to design the appropriate assay conditions for optimal cross-linking of LAMP-1 during the kinetic experiments, diagrammatically represented in figure 4.1.27. To ensure maximal cross-linking of LAMP-1 in the endocytic pathway, HRP (1 mg/ml) was internalised for at least 100 min to fill the entire endocytic pathway before a 5 min ^{35}S-methionine pulse was chased into the endocytic pathway in the continued presence of HRP (figure 4.1.27, A). To cross-link LAMP-1 in early endosomes, the 5 min ^{35}S-methionine pulse was first chased into the cells and HRP (1 mg/ml) was internalised during the last 5 min of every chase period (figure 4.1.27, B). To ensure maximal cross-linking of LAMP-1 in lysosomes, an HRP (1 mg/ml) pulse of 30 min was chased for 70 min (a total delivery time of 100 min) to lysosomes before the 5 min ^{35}S-methionine pulse was chased into the endocytic pathway (figure 4.1.27, C). These conditions were applied in the actual pulse-chase experiments to observe the kinetics of entry of newly-synthesised ^{35}S-LAMP-1 into the endocytic pathway, early endosomes or lysosomes.

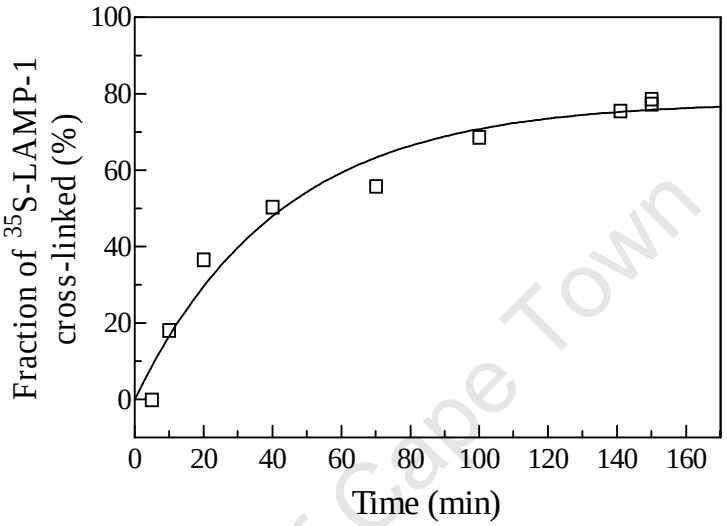

Figure 4.1.26 Maximal cross-linking of LAMP-1 in the endocytic pathway. $P388D_1$ cells were metabolically labelled with ^{35}S-methionine to produce ^{35}S-LAMP-1. Horse-radish peroxidase (HRP) (3 mg/ml) was endocytosed for the indicated times, when samples were taken and cooled on ice. Samples were analysed for the degree of cross-linking, as described in figure 4.1.25. A curve was fitted manually and indicated a maximum cross-linking of 76% after about 150 min. **Labelling method:** $P388D_1$ cells were starved in methionine-free medium for 30 min and metabolically labelled with ^{35}S-methionine for 60 min. The ^{35}S-methionine labelled proteins were equilibrated to steady-state levels by incubation of the cells in medium with unlabelled methionine at 37ºC for 1 h.

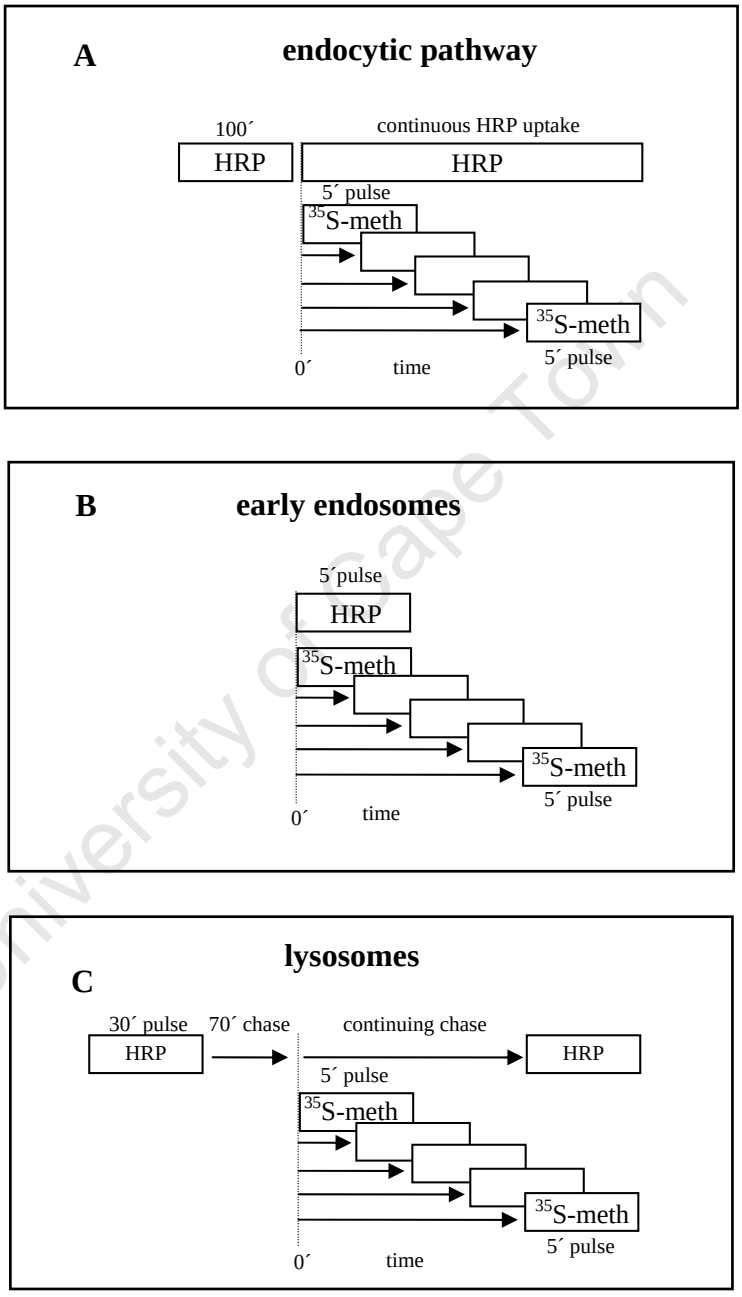

Figure 4.1.27 A diagrammatic representation of the pulse-chase experiments.

4.1.4 Biosynthetic pathway for LAMP-1

Having established the conditions for the quantitative localisation of newly-synthesised LAMP-1 along the endocytic pathway, the following experiments were aimed to observe its pathway *en route* to lysosomes. As described in the Introduction (3.4), two different pathways can be considered. LAMP-1 can enter the endocytic pathway either via early endosomes, or be delivered directly into lysosomes. Because these two scenarios lead to markedly different kinetics for the entry of LAMP-1 into the respective organelles (see figures 3.4.1 and 3.4.2), an unambiguous conclusion seemed feasible, despite the known potential for a high degree of experimental variation of the present approach.

4.1.4.1 The biosynthetic processing of newly-synthesised ^{35}S-LAMP-1

As a basis for studying its delivery into the endocytic pathway, the rate of protein synthesis in general, and LAMP-1 in particular, had to be established. As shown in figure 4.1.28, the rate of ^{35}S-protein synthesis remained constant throughout the 5 min ^{35}S-methionine pulse, as was reflected by the linear increase in TCA-precipitation of total protein. When the ^{35}S-methionine was replaced with excess unlabelled methionine after 5 min, the ^{35}S-methionine concentration in the cells was diluted. ^{35}S-methionine incorporation into protein became negligible and no further increase was observed. In contrast to the TCA-precipitation of total ^{35}S-labelled protein, ^{35}S-LAMP-1 was observed via immunoprecipitation. Accordingly, it would only be observed once it had become antigenic. The kinetics of processing of newly-synthesised ^{35}S-LAMP-1 were determined by combining the data of total newly-synthesised soluble immunoprecipitable ^{35}S-LAMP-1 (dpm) formed with time in the non-cross-linked fractions of all the kinetic experiments to follow into one graph, as in figure 4.1.29. The 5 min pulse of ^{35}S-LAMP-1 was processed within 50-60 min into mature immunoprecipitable ^{35}S-LAMP-1 with a half-time of approximately 14 min. Because the methionine concentration in the cells under the above experimental conditions remained in excess, the rate of protein synthesis, including LAMP-1,

in the cells was constant. The gradual decrease in the rate at which mature ^{35}S-LAMP-1 became immunoprecipitable with time was thus not due to a decrease in the rate of total LAMP-1 synthesis. It was also not due to gradual dilution of the ^{35}S-methionine concentration when the ^{35}S-methionine was replaced by excess unlabelled methionine, as judged by the rapid termination in the incorporation of ^{35}S-methionine into total protein after 5 min (figure 4.1.28). Because ^{35}S-LAMP-1 was observed with immunoprecipitation and SDS-PAGE, it would only be detected once it had become immunoprecipitable. The gradual decrease in the rate at which ^{35}S-LAMP-1 became immunoprecipitable suggests that unprocessed ^{35}S-LAMP-1 in the Golgi was mixed and gradually diluted with incoming unlabelled LAMP-1 and was then processed into immunoprecipitable protein on a random basis rather than on a first-come-first-serve basis.

4.1.4.2 Entry of ^{35}S-LAMP-1 into the endocytic pathway

The next step was to determine the kinetics with which newly-synthesised LAMP-1 entered the endocytic pathway in general. This served as a reference for the more detailed pathways of entry into either early endosomes or directly into lysosomes. The total endocytic pathway was defined by its accessibility to endocytosed HRP (figures 4.1.24 and 4.1.26) and entry of ^{35}S-LAMP-1 was determined by HRP-mediated cross-linking as in figure 4.1.30. The rate of LAMP-1 entry into the endocytic pathway at steady state can be expected to remain constant under the experimental conditions used. The initial 15 to 20 min lag can be ascribed to movement of ^{35}S-LAMP-1 through the endoplasmic reticulum and Golgi. The initial slowly increasing rate at which ^{35}S-LAMP-1 entered the endocytic pathway could be expected as previously formed unlabelled LAMP-1 is gradually replaced by ^{35}S-LAMP-1. The slow decrease in the rate at the end of the ^{35}S-LAMP-1 pulse (around 50 to 60 min) reflects the dilutions with subsequently synthesised unlabelled LAMP-1.

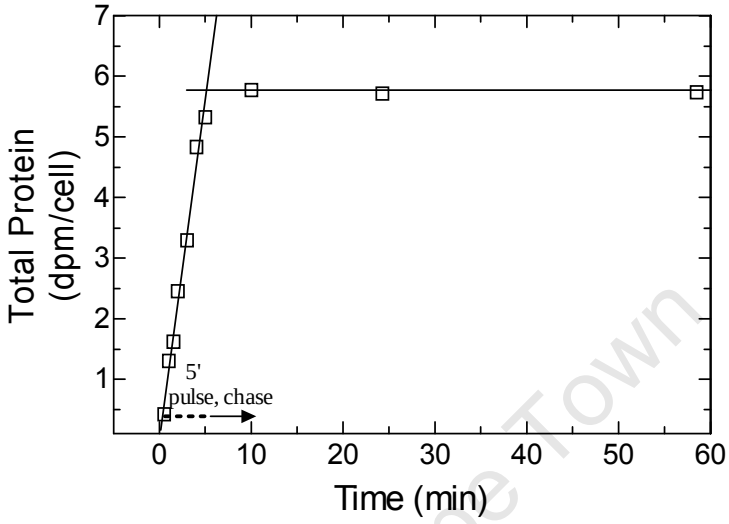

Figure 4.1.28 Determination of the kinetics with which total protein is processed. Cells were metabolically labelled with ^{35}S-methionine for 5 min after which the labelled protein was chased. Samples were taken for the indicated times. The amount of radio-actively labelled total protein synthesised per cell was determined using TCA-precipitation. **Method**: Cells (10^7 cells/ml) were starved for 30 min in methionine-free medium. At time = 0 min ^{35}S-methionine at 10^{-7} M (specific-activity, 1175 Ci/mmole) was added to the medium and the cells were metabolically labelled at 37ºC, 5% CO_2 for 5 min. The cells were then cooled immediately to stop the internalisation of ^{35}S-methionine. Cells were washed and re-incubated with unlabelled medium. Samples were taken during the 5 min labelling period and the chase period at the indicated times. Cells were washed thrice with HeSBSA (10 ml) and transferred to an eppendorf in 1 ml HeSBSA. Cells were centrifuged at 200 g for 3 min, resuspended in 100 µl HeSBSA and subjected to TCA-precipitation (see Methods 6.9.3).

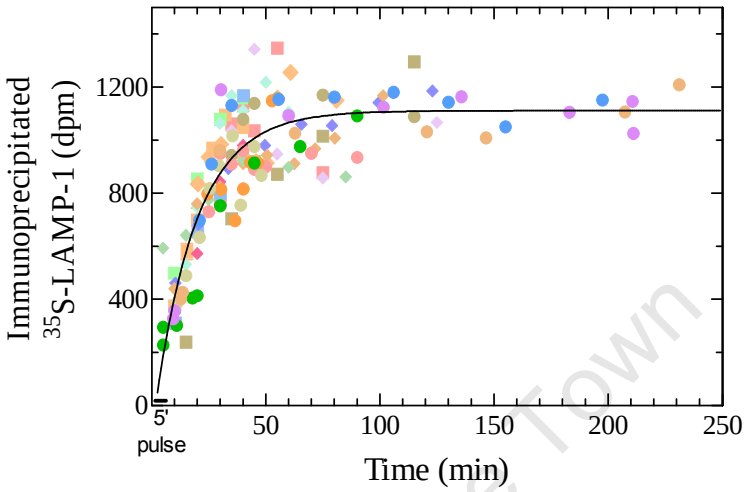

Figure 4.1.29 Biosynthetic processing of immunoprecipitable ^{35}S-LAMP-1. P388D$_1$ cells were starved in methionine-free medium for 30 min at 37°C. At time zero, ^{35}S-methionine was added at 10^{-7} M (specific-activity = 1175 Ci/mmole) and cells were labelled for 5 min. ^{35}S-LAMP-1 was then chased by replacing the ^{35}S-methionine-containing medium with unlabelled methionine-containing medium. Cells were washed and lysed. ^{35}S-LAMP-1 was immunoprecipitated from the detergent-soluble fraction of the lysate, processed via SDS-PAGE and quantitated by scintillation counting (see Methods). Differently coloured symbols refer to independent experiments. Since all experiments did not extend across the entire time-course, individual experiments were normalised to a best-fit steady state that started at approximately 60 min and averaged around 1000 dpm. An exponential curve, allowing for background as a degree of freedom, was chosen as a best-fit to the data for ^{35}S-LAMP-1. The data were compatible with a half-time of 14 min for the processing of LAMP-1 into immunoprecipitable LAMP-1.

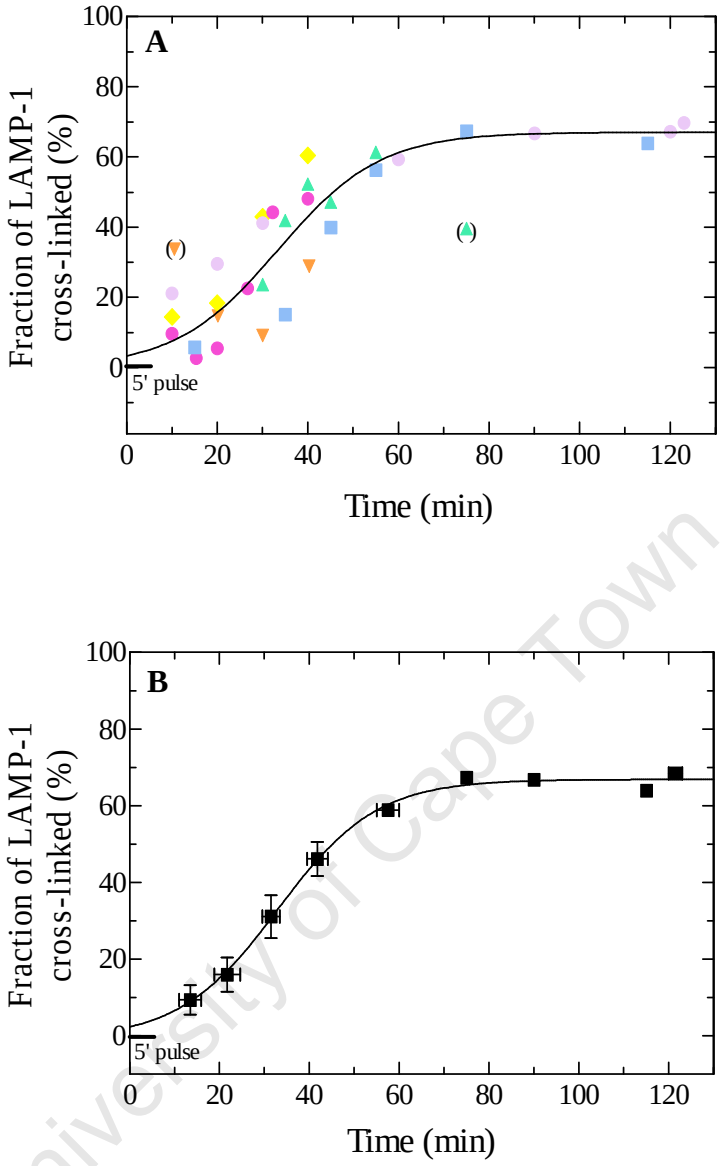

Figure 4.1.30 Delivery of newly-synthesised ^{35}S-LAMP-1 into the endocytic pathway. The endocytic pathway of P388D$_1$ cells was filled with HRP (70 min). In the continued presence of HRP, cells were starved in methionine-free medium (30 min), metabolically labelled with ^{35}S-methionine for 5 min and further incubated in the presence of unlabelled methionine for the indicated times, when samples were taken and cooled on ice. One half of each sample was treated for HRP–DAB cross-linking. The other half served as a measure for total ^{35}S-LAMP-1. In both cases, the soluble (non-cross-linked) ^{35}S-LAMP-1 was quantified by scintillation counting of the appropriate band after SDS-PAGE of the immunoprecipitated soluble LAMP-1 (see Methods). Delivery of ^{35}S-LAMP-1 into the endocytic pathway was expressed as the amount of cross-linked ^{35}S-LAMP-1, as a fraction of the total ^{35}S-LAMP-1, in each sample. The curve was fitted manually. The fraction of ^{35}S-LAMP-1 cross-linked at steady state was 67%. In **A,** different symbols refer to independent experiments. In **B**, the average from the different experiments is shown. Vertical error bars indicate variation (SEM) among the data obtained in the time intervals indicated by the horizontal error bars.

The entry of ^{35}S-LAMP-1 into the endocytic pathway thus appears sigmoidal. A curve predicted in Introduction 3.4 could not be fitted to the data and was thus fitted manually. A steady-state level of about 67% ^{35}S-LAMP-1 was reached after 60 to 70 min. The fact that the 5 min pulse of ^{35}S-LAMP-1 was processed within 50 to 60 min into mature immunoprecipitable ^{35}S-LAMP-1 (figure 4.1.29) and entered the endocytic pathway in about the same time (figure 4.1.30) suggested that entry into the endocytic pathway is a rapid process. This is in accordance with previous results that for most proteins the rate-limiting step in their trafficking from the site of their synthesis to their final destination is exit from the ER, with subsequent steps being rapid (Lodish *et al.*, 1983).

4.1.4.3 Entry of ^{35}S-LAMP-1 into lysosomes

The kinetics of entry of ^{35}S-LAMP-1 into lysosomes were observed by cross-linking ^{35}S-LAMP-1 as it entered lysosomes (figure 4.1.31). A curve was manually fitted to the data. A steady-state level of about 38% ^{35}S-LAMP-1 was reached after 60 to 70 min. When the entry of ^{35}S-LAMP-1 into lysosomes was compared to its entry into the endocytic pathway, it was observed that ^{35}S-LAMP-1 entered lysosomes with a more pronounced biological lag (figure 4.1.33). This suggests that the bulk of ^{35}S-LAMP-1 entered the endocytic pathway via an endocytic organelle other than the lysosomes.

4.1.4.4 Entry of ^{35}S-LAMP-1 into early endosomes

The kinetics of entry of ^{35}S-LAMP-1 into early endosomes were observed by cross-linking ^{35}S-LAMP-1 as it entered early endosomes, see figure 4.1.32. A transient presence of ^{35}S-LAMP-1 was observed in early endosomes. Because of the overall low amounts of ^{35}S-LAMP-1 in this compartment, the quantitation was less accurate and resulted in substantial scattering of the data.

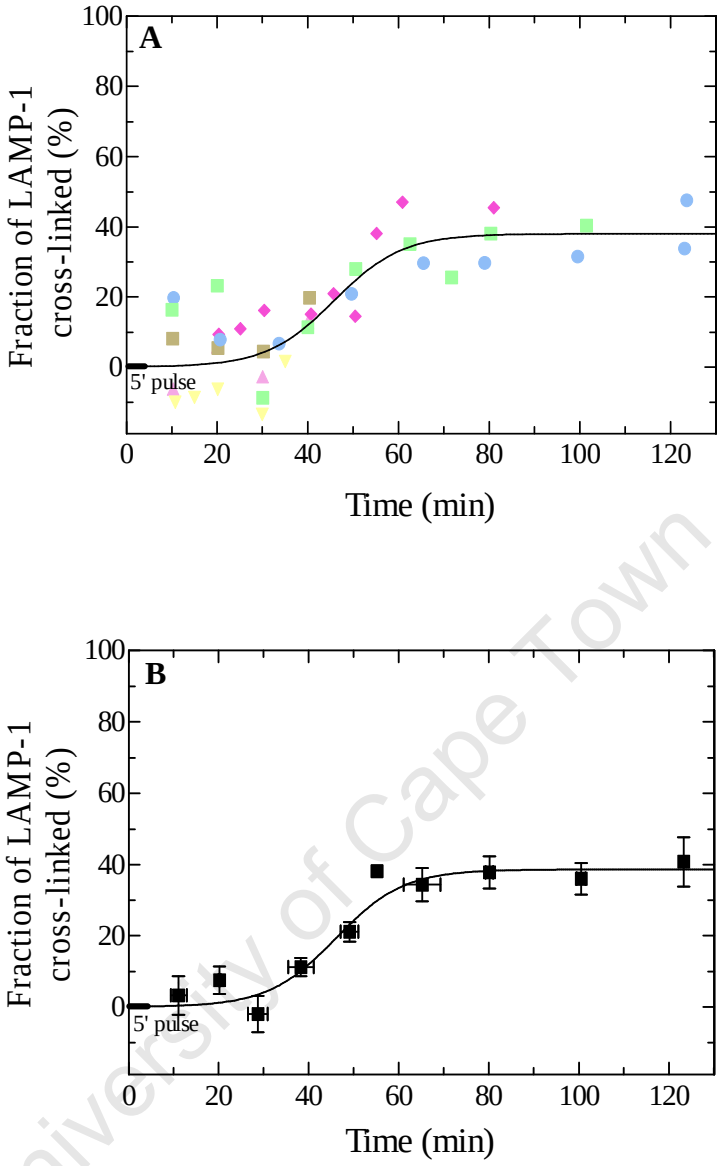

Figure 4.1.31 Delivery of newly-synthesised ^{35}S-LAMP-1 to lysosomes. An HRP-uptake pulse (30 min) was chased into lysosomes for 40 min in P388D$_1$ cells. The cells were then starved in methionine-free medium for 30 min (HRP was chased for a total period of 70 min, equivalent to a delivery time of 100 min.), labelled with ^{35}S-methionine for 5 min, followed by further incubation in the presence of unlabelled methionine for the indicated times when samples were taken and cooled on ice. Samples were processed as in figure 4.1.30. Delivery of ^{35}S-LAMP-1 into lysosomes was expressed as the amount of cross-linked ^{35}S-LAMP-1, as a fraction of the total ^{35}S-LAMP-1, in each sample. The curve was fitted manually. The fraction of ^{35}S-LAMP-1 cross-linked at steady state was ~38%. In **A,** different symbols refer to independent experiments. In **B,** the average from the different experiments is shown. Vertical error bars indicate variation (SEM) among data obtained from the independent experiments in the time intervals indicated by horizontal error bars.

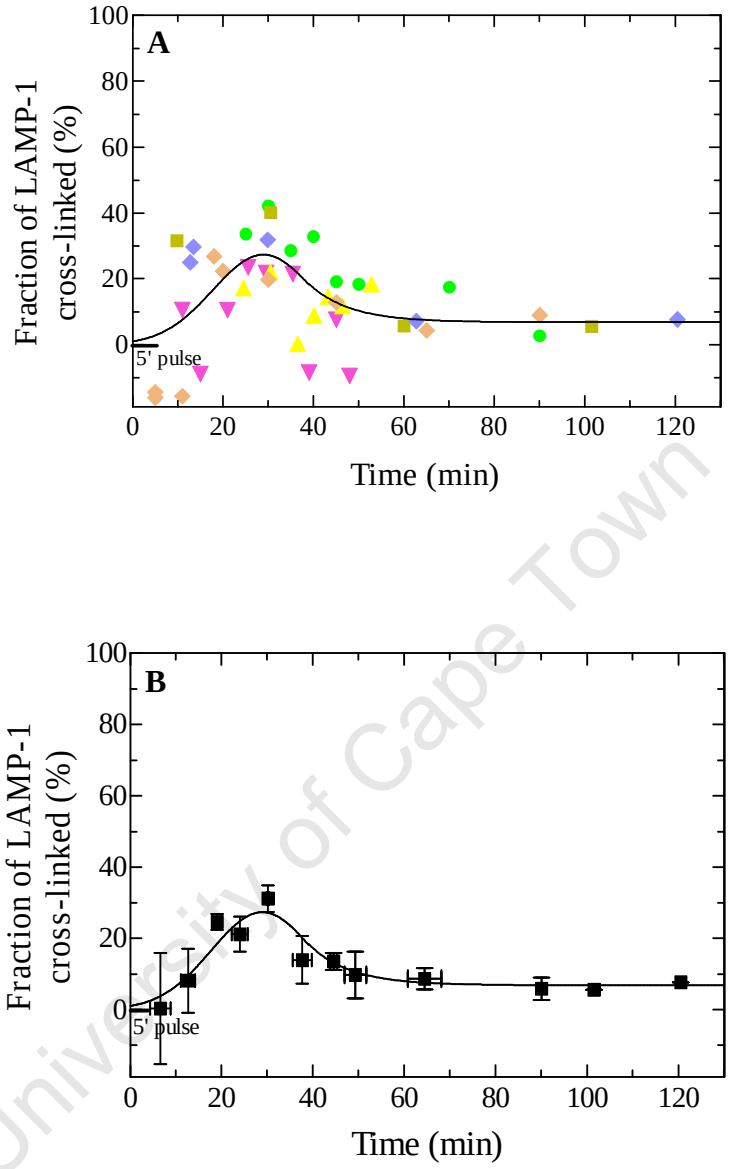

Figure 4.1.32 Delivery of newly-synthesised ^{35}S-LAMP-1 to early endosomes. P388D$_1$ cells were starved in methionine-free medium (30 min), labelled with ^{35}S-methionine (5 min) and further incubated at the indicated times when samples were taken and cooled on ice. HRP was internalised during the last 5 min of each time point. Samples were processed as in figure 4.1.30. Delivery of LAMP-1 into early endosomes was expressed as the amount of cross-linked LAMP-1, as a fraction of the total LAMP-1, in each sample. The curve was fitted manually. The fraction of ^{35}S-LAMP-1 cross-linked at steady state was ~5.5%. The data are compatible with a transient presence of LAMP-1 in early endosomes. In **A**, different symbols refer to independent experiments. In **B**, the average from the different experiments is shown. Vertical error bars indicate variation (SEM) among data from the independent experiments in the time intervals indicated by the horizontal error bars.

In this regard it should be realised that due to technical constraints no more than 9 data points could be obtained for a single experiment. When averaged between independent experiments (figure 4.1.32 B), the data nevertheless allowed an unambiguous distinction between the two different scenarios as presented in figures 3.4.1 and 3.4.2. When the entry of ^{35}S-LAMP-1 into early endosomes was compared with its entry into the endocytic pathway, it was observed that during the initial period of the time course the two curves were co-incident, see figure 4.1.33. This implies that the bulk of the ^{35}S-LAMP-1 entered the endocytic pathway via early endosomes. The transient presence of ^{35}S-LAMP-1 in early endosomes suggests that the early endosome is a station *en route* to lysosomes.

4.1.4.5 Entry of ^{35}S-LAMP-1 into late endosomes and conclusion

Taken together, these results imply that the bulk of ^{35}S-LAMP-1 entered the endocytic pathway via early endosomes before its delivery to lysosomes. It can be expected that this delivery occurs via the late endosomes as an intermediate stage. Because HRP could not be loaded exclusively into the late endosomes, it was not possible to measure specific cross-linking of ^{35}S-LAMP-1 in this compartment. Entry of ^{35}S-LAMP-1 into late endosomes could be calculated as the difference between the amount of LAMP-1 in the total endocytic pathway and the combined amounts in early endosomes and lysosomes. When the curves in figures 4.1.30, 4.1.31 and 4.1.32 were combined in this way, the kinetics of delivery to late endosomes could be constructed as in figure 4.1.33. From the curves, it was observed that at steady state about 67% ^{35}S-LAMP-1 occurred in the endocytic pathway, 38% in lysosomes, 23% in late endosomes and 6% in early endosomes. At steady state, LAMP-1 is present in early endosomes at an insignificant level. However, a comparison of the curves in figure 4.1.33 with those for the two scenarios as in Introduction 3.4 (see figures 3.4.1 and 3.4.2) allowed the unambiguous conclusion that LAMP-1 enters the endocytic pathway via early endosomes.

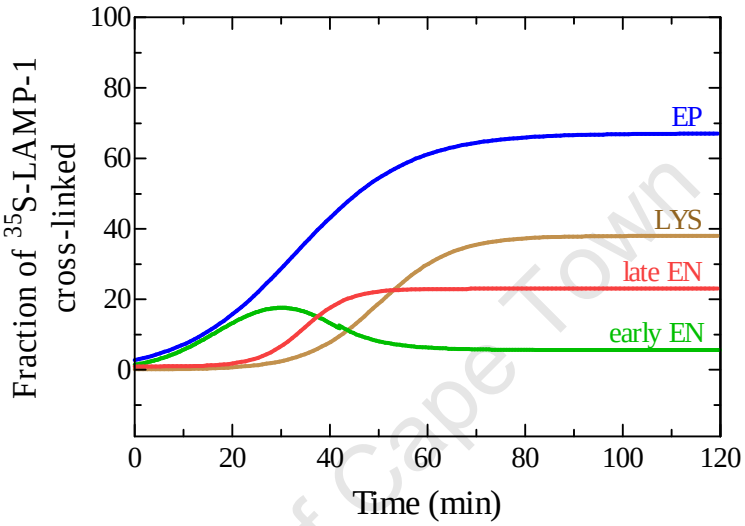

Figure 4.1.33 Comparison of the entry of ^{35}S-LAMP-1 into individual compartments. The curves obtained for the experiments where ^{35}S-LAMP-1 was cross-linked in the endocytic pathway (EP), lysosomes (LYS) and early endosomes (early EN) were used to calculate the curve for ^{35}S-LAMP-1 entry into the late endosomes (late EN) by subtracting the sum of the early endosomal and lysosomal curves from that of the endocytic pathway. At steady state, the LAMP-1 level was at about 23% in late endosomes.

4.1.4.6 Technical limitations of the experimental system

Kinetic experiments were repeated several times because of technical limitations. The number of time-points that could be accommodated per experiment was limited to 9. The inter-experimental variation in LAMP-1 cross-linking at a single time-point was ±12% on average. It was as low as ±5% when the LAMP-1 signal and the cross-linked fraction were high and as high as ±20% when the LAMP-1 signal and the cross-linked fraction were low. This variability in the variation of cross-linking may find an explanation in the equation used to calculate the fraction of cross-linking: Y = [1 - (S-X)/(T-X)] * 100, where Y = the fraction of cross-linked LAMP-1 (%), X = lane background (dpm), S = soluble LAMP-1 (dpm) from the cross-linked sample, T = soluble LAMP-1 (dpm) from the non-cross-linked sample (total LAMP-1). From the equation, the amount of soluble LAMP-1 (dpm) in the cross-linked (S) and non-cross-linked (T) samples determines the fraction of LAMP-1 cross-linked (Y). Any variation in lane background (X) will affect the accuracy with which the effective soluble LAMP-1 (S and T) is determined. To examine the effect of lane background (X) on Y, theoretical curves were simulated for a specified range of lane background (X) values at low and high levels of LAMP-1 signal and cross-linking. Curves were generated for two scenarios with comparable levels of cross-linking (≤10%), but different levels of LAMP-1 signal:

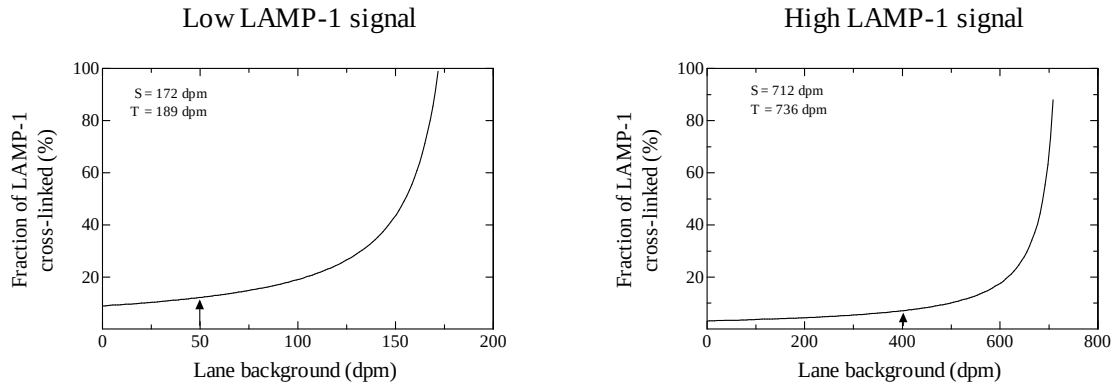

From these simulations it can be concluded that there is a critical point (arrows) above which the fraction of cross-linking (%) becomes sensitive to variation in lane background. The cross-

linked fraction is more sensitive to lane background when the LAMP-1 signal is low. The following curves were generated for two scenarios with comparable levels of total LAMP-1 signal, but different levels of cross-linking:

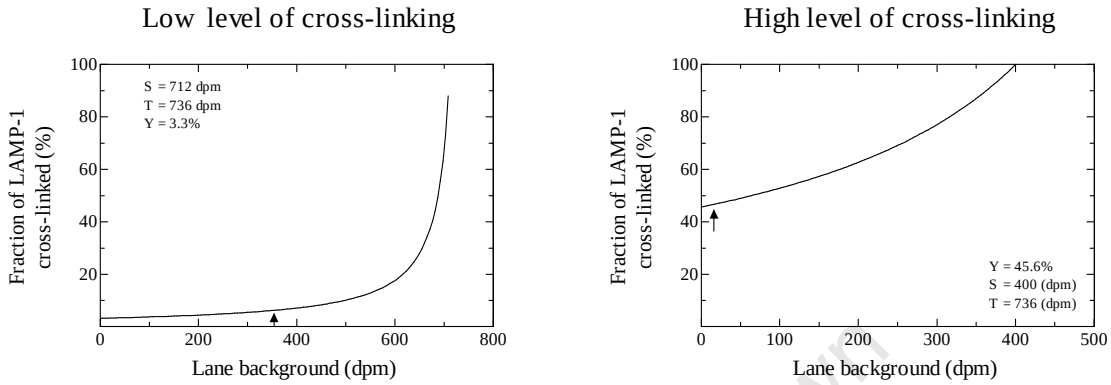

High levels of cross-linking are more sensitive to lane background than low levels of cross-linking. Lane background therefore probably contributed to the high degree of variation in Y (±15 to ±20%) observed during the initial time points when cross-linking was low, mainly due to low LAMP-1 signal. However, considerable variation in Y was also observed when cross-linking was low and LAMP-1 signal was high, for example, during the later time points of the experiment when LAMP-1 was cross-linked in early endosomes. When the cross-linked LAMP-1 fraction is low, the difference in T and S is small even though the LAMP-1 signal in general is high and so resolution would be compromised. Lane background was sometimes affected by cross-linking. In such cases, lane background for cross-linked samples (X_1) was observed to be lower than lane background for non-cross-linked samples (X_2). This could be explained by the cross-linking of non-specific proteins. This difference in lane background sometimes resulted in negative cross-linking. Negative cross-linking comes about when $(S-X_1) > (T-X_2)$. This will be the case when $S \sim T$ and $X_1 > X_2$. By repeating the cross-linking of LAMP-1 in a particular compartment in several experiments, a sufficient number of reproducible points from independent samples were obtained to generate a curve through which the kinetics of LAMP-1 trafficking could be determined.

4.2 CD-MPR

The CD-MPR is an example of a protein that behaves differently to LAMP-1 in terms of the kinetics with which it enters early endosomes, lysosomes or the endocytic pathway. It is functionally distinct and has a different steady-state distribution from LAMP-1. The CD-MPR mediates delivery of lysosomal enzymes from the TGN into the endocytic pathway. LAMP-1 is predominantly localised to lysosomes whereas the CD-MPR is predominantly localised to the TGN and the endosomes, in particular, the late endosome. Newly-synthesised ^{35}S-methionine-labelled CD-MPR was chased for various periods and trapped by HRP–DAB cross-linking in early endosomes, lysosomes or the endocytic pathway. Rabbit antiserum against bovine-liver CD-MPR, known to cross-react with mouse CD-MPR, was used to immunoprecipitate the CD-MPR from the soluble fraction of a cell lysate to quantitate the complimentary fraction of ^{35}S-CD-MPR that became trapped. Accordingly, the conditions for quantitative detection of the CD-MPR had to be optimised.

4.2.1 Cross-reactivity of anti-bovine-CD-MPR serum with mouse CD-MPR

First I had to establish whether rabbit anti-bovine-CD-MPR serum was able to cross-react with mouse CD-MPR in P388D$_1$ cells. This was done via Western blotting (figure 4.2.1).

The CD-MPR has a molecular weight of about 46 kDa. The band in the 50 kDa position was presumed to be the CD-MPR, confirming that the rabbit anti-bovine-CD-MPR serum was able to cross-react with mouse CD-MPR.

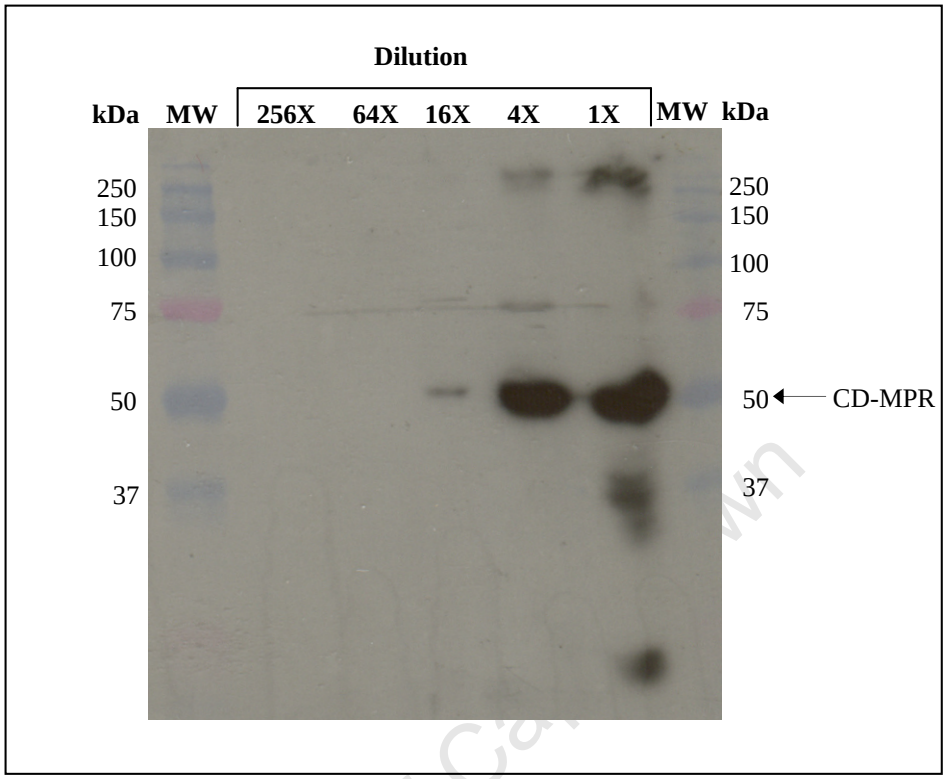

Figure 4.2.1 Cross-reactivity of rabbit anti-bovine-CD-MPR serum with mouse CD-MPR. A post-nuclear supernatant (PNS) was prepared as in Methods 6.5.2 at $20 \cdot 10^6$ cells/ml. The PNS was lysed at 0.5% Triton X-100 and diluted as indicated: 4X, 16X, 64X, 256X. Proteins were resolved on a non-reducing 10% SDS-polyacrylamide gel and subjected to Western blotting, see Methods 6.7.2. The blot was incubated with anti-bovine-liver-CD-MPR rabbit serum, diluted 100-fold. The primary antibody was detected by HRP-linked donkey anti-rabbit whole antibody (cat. no. NA934, Amersham) diluted 5000-fold. The blot was developed with an ECL detection system. The arrow indicates the CD-MPR.

4.2.2 Development of quantification methods for the ^{35}S-CD-MPR

Quantification of soluble newly-synthesised ^{35}S-CD-MPR from the cross-linking assay was to be done by immunoprecipitation. This required an immunoprecipitation assay that was specific and quantitative. Initially an unoptimised immunoprecipitation assay was set up, using the LAMP-1 immunoprecipitation assays and methods from the literature as a guide. It was generally performed as follows, with details and variations specified in the legends of figures where necessary: P388D$_1$ cells were metabolically labelled, washed 3 times with 10 ml HeSBSA and lysed in lysis buffer. After preclearing by centrifugation at 8 000 g, the detergent-soluble fraction of the lysate was incubated with anti-bovine-CD-MPR antiserum. The ag-ab complexes were removed from solution by incubation with protein-A agarose beads for 2 h at 4°C. The beads were washed 6 times with 1 ml washing buffer and then once with 1 ml dH_2O. The ag-ab complexes were eluted from the beads, analysed by 10% SDS-PAGE, followed by autoradiography and densitometric analyses using InstantImager software. In an attempt to develop the immunoprecipitation assay, a minimum metabolic labelling time required to give a measurable signal was determined in figure 4.2.2. In light of the different elution profiles obtained for LAMP-1 when either SDS-reducing sample buffer or Gly/HCl, pH 2.5 was used to elute the ag-ab complexes, the effect of these two elution buffers on the elution of the CD-MPR was compared in figure 4.2.2. Two bands (labelled I and II), one on either side of the 45 kDa band, were observed and assumed to be the CD-MPR. By using InstantImager software, regions of interest in the gel lanes were scanned and quantified. A region where counts were comparable to background (between the 24 and 20 kDa markers (box)) was designated as lane background. Different levels of lane background were observed for the two elution buffers. In the lanes where the metabolic labelling was 1 h, the levels of background were 18% (sample buffer) and 12.5% (Gly/HCl) of the specific CD-MPR signal (box). The percentage of background decreased with increasing times of metabolic labelling.

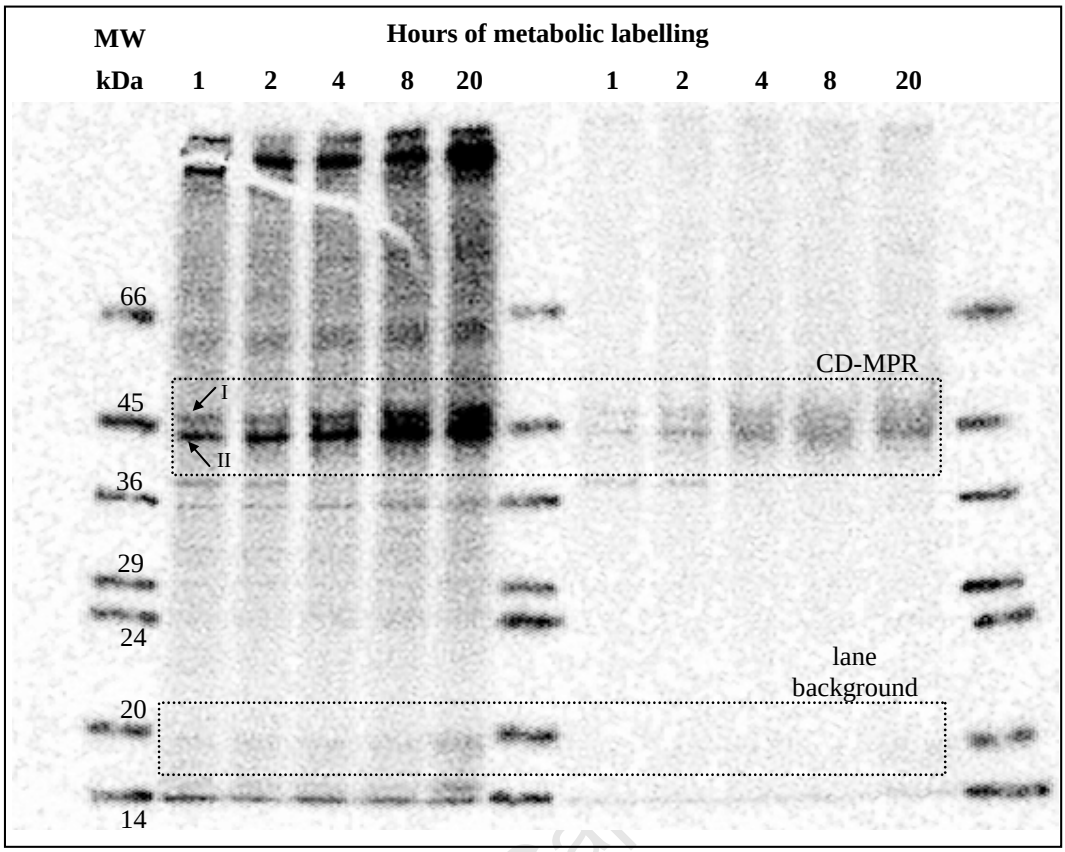

Figure 4.2.2 Immunoprecipitation of CD-MPR after increasing times of metabolic labelling. P388D$_1$ cells were metabolically labelled with ^{35}S-methionine at 100 μCi/ml (specific-activity of 1000 Ci/mMole) for 1 h, 2 h, 4 h, 8 h and 20 h, as indicated. The CD-MPR was immunoprecipitated from the soluble fraction of the cell lysate using anti-CD-MPR serum and protein-A beads. Bead fractions were split in half. Ag-ab complexes were either eluted with SDS-reducing sample buffer or Gly/HCl, pH 2.5. Proteins were analysed by SDS-PAGE, followed by autoradiography. Bands labelled I and II were presumed to be the CD-MPR. **Method:** Cell samples from each labelling time were washed and then lysed at ~$20{\cdot}10^6$ cells/ml imidazole lysis buffer (see Reagents 7.5)**.** The lysate was precleared twice by centrifugation at 8 000 g for 15 min. The precleared lysate ($3.26{\cdot}10^6$ cells ≈ 170 μl) was incubated with 10 μl anti-CD-MPR ab, overnight at 4ºC, followed by incubation with protein-A agarose beads (100 μl) for 2 h at 4ºC. Beads were washed 8 times with 1 ml imidazole washing buffer and once with 1 ml dH_2O. Bead fractions were split in half (50 μl) during the 5th wash. Proteins were eluted with 1X reducing SDS-sample buffer or 0.1 M Gly/HCl, pH 2.5: two rounds (60 μl and then 40 μl) of 1X reducing SDS-sample buffer for 5 min at 95°C, or two rounds (50 μl and then 24 μl) of 0.1 M Gly/HCl, pH 2.5 for 5 min at room temperature. The pH was subsequently neutralised with 2 M Tris, pH 8 (0.6 μl Tris / 10 μl Gly/HCl). Samples were analysed by SDS-PAGE, followed by autoradiography for 19 h. (Positions of molecular-weight markers were traced with ^{14}C-labelled ink.)

Since the reducing sample buffer gave a higher yield and the variation in lane background was within experimental error, the reducing sample buffer was chosen as the provisional elution buffer. 1 to 2 h of metabolic labelling yielded a sufficient signal for further experiments.

4.2.2.1 The specificity of the immunoprecipitation assay

The specificity of the immunoprecipitation of the CD-MPR was improved by the introduction of two additional centrifugation steps and the selection of different lysis and elution conditions. This resulted in the reduction of non-specific proteins.

To determine the specificity of the CD-MPR immunoprecipitation assay (figure 4.2.3)**,** the assay was performed in the presence of ab-serum (lanes 1 & 2), in the presence of control rabbit serum (lane 3) and in the absence of serum (lane 4). Two bands, similar to those assumed to be the CD-MPR in figure 4.2.2, were observed in lanes 1, 2 and 3 (box, arrows labelled I and II). These bands will henceforth be referred to as band I and band II. The observation of band II in lane 4 implied that at least a fraction of this band was due to non-specific binding of labelled protein in the soluble fraction of the lysate to the beads. The observation of both bands I and II in lane 3 implied that at least a fraction of these bands was due to non-specific binding of labelled protein in the soluble fraction of the lysate to proteins in rabbit serum. An additional centrifugation step (↺: 8 000 g for 10 min at 4°C) prior to the introduction of the beads (lane 1) resulted in a reduction, but not complete removal, of bands I and II. The reduction of band II that corresponded to the non-specific band II observed in lane 4 was confirmed in figure 4.2.4. The introduction of a higher speed centrifugation step (100 000 g for 30 min) before the immunoprecipitation assay precleared the lysate more efficiently in figure 4.2.5. The intensity of the non-specific bands I and II was reduced, when compared to figure 4.2.3. A smear (brackets & dashed line in profile) became visible behind band II in the ab lane and was absent from the control sera lanes.

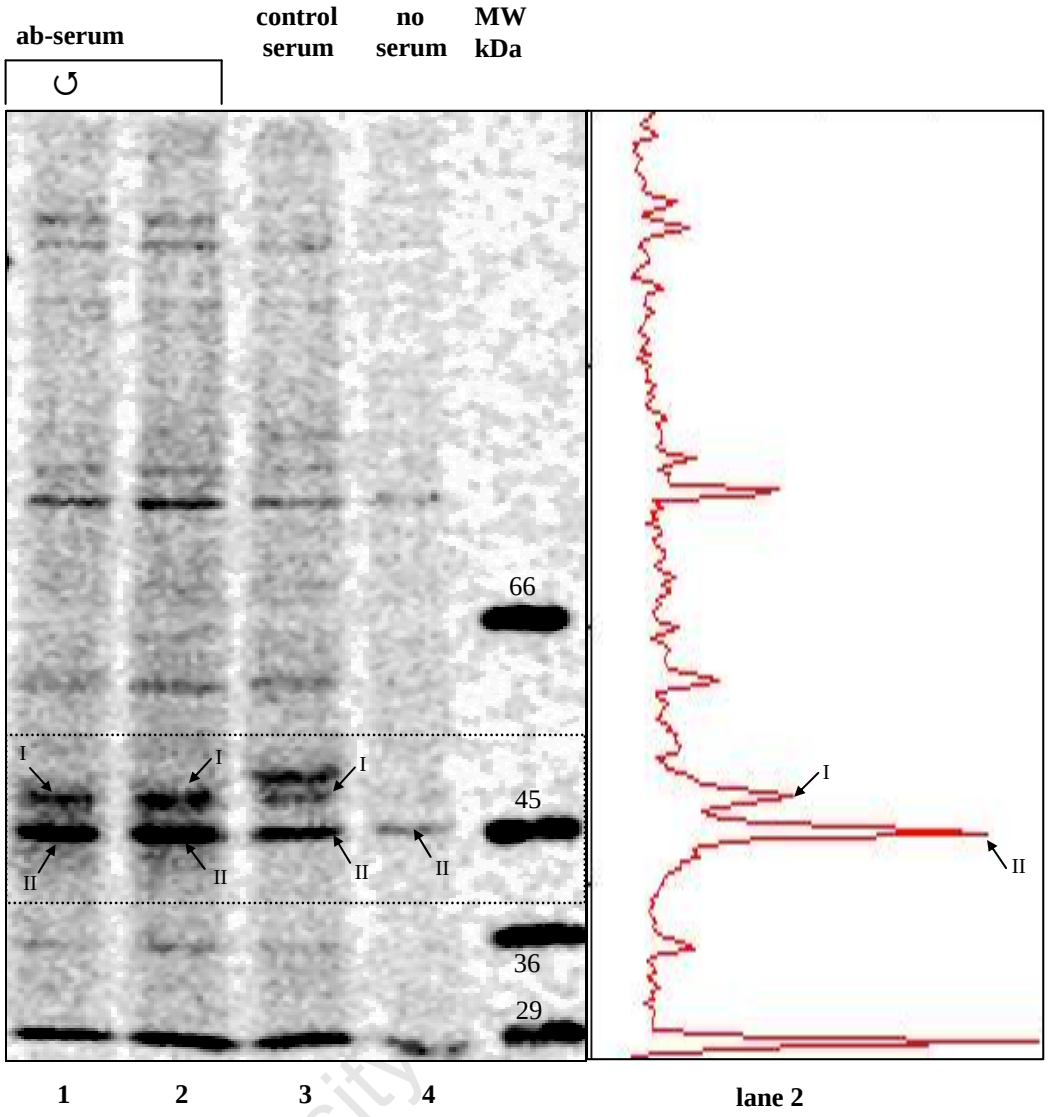

Figure 4.2.3 Specificity of the CD-MPR immunoprecipitation assay. The soluble fraction of metabolically labelled cell lysate was incubated with anti-CD-MPR serum (lanes 1 and 2), control rabbit serum (lane 3) and without serum (lane 4). To remove non-specific aggregates, the mixture for lane 1 was subjected to centrifugation before the introduction of the beads. Ag-ab complexes were collected by protein-A beads, eluted with SDS-reducing sample buffer and subjected to SDS-PAGE and InstantImager analyses. The lane profile for lane 2 was obtained through InstantImager scanning software and aligned to the lane by eye. At least a fraction of bands labelled I and II, previously presumed to be the CD-MPR, is non-specific. **Method:** Cells were metabolically labelled for 1 h. The labelled protein was then chased for 1 h. Cell lysate was prepared as in figure 4.2.2, except that cells were lysed at a 2.5-fold higher concentration ($50 \cdot 10^6$ cells/ml). For lanes 1 and 2, 10 µl of anti-CD-MPR serum was incubated for 1 h at 4°C with 40 µl ($2 \cdot 10^6$ cells) of detergent-soluble cell lysate made up to a final volume of 180 µl with imidazole immunoprecipitation buffer (see Reagents 7.5). For lane 3, control rabbit serum was used and for lane 4, no serum was used. For lane 1, an additional centrifugation step (↺: 8 000 g for 10 min at 4°C) was performed prior to the introduction of the beads. Ag-ab complexes were removed from solution with 50 µl protein-A beads which were then washed 5 times with 1 ml imidazole washing buffer (see Reagents 7.5) and once with 1 ml dH_2O. Proteins were eluted from the beads with SDS-reducing sample buffer and processed as in figure 4.2.2.

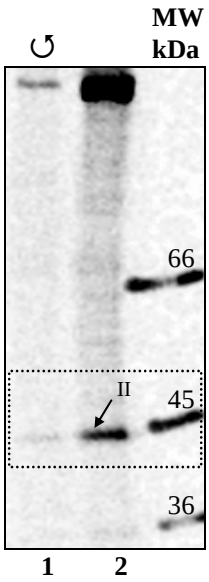

Figure 4.2.4 Removal of non-specific band II by centrifugation. The immunoprecipitation was simulated in the absence of serum (lane 2). For lane 1, an additional centrifugation step (↺: 8 000 g for 10 min at 4ºC) was performed prior to the introduction of the beads. A comparison with lane 2 and lane 4 in figure 4.2.3 suggested that the fraction of band II that was due to non-specific binding of proteins in the soluble fraction of the lysate to the beads could be removed by centrifugation.

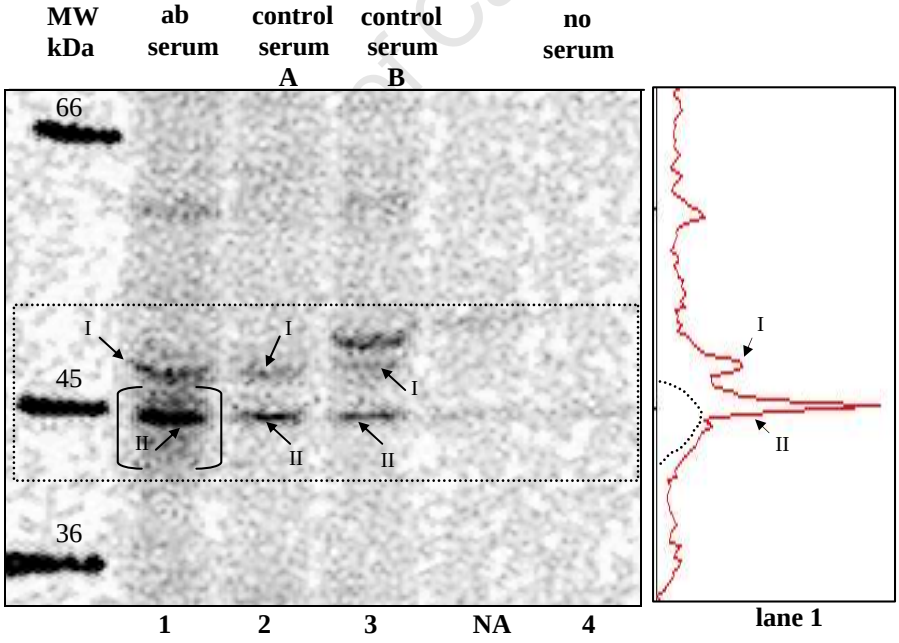

Figure 4.2.5 Immunoprecipitation of CD-MPR after a high-speed preclearing centrifugation step. Cell lysate was prepared as in figure 4.2.3, except now the cell lysate was precleared by centrifugation as follows, once at 8 000 g for 15 min and once at 100 000 g for 30 min at 4°C. The immunoprecipitation was performed with ab serum (lane 1), two different control sera (A and B, lane 2 and 3) and no sera (lane 4). Samples were processed and analysed as in figure 4.2.3. A smear (brackets and dashed line in profile) became visible behind band II in lane 1 and was absent from the control sera lanes. Band II was also more intense in lane 1. This smear and at least a fraction of band II appeared to be the CD-MPR. (NA: not applicable)

The CD-MPR is glycosylated and thus a broad band was not unexpected. The smear and at least part of band II thus appeared specific. To further improve the specificity of the immunoprecipitation assay a different set of lysis conditions was tested (figure 4.2.6). Cells were lysed in a Tris lysis buffer (CD-MPR lysis buffer, see Reagents 7.5) with additional protease inhibitors and gentle mixing overnight at 4°C**.** While PMSF is just a ser and cys protease inhibitor and leupeptin is a trypsin inhibitor, the Complete Protease Inhibitor Cocktail Tablet contains inhibitors of a broad range of ser-, cys- and metalloproteases, as well as calpains. The smear (bracket) surrounding band II (lane 3) was more intense relative to the non-specific bands I and II, when compared to the previous lysis conditions (figure 4.2.5). Extending the ag-ab incubation period had no effect on the relative intensities of the specific band (smear) and the non-specific bands I and II, lane 3 (1 h ag-ab incubation) versus lane 4 (16 h ag-ab incubation). The 16 h incubation was chosen because it was more convenient. Centrifugation after 16 h ag-ab incubation seemed to remove some background, though not significantly (lane 4 versus lane 5).

In an attempt to further optimise the elimination of the non-specific band II, the fact that it may be a reduced product of a higher molecular-weight protein was considered. If so, it could be shifted to a higher molecular-weight position by performing the elution under non-reducing conditions. To examine the effect of non-reducing elution conditions on the relative intensities of the specific and non-specific bands, the CD-MPR immunoprecipitate was eluted from the beads and analysed with non-reducing sample buffer **(**figure 4.2.7). The contaminating bands disappeared for the control serum lane 2 (arrow). In addition to the broad band in the 45 kDa range (box), another broad band in the ~90 kDa range (box) appeared. This was indicative of the CD-MPR dimer and, was not unexpected since interchain disulphide bonds can be formed during the solubilisation process (Li *et al.*, 1990).

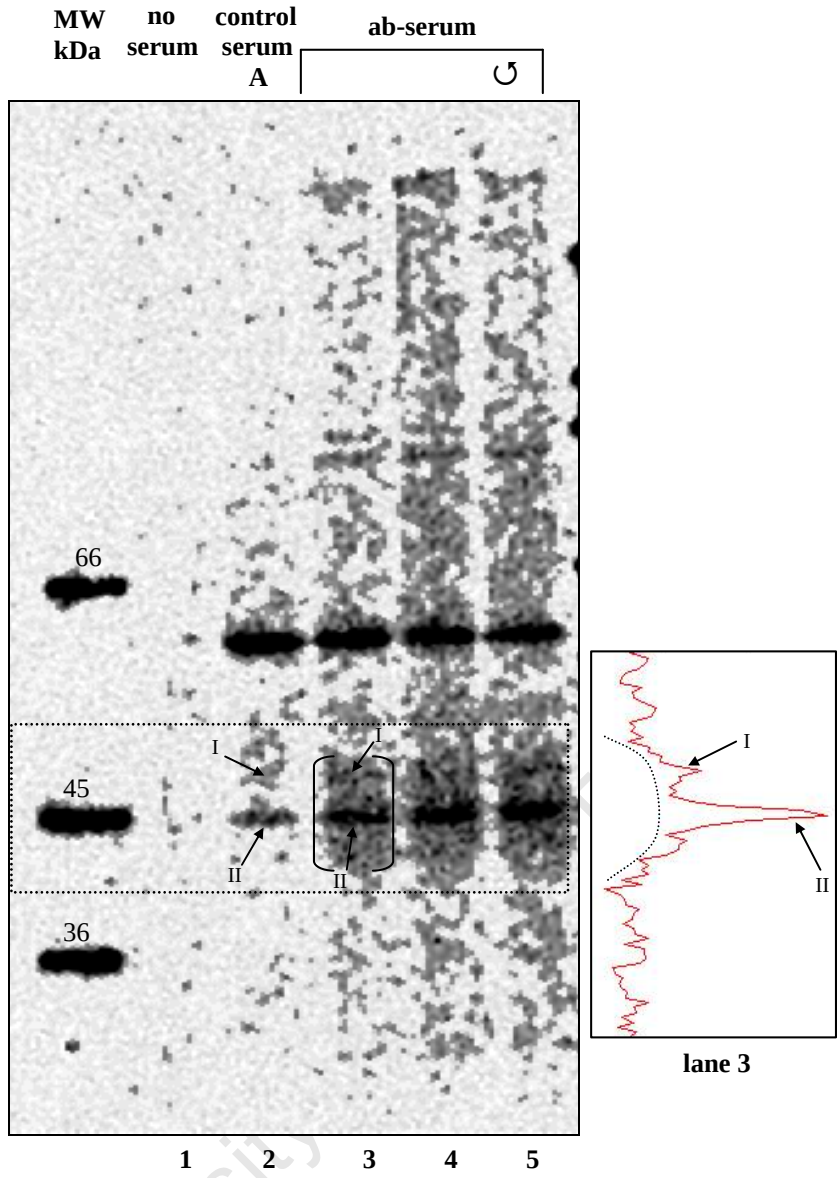

Figure 4.2.6 Immunoprecipitation of CD-MPR after different lysis conditions. Cells were metabolically labelled for 2 h and the labelled protein was chased for 1 h. For lysis, cells were incubated at $50 \cdot 10^6$ cells/ml in a Tris lysis buffer (CD-MPR lysis buffer, see Reagents 7.5) with gentle mixing overnight at 4°C, followed by centrifugation once at 8 000g for 15 min, to remove the major fraction of the insoluble material, and once at 100 000 g for 30 min, as in figure 4.2.5. The immunoprecipitation assay was performed in the absence of serum (lane 1), presence of contol serum (lane 2) or in the presence of ab-serum (lanes 3, 4 and 5). For lanes 1, 2 and 3 the incubation was 1 h and for lanes 4 and 5, 16 h. For lane 5 an additional centrifugation (↺: 8 000 g for 10 min at 4ºC) step was introduced prior to the addition of the beads. The ag-ab complexes were processed and analysed as in figure 4.2.3, except that 5 µl (instead of 10 µl) ab-serum or control serum was used and beads were washed with a Tris washing buffer (CD-MPR washing buffer, see Reagents 7.5) instead of imidazole washing buffer. The smear behind band II (brackets and dashed line in profile) was more intense. The non-specific band I was reduced to negligible levels.

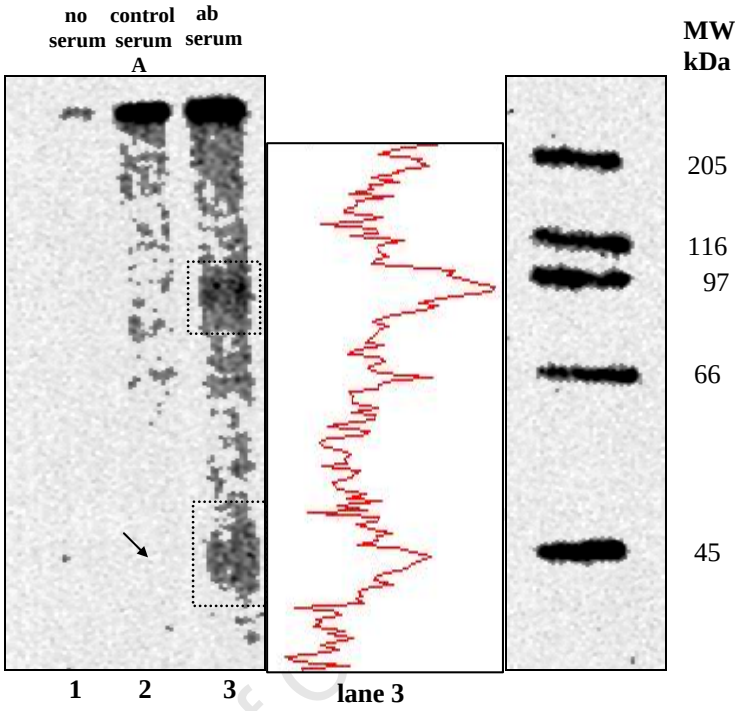

Figure 4.2.7 CD-MPR immunoprecipitate analysis under non-reducing conditions. Cells were metabolically labelled for 2 h, followed by a chase for 2 h. Cell lysate was prepared and the immunoprecipitation performed as in figure 4.2.6. The cell lysate was incubated with ab for 16 h and the ag-ab incubation mixture was precleared by centrifugation (8 000 g for 10 min). Non-reducing conditions were used for both elution and subsequent SDS-PAGE. The lane profile was obtained through InstantImager scanning software. The boxes indicate the possible two forms of the CD-MPR. The arrow shows the absence of non-specific bands.

The two bands (boxes) obtained under non-reducing conditions were fairly specific. However, such conditions were not ideal. Future experiments would be based on very low counts for which gel bands would have to be cut out and solubilised for counting. Cutting out two bands would require more hands-on manipulation and would thus increase experimental error. The possible dimer would therefore have to be reduced. When the CD-MPR immunoprecipitate was reduced by the addition of β-mercapto-ethanol after its elution from the beads with non-reducing sample buffer (figure 4.2.8), the 90 kDa band was partially reduced to a 45 kDa band. This confirmed that at least some of the 90 kDa band consisted of a non-reduced dimer of the CD-MPR. The fact that not all protein at the 90 kDa position were reduced, implied either incomplete reduction or the presence of non-specific protein. The contaminating bands (arrows) in the 45 kDa range of the control-serum lane reappeared under reducing conditions. The results therefore suggested that elution with sample buffer (reducing or non-reducing) was not suitable. In an attempt to avoid the elution of these contaminating proteins, the immunoprecipitation products were eluted with a milder non-reducing buffer (0.1 M Gly/HCl, pH 2.5). Samples were then separated on SDS-PAGE under non-reducing or reducing conditions (figures 4.2.9 & 4.2.10). Complete reduction of the protein in the 90 kDa range was observed. Results confirmed the band below the 97 kDa position was a dimer of the 45 kDa band. The contaminating bands in the 45 kDa range (control-serum lane 2) were negligible. Background in this region remained constant under non-reducing and reducing conditions. When the two non-reducing elution buffers were compared under reducing SDS-PAGE conditions, the contaminating bands in the control-serum lanes contributed 41% to the specific signal in the ab-serum lane when sample buffer was used (figure 4.2.8) and 20 – 25% when Gly/HCl, pH 2.5 was used (figure 4.2.9 and figure 4.2.10). Gly/HCl was thus a more specific elution buffer and was chosen for subsequent experiments. It must be noted, however, that the effective yield of the specific signal was 25% less when Gly/HCl was used.

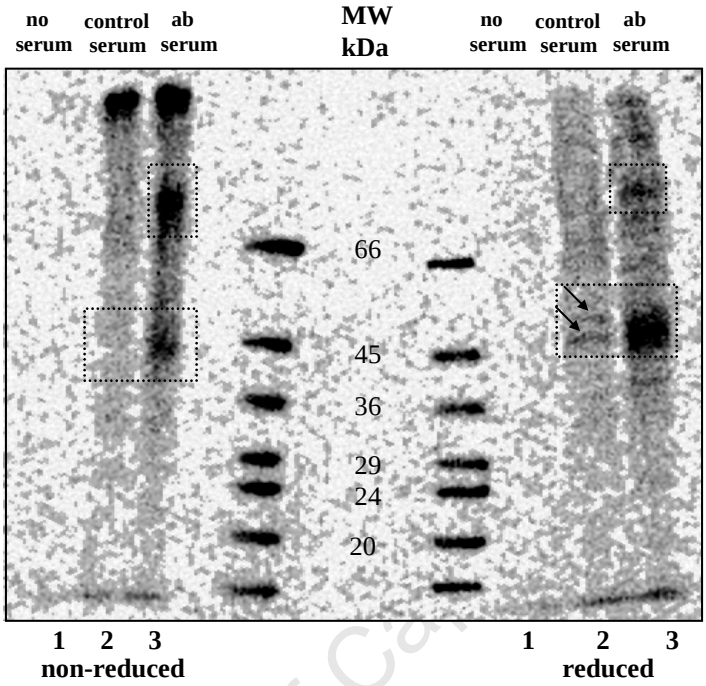

Figure 4.2.8 CD-MPR immunocomplex analysis under non-reducing or reducing conditions. Cell lysate was prepared and immunoprecipitation performed as in figure 4.2.6 in the absence of serum (lane 1) or in the presence of control serum (lane 2) or ab serum (lane 3). CD-MPR immunocomplexes were eluted from the beads with non-reducing sample buffer and resolved using SDS-PAGE under non-reducing or reducing conditions. The gel was exposed to the InstantImager and subjected to densitometric analyses.

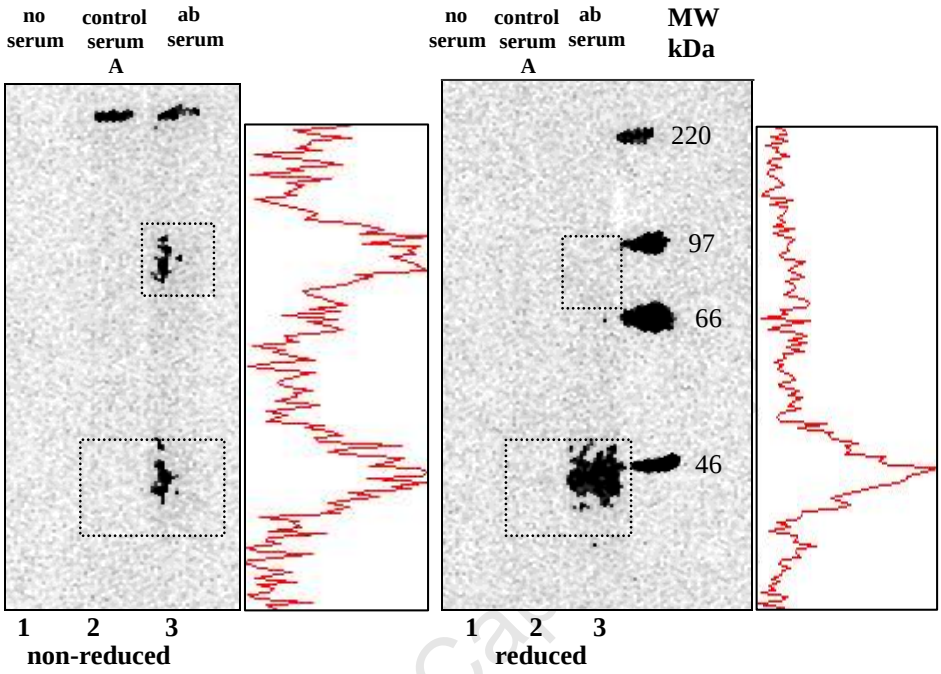

Figure 4.2.9 CD-MPR elution with a gentler non-reducing buffer. Cell lysate was prepared and immunoprecipitation performed as in figure 4.2.6. The ag-ab complexes were eluted with a gentler non-reducing buffer (0.1 M Gly/HCl, pH 2.5). The eluted products were resolved using SDS-PAGE under non-reducing or reducing conditions. The gel was exposed to the InstantImager and subjected to densitometric analyses.

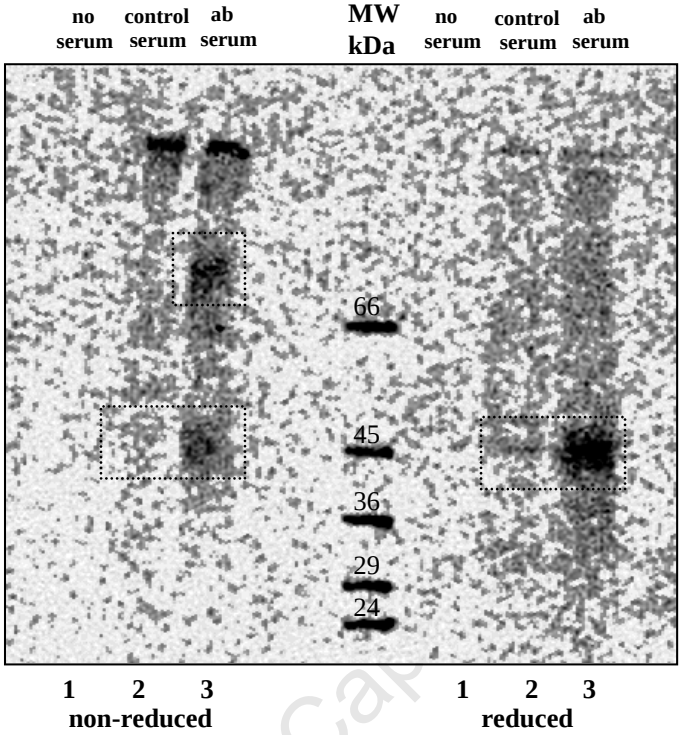

Figure 4.2.10 A repeat of figure 4.2.9. The band pattern in figure 4.2.9 was reproduced.

4.2.2.2 Quantitative immunoprecipitation of the CD-MPR

The immunoprecipitation conditions derived above and summarised in Methods were used to determine the range of protein concentration that would generate a linear dose-response of the immunoprecipitated CD-MPR. Fixed amounts of protein-A beads (50 µl) and anti-CD-MPR serum (5 µl) were used to precipitate CD-MPRs from increasingly higher concentrations of this antigen. Two different methods were compared for the quantification of the CD-MPR, namely InstantImager software analyses and scintillation counting. Immunoprecipitation products were divided into two sets, each of which was resolved on separate gels. One gel was dried and exposed to the InstantImager (figure 4.2.11). The specific signal of the CD-MPR was quantitated using InstantImager software. A region above the 20 kDa marker (box) was chosen as lane background on the basis that radioactivity in this region was consistently lower than the rest of the lane. Lane background was subtracted from the corresponding signal in the 45 kDa range (box) to obtain the specific signal due to the CD-MPR. After lane background was removed from corresponding regions A and B in control-sera lanes 1 and 8, regions A and B still contributed about 17% of the comparable specific CD-MPR signal in lanes 2 and 7, respectively. This was probably due to non-specific labelled proteins that were bound by non-specific proteins in the polyclonal anti-serum. Gel pieces corresponding to the CD-MPR signal and suitable lane background (boxes) were excised and processed for scintillation counting. Data obtained from scintillation counting were analysed similar to those obtained using the InstantImager. The two detection methods were reproducible as can be seen from the linear relationship between the data obtained from the respective methods (figure 4.2.12). The scintillation counter yielded 180-fold higher counts per min than the InstantImager as was determined from the slope of the graph. The excision of CD-MPR gel bands and scintillation counting was chosen as the method for ^{35}S-CD-MPR quantification because of its 180-fold higher detection sensitivity that would result in better experimental resolution.

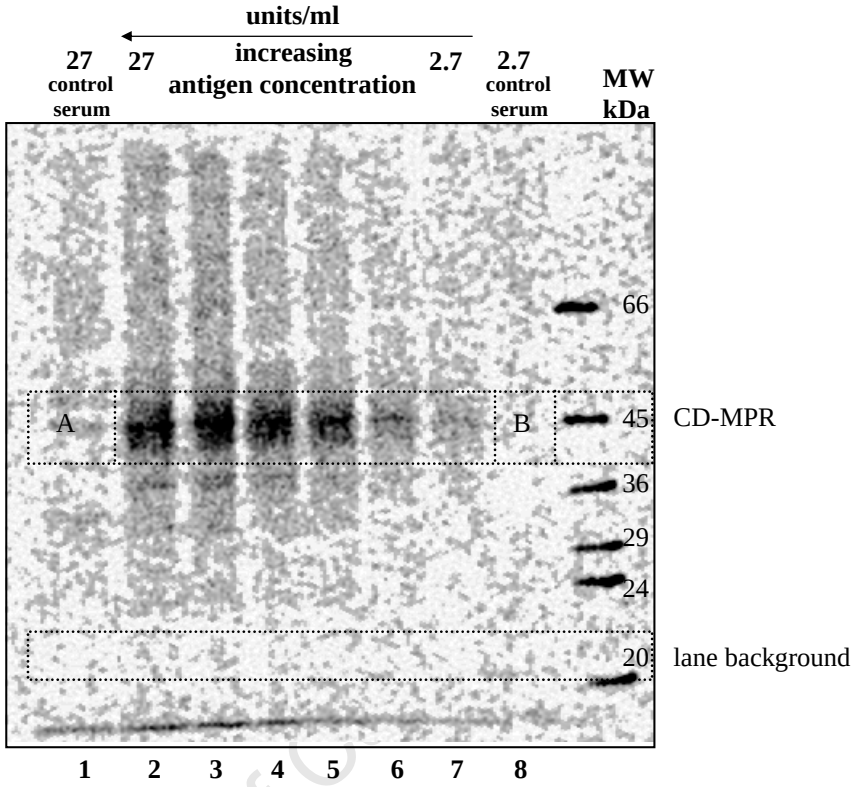

Figure 4.2.11 Quantification of immunoprecipitated ^{35}S-CD-MPR. P388D$_1$ cells were metabolically labelled with ^{35}S-methionine for 2h and lysed to prepare ^{35}S-CD-MPR. Increasing amounts of the detergent-soluble fraction of the cell lysate were added to the immunoprecipitation assay in order to apply an increasing concentration of ^{35}S-CD-MPR (indicated as the antigen concentration, where 1 unit of antigen is that amount of ^{35}S-CD-MPR obtained from 10^6 cells). ^{35}S-CD-MPR was immunoprecipitated with a constant amount of ab serum (5 μl) and protein-A beads (50 μl). In lanes 1 and 8 control rabbit anti-serum was used. The ag-ab complexes were processed as in figures 4.2.9 B and 4.2.10 B. The eluted products were divided into two sets, each of which was resolved on separate gels. One gel was dried and exposed to the InstantImager, as in this figure. The CD-MPR signal for the corresponding antigen concentrations was determined from the dried gel using InstantImager software. The other gel was processed wet. The InstantImager generated image was used to determine the position of the CD-MPR relative to molecular-weight markers. These parameters were used to excise the CD-MPR band from the dried and silver-stained wet gels for solubilisation and scintillation counting. The results were analysed graphically as illustrated in figures 4.2.12 and 4.2.13.

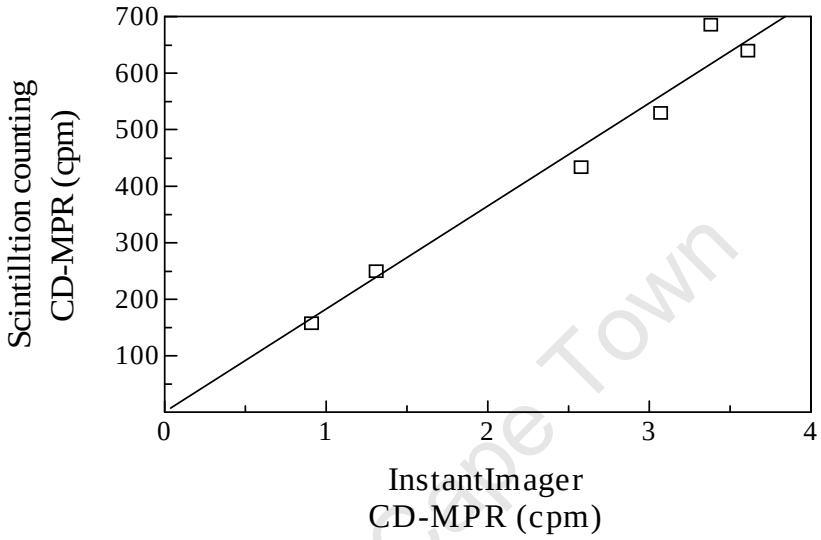

Figure 4.2.12 Comparison of two methods for the quantification of immunoprecipitated CD-MPR, InstantImager scanning software versus scintillation counting. The ^{35}S-CD-MPR signal was determined from the dried gel that was exposed to the InstantImager (figure 4.2.11) using the InstantImager software. It was then processed for scintillation counting. The data obtained from the scintillation counter were plotted against the data obtained from the Imager. Results reflected a linear relationship with a slope of 182.1±5.9.

The second gel was processed and analysed in the wet state, in exactly the same way as the dried gel was for scintillation counting. The results obtained for the two independent gels and the two different detection methods were normalised against their respective maximum signal to allow direct comparison on the same graph (figure 4.2.13). Results obtained from the two different quantitation methods (squares) were more reproducible than results from two different gels (circles and open squares). A curve representing Michaelis-Menton kinetics was fitted to the data and generated a K_m of 6.04 units/ml. The response could be considered approximately linear up to an antigen concentration of about 6 units/ml. This concentration of antigen is equivalent to the concentration of CD-MPR in the detergent-soluble fraction of a cell lysate prepared at a concentration of $6 \cdot 10^6$ cells/ml. Pulse-chase experiments were designed such that the theoretical maximal concentration of the cells in the final sample is about $10 \cdot 10^6$ cells/ml. When cell loss due to washes in between experimental steps was factored in, the working cell lysate concentration range was most likely in the range of $6 \cdot 10^6$ cells/ml, within the linear dose-response range.

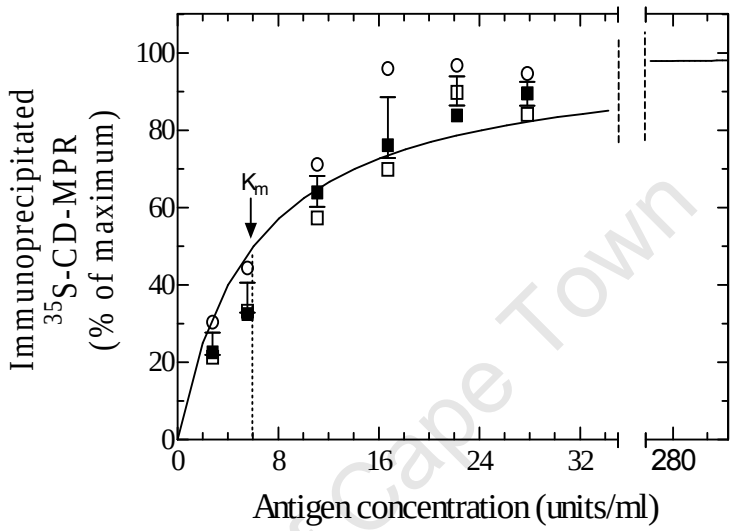

Figure 4.2.13 Optimisation of the cell-concentration range to be used for the quantitative immunoprecipitation of ^{35}S-CD-MPR. For direct comparison, the ^{35}S-CD-MPR signal for the corresponding antigen concentrations determined using InstantImager software (closed squares) or scintillation counting (open symbols - from two independent gels), as explained in figure 4.2.11, were normalised by expressing the individual values as a percentage of the maximum signal of immunoprecipitated ^{35}S-CD-MPR. The curve shows Michaelis-Menton kinetics with a K_m = 6.04 units/ml.

4.2.3 Biosynthetic pathway for the CD-MPR

Having established the conditions for the quantitative immunoprecipitation of the CD-MPR, the following experiments were performed to observe the pathway of newly-synthesised CD-MPR for the delivery of lysosomal enzymes into lysosomes. Conditions for quantitative localisation along the endocytic pathway, as were set up using NAGA and LAMP-1 (4.1.3.2), were applied to the kinetic experiments for the CD-MPR. To observe the kinetics of entry of newly-synthesised CD-MPR into the endocytic pathway, early endosomes or lysosomes, newly-synthesised CD-MPR was labelled with ^{35}S-methionine and chased through the endoplasmic reticulum, Golgi, TGN and into the endocytic pathway. The newly-synthesised ^{35}S-CD-MPR was trapped as it entered early endosomes, lysosomes or the endocytic pathway by HRP–DAB cross-linking (see Introduction 3.3 and Results 4.1.3.2). In control samples, the CD-MPR was not cross-linked. Samples were processed for the quantification of soluble ^{35}S-CD-MPR by using the optimised conditions as obtained in 4.2.2. The fraction of cross-linked ^{35}S-CD-MPR was then determined by comparing the soluble ^{35}S-CD-MPR of the cross-linked samples with that of the controls. The fraction of cross-linked ^{35}S-CD-MPR was plotted against time, where time zero was when the ^{35}S-methionine was added to the incubation medium.

4.2.3.1 The biosynthetic processing of newly-synthesised ^{35}S-CD-MPR

To determine the kinetics of processing of newly-synthesised ^{35}S-CD-MPR, the data of total newly-synthesised immunoprecipitable ^{35}S-CD-MPR (dpm) formed with time in the non-cross-linked fractions of all the kinetic experiments were combined into one graph, as in figure 4.2.14. CD-MPR expression levels and/or ^{35}S-methionine incorporation into mature protein were much lower than for LAMP-1. Even though the CD-MPR was metabolically labelled at five-fold higher concentrations of ^{35}S-methionine, it generally yielded lower counts (dpms). These data could be analysed in one of two ways.

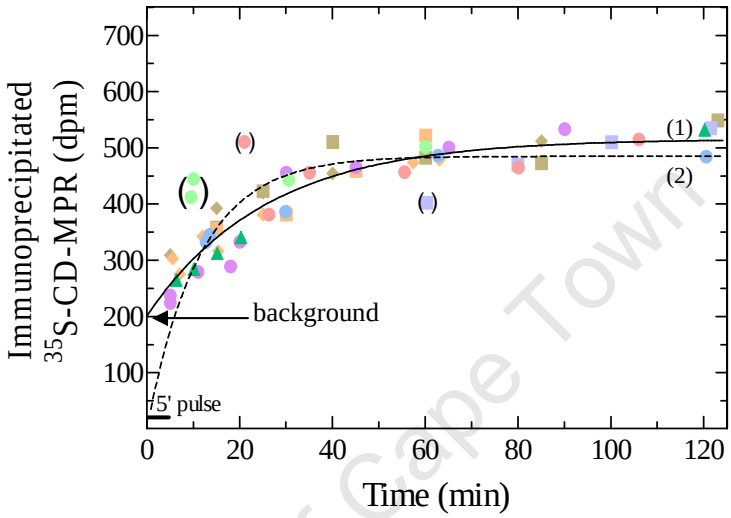

Figure 4.2.14 Biosynthetic processing of ^{35}S-CD-MPR. P388D$_1$ cells were starved in methionine-free medium for 30 min at 37°C. At time zero, ^{35}S-methionine was added at $5 \cdot 10^{-7}$ M (specific-activity = 1175 Ci/mmole) and cells were labelled for 5 min. ^{35}S-CD-MPR was then chased by replacing the ^{35}S-methionine-containing medium with unlabelled methionine-containing medium. Cells were washed and lysed. ^{35}S-CD-MPR was immunoprecipitated from the detergent-soluble fraction of the lysate, processed via SDS-PAGE and quantitated by scintillation counting (see Methods). Different coloured symbols refer to independent experiments. Since all experiments did not extend across the entire time-course, individual experiments were normalised to a best-fit steady state that started at approximately 60 min and averaged around 500 dpm. An exponential curve, with (1) or without (2) background, was manually fitted to the points. The data were compatible with a half-time of 8 (curve 2) or 18 (curve 1) min for the processing into immunoprecipitable CD-MPR.

When an exponential curve (figure 4.2.14, curve 1), allowing for background as a degree of freedom, was plotted through the data, as for LAMP-1, the 5 min pulse of ^{35}S-CD-MPR was processed within 60-80 min into mature immunoprecipitable ^{35}S-CD-MPR with a half-time of 18 min. With this type of analysis, a substantial background (arrow) is indicated by the curve. The background was that which remained after lane background was subtracted. It could probably be due to non-specific labelled proteins that bound to non-specific proteins in the polyclonal antiserum. Although the non-specific bands observed in figure 4.2.6 were predominantly removed after a change in the elution conditions and were only faintly visible in figure 4.2.11 (regions A and B, 17% of the ^{35}S-CD-MPR after a 2 h labelling period), depending on the labelling kinetics and the turnover time of the non-specific proteins compared to that of the CD-MPR, these non-specific proteins could potentially have been present at levels that influenced the CD-MPR count after a 5 min labelling period.

However, it is also possible that the substantial amount of signal detectable within 5 min could be specific. Figure 4.1.28 shows that a 5 min methionine pulse was incorporated into TCA-precipitable protein within 5 min. If the epitopes for the polyclonal anti-CD-MPR became available within this initial 5 min period, a specific signal could be expected at these early time points. In this scenario, a linear increase would start from zero (cf. figure 4.1.28) to be followed, after the end of the 5 min pulse, by a first-order process to steady state. If this was the case, subsequent processing occurred with a half-time of 8 min (figure 4.2.14, curve 2). This option (curve 2) was used to analyse my results.

4.2.3.2 Entry of ^{35}S-CD-MPR into the endocytic pathway

The endocytic pathway includes early endosomes, late endosomes and lysosomes. Based on previous studies, a steady-state presence of the CD-MPR has been observed in both early and late endosomes, predominantly the late endosomes, and has generally not been detected in lysosomes (see Introduction 3.2.2). Here, the kinetics of entry of newly-synthesised ^{35}S-CD-MPR into the endocytic pathway was observed by cross-linking ^{35}S-CD-MPR as it entered the endocytic pathway, see figure 4.2.15. This provides the time-course for how newly-synthesised ^{35}S-CD-MPR entered the endocytic pathway as a whole.

The data are compatible with a rapid (relative to ^{35}S-LAMP-1) entry of ^{35}S-CD-MPR into the endocytic pathway. Within the resolution allowed for by the scatter of the data, no early rise of cross-linked ^{35}S-CD-MPR could be observed. Maximum cross-linking had already been reached at 10 min (5 min after completion of the 5 min pulse). On average, the fraction of ^{35}S-CD-MPR that could be cross-linked in the endocytic pathway at steady state was about 42%. A comparative set of data was obtained with a different experimental approach. The CD-MPR was first labelled with ^{35}S-methionine and then chased to steady state. HRP was then internalised for the indicated times (figure 4.2.16) to indicate its progressive colocalisation with CD-MPRs at steady state. The highest fraction of CD-MPR that could be cross-linked once HRP had filled the entire endocytic pathway after about 60 min was about 30%. Within the experimental variation, this confirmed the previous value for the fraction of CD-MPR in the entire endocytic pathway at steady state. (It has been reported that 20% of intracellular CD-MPRs reside in the endocytic pathway of fibroblasts (Stein *et al.*, 1987a)).

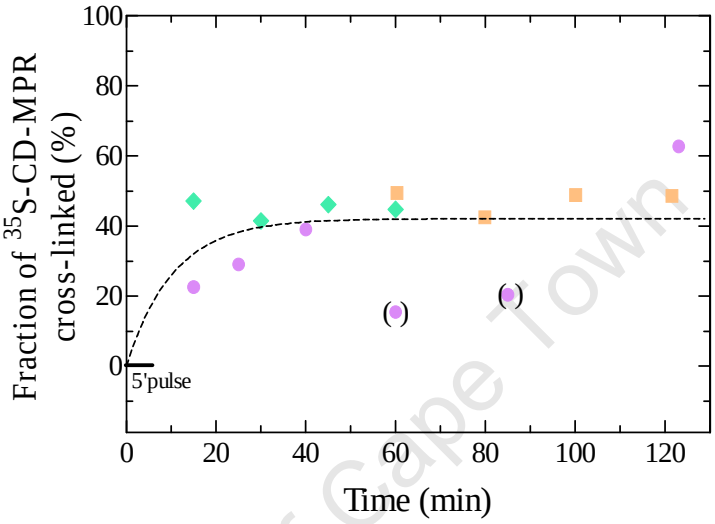

Figure 4.2.15 Delivery of newly-synthesised ^{35}S-CD-MPR to the endocytic pathway. The endocytic pathway of P388D$_1$ cells was filled with HRP (70 min). In the continued presence of HRP, cells were starved in methionine-free medium (30 min), metabolically labelled with ^{35}S-methionine for 5 min and further incubated in the presence of unlabelled methionine for the indicated times, when samples were taken and cooled on ice. One half of each sample was treated for HRP–DAB cross-linking. The other half served as a measure for total CD-MPR. In both cases, soluble (non-cross-linked) CD-MPR was quantified by scintillation counting of the appropriate band after SDS-PAGE of immunoprecipitated soluble CD-MPR (see Methods). Delivery of ^{35}S-CD-MPR into the endocytic pathway was expressed as the amount of cross-linked ^{35}S-CD-MPR, as a fraction of the total ^{35}S-CD-MPR, in each sample. The curve through the data points was fitted manually and suggested that the fraction of ^{35}S-CD-MPR cross-linked at steady state was about 42%. Different coloured symbols refer to independent experiments.

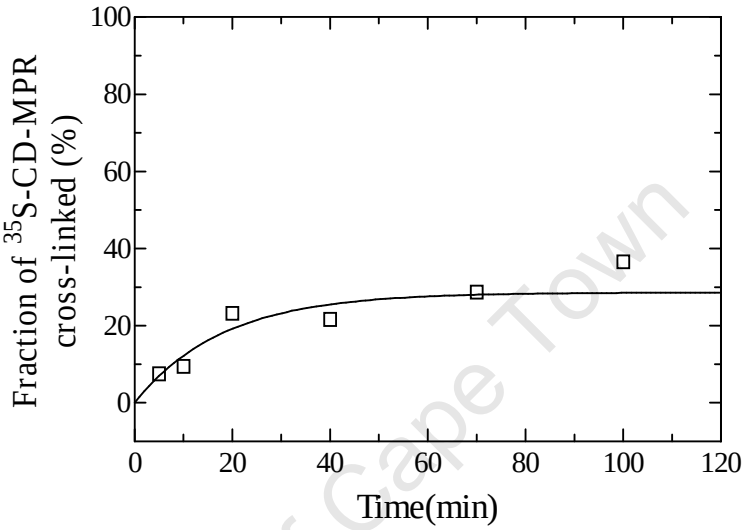

Figure 4.2.16 Colocalisation of endocytosed HRP with CD-MPR at steady state. P388D$_1$ cells were starved in methionine-free medium for 30 min and metabolically labelled with ^{35}S-methionine for 1 h. The ^{35}S-methionine-labelled proteins were equilibrated to steady-state levels by incubation of the cells in medium with unlabelled methionine at 37ºC for 1 h. HRP (3 mg/ml) was endocytosed for the indicated times, when samples were taken and cooled on ice. Samples were processed as in figure 4.2.15. The curve through the data points was fitted manually. Maximal colocalisation of HRP with CD-MPR was ~30% after about 60 min of HRP internalisation.

4.2.3.3 Entry of ^{35}S-CD-MPR into lysosomes

CD-MPRs have generally not been detected in lysosomes. It has thus been assumed that they do not enter lysosomes. However, rapid entry into and exit from lysosomes, such that they are present at undetectable levels at steady state, cannot be excluded. The kinetics of any possible entry of newly-synthesised ^{35}S-CD-MPR into lysosomes was followed by cross-linking protein in lysosomes and measuring any loss of ^{35}S-CD-MPR from the soluble lysate by immunoprecipitation (figure 4.2.17). Variation between duplicate immunoprecipitations from the same sample ranged from ±10% during initial time points to ±3% at later time points. The pattern of the data points is compatible with an initial increase in the fraction of ^{35}S-CD-MPR in lysosomes, followed by a decrease toward a very low steady-state level of about 5%. Results thus suggest a transient presence of the CD-MPR in lysosomes. When the entry of ^{35}S-CD-MPR into lysosomes was compared with its entry into the endocytic pathway (figure 4.2.19), it was observed that during the initial period of the time-course the two curves could be considered as being co-incident. This would suggest that the bulk of the ^{35}S-CD-MPR entered the endocytic pathway directly via lysosomes. Presumably, once the lysosomal enzymes have dissociated, the CD-MPRs would leave the lysosomes and enter the late endosomes from where they are recycled to the TGN. In view of the observed fast kinetics of the CD-MPR and the extent of experimental variation as a result of low CD-MPR expression levels, I have not been able to clearly resolve the passage of the CD-MPR through lysosomes.

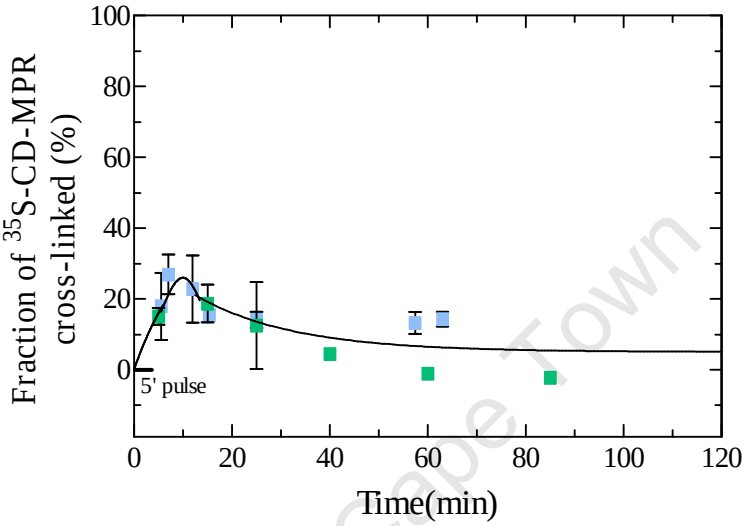

Figure 4.2.17 Delivery of newly-synthesised ^{35}S-CD-MPR into lysosomes. An HRP-uptake pulse (30 min) was chased into lysosomes for 40 min in P388D$_1$ cells. The cells were then starved in methionine-free medium for 30 min (HRP was chased for a total period of 70 min, equivalent to a delivery time of 100 min.), labelled with ^{35}S-methionine for 5 min, followed by further incubation in the presence of unlabelled methionine for the indicated times when samples were taken and cooled on ice. Samples were processed for measuring non-cross-linked ^{35}S-CD-MPR as in figure 4.2.15. Delivery of ^{35}S-CD-MPR into lysosomes was expressed as the amount of cross-linked ^{35}S-CD-MPR, as a fraction of the total ^{35}S-CD-MPR, in each sample. The curve through the data points was fitted manually and suggested that the fraction of ^{35}S-CD-MPR cross-linked at steady state was about 5%. Error bars indicate variation (SEM) between duplicate immunoprecipitations from the same sample. Different coloured symbols refer to independent experiments.

4.2.3.4 Entry of ^{35}S-CD-MPR into early endosomes

The kinetics of entry of ^{35}S-CD-MPR into early endosomes were observed by cross-linking protein in early endosomes and measuring any loss of ^{35}S-CD-MPR from the soluble lysate by immunoprecipitation, see figure 4.2.18. The data reflect systematic variation and scatter around a straight line. The points were thus averaged to calculate the average level of the ^{35}S-CD-MPR in early endosomes at steady state. The average level of 7% suggests a low degree of entry of the ^{35}S-CD-MPR into early endosomes, probably due to residual recycling from late endomes.

4.2.3.5 Entry of ^{35}S-CD-MPR into late endosomes and conclusion

Taken together, the data for the CD-MPR suggest that newly-synthesised CD-MPRs entered the endocytic pathway directly via lysosomes where they remained transiently. Presumably the receptors left the lysosomes as soon as the hydrolytic enzymes had dissociated. This would explain their low steady-state levels in lysosomes, as is suggested by the data and confirmed by other studies. The receptors would then probably return to the TGN via late endosomes, re-bind enzymes and then cycle between the TGN and late endosomes, as reported in the literature. Because HRP could not be loaded exclusively into late endosomes, it was not possible to measure specific cross-linking of ^{35}S-CD-MPR in this compartment. Entry of ^{35}S-CD-MPR into late endosomes could be calculated as the difference between the amount of ^{35}S-CD-MPR in the total endocytic pathway and the combined amounts in early endosomes and lysosomes. However, the entry of ^{35}S-CD-MPR into early endosomes could not be kinetically resolved due to low CD-MPR expression levels. The steady-state level of the ^{35}S-CD-MPR in early endosomes was calculated from the average of the data points. The entry of the ^{35}S-CD-MPR into late endosomes was thus calculated as the difference between the amount of ^{35}S-CD-MPR in the total endocytic pathway and lysosomes, while the calculation of its steady-state level in late endosomes took the early endosomes into account.

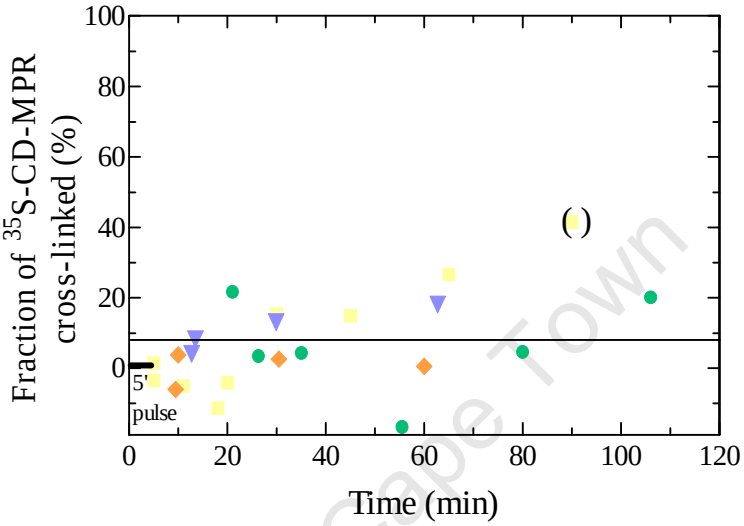

Figure 4.2.18 Delivery of newly-synthesised ^{35}S-CD-MPR to early endosomes. P388D$_1$ cells were starved in methionine-free medium (30 min), labelled with ^{35}S-methionine (5 min) and further incubated in the presence of unlabelled methionine for the indicated times when samples were taken and cooled on ice. HRP was internalised during the last 5 min of each time point. Samples were processed for measuring non-cross-linked ^{35}S-CD-MPR as in figure 4.2.15. Delivery of ^{35}S-CD-MPR into early endosomes was expressed as the amount of cross-linked ^{35}S-CD-MPR, as a fraction of the total ^{35}S-CD-MPR, in each sample. The average of the data points were calculated to be about 7% and taken to be the steady-state level in early endosomes. Different symbols refer to independent experiments.

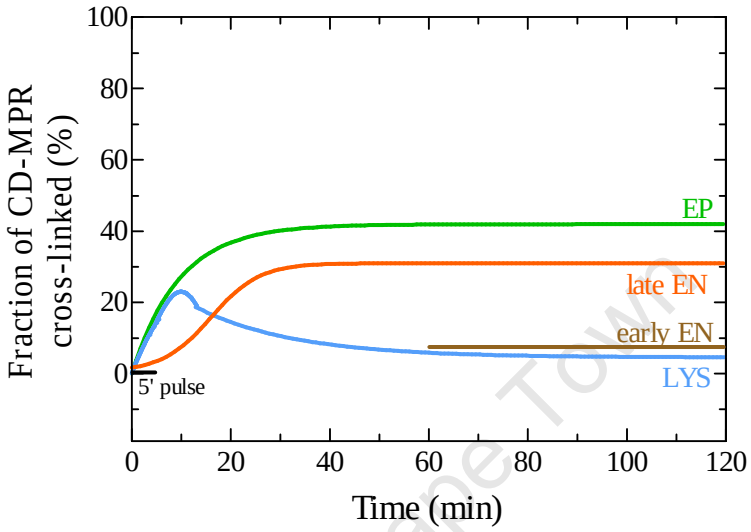

Figure 4.2.19 Comparison of the entry of ^{35}S-CD-MPR into individual compartments. The data obtained for the experiments where ^{35}S-CD-MPR was cross-linked in the endocytic pathway (EP), lysosomes (LYS) and early endosomes (early EN) were used to calculate the curve for ^{35}S-CD-MPR entry into late endosomes (late EN). The ^{35}S-CD-MPR's entry was determined by subtracting the lysosomal curve from the endocytic pathway curve while its steady-state level was calculated by taking into consideration the steady-state of the ^{35}S-CD-MPR in early endosomes as well. At steady state, the ^{35}S-CD-MPR level was at about 31% in late endosomes.

When the data in figures 4.2.15, 4.2.17 and 4.2.18 were combined in this way, the kinetics of delivery to late endosomes could be constructed as in figure 4.2.19. From the curves, it was observed that at steady state about 42% ^{35}S-CD-MPR occurs in the endocytic pathway, 5% in lysosomes, 30% in late endosomes and 7% in early endosomes. At steady state, the CD-MPR is present in early endosomes and lysosomes at an insignificant level. In view of the extent of experimental variation and statistical inaccuracies of the results due to low CD-MPR expression levels, no definite conclusions can be made about the CD-MPR pathway.

4.2.3.6 Technical limitations of the experimental system

In addition to the technical limitations discussed for LAMP-1 in section 4.1.4.6, kinetic results for the CD-MPR were also restricted by various aspects that were intrinsic to the CD-MPR. The CD-MPR had lower expression levels and possibly higher background (discussed in 4.2.3.1) relative to the specific signal. The fraction of the CD-MPR in the endocytic pathway was lower than for LAMP-1, further reducing the scope for resolution of the kinetics. The CD-MPR had a much smaller lumenal domain than LAMP-1 (cf. figures 3.2.1 and 3.1.1). Since the physical process of cross-linking involved trapping of the lumenal portion of a protein, a protein with a very small lumenal domain as the CD-MPR could easily escape the cross-linking process or leak from the cross-linked meshwork. This could contribute to variation in the cross-linking efficiency.

5 DISCUSSION AND CONCLUSION

The aim of this project was to characterise the pathway of newly-synthesised LAMP-1 for delivery into lysosomes.

Most previous studies toward answering this question have considered the steady-state distribution of LAMP-1. The absence of LAMP-1 from a particular compartment has been interpreted to imply that it did not move through the compartment at all. However, it is possible that LAMP-1 moved rapidly in and out of this compartment, so that LAMP-1 did not accumulate to levels that were detectable by the techniques employed. The presence of LAMP-1 in a compartment other than lysosomes has sometimes been interpreted to imply that this compartment is a station *en route* to lysosomes. The fraction of total cellular LAMP-1 in this compartment has been taken to be a measure of the importance of this route. However, the presence of LAMP-1 in a particular compartment could also be a result of recycling from other compartments. The fraction of total cellular LAMP-1 in a particular compartment at steady state is in no way a measure of the fraction of newly-synthesised LAMP-1 that actually moves in and out of the compartment. Hence, steady-state distribution levels provide insufficient information for outlining the pathway followed by LAMP-1 *en route* to lysosomes.

In studies where a kinetic approach has been used, the newly-synthesised LAMP-1 was labelled with radio-active material (eg. ^{35}S-methionine) for relatively long pulse periods, thus yielding poor kinetic resolution. In some cases, the half-times ($T_{½}$ [time]) of the appearance of newly-synthesised labelled material in specific compartments were correlated to the rate at which the newly-synthesised material was delivered to these compartments. However, the half-time of accumulation in a specific compartment depends on the flux ($f \alpha m/T_{½}$ [molecules per time]) of the specific protein into the compartment in relation to its pool-size (m [molecules]) in the compartment at steady state. Hence, the half-time alone cannot serve as a direct measure

of the rate at which the protein travels to the compartment. In studies where the shapes of the time-courses for newly-synthesised LAMP entry into compartments have been compared and interpreted as determining the pathways followed by LAMP proteins, no controls were in place to clearly define the source of these incoming proteins. For example, a simultaneous increase of LAMPs in two different compartments does not necessarily imply that the source is the biosynthetic pathway. An increase of LAMP in a particular compartment is the net result of LAMP moving in and out of this compartment. The LAMP that is leaving could thus enter another compartment. As a result, it is not correct to assume that the protein moving into a compartment is coming from the biosynthetic pathway. Differences between curves were sometimes based on one or two experimental points, hence making definitive interpretations difficult.

Only one study (Cook *et al.*, 2004) has thus far managed to show transient presence of labelled newly-synthesised LAMP-1 in early endosomes. While these observations have identified early endosomes as a compartment that lies *en route* to lysosomes, the authors have relied on *in vitro* studies to suggest that delivery via early endosomes is the major pathway.

In the present study, I observed the movement of newly-synthesised LAMP-1 into either early endosomes or lysosomes relative to the movement into both compartments. By comparing the shapes of the resulting time-courses, I am able to conclusively say that the bulk of newly-synthesised LAMP-1 that entered the endocytic pathway was delivered to lysosomes via early endosomes, and that this was the major pathway.

At steady state LAMP-1 is predominantly localised to late endosomes and lysosomes, more so lysosomes. It has been reported that 2% of LAMP-1 occurs on the cell surface of chicken fibroblasts (Lippencott-Schwartz and Fambrough, 1986) and HL60 cells (Carlsson and Fukuda,

1992). Results obtained here suggest that at steady state about 67% LAMP-1 occurs in the endocytic pathway (figure 4.1.30), 38% in lysosomes (figure 4.1.31), 6% in early endosomes (figure 4.1.32) and 23% in late endosomes (figure 4.1.33). At steady state, the maximal fraction of LAMP-1 that could be cross-linked in the endocytic pathway was 76% (figure 4.1.26). Within experimental error, this compares well with the 67% observed for the kinetic experiments (figure 4.1.31). The remaining 24 – 33% seems too large an amount to be accounted for by compartments outside of the endocytic pathway. A substantial fraction could therefore be due to incomplete cross-linking.

From the individual curves of the kinetic experiments of LAMP-1, significant experimental variation in the fraction of cross-linking was observed during the first 10 min when LAMP-1 was cross-linked in the endocytic pathway (figure 4.1.30), 30 min when LAMP-1 was cross-linked in lysosomes (figure 4.1.31) and 15 min, as well as during the 40-50 min interval, when LAMP-1 was cross-linked in early endosomes (figure 4.1.32). Increased experimental variation in the fraction of cross-linking correlated with conditions when less than 50% of newly-synthesised-labelled LAMP-1 was processed to immunoprecipitable LAMP-1 (during the first 15 min, figure 4.1.29) and/or when the fraction of cross-linked LAMP-1 was low. Factors that may potentially have contributed to experimental variations were discussed in Results 4.1.4.6.

The experimental variations do not negatively affect the interpretation of the results however, since conclusions about the movement of LAMP-1 are not dependent on any particular time point(s). They are based on the general trend and shape of the experimental kinetic curves in comparison to predicted kinetic curves (see figures 3.4.1 and 3.4.2). There is a clear difference in the pattern of the two sets of curves predicted for the two alternative scenarios. For the scenario where LAMP-1 is delivered to lysosomes via early endosomes (figure 3.4.1): During the initial time-points curve (3), which depicts LAMP-1 cross-linked in early endosomes, is co-

incident with curve (1), which depicts LAMP-1 cross-linked in the endocytic pathway. This implies that initially the bulk of newly-synthesised LAMP-1 in the endocytic pathway is present in early endosomes. Curve (3) rises as the net flow of newly-synthesised LAMP-1 into early endosomes increases. The slope of the curve decreases as the net flow into early endosomes reaches a maximum and then becomes negative as the net flow of newly-synthesised LAMP-1 is movement out of early endosomes. Curve (3) is thus indicative of a transient presence of newly-synthesised LAMP-1 in early endosomes. During the early time-points when the bulk of newly-synthesised LAMP-1 occurs in early endosomes, it could be present in lysosomes at insignificant levels, hence the observed delay in curve (2). When this set of curves is compared with that which depicts LAMP-1 entry into lysosomes directly (figure 3.4.2), the curve that is co-incident with the endocytic pathway curve (1) during the initial time points varies and there is a marked difference in the amplitude of curve (3). The experimentally obtained curves, super-imposed on the same graph (figure 4.1.33), best fit the pattern of the set of predicted curves that depicts LAMP-1 delivery via early endosomes (figure 3.4.1). It was observed that the bulk of newly-synthesised-labelled LAMP-1 entered the endocytic pathway via early endosomes with subsequent delivery to lysosomes. I can conclude that the pathway via early endosomes is the only major pathway during the initial stages of entry into the endocytic pathway.

The study was extended to the CD-MPR to serve as a control of a protein that behaves differently to LAMP-1. LAMP-1 is predominantly localised to late endosomes and lysosomes whereas the CD-MPR delivers resident lysosomal hydrolytic enzymes to lysosomes and is predominantly localised to the TGN and endosomes, more specifically late endosomes. It has been reported that 20% of the intracellular CD-MPRs reside in the endocytic pathway of fibroblasts (Stein *et al.*, 1987a). Results obtained here show that at steady state about 42% of the CD-MPR occurs in the endocytic pathway (figure 4.2.15), 5% in lysosomes (figure 4.1.17),

7% in early endosomes (figure 4.2.18) and 30% in late endosomes (figure 4.2.19). Using a different approach, the maximal fraction of CD-MPR that could be cross-linked in the endocytic pathway was 30% (figure 4.2.16). Within experimental error, this compares well with the 42% observed for the kinetic experiments (figure 4.2.15). A large amount of the remaining 58 – 70% is localised to compartments outside of the endocytic pathway, presumably the TGN. A substantial fraction could probably also be due to incomplete cross-linking.

The CD-MPR suffice as a control for the experimental approach. The kinetic results for the CD-MPR are different from that of LAMP-1. The data suggest that CD-MPRs are delivered into the endocytic pathway via lysosomes, remain in lysosomes transiently and at steady state are present in early endosomes and lysosomes at insignificant levels. This would support the observations in the literature that CD-MPRs have generally not been detected in lysosomes. Presumably the CD-MPR would leave the lysosomes as soon as the lysosomal enzymes have dissociated and enter late endosomes from where they would be recycled to the TGN. However, the entry of CD-MPR-enzyme complexes into lysosomes would be contrary to the observations from studies that involved the inhibition of intra-organellar ATP-dependent acidification in CHO mutants (Merion *et al.*, 1983; Robbins et al., 1983; Robbins *et al.*, 1984). These have suggested that enzymes dissociate from MPRs in an acidic pre-lysosomal organelle. In view of the extent of experimental variation and statistical inaccuracies due to low CD-MPR expression levels, results are not conclusive. Factors that may potentially have contributed to experimental variation were discussed in Results 4.1.4.6 and 4.2.3.6.

Based on my results and previous studies, I propose that LAMP-1 is sorted at the TGN into vesicles that deliver their contents to lysosomes along the indirect pathway, intracellularly via early endosomes or along the secretory route, plasma membrane and endocytosis. While my

results show delivery via early endosomes (figure 5.1), it does not preclude the possibility that LAMP-1 is transported to early endosomes along the secretory route, plasma membrane and endocytosis. Results for AP-1 are very contradictory and might imply that AP-1 only plays a minor or a secondary role in LAMP-1 trafficking. LAMP-1 sorting is not affected in μ1A-deficient mouse fibroblasts (Meyer *et al.*, 2000). However, depletion of AP-1 by ribonucleic-acid (RNA) interference did increase cell-surface expression (less than two fold), although the effects were much lower than for other adaptors (Le Borgne *et al.*, 1998). Immunofluorescence in mammalian cells has localised AP-3 to perinuclear buds or vesicles of the TGN as well as those in the cell periphery (Dell'Angelica *et al.*, 1997; Dell'Angelica *et al.*, 1998; Simpson *et al.*, 1996; Simpson *et al.*, 1997). AP-3 may thus function at both the TGN and early endosomes. Using immuno-electron microscopy, LAMPs have been colocalised with AP-3 to a novel tubular sorting endosome where AP-3 has been implicated in sorting LAMPs from recycling membrane proteins destined for the plasma membrane or the TGN (Peden et al., 2004). AP-2 depletion results in a five to ten-fold increase in cell-surface expression of LAMPs, much more than did the depletion of other adaptor proteins (Janvier and Bonifacino, 2005). If LAMP-1 is delivered intracellularly via early endosomes, LAMP-1 could be sorted into AP-3–containing vesicles at the TGN, transported to early endosomes where it would possibly be prevented from recycling to the plasma membrane by AP-3 and then delivered to lysosomes along the endocytic pathway. Due to rapid and extensive membrane traffic between the plasma membrane and early endosomes, LAMPs which escape the AP-3 sorting machinery in early endosomes would appear on the plasma membrane from where they would be sorted by AP-2 and re-internalised. If LAMP-1 was transported to early endosomes via the secretory pathway and cell surface, AP-2–mediated sorting at the cell surface would be encountered first. Sorting machineries are saturable and specific for molecular determinants located in the cytoplasmic tail of lysosomal membrane proteins, as has been shown by experiments in which lysosomal membrane proteins were overexpressed or the tyr motif of the cytoplasmic tail was

mutated (Harter and Mellman, 1992; Honing and Hunziker, 1995; Honing *et al.*, 1996; Marks *et al.*, 1996). If the sorting process in the plasma-membrane/early endosomal compartment is efficient, LAMP-1 is delivered to lysosomes without being detected on the cell surface, since the movement through the plasma-membrane/early endosomal compartment is transient and rapid. When there is an excess of LAMP-1 and the sorting machinery is saturated or the signalling motifs in the cytoplasmic tail are altered and the sorting machinery are inefficient, movement of LAMP-1 through the plasma-membrane/early endosomal compartment would become slower, the steady-state concentration of LAMP-1 on the plasma membrane would increase and thus LAMP-1 would be detected on the cell surface. This would explain why lysosomal membrane proteins with variable tyr motifs in their cytoplasmic tails have different cell-surface steady-state distributions. The variation in the tyr-based sorting signal causes the different lysosomal membrane proteins to bind to the sorting machinery in the plasma-membrane/early endosomal compartment with different affinities. High-affinity binding would result in efficient sorting, rapid flow through the cell surface and no detection on the plasma membrane. Low-affinity binding would result in inefficient sorting, slower movement through the cell surface and a higher cell-surface steady-state distribution. Delivery of newly-synthesised LAMP-1 to lysosomes via the plasma-membrane/early endosomal compartment is thus compatible with the apparent contradictory observations in the literature, that is, the presence or the absence of LAMP-1 on the cell surface at steady state.

Delivery of newly-synthesised lysosomal material via early endosomes could also explain why small quantities of lysosomal material were observed in early endosome-like mycobacterial phagosomes (Clemens and Horwitz, 1995; Thilo and de Chastellier, 1995). In light of the findings that mycobacteria are able to survive in the lysosomal environment (Gomes *et al.*, 1999) and that an adaptive immune response against mycobacteria is not determined by the degree of lysosomal delivery (Majlessi *et al.*, 2007), the reason that mycobacteria generally

remain in immature phagosomes is probably not to avoid lysosomes *per se*. It could be because the early endosome is a strategic site where they would have continued access to newly-synthesised cellular material, sustenance for their intracellular survival.

In addition to functioning in lysosomes, lysosomal membrane proteins may also function at the cell surface and in early endosomes. In human peripheral blood mononuclear cells LAMP-1 and LAMP-2 are activation-dependent cell-surface glycoproteins that mediate cell adhesion to the vascular endothelium (Kannan *et al.*, 1996). LAMP-2 and LAMP-3 might be indicators of platelet activation (Kannan *et al.*, 1995). Recently it has been shown that LAMPs are required for the maturation of phagosomes, specifically the transition from the early to the late stage (Huynh *et al.*, 2007). LAMP-1– and LAMP-2–deficient phagosomes from FcγIIA-transfected MEFs (isolated from double-knockout mice) were positive for early endosomal markers Rab5 and phosphatidylinostol 3-phosphate, failed to accumulate the late endosomal marker Rab7 and did not fuse with lysosomes. This introduces the possibility that newly-synthesised LAMPs could be delivered to early endosomes for the purpose of facilitating their maturation. Lysosomal membrane proteins may thus be transported along the indirect pathway to reach the different destinations where they are required to function. In addition to targeting the lysosomal membrane proteins to the correct destinations, the variable targeting signals could also ensure that these proteins are present at the required concentrations. Proteins which only function in lysosomes may then follow the direct pathway that could involve the ubiquitin-ligase Nedd4 and ubiquitinated GGA3, as for LAPTM5 (Pak *et al.*, 2006).

OUTLOOK

Future studies could use our approach to explore whether other lysosomal proteins are also delivered to lysosomes via early endosomes. Maybe only certain lysosomal proteins with a common purpose are delivered via early endosomes. This purpose might be to promote the maturation of the early endosome, as has been inferred to by Huynh *et al.* (2007). By identifying these proteins we could home in on what they have in common and subsequently also the possible mechanism that they employ in the maturation process.

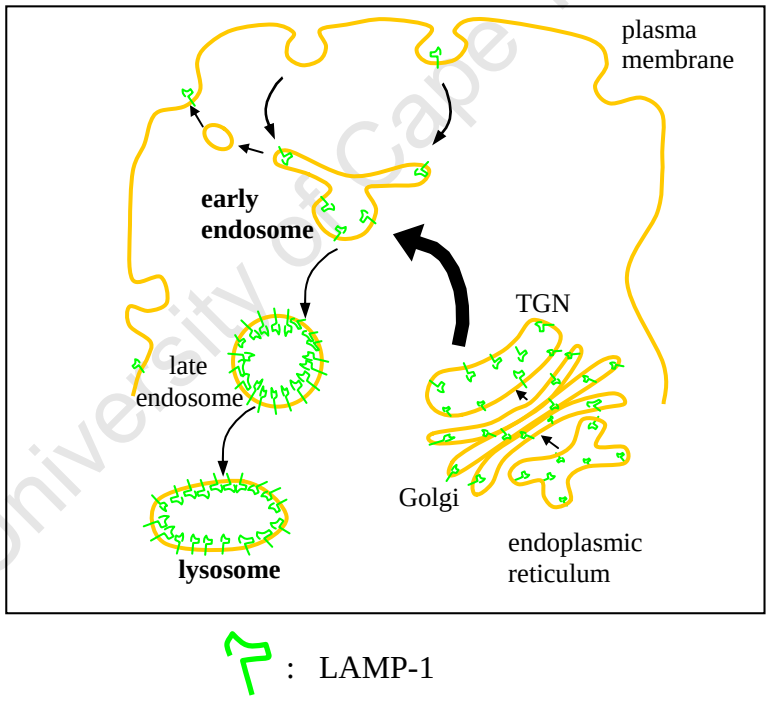

Figure 5.1 Model proposed for LAMP-1 delivery to lysosomes. Newly-synthesised LAMP-1 from the biosynthetic pathway is delivered to lysosomes via early endosomes.

6 METHODS

6.1 MATERIALS

The rat hybridoma cell line which secretes the monoclonal antibody against mouse LAMP-1 (ID4B) was purchased from the Developmental Studies Hybridoma Bank, Department of Biology, University of Iowa. (The immunogen was NIH/3T3 mouse embryo fibroblast tissue culture cell membranes). The mouse macrophage cell line, $P388D_1$, was obtained from the Institute of Genetics, University of Cologne, Cologne, Germany. **D**ulbecco's **M**inimum **E**ssential **M**edium, DMEM, used to culture the hybridomas, RPMI-1640 (developed by Moore *et al.* in 1966 at the **R**oswell **P**ark **M**emorial **I**nstitute), used to culture the macrophages, and the bovine foetal-calf serum were purchased from Highveld Biological, South Africa. Methionine-free minimum essential medium (MEM) or methionine-free RPMI 1460 and trans-label ^{35}S-L-Methionine (Specific-Activity = 1175 µCi/mmole) (cat. no. 51006) were purchased from MP (formerly ICN) Biomedicals, Solon, Ohio, USA. NCTC-135 medium (developed by the **T**issue **C**ulture Section, Laboratory of Biology, **N**ational **C**ancer Institute (NCI), Bethesda, MD; cat. no. N-3262) and opi media supplement (**o**xaloacetate, **p**yruvate, and bovine **i**nsulin; cat. no. O-5003) were obtained from Sigma-Aldrich, St. Louis, MO, USA. Precision Plus protein standards (cat. no. 161-0374) were purchased from Biorad, Hercules, California. Complete Protease Inhibitor Cocktail Tablets were bought from Roche Pharmaceuticals, F. Hoffmann-La Roche Ltd., Basel, Switzerland. The Enhanced Chemiluminescence Detection (ECL) kit (cat. no. RPN2132) from Amersham Biosciences, Piscataway, USA or the KPL LumiGLO (cat. no. 54-61-02) from KPL, Inc., Gaithersburg, Maryland USA was used for Western blotting detection. Control antibody against the low-density lipoprotein (LDL) receptor was a gift from the LDL group, Department of Medical Biochemistry, UCT, Cape Town, South Africa. Rabbit anti-bovine liver CD-MPR antibody was a gift from Nancy Dahms at the Department of Biochemistry, Medical College of Wisconsin, Milwaukee, Wisconsin, USA. Sheep anti-rat-Fc immunoglobulin (AAR02) was purchased from Serotec, Dusseldorf,

Germany. Rabbit polyclonal anti-mouse EEA1 antibody (cat. no. ab14453-50) was purchased from Abcam, Cambridge, UK. Rabbit polyclonal anti-human Rab 5b IgG (cat. no. SC-598, cross-reacts with mouse Rab 5b) was obtained from Santa Cruz Biotechnology, Santa Cruz, USA. HRP-linked goat anti-rat whole antibody (cat. no. NA935), HRP-linked donkey anti-rabbit whole antibody (cat. no. NA934) and peroxidase-linked polyclonal anti-rabbit secondary antibody (cat. no. NIF824) were products from GE Healthcare, Buckinghamshire, UK. Horseradish-peroxidase was supplied by Seravac Biotech (Pty) Ltd., Epping, Cape Town, South Africa. 3'3 Diaminobenzidine was a product from Sigma. ImmunoPure Immobilized Protein-G (cat. no. 20398/9) and Protein-A (cat. no. 20333) beads were purchased from Pierce, Rockford, USA. Ultrafree-15 centrifugal filter devices were products from Millipore, Millipore Corporation, USA. High-speed spins at 40 − 100 000 g were performed using polyallomer centrifuge tubes, (5 X 20 mm and 14 X 95 mm) purchased from Beckman Coulter, Inc., Fullerton, CA, USA.

6.2 SPECIALISED EQUIPMENT AND SOFTWARE

Cells were counted using a Z1 Coulter Particle Counter, Beckman Coulter. A transfer apparatus that was custom made by Mr Hall at the Department of Medical Biochemistry, UCT and BioRad's miniprotein II and III were used for Western blotting. Developed Western blot films were scanned with BioRad's Gel Doc 1000 system. Radio-actively labelled protein bands on dried gels were visualised by radio-active scanning and digitally analysed using an Instant Imager electronic autoradiographer from Packard InstantImager Co., Meriden, CT, USA. Radioactivity in solubilised gel pieces was quantified using a scintillation counter (Packard Liquid Scintillation Analyzer).

6.3 CELL CULTURE

The hybridoma cell line, ID4B, and the macrophage cell line, $P388D_1$, were cultured as monolayers on 175 cm^2 tissue culture flasks. These were maintained in 30 ml medium in an incubator (Queue) with a 37°C, 5% CO_2 environment.

6.3.1 Culturing of the hybridoma cell line, ID4B, and harvesting ab-TCM

This cell line was cultured in DMEM, supplemented with 10% (v/v) NCTC-135, 20% (v/v) heat-inactivated (56°C, 0.5 h) foetal-bovine serum and opi (1vial/l medium). The anti-LAMP-1 rat antibodies secreted into the medium (ID4B-TCM) were harvested and the medium was replenished every 36 h. The harvested ab-TCM was centrifuged at 200 g for 4 min. The pelleted cells were returned to the cell culture. The medium was centrifuged again at 1250 g for 10 min to remove any remaining cells. The supernatant was retained and stored as the first batch of ab-TCM. This process was repeated until the cells were approximately 70% confluent. The ab-TCM from the 70% confluent cells was harvested as the second batch of ab-TCM until the morphology of ~30% of cells was indicative of dying cells. The ab-TCM was then collected only once all cells were dead. This was then pooled and stored with the second batch of ab-TCM, which were kept separate. Initially, when the cells are few, the amount of antibody secreted into the medium is low and thus the antibody concentration of the first batch of ab-TCM is low. When the cells are confluent, a large amount of antibody is secreted into the medium as a result of the greater number of cells. When the cells die, they break-up and release a greater amount of antibody relative to the living cells. The antibody concentration of the second batch is thus higher.

6.3.2 Culturing and harvesting of the mouse macrophage cell line, $P388D_1$

This cell line was cultured in RPMI 1640 medium (Koren et al., 1975) containing 10% heat-inactivated (56°C, 0.5 h) foetal-bovine serum, 100 U/ml penicillin, 100 μg/ml streptomycin. The medium was replenished every 48 h. Two or three days before cells were to be used for an experiment, the medium was replenished every 24 h. Cells in suspension were harvested from 6 flasks into a 500 ml sterile bottle and transferred to 50 ml tubes or directly into sterile 50 ml tubes. These were then centrifuged (200 g, 3 min) at 4°C. Cell pellets were pooled with 8 ml HeSBSA (10 mM Hepes, 140 mM NaCl, 1 mg/ml BSA, pH 7.4) or the appropriate medium, depending on the purpose for which the cells were to be used. Cells were washed with 10 ml of the appropriate buffer/medium and counted. (A wash step entailed the following: The cells were suspended in 10 ml of the appropriate buffer/medium and then pelleted at 200 g, 4 min at 4ºC.)

6.4 PREPARATION OF ANTIBODY

6.4.1 Storage of ab-TCM

Storage of ab-TCM: The harvested ab-TCM was centrifuged at 1250 g for 10 min to remove suspended cells. Tris(hydroxymethyl)amino methane (Tris), 1 M at pH 8.0 and NaN_3 were then added to the supernatant (ab-TCM) at a final concentration of 5% (v/v) and 0.02% (w/v), respectively. The medium was stored at -20°C or -70°C for long-term storage. When ab-TCM was thawed for use, it was centrifuged again at 1250 g for 15 min to remove any precipitable protein (Harlow and Lane, 1988).

6.4.2 Purification of antibody using protein-G affinity chromatography

ID4B antibody was purified using a column packed with protein-G (Akerstrom and Bjorck, 1986; Akerstrom *et al.*, 1987) beads as per manufacturer's instructions (Pierce). ID4B-TCM was mixed with binding buffer (0.1 M Na-acetate, pH 4) at a ratio of 1:1. The mixture was run through a 2 ml protein-G column at a flow rate of 1 ml/min. The column was washed with binding buffer. The bound protein (antibody) was eluted with 100 mM Glyc/HCl, pH 2.65. The acidity of the eluted antibody solution was neutralised by the addition of 50 µl of 1 M Tris per 1 ml fraction. This solution was dialysed against phosphate-buffered saline (PBS), 8 mM Na_2HPO_4, 2 mM NaH_2PO_4, 47 mM NaCl, pH7.4.

6.4.3 Concentration of antibody

The second batch of harvested ab-TCM (refer to 6.3.1 and 6.4.1) was concentrated by filtration through an Ultrafree-15 centrifugal filter device. 15 ml ab-TCM was poured into Ultrafree-15 centrifugal filter device and the cap was closed tightly. This was then placed into a standard, disposable 50 ml centrifuge tube. The assembled device was centrifuged at 1250 g for 1 h. The concentrated ab-TCM was retrieved from the concentrate "pocket" located below the membrane surface. The filtrate was discarded and the process was repeated. It took ~15 h to concentrate 1395 ml to 62 ml, ie. to produce 22,5 X concentrated ab-TCM.

6.5 PREPARATION OF LYSOSOMAL MEMBRANE

This method was adapted from Haylett and Thilo (1986).

6.5.1 ^{35}S-Labelled lysosomal membrane

Harvested P388D$_1$ cells were washed twice with methionine-free medium and resuspended in this medium at $10 \cdot 10^6$ cells/ml. ^{35}S-Methionine (specific-activity = 1175 Ci/mmol) and methionine were added such that the final methionine concentration was $2 \cdot 10^6$ M and specific activity was 20 Ci/mmol. Cells were labelled for 2 h at 37ºC, 5 % CO_2 in a conical flask on a shaker or with occasional mixing (every 15 min). Cells were washed once with 50 ml, transferred to a new tube and washed five times with 10 ml HeSBSA. The process was then the same as for the unlabelled lysosomal membrane (below).

6.5.2 Unlabelled lysosomal membrane

Harvested P388D$_1$ cells were pooled into 10 ml HeSBSA in a 10 ml tube. Cells were washed once with 10 ml HeSBSA and once with 10 ml homogenisation buffer (HB: 23 ml dH_2O +73 ml HB27 (see Reagents 7.5)). Cells were resuspended in HB that contained 1mM PMSF, 0.1 mM leupeptin at $20 - 40 \cdot 10^6$ cells/ml. Cells were cracked in a cell cracker with 12 passes. The cracked cells were transferred to a 10 ml tube and centrifuged at 1000 g for 15 min. If the separation between the pellet and supernatant was not clear, the pellet was resuspended in 2 ml HB, PMSF, leupeptin. The resuspended pellet and supernatant were centrifuged again at 1000 g for 15 min. The post-nuclear supernatants (PNS) were pooled. The PNS (1.7 ml) was carefully layered on top of 10 ml 27% Percoll in HB (27 ml Percoll + 73 ml HB27), resting on a 0.5 ml sucrose cushion at the bottom of a polyallomer tube. These tubes and their content were then subjected to centrifugation in an ultra-centrifuge at 50 000 g for 1.5 h at 4ºC in a SW40Ti swing-out rotor. Two bands were visible on the resultant gradient. Lysosomes were present in the lower band and early endosomes in the upper band (previously established in our laboratory using lysosomal and early endosomal markers). Fractions (0.5 ml) were collected

from the bottom of the gradient using a fraction collector. The fractions that corresponded to the lysosomal band were pooled and stored at -20ºC or -70ºC if stored for long periods. To remove the Percoll, the lysosomal membrane was resuspended in HB, 1 mM PMSF, 0.1 mM leupeptin (final volume = 11.5 ml), transferred to polyallomer tubes and centrifuged at 100 000 g, for 1 h at 4ºC in an SW40Ti swing-out rotor. The supernatant was removed with a Pasteur pipette and discarded. A little supernatant was left to collect the lysosomal membrane which slid off the Percoll easily. To remove lumenal lysosomal protein, the lysosomal membrane was resuspended in 5 ml HB, 1 mM PMSF, 0.1 mM leupeptin and sonicated for ~2 min at 30 seconds bursts. (NB. The lysosomal membrane was returned to ice at every interval.) The polyallomer tubes were filled to the top and centrifuged again at 100 000 g for 1 h at 4ºC in a SW40Ti swing-out rotor. The lysosomal membrane was collected as described above. To remove the remaining Percoll, the lysosomal membranes were centrifuged once or twice for 20 min at 100 000 g (30 psi) in an airfuge at 4ºC. The lysosomal membranes were solubilised in lysis buffer (10 mM Tris (pH 7.5), 5 mM EDTA, 150 mM NaCl, 0.05% NP-40, 1 mM PMSF, 0.1 mM leupeptin) (D'Souza and August, 1986) and stored at 4ºC if used the next day or at -20ºC until use.

6.5.3 Preparation of cross-linked early endosomes and lysosomes

$P388D_1$ cells were harvested and washed twice with 10 ml RPMI/Hepes/BSA (1 mg/ml). Cells were split in half and both sets were resuspended at $5 \cdot 10^6$ cells/ml RPMI/Hepes/BSA. Mannan (1 mg/ml) was added to both cell suspensions. Cells were warmed for 10 min at 37°C and then HRP (1 mg/ml) was added. One batch of cells was allowed to internalise HRP for 5 min to prepare early endosomes and the other batch for 30 min to prepare lysosomes. HRP internalisation was stopped by adding 50 ml cold HeSBSA and placing the flasks containing the suspended cells in a mixture of ice and water (ice-water). Cells were pelleted (200 g for 4 min). The cells that contained the HRP-filled early endosomes were washed twice with 10 ml

cold HeSBSA and kept aside on ice for further processing. The cells that contained the 30 min HRP pulse were washed thrice with cold 10 ml RPMI/Hepes/BSA and resuspended at $5 \cdot 10^6$ cells/ml RPMI/Hepes/BSA. HRP was chased into lysosomes by incubating the cells for 70 min at 37°C after which the flask that contained the suspended cells was placed in ice-water. The cells were washed twice with 10 ml cold HeSBSA. Both sets of cells were then processed for HRP–DAB cross-linking (refer to section 6.11.4). The cells were washed once with 10 ml HB and resuspended at $40 \cdot 10^6$ cells/ml cold HB that contained Complete Protease Inhibitors (diluted 25-fold, see Reagents 7.5). Each set of cells were cracked separately in a cell cracker with 12 passes. The homogenates were centrifuged at 800 g for 5 min and 2 – 3 ml of each supernatant were layered on top of 9 ml 27% Percoll in HB, resting on a 0.5 ml sucrose cushion at the bottom of a polyallomer tube. If necessary, more HB was added to fill the tube to the top. These tubes and their contents were then subjected to centrifugation in an ultra-centrifuge at 35 000 g for 1.5 h at 4ºC in a SW40Ti swing-out rotor. The brown band at the top that corresponded to the early endosomes was collected from the gradient that contained the material of the cells in which the early endosomes were cross-linked. The brown band at the bottom that corresponded to the lysosomes was collected from the gradient that contained the material of the cells in which the lysosomes were cross-linked. The fractions were stored at 4ºC and were washed the next day in a final volume of about 12.5 ml HB to remove the Percoll (100 000 g for 2 h at 4ºC). The cross-linked material was collected and concentrated by centrifugation (8 000 g for 30 min at 4ºC). Membranes were solubilised in 10 mM Tris/HCL pH 7.4, 0.9% NaCl (TBS), 1% Triton-X 100, 25-fold diluted Complete Protease Inhibitors Cocktail (see Reagents 7.5). Detergent-resistant material was pelleted at 8 000 g for 30 min and the supernatant collected. The protein concentration was determined using the bicinchoninic acid (BCA) assay, see section 6.9.2.

6.6 SDS-PAGE

This method was adapted from (Laemmli, 1970). Proteins were separated on mini-gels using gel electrophoresis. The dimensions of the lower gels were ~ 800 mm long, 140 mm wide and 1.5 mm thick. The required concentrations of polyacrylamide solutions were prepared from a 30% Acrylamide, 0.8% bisacrylamide stock solution. For the lower gel solutions, the stock acrylamide was diluted with a lower gel buffer, 1.5 M Tris, 0.4% SDS, pH 8.8, such that the solution was in 0.375 M Tris, 0.1% SDS, pH 8.8. Ammonium persulphate (AMPS) and N,N,N',N'-tetramethylethylendiamine (TEMED) were added to final concentrations of 0.02% and 0.039% TEMED, respectively. For the upper gel solution, the stock acrylamide was diluted to 4.2% with an upper gel buffer, 0.5 M Tris, 0.4% SDS, pH 6.3 such that the solution was in 0.125 M Tris, 0.1 SDS, pH 6.3. AMPS and TEMED were added to final concentrations of 0.085% and 0.426%, respectively. Gels were run in a discontinuous buffering system using running buffer, 0.025 M Tris, 0.192 M Glycine, 0.1% SDS, pH 8.3, at 25 mA until the samples had gone into the stacker and then at 30 mA for ~3 h.

6.7 WESTERN BLOT

Proteins were resolved using SDS-PAGE and Amersham's Rainbow molecular-weight markers or BioRad's Precision Plus protein standards. The proteins were transferred from SDS-polyacrylamide gels to nitrocellulose membranes (Burnette, 1981) using transfer buffer, 20 mM Tris, 150 mM Glyc, 20% methanol at 4ºC.

6.7.1 Western blot no.1

A transfer apparatus that was custom made for 800 mm X 140 mm gels by Mr Hall for the LDL laboratory at the Department of Medical Biochemistry was used. The transfer was performed at 100 mA for 16 to 20 h.

Treatment of the blot after transfer

Immediately following transfer, the nitrocellulose (NC) membrane was incubated in 200 ml blocker (10 mM Tris/HCl pH 7.4, 0.9% NaCl, 5% BSA) at 4ºC for 30 min on a rocking platform. NaCl prevents non-specific ionic bonds and BSA prevents non-specific hydrophobic bonds. The NC membrane was cut into strips (one lane per strip). A strip was then incubated with anti-LAMP-1 primary antibody (ID4B-TCM, 20-50 µg/ml), diluted 5- or 25-fold with the blocker, for 90 min at room temperature (RT) on a rocking platform. The NC membrane was then washed once in 200 ml solution 1 (10 mM Tris/HCl pH 7.4, 0.9% NaCl) for 10 min, twice in 200 ml solution 1, 0.05% NP40, for 20 min and then once in 200 ml solution 1 for 10 min. The detergent removes probe bound to the NC non-specifically, through hydrophobic bonds. This process was then repeated with the secondary antibody (sheep anti-mouse serum diluted 500-fold) and the tertiary antibody (rabbit anti-sheep/goat horseradish-peroxidase-linked antibody diluted 2000-fold). To minimise the volumes of antibodies used, cling-wrap (Glad-wrap) was sealed around the NC membrane to serve as containers. The minimum volume required was 100 µl/cm^2.) The NC was briefly blotted with paper towels or dried between 2

pieces of 3M Whatman papers (~1 h at RT or 15 min at 37ºC). It was then wrapped in cling-wrap and developed with the enhanced chemiluminescence detection system.

6.7.2 Western blot no.2

BioRad's Miniprotein II or III cell system was used to resolve the proteins by SDS-PAGE (200 V for 45 min) and to transfer the proteins to a NC membrane (100 V for 1 h) at 4ºC.

Treatment of the blot after transfer

Immediately following transfer, the NC membrane was blocked in 5% fat-free milk powder, TBS-T (10 mM Tris/HCL pH 7.4, 0.9% NaCl, 0.1% Tween 20) overnight at 4ºC and washed with TBS-T as follows: two quick washes, one 15 min wash and two 5 min washes. The blot was then incubated in primary antibody in TBS-T, 0.5% fat-free milk powder for 1 h at room temperature and the washing process was repeated. The primary antibody was detected with peroxidase-linked secondary antibody in TBS-T, 0.5% fat-free milk powder and the washing process was repeated. The blot was developed with the enhanced chemiluminescence detection system (ECL) or KPL luminoglo.

6.8 LINKAGE OF ANTI-RAT-Fc ANTIBODY TO CN-Br–ACTIVATED SEPHAROSE 4B

(This method was adapted from the Pharmacia protocol on Affinity Chromatography by the LDL group, department of Medical Biochemistry, UCT.)

To 8 mg of ligand (AAR-02), 0.5 volumes of 0.6 M $NaHCO_3$ (pH 8.6), 1.5 M NaCl was added. The mixture was made up to a volume such that the final coupling buffer concentrations were 0.2 M $NaHCO_3$ (pH 8.6), 0.5 M NaCl. This constituted the coupling solution. Freeze-dried, cyanogen bromide(CNBr)-activated Sepharose 4B beads (0.57 g) were suspended in 5 ml 1 mM HCl at 4ºC. The beads were washed on a sintered glass filter (porosity G3) with approximately 120 ml 1 mM HCl (4ºC) and dried until cracks appeared in the gel cake. The gel was immediately transferred to coupling solution which contained the ligand at a gel:buffer ratio of 1:2. (NB. The 12 ml Greiner blue-capped tube is suitable for this). The suspension was rotated for 2 h at room temperature or overnight at 4ºC. The residual active groups on the gel were blocked by incubating the gel in a solution of 0.2 M Glyc, pH 8 for 2 h at room temperature or 16 h at 4ºC. The excess absorbed protein was washed away with alternative high and low pH solutions; coupling buffer (0.2 M $NaHCO_3$, pH 8.3; 0.5 M NaCl) followed by acetate buffer (0.1 M Na-acetate pH 4, 0.5 M NaCl). This was repeated 4 or 5 times. The coupled gel was stored at 4 to 8ºC.

6.9 PROTEIN DETERMINATION

6.9.1 Lowry protein assay

This method was reviewed as a standard protocol for the quantitation of proteins in (Peterson, 1979). Protein standards in the concentration range of 0.04 − 0.30 mg/ml were prepared from 1 mg/ml BSA in a final volume of 250 µl. An equal volume (250 µl) of 1 M NaOH was added to the BSA standards. The unknown sample was prepared such that it contained 20 − 40 µg protein in 500 µl 0.5 M NaOH. NaOH (0.5 M, 500 µl) was used as a blank. A mixture (2.5 ml) consisting of (0.01%) $CuSO_4$ / (0.02%) NaK Tartrate / (1.96%) Na_2CO_3 was added to all tubes. The solutions were thoroughly mixed and incubated at room temperature for 10 min. Folin reagent (Folin − Ciocalteu's phenol reagent, Merck Art 9001, diluted 1 + 1.5 ml H_2O, 250 µl) was added to each tube and the solutions were immediately mixed. The solutions were incubated at room temperature for 30 min. Absorbances of all standards and samples were read at 660 nm.

6.9.2 BCA protein assay

(This method was done in a microplate as per the Pierce protocol.)

Protein standards in the concentration range of 5 − 250 µg/ml were prepared from BSA (2 mg/ml). Sample buffer and dH_2O were used as blanks. The standards or samples (25 µl) were pipetted into microplate wells. The BCA working reagent was prepared such that it contained reagent A and reagent B in a ratio of 50:1. The working reagent (200 µl) was then added to the wells. The microplate was gently agitated such that the samples were thoroughly mixed. The plate was covered and incubated at 37ºC for 30 min. After the incubation period the plate was cooled to room temperature and absorbances were read at 562 nm.

6.9.3 TCA precipitation

Radio-actively−labelled samples (5 µl) were aliqouted in 1 ml eppendorf tubes and diluted with 100 µl HeSBSA (1 mg/ml). TCA (1ml, 10%) was added to each sample. The suspension was thoroughly mixed and duplicate aliquots (100 µl) were taken for scintillation counting. The samples were placed on ice for 30 min and then centrifuged at 8 000 g for 30 min. Aliquots (100 µl) were again taken for scintillation counting. The radio-actively−labelled precipitated protein was then determined as a fraction of the total radioactivity or an amount in dpm.

6.9.4 NAGA assay

The Oxford glucose method was used. NAGA is only active at the low pH of 5. The assay was thus performed in a Na_2HPO_4 (anhydrous) /citric acid.H_2O buffer, pH 5 that was prepared by diluting 20 ml of 100 mM Na_2HPO_4 (anhydrous) with ~10 ml of 100 mM citric acid.H_2O. The unknown samples (5 or 10 µl) were aliqouted into eppendorfs and placed on ice. The substrate solution (200 µl, 3 mM p-nitrophenyl acetyl glucosaminade in Na_2HPO_4/citric acid buffer) was added to the samples, mixed and placed on ice. (The activity of NAGA is very low on ice.) The samples were then incubated at 37ºC for 20 min after which the reaction was slowed down by placing the samples in ice-water. The reaction was stopped by the addition of 700 µl 0.05 M NaOH to each sample. Lysis buffer and dH_2O were used as controls. NAGA releases acetyl glucosaminade from the substrate. p-Nitrophenol, a coloured product of which the absorbance can be read at 405 nm, is generated in the process.

6.10 METABOLIC LABELLING OF CELLS

6.10.1 Continuous labelling

Cells were washed once with MEM and incubated at 37°C for 2 h in MEM containing ^{35}S-methionine at $1.16 \cdot 10^{-7}$ M (specific-activity = 1175 Ci/mmole) and 5% CO_2 at $10 \cdot 10^6$ cells/ml. The labelling process was stopped by placing the cells on ice. Cells were lysed as described in section 6.12.1.

6.10.2 Pulse-chase experiments

Cells were washed twice with 4 ºC methionine-free RPMI 1640 and starved in this medium at $10 \cdot 10^6$ cells/ml for 30 min at 37ºC, 5% CO_2. ^{35}S-Methionine was then added to the warm medium at 10^{-6} to 10^{-7} M (specific-activity = 1175 Ci/mmole) and the cells were metabolically labelled at 37°C, 5% CO_2 for 5 min. The labelling was stopped by placing the flask containing the suspension of cells in ice-water. Cells were pelleted by centrifugation at 200 g for 4 min at 4°C and washed thrice with 10 ml cold RPMI/Hepes/BSA (1 mg/ml). A volume of RPMI/Hepe/BSA(1 mg/ml) that would result in a $5 \cdot 10^6$ cells/ml suspension of cells was warmed to 37°C. The pelleted cells were resuspended in 1 ml cold RPMI/Hepes/BSA (1 mg/ml) and transferred to the warmed medium. This was time zero. The cells were then incubated for the specified chase periods. The chase was stopped by collecting samples of 1 ml ($5 \cdot 10^6$ cells) and transferring them to 10 volumes of cold HeS-BSA. During the labelling process HRP was either localised to the endocytic pathway, lysosomes or early endosomes.

6.11 LOCALISATION OF HRP IN ENDOSOMES TO TRAP PROTEINS

During endocytosis of HRP, the medium contained 1 mg/ml HRP and 1 mg/ml mannan, unless otherwise stated. Mannan was always added at least 5 min prior to the addition of HRP.

6.11.1 The endocytic pathway

HRP was endocytosed for 70 min before the starvation of the cells, during the 30 min starvation and throughout the experiment.

6.11.2 The early endosomes

HRP was endocytosed during the last 5 min of the chase periods.

6.11.3 The lysosomes

HRP was endocytosed for 30 min and then chased for 40 min prior to the starvation period. The rest of the experiment was performed in the absence of HRP.

6.11.4 HRP–DAB cross-linking

To cross-link the proteins in the HRP-containing endosomes/lysosomes the metabolically labelled and HRP-containing cells were subjected to HRP–DAB cross-linking. The cells (~$5 \cdot 10^6$ cells) were washed twice with cold HeS-BSA (10 ml) and once with 10 ml Hepes-Saline (HeS, 10 mM Hepes, 140 mM NaCl, pH 7.4) during which the cells were transferred to a clean tube. Cells were resuspended in 2 ml HeS and split into two 1 ml aliquots. One aliquot (~$2 \cdot 10^6$ cells) was treated with diaminobenzidine (DAB) and hydrogen peroxide (H_20_2) as follows: DAB was prepared fresh at 3 mg/ml in HeS. The DAB suspension was mixed in a sonicator bath for 5 min and filtered through a 0.4 μm Millipore filter. The filtered DAB was added at 180 μl/ml of cell suspension. The cells were gently mixed and incubated in the dark on ice for 30 min, with occasional mixing. The cells were then warmed to room temperature in a 37°C waterbath. H_20_2 (0.3%) was added to the cells at 20 μl/ml of cell suspension, such that the final concentration of H_20_2 was 0.03%. Cells were incubated in the dark for 20 min at

room temperature with occasional mixing. The cross-linking process was stopped by adding 4 volumes of cold HeS-BSA. The other aliquot was treated exactly the same, but DAB and H_20_2 were not added. This served as the control. The cells were washed three times with 10 ml cold Hepes-Saline BSA (HeS-BSA). Cells were lysed as described in section 6.12.2.

6.12 LYSIS

6.12.1 General lysate preparation of metabolically labelled cells for immunoprecipitation of LAMP-1

The cells were washed three times with 10 ml cold Hepes-Saline BSA (HeS-BSA). On the third wash the cells were transferred to a clean tube. The labelled cells were then incubated on ice for 30 min in LAMP-1 lysis buffer at a final cellular concentration of ~$40 \cdot 10^6$ cells/ml, with occasional mixing on a vortex. The lysate was freeze-thawed three times, using liquid N_2 for snap freezing and a 37°C water-bath for rapid thawing. Detergent-resistant material was removed by centrifugation in a microfuge twice at 8 000 g for 15 min at 4ºC. The detergent-soluble material was retained for immunoprecipitation. If kept for long periods, lysates were stored at -70°C.

6.12.2 Lysate preparation for cross-linking experiments

Cells in the samples collected during pulse-chase experiments were centrifuged at 200 g for 3 min, resuspended in ~1 ml HeSBSA and transferred to an eppendorf tube (1.5 ml). Cells ($<2.5 \cdot 10^6$) were then pelleted at 200 g for 3 min and resuspended in 200 µl LAMP/CD-MPR lysis buffer (see Reagents 7.5). The lysate was incubated overnight on a shaker or a roller at 4ºC. (Freeze-thawing was not appropriate for cross-linked material. It led to inconsistent results.) Detergent-resistant material was removed by centrifugation, twice at 8 000 g for 30 min at 4ºC for LAMP-1; or once at 8 000 g for 30 min and once at 100 000 g for 30 min at 4ºC

for the CD-MPR. The detergent-soluble material was retained for immunoprecipitation as described in 6.13.

6.13 IMMUNOPRECIPITATION

Antibody (10 µl of 10-fold concentrated ID4B-TCM or 5 µl rabbit anti-bovine-CD-MPR serum) was added to 160-180 µl of the detergent-soluble fraction of the lysate, prepared in 6.12. The antibody-lysate mixture was incubated on a vortex shaker, overnight at 4°C. The following day it was centrifuged at 8 000 g for 15 min at 4°C to remove any precipitable material. The supernatant was then incubated with 50 µl beads (protein-G for rat antibodies and protein-A for rabbit antibodies) for 2 h at 4°C on a vortex shaker. The immuno-complexed beads were washed thrice with cold LAMP lysis buffer/CD-MPR washing buffer (see Reagents 7.5), transferred to a clean tube during the 4th wash, washed again twice with cold LAMP lysis buffer/CD-MPR washing buffer and once with dH_2O. Immunocomplexes were eluted as in 6.14.

6.14 ELUTION OF IMMUNOCOMPLEXES FROM BEADS

The antigen-antibody complexes were eluted with 0.1 M Gly/HCl, pH 2.6 at room temperature. Beads were incubated with 55 µl of buffer for 5 min, on a vortex shaker. The beads were pelleted and 40 µl of the eluent was collected. The elution was repeated with 20 µl elution buffer, 20 µl eluent was collected and pooled with the first eluent. The pH of the eluent was increased to 7.0 with 3.6 µl of 2 M Tris at pH 8.0.

6.15 SDS-PAGE AND PRODUCT ANALYSES OF SAMPLES FROM CROSS-LINKING EXPERIMENTS

Three-fold–concentrated, reducing-SDS-sample buffer (31.8 µl) was added to the total eluent of 60 µl. Samples were incubated at 95°C for 5 min. High molecular-weight markers or precision-plus dual-colour molecular-weight markers (2.5 µl) were added per sample to aid in the cutting-out of the LAMP-1/CD-MPR bands. The eluents were then resolved by SDS-PAGE on mini-gels (7% for LAMP-1 and 10% for CD-MPR). Samples were run through a 5% stacker at 25 mA. Thereafter the current was maintained at 30 mA until the appropriate separation was attained. For the LAMP-1, the front was run off the gel for 40 min. For the CD-MPR, the front was run to a position 1 cm from the edge of the gel. The gel was silver-stained and the LAMP-1/CD-MPR bands were excised from the gel using the molecular-weight markers as reference points. The gel pieces (1.5 mm thick, ~1 cm wide, ~1 − 2 cm long) were solubilised in 2 ml 30% H_2O_2 at 60°C overnight. The solubilised gel pieces were then counted in a Packard Liquid Scintillation Analyzer.

6.16 GEL-STAINING

6.16.1 Coomassie Staining

The staining solution (46% methanol, 8% glacial acetic acid, 0.1% Coomassie brilliant blue R) was freshly made before use. A fraction of the methanol was added to the dye to solubilise the dye. The suspension was stirred and the solubilised dye carefully decanted. The process was repeated until only white sediment remained and was discarded. The rest of the methanol, the glacial acetic acid and dH_2O were then added. The gel was incubated in staining solution for 15 min. The gel was rinsed once quickly (30 sec) in dH_2O to remove the excess dye. The gel was incubated in ~150 ml destain solution (20% methanol, 8% glacial acetic acid) for 30 min to 1 h after which the destain solution was replaced with fresh destain solution. Sponges (~2 cm^3) were immersed in the destain solution (~400 ml) and suspended above the gel to facilitate the destain process. Gel was left to destain overnight.

6.16.2 Silver Staining

This method was adapted from (Meril et al., 1984). Protein bands on the gels were fixed overnight in 12% TCA, 2% $Cu(II)Cl_2$ and 50% methanol. Gels were then sequentially soaked in the following solutions while continually being agitated: 10% ethanol, 5% acetic acid (solution 1) for 30-40 min; 0.01% $KMnO_4$ for 10 min; solution 1 for 20 min; 10% ethanol for 40 min; de-ionised water for 30 min; 0.1% $AgNO_3$ for 20 min; de-ionised water for 1 min; 10% K_2CO_3 for 1.5 min; 2% K_2CO_3, 0.01% formaldehyde until the protein bands became visible, usually for ~3-4 min; de-ionised water for 30 seconds, 3% acetic acid overnight. The following day protein bands were cut from the wet gels using molecular-weight markers as a reference.

7 ADDENDUM

7.1 ABBREVIATIONS

- AAR-02 : rabbit anti-rat IgG antibody
- ab : antibody
- ABL93 : rat anti-mouse LAMP-2 antibody
- ab-TCM : antibody-containing tissue-culture medium
- ag-ab : antigen complexed to antibody
- AP : adaptor protein
- cat. no. : catalogue number
- CD8 : a cell-surface protein
- CD-MPR : cation-dependent mannose 6-phospate receptor
- cf. : compare
- chs: chapters
- CI-MPR : cation-independent mannose 6-phosphate receptor
- CN-Br : cyanogen-bromide
- CO_2 : carbon dioxide
- COS-1 : transformed African Green Monkey Kidney Fibroblasts
- CURL : compartment of uncoupling of receptor and ligand
- DAB : diaminobenzidine
- dH_2O : distilled water
- EDTA : ethylenediaminotetra-acetic disodium salt
- EN : endosomes
- EP : endocytic pathway
- Endo H : endoglycosidase H
- FITC-D : Fluorescein isothiocyanate-dextran

- GST : Glutathione-S-transferase
- g : gravitational acceleration
- HCl : hydrochloric acid
- H_2O_2 : hydrogen peroxide
- HeLa : An immortalised cell line derived from Henrietta Lacks' cervical cancer cells.
- HeS : hepes-saline
- HeS-BSA : hepes-saline – bovine serum albumin
- HMW : high molecular-weight markers
- HRP : horse-radish peroxidase
- ID4B : rat-anti-mouse LAMP-1 antibody
- LAMP : lysosomal-associated membrane protein
- LAP : lysosomal acid phosphatase
- LAPTM5 : lysosomal-associated multispanning membrane protein 5
- LEP 100 : chicken LAMP-1
- LIMP : lysosomal integral membrane protein
- LDL : low density lipoprotein
- LYS : lysosomes
- MEM : methionine-free minimum essential medium
- MEF : mouse embryonic fibroblasts
- MW : molecular-weight
- NAGA : N-acetyl glucosaminidase
- NRK : normal rat kidney cells
- N_2 : nitrogen
- Na-acetate : sodium acetate
- NaCl : sodium chloride

- NP_{40} : non-ionic detergent P_{40}
- P : page
- $P388D_1$: mouse macrophage cell line
- PMSF : para-methyl sulphonyl fluoride
- protein-G −ID4B : rat-anti-mouse LAMP-1 antibody complexed to protein-G beads
- RNA : ribonucleic acid
- SDS : sodium dodecyl sulphate
- SDS-PAGE : sodium dodecyl sulphate - polyacrylamide gel electrophoresis
- TCA : trichloro-acetic acid
- TCM : tissue-culture medium
- Tris : Tris(hydroxymethyl) amino methane
- β-counter : beta-counter or scintillation counter
- µ1B : subunit of the AP-1 complex in polarised epithelial and glandular cells
- µ3B : subunit of the AP-3 complex in neuronal cells

7.2 SINGLE AMINO-ACID CODE

A	Ala	alanine	M	Met	methionine
C	Cys	cysteine	N	Asn	asparagine
D	Asp	aspartic acid	P	Pro	proline
E	Glu	glutamic acid	Q	Gln	glutamine
F	Phe	phenylalanine	R	Arg	arginine
G	Gly	glycine	S	Ser	serine
H	His	histidine	T	Thr	threonine
K	Lys	lysine	V	Val	valine
I	Ile	isoleucine	W	Trp	tryptophan
L	Leu	leucine	Y	Tyr	tyrosine

7.3 UNITS

1. Ci : Curies
2. Ci/mmol : Curie per mmole
3. h : hour/s
4. kDa : kilo-Dalton
5. lr : litre
6. M : molar (moles per litre)
7. mA : milliamps
8. min : minute/s
9. mM : milli-molar (millimoles per litre)
10. U/ml : Units per ml
11. v/v : volume by volume
12. w/v : weight by volume
13. °C : degree Celsius
14. µCi/ml : micro-Curie per millilitre
15. µg/ml : microgram per millilitre
16. µl : microlitre

7.4 EQUATIONS

1. The amount of sample eluted from beads with every elution round (figure 4.1.12).

$\mathbf{E_n = f.L.(1-f)^{(n-1)}}$,

where $\mathbf{E_n}$ is the amount of LAMP eluted at round **n**

L is total bead load

f is the fraction of LAMP-1 eluted with each elution round

2. The total amount of protein synthesised in terms of the total amount of methionine (mmoles) incorporated into protein as determined in figure 4.1.20.

$\mathbf{M = p / (f . S)}$,

where **M** is the total amount of methionine incorporated into protein (mmoles)

p is the total amount of protein precipitated in terms of ^{35}S-methonine counts (dpm)

f is the dpm to Ci conversion factor : $2200 \cdot 10^9$ dpm/Ci

S is the specific-activity of methionine in the medium (Ci/mmol)

3. The fraction of ^{35}S-LAMP-1 or ^{35}S-CD-MPR cross-linked.

$\mathbf{Y = (1-(S-X)/(T-X))*100}$,

where **Y** is the fraction of cross-linked LAMP-1/CD-MPR (%)

X is lane background (dpm)

S is soluble LAMP-1 (dpm) from the cross-linked sample

T is soluble LAMP-1 (dpm) from the non-cross-linked sample (total LAMP-1)

7.5 REAGENTS

1) HeSBSA (Hepes-saline with bovine serum albumin) : 10 mM Hepes, 140 mM NaCl, 1 mg/ml BSA, pH 7.4.
2) HeS (Hepes-saline) : 10 mM Hepes, 140 mM NaCl, pH 7.4.
3) Binding buffer : 0.1 M Na-acetate, pH 4
4) Complete Protease Inhibitor Cocktail Tablets (commercially-purchased tablets that contain a cocktail of a broad range of ser-, cys- and metalloproteases, as well as calpains)

   Stock: One tablet was dissolved in 1 ml of dH_2O.

   Working solution: stock was diluted 25-fold with the buffer that was used for lysis.
5) LAMP-1 lysis buffer : 10 mM Tris (pH 7.5), 5 mM EDTA, 150 mM NaCl, 0.05% NP-40, inhibitors (1 mM PMSF, 1 μM leupeptin or 25-fold diluted Complete Protease Inhibitors Cocktail).
6) Elution buffer : 0.1 M Gly/HCl, pH 2.6
7) Imidazole buffer : 50 mM imidazole, 150 mM NaCl, 2 mM EDTA, 1 mg/ml BSA, 5 mM Na-β-glycerophosphate, pH 7
8) Imidazole lysis buffer : imidazole buffer, 1% Triton, 0.1% Na-deoxycholate, 1 mM PMSF, 1 μM pepstatin.
9) Imidazole immunoprecipitation/washing buffer : imidazole buffer, 0.05% Triton
10) CD-MPR buffer (Tris buffer) : 25 mM Tris, 5 mM EDTA, 150 mM NaCl, pH 7.5
11) CD-MPR lysis buffer (Tris lysis buffer) : Tris buffer, 1% Triton, 0.1% Na-Deoxycholate, 1 mM PMSF, 25-fold diluted Complete Protease Inhibitors Cocktail.
12) CD-MPR immunoprecipitation/washing buffer (Tris washing buffer) : Tris buffer, 0.05% Triton.
13) Lower gel buffer : 1.5 M Tris, 0.4% SDS, pH 8.8
14) Upper gel buffer : 0.5 M Tris, 0.4% SDS, pH 6.3

15) Running buffer : 0.025 M Tris, 0.192 M Glycine, 0.1% SDS, pH 8.3
16) Non-reducing SDS-sample buffer (concentrated 4-fold) : 40% (v/v) glycerol, 9.2% (w/v) SDS, 0.001% (w/v) Bromophenol blue, 33.2% (v/v) upper gel buffer
17) Reducing SDS-sample buffer (concentrated 4-fold) : Non-reducing SDS-sample buffer (concentrated 4-fold), 20% (v/v) β-mercaptoethanol
18) Coomassie stain : 46% methanol, 8% glacial acetic acid, 0.1%Coomassie Brilliant BlueR
19) Destain : 20% methanol, 8% glacial acetic acid
20) Gel drying solution : 3% glacial acetic acid, 2% glycerol (glycerol was not included when gel was cut-up for solubilisation)
21) Transfer buffer : 20 mM Tris, 150 mM Glycine, 20% methanol
22) Phosphate buffered saline (PBS) : 8 mM Na_2HPO_4, 2 mM NaH_2PO_4, 47 mM NaCl, pH7.4
23) Tris buffered saline (TBS) : 10 mM Tris/HCL pH 7.4, 0.9% NaCl
24) Tris buffered saline-Tween 20 (TBS-T) : 10 mM Tris/HCL pH 7.4, 0.9% NaCl, 0.1% Tween 20
25) HB27 : 342 mM Sucrose, 2.74 mM EDTA, 13.7 mM Hepes

7.6 LIST OF FIGURES

7.7 LIST OF TABLES

7.8 REFERENCES

Ahle, S., Mann, A., Eichelsbacher, U. and Ungewickell, E. (1988). Structural relationships between clathrin assembly proteins from the Golgi and the plasma membrane. *EMBO J.* **7,** 919-929.

Akasaki, K., Fukuzawa, M., Kinoshita, H., Furuno, K. and Tsuji, H. (1993). Cycling of two endogenous lysosomal membrane proteins, lamp-2 and acid phosphatase between the cell surface and lysosomes in cultured rat hepatocytes. *J. Biochem.* **114,** 598-604.

Akasaki, K., Michihara, A., Fujiwara, Y., Mibuka, K. and Tsuji, H. (1996). Biosynthetic transport of a major lysosome-associated membrane glycoprotein 2, LAMP-2: A significant fraction of newly synthesized LAMP-2 is delivered to lysosomes by way of early endosomes. *J. Biochem.* **120,** 1088-1094.

Akasaki, K., Michihara, A., Fukuzawa, M., Kinoshita, H. and Tsuji, H. (1994). Cycling of an 85 kDa lysosomal membrane glycoprotein between the cell surface and lysosomes in cultured rat hepatocytes. *J. Biochem.* **116,** 670-676.

Akasaki, K., Michihara, A., Mibuka, K., Fujiwara, Y. and Tsuji, H. (1995). Biosynthetic transport of a major lysosomal membrane glycoprotein, lamp-1: Convergence of biosynthetic and endocytic pathways occurs at three distinctive points. *Exp. Cell Res.* **220,** 464-473.

Akerstrom, B. and Bjorck, L. (1986). A physicochemical study of protein G, a molecule with unique immunoglobulin G-binding properties. *J. Biol. Chem.* **261,** 10240-10247.

Akerstrom, B., Nielsen, E. and Bjorck, L. (1987). Definition of IgG- and albumin binding regions of streptococcal protein G. *J. Biol. Chem.* **262,** 13388-13391.

Barriocanal, J. G., Bonifacino, J. S., Yuan, L. and Sandoval, I. V. (1986). Biosynthesis, glycosylation, movement through the Golgi system, and transport to lysosomes by an N-linked carbohydrate-independent mechanism of three lysosomal integral membrane proteins. *J. Biol. Chem.* **261,** 16755-16763.

Beguinot, L., Lyall, R. M., Willingham, M. C. and Pastan, I. (1984). Down-regulation of the epidermal growth factor receptor in KB cells is due to receptor internalization and subsequent degradation in lysosomes. *Proc. Natl. Acad. Sci. USA* **81,** 2384-2388.

Bittencourt, Marcello de Carvalho, Herren, S., Graber, P., Vilbois, F., Pasquali, C., Berney, C., Plitz, T., Nicoletti, F. and Kosco-Vilbois, M. H. (2005). Extracellular lysosome-associated membrane protein-1 (LAMP-1) mediates autoimmune disease progression in the NOD model of type 1 diabetes. *Eur. J. of Immunol.* **35,** 1501-1509.

Black, M. W. and Pelham, H. R. B. (2000). A selective transport route from the Golgi to late endosomes that requires the yeast GGA proteins. *J. Cell Biol.* **151,** 587-600.

Bleekemolen, J. E., Stein, M., Slot, J. W. and Geuze, H. J. (1988). The two mannose 6-phosphate receptors have almost identical subcellular distributions in U937 monocytes. *Eur. J. Cell Biol.* **47,** 366-372.

Bonifacino, J. S. (2004). Role of the mammalian retromer in sorting of the cation-independent mannose-6-phosphate receptor. *J. Cell Biol.* **165,** 123-133.

Bonifacino, J. S. and Dell'Angelica, E. C. (1999). Molecular bases for the recognition of tyrosine-based sorting signals. *J. Cell Biol.* **145,** 923-926.

Braun, M., Waheed, A. and von Figura, K. (1989). Lysosomal acid phosphatase is transported to lysosomes via the cell surface. *EMBO J.* **8,** 3633-3640.

Bright, N. A., Gratian, M. J. and Luzio, J. P. (2005). Endocytic delivery to lysosomes mediated by concurrent fusion and kissing events in living cells. *Current Biol.* **15,** 360-365.

Brown, M. S. and Goldstein, J. L. (1976). Receptor-mediated control of cholesterol metabolism. *Science* **191,** 150-154.

Brown, W. J., Constantinescu, E. and Farquhar, M. G. (1984). Redistribution of mannose-6-phosphate receptors induced by tunicamycin and chloroquine. *J. Cell Biol.* **99,** 320-326.

Brown, W. J., Goodhouse, J. and Farquhar, M. G. (1986). Mannose-6-phosphate receptors for lysosomal enzymes cycle between the Golgi complex and endosomes. *J. Cell Biol.* **103,** 1235-1247.

Brown, W. J. and Farquhar, M. G. (1984a). Accumulation of coated vesicles bearing mannose 6-phosphate receptors for lysosomal enzymes in the Golgi region of I-cell fibroblasts. *Proc. Natl. Acad. Sci. USA* **81,** 5135-5139.

Brown, W. J. and Farquhar, M. G. (1984b). The mannose-6-phosphate receptor for lysosomal enzymes is concentrated in *cis*-Golgi cisternae. *Cell* **36,** 295-307.

Burnette, W. N. (1981). "Western blotting": Electrophoretic transfer of proteins from SDS-PAGE to unmodified nitrocellulose and radiographic detection with antibody and radioiodinated protein A. *Anal. Biochem.* **112,** 195-203.

Canfield, W. M., Johnson, K. F., Ye, R. D., Gregory, W. and Kornfeld, S. (1991). Localization of the signal for rapid internalization of the bovine cation-independent mannose 6-phosphate/insulin-like growth factor-II receptor to amino acids 24-29 of the cytoplasmic tail. *J. Biol. Chem.* **266,** 5682-5688.

Carlsson, S. R., Lycksell, P. O. and Fukuda, M. (1993). Assignment of O-glycan attachment sites to the hinge-like regions of human lysosomal membrane glycoproteins lamp-1 and lamp-2. *Arch. Biochem. Biophys.* **304,** 65-73.

Carlsson, S. R., Roth, J., Piller, F. and Fukuda, M. (1988). Isolation and characterization of human lysosomal membrane glycoproteins, h-lamp-1 and h-lamp-2. Major sialoglycoproteins carrying polylactosaminoglycan. *J. Biol. Chem.* **263,** 18911-18919.

Carlsson, S. R. and Fukuda, M. (1990). The polylactosaminoglycans of human lysosomal membrane glycoproteins lamp-1 and lamp-2. Localization on the peptide backbones. *J. Biol. Chem.* **265,** 20488-20495.

Carlsson, S. R. and Fukuda, M. (1992). The lysosomal membrane glycoprotein lamp-1 is transported to lysosomes by two alternative pathways. *Arch. Biochem. Biophys.* **296,** 630-639.

Chang, T., Reid, P. C., Sugi, S., Ohgami, N., Cruz, J. C. and Chang, Catherine C. Y. (2005). Niemann-pick type C disease and intracellular cholesterol trafficking. *J. Biol. Chem.* **280,** 20917-20920.

Chao, H. H., Waheed, A., Pohlmann, R., Hille, A. and von Figura, K. (1990). Mannose 6-phosphate receptor dependent secretion of lysosomal enzymes. *EMBO J.* **9,** 3507-3513.

Chavez, C. A., Bohnsack, R. N., Kudo, M., Gotschall, R. R., Canfield, W. M. and Dahms, N. M. (2007). Domain 5 of the cation-independent mannose 6-phosphate receptor preferentially binds phophodiesters (mannose 6-phophate N-acetylglucosamine ester). *Biochemistry-US.* **46,** 12604-12617.

Chavrier, P., Parton, R. G., Hauri, H. P., Simons, K. and Zerial M. (1990). Localisation of low molecular weight GTP binding proteins to exocytic and endocytic compartments. *Cell* **62,** 317-329.

Chen, J. W., Goldstein, J. L. and Brown, M. S. (1990). NPXY, a sequence often found in cytoplasmic tails, is required for coated pit-mediated internalization of the low density lipoprotein receptor. *J. Biol. Chem.* **265,** 3116-3123.

Chen, J. W., Pan, W., D'Souza, M. P. and August, J. T. (1985). Lysosome-associated membrane proteins: Characterisation of LAMP-1 of macrophage P388 and mouse embryo 3T3 cultured cells. *Arch. Biochem. Biophys.* **239,** 574-586.

Clague, M. J., Urbe, S., Aniento, F. and Gruenberg, J. (1994). Vacuolar ATPase activity is required for endosomal carrier vesicle formation. *J. Biol. Chem.* **269,** 21-24.

Clemens, D. L. and Horwitz, M. A. (1995). Characterisation of the mycobacterium tuberculosis phagosome and evidence that phagosomal maturation is inhibited. *J. Exp. Med.* **181,** 257-270.

Cohn, Z. A. and Ehrenreich, B. A. (1969). The uptake, storage, and intracellular hydrolysis of carbohydrates by macrophages. *J. Exp. Med.* **129,** 201-225.

Cook, N. R., Row, P. E. and Davidson, H. W. (2004). Lysosome-associated membrane protein 1 (Lamp1) traffics directly from the TGN to early endosomes. *Traffic* **5,** 685-699.

Courtoy, P. J. (1993). Analytical subcellular fractionation of endosomal compartments in rat hepatocytes. *Subcell. Biochem.* **19,** 29-68.

Courtoy, P. J., Quintart J. and Baudhuin, P. (1984). Shift of equilibrium density induced by 3,3'-diaminobenzidine cytochemistry: A new procedure for the analysis and purification of peroxidase-containing organelles. *J. Cell Biol.* **98,** 870-876.

Croze, E., Ivanov, I. E., Kreibich, G., Adenisk, M., Sabatini, D. D. and Rosenfeld, M. G. (1989). Endolyn-78, a membrane glycoprotein present in morphologically diverse components of the endosomal and lysosomal compartments: Implications for lysosome biogenesis. *J. Cell Biol.* **108,** 1597-1613.

Crump, C. M., Xiang, Y., Thomas, L., Gu, F., Austin, C., Tooze, S. A. and Thomas, G. (2001). PACS-1 binding to adaptors is required for acidic cluster motif-mediated protein traffic. *EMBO J.* **20,** 2191-2201.

Cuervo, A. M. and Dice, J. F. (1996). A receptor for the selective uptake and degradation of proteins by lysosomes. *Science* **273,** 501-503.

Dahms, N. M. and Kornfeld, S. (1987). 46 kDa Mannose 6-phosphate receptor: Cloning, expression, and homology to the 215 kDa mannose 6-phosphate receptor. *Cell* **50,** 181-192.

Dahms, N. M. and Kornfeld, S. (1989). The cation-dependent mannose 6-phosphate receptor (structural requirements for mannose 6-phosphate binding and oligomerization). *J. Biol. Chem.* **264,** 11458-11467.

Dahms, N. M., Lobel, P. and Kornfeld, S. (1989). Mannose 6-phosphate receptors and lysosomal enzyme targeting. *J. Biol. Chem.* **264,** 12115-12118.

Davidson, H. W. (1995). Wortmanin causes mistargeting of procathepsin D. evidence for the involvement of a phosphatidylinositol 3-kinase in vesicular transport to lysosomes. *J. Cell Biol.* **130,** 797-805.

Dell'Angelica, E. C., Klumperman, J., Stoorvogel, W. and Bonifacino, J. S. (1998). Association of the AP-3 adaptor complex with clathrin. *Science* **280,** 431.

Dell'Angelica, E. C., Mullins, C., Caplan, S. and Bonifacino, J. S. (2000). Lysosome-related organelles. *FASEB J.* **14,** 1265-1278.

Dell'Angelica, E. C., Ooi, C. E. and Bonifacino, J. S. (1997). β3A-adaptin, a subunit of the adaptor-like complex AP-3. *J. Biol. Chem.* **272,** 15078-15084.

Dell'Angelica, E. C., Puertollano, R., Mullins, C., Aguilar, R. C., Vargas, J. D., Hartnell, L. M. and Bonifacino, J. S. (2000). GGAs: A family of ADP ribosylation factor-binding proteins related to adaptors and associated with the Golgi complex. *J. Cell Biol.* **149,** 81-94.

Dell'Angelica, E. C., Shotelersuk, V., Aguilar, R. C., Gahl, W. A. and Bonifacino, J. S. (1999). Altered trafficking of lysosomal proteins in Hermansky-Pudlak syndrome due to mutations in the β3A subunit of the AP-3 adaptor. *Mol. Cell* **3,** 11-21.

Denzer, K., Weber, B., Hille-Rehfeld, A., von Figura, K. and Pohlmann, R. (1997). Identification of three internalization sequences in the cytoplasmic tail of the 46 kDa mannose 6-phosphate receptor. *Biochem. J.* **326 (Pt 2),** 497-505.

Diment, S., Sandoval, I. V. and von Figura, K. (1998). A di-leucine-based motif in the cytoplasmic tail of LIMP-II and tyrosine mediate selective binding of AP-3. *EMBO J.* **17,** 1304-1314.

Dintzis, S. M. and Pfeffer, S. R. (1990). The mannose 6-phosphate receptor cytoplasmic domain is not sufficient to alter the cellular distribution of a chimeric EGF receptor. *EMBO J.* **9,** 77-84.

Dintzis, S. M., Velculescu, V. E. and Pfeffer, S. R. (1994). Receptor extracellular domains may contain trafficking information. *J. Biol. Chem.* **269,** 12159-12166.

Doray, B., Ghosh, P., Griffith, J., Geuze, H. J. and Kornfeld, S. (2002a). Cooperation of GGAs and AP-1 in packaging MPRs at the trans-Golgi network. *Science* **297,** 1700-1703.

Doray, B., Bruns, K., Ghosh, P. and Kornfeld, S. (2002b). Interaction of the cation-dependent mannose 6-phosphate receptor with GGA proteins. *J. Biol. Chem.* **277,** 18477-18482.

D'Souza, P. M. and August, J. T. (1986). A kinetic analysis of biosynthesis and localisation of a lysosome-associated membrane glycoprotein. *Arch. Biochem. Biophys.* **249,** 522-532.

Duncan, J. R. and Kornfeld, S. (1988). Intracellular movement of two mannose 6-phosphate receptors: Return to the Golgi apparatus. *J. Cell Biol.* **106,** 617-628.

De Duve, C. (1983). Lysosomes revisited. *Eur. J. Biochem.* **137**, 391-397.

Ehrenreich, B. A. and Cohn, Z. A. (1969). The fate of peptides pinocytosed by macrophages in vitro. *J. Exp. Med.* **129,** 227-245.

Eskelinen, E., Cuervo, A. M., Taylor, Matthew R. G., Nishino, I., Blum, J. S., Dice, J. F., Sandoval, I. V., Lippincott-Schwartz, J., August, J. T. and Saftig, P. (2005). Unifying nomenclature for the isoforms of the lysosomal membrane protein LAMP-2. *Traffic* **6,** 1058-1061.

Eskelinen, E., Schmidt, C. K., Neu, S., Willenborg, M., Fuertes, G., Salvador, N., Tanaka, Y., Lullmann-Rauch, R., Hartmann, D., Heeren, J. et al. (2004). Disturbed cholesterol traffic but normal proteolytic function in LAMP-1/LAMP-2 double-deficient fibroblasts. *Mol. Biol. Cell* **15,** 3132-3145.

Eskelinen, E., Tanaka, Y. and Saftig, P. (2003). At the acidic edge: Emerging functions for lysosomal membrane proteins. *Trends Cell Biol.* **13,** 137-145.

Fambrough, D. M. (1995). The family of LAMP-2 proteins arises by alternative splicing from a single gene: Characterisation of avian LAMP-2 gene and identification of mammalian homologues of LAMP-2b and LAMP-2c. *DNA Cell Biol.* **14,** 863-867.

Fukuda, M., Viitala, J., Matteson, J. and Carlsson, S. R. (1988). Cloning of cDNAs encoding human lysosomal membrane glycoproteins, h-lamp-1 and h-lamp-2. Comparison of their deduced amino acid sequences. *J. Biol. Chem.* **263,** 18920-18928.

Fukuda, M. (1990). Lysosomal membrane glycoproteins. *J. Biol. Chem.* **265,** 7548-7551.

Fukuda, M. (1991). Lysosomal membrane glycoproteins. *J. Biol. Chem.* **266,** 21327-21330.

Furuno, K., Ishikawa, T., Akasaki, K., Yano, S., Tanaka, Y., Yamaguchi, Y., Tsuji, H., Himeno, M. and Kato, K. (1989a). Morphological localisation of a major lysosomal membrane glycoprotein in the endocytic membrane system. *J. Biochem.* **106,** 708-716.

Furuno, K., Yano, S., Akasaki, K., Tanaka, Y., Yamaguchi, Y., Tsuji, H., Himeno, M. and Kato, K. (1989b). Biochemical analysis of the movement of a major lysosomal membrane glycoprotein in the endocytic membrane system. *J. Biochem.* **106,** 717-722.

Furuta, K., Ikeda, M., Nakayama, Y., Nakamura, K., Tanaka, M., Hamasaki, N., Himeno, M., Hamilton, S. R. and August, J. T. (2001). Expression of lysosome-associated membrane proteins in human colorectal neoplasms and inflammatory diseases. *Am. J. Pathol.* **159,** 449-455.

Gabel, C. A., Goldberg, D. E. and Kornfeld, S. (1983). Identification and characterization of cells deficient in the mannose 6-phosphate receptor: Evidence for an alternate pathway for lysosomal enzyme targeting. *Proc. Natl. Acad. Sci. USA* **80,** 775-779.

Gamp, A., Tanaka, Y., Lullmann-Rauch, R., Wittke, D., D'Hooge, R., De Deyn, Peter P., Moser, T., Maier, H., Hartmann, D., Reiss, K. et al. (2003). LIMP-2/LGP85 deficiency causes ureteric pelvic junction obstruction, deafness and peripheral neuropathy in mice. *Human Molecular Genetics* **12,** 631-646.

Geuze, H. J., Slot, J. W., Strous, Ger J. A. M., Hasilik, A. and von Figura, K. (1984). Ultrastructural localisation of the mannose 6-phosphate receptor in rat liver. *J. Cell Biol.* **98,** 2047-2054.

Geuze, H. J., Slot, J. W., Strous, Ger J. A. M., Hasilik, A. and von Figura, K. (1985). Possible pathway for lysosomal enzyme delivery. *J. Cell Biol.* **101,** 2253-2262.

Geuze, H. J., Slot, J. W., Strous, Ger J. A. M., Lodish, H. F. and Schwartz, A. L. (1983). Intracellular site of asialoglycoprotein receptor-ligand uncoupling: Double-label immunoelectron microscopy during receptor-mediated endocytosis. *Cell* **32,** 277-287.

Geuze, H. J., Stoorvogel, W., Strous, Ger J. A. M., Slot, J. W. and Bleekemolen, J. E. (1988). Sorting of mannose 6-phosphate receptors and lysosomal membrane proteins in endocytic vesicles. *J. Cell Biol.* **107,** 2491-2501.

Glickman, J. N., Conibear, E. and Pearse, B. M. (1989). Specificity of binding of clathrin adaptors to signals on the mannose-6-phosphate/insulin-like growth factor II receptor. *EMBO J.* **8,** 1041-1047.

Gomes, M. S., Paul, S., Moreira, A. L., Appelberg, R., Rabinovitch, M. and Kaplan, G. (1999). Survival of mycobacterium avium and mycobacterium tuberculosis in acidified vacuoles of murine macrophages. *Infect. Immun.* **67,** 3199-3206.

Gonzalez-Noriega, A., Grubb, J. H., Talkad, V. and Sly, W. S. (1980). Chloroquine inhibits lysosomal enzyme pinocytosis and enhances lysosomal enzyme secretion by impairing receptor recycling. *J. Cell Biol.* **85,** 839-852.

Gough, N. R. and Fambrough, D. M. (1997). Different steady state subcellular distributions of the three splice variants of lysosome-associated membrane protein LAMP-2 are determined largely by the COOH-terminal amino acid residue. *J. Cell Biol.* **137,** 1161-1169.

Gough, N. R., Zweifel, M. E., Martinez-Augustin, O., Aguilar, R. C., Bonifacino, J. S. and Fambrough, D. M. (1999). Utilization of the indirect lysosome targeting pathway by lysosome-associated membrane proteins (LAMPs) is influenced largely by the C-terminal residue of their GYXXϕ targeting signals. *J. Cell Sci.* **112,** 4257-4269.

Granger, B. L., Green, S. A., Gabel, C. A., Howe, C. L. and Helenius, A. (1990). Characterisation and cloning of lgp110, a lysosomal membrane glycoprotein from mouse and rat cells. *J. Biol. Chem.*

Green, S. A., Zimmer, K., Griffiths, G. and Mellman, I. (1987). Kinetics of intracellular transport and sorting of lysosomal membrane and plasma membrane proteins. *J. Cell Biol.* **105,** 1227-1240.

Griffiths, G., Hoflack, B. and Simons, K. (1988). The mannose 6-phosphate receptor and the biogenesis of lysosomes. *Cell* **52,** 329-341.

Griffiths, G. and Simons, K. (1986). The trans-Golgi network: Sorting at the exit site of the Golgi complex. *Science* **234,** 438-443.

Guarnieri, F. G., Arterburn, L. M., Penno, M. B. and Cha, Y. (1993). The motif tyr-X-X-hydrophobic residue mediates lysosomal membrane targeting of lysosome-associated membrane protein1. *J. Biol. Chem.* **268,** 1941-1946.

Hall, C. W., Liebaers, I., DiNatale, P., and Neufeld, E. F. (1978). Enzymatic diagnosis of the genetic mucopolysaccharide storage disorders. *Methods Enzymol.* **50**, 439-456.

Hancock, M. K., Haskins, D. J., Sun, G. and Dahms, N. M. (2002a). Identification of residues essential for carbohydrate recognition by the insulin-like growth factor II/Mannose 6-phosphate receptor. *J. Biol. Chem.* **277,** 11255-11264.

Hancock, M. K., Yammani, R. D. and Dahms, N. M. (2002b). Localization of the carbohydrate recognition sites of the insulin-like growth factor II / mannose 6-phosphate receptor to domains 3 and 9 of the extracytoplasmic region. *J. Biol. Chem.* **277,** 47205-47212.

Harding, C. V. and Geuze, H. J. (1993). Immunogenic peptides bind to class II MHC molecules in an early lysosomal compartment. *J. Immunol.* **151,** 3988-3998.

Harlow, E. and Lane, D. (1988). Antibodies: A laboratory manual. Chs. 6, 7, 8 & 11. New York: Cold Spring Harbor Laboratory.

Harter, C. and Mellman, I. (1992). Transport of the lysosomal membrane glycoprotein lgp120 to lysosome does not require appearance on the plasma membrane. *J. Cell Biol.* **117,** 311-325.

Hasilik, A. and Neufeld, E. F. (1980a). Biosynthesis of lysosomal enzymes in fibroblasts. Phosphorylation of mannose residues. *J. Biol. Chem.* **255,** 4946-4950.

Hasilik, A. and Neufeld, E. F. (1980b). Biosynthesis of lysosomal enzymes in fibroblasts. Synthesis as precursors of higher molecular weight. *J. Biol. Chem.* **255,** 4937-4945.

Hatem, C. L., Gough, N. R. and Fambrough, D. M. (1995). Multiple mRNAs encode the avian lysosomal membrane protein LAMP-2, resulting in alternative transmembrane and cytoplasmic domains. *J. Cell Sci.* **108,** 2093-2100.

Haylett, T. and Thilo, L. (1986). Limited and selective transfer of plasma-membrane glycoproteins to membrane of secondary lysosomes. *J. Cell Biol.* **103,** 1249-1256.

Hemer, F., Korner, C. and Braulke, T. (1993). Phosphorylation of the human 46-kDa mannose 6-phosphate receptor in the cytoplasmic domain at serine 56. *J. Biol. Chem.* **268,** 17108-17113.

Hickman, S., Shapiro, L. J. and Neufeld, E. F. (1974). A recognition marker required for uptake of a lysosomal enzyme by cultured fibroblasts. *Biochem. Biophys. Res. Commun.* **57,** 55-61.

Hieber, V., Distler, J., Myerowitz, R., Schmickel, R. D. and Jourdian, G. W. (1976). The role of glycosidically bound mannose in the assimilation of β-galactosidase by generalized gangliosidosis fibroblasts. *Biochem. Biophys. Res. Commun.* **73,** 710-717.

Hille-Rehfeld, A. (1995). Mannose 6-phosphate receptors in sorting and transport of lysosomal enzymes. *Biochim. Biophys. Acta* **1241,** 177-194.

Hirsch, D. S., Stanley, K. T., Chen, L., Jacques, K. M., Puertollano, R. and Randazzo, P. A. (2003). Arf regulates interaction of GGA with mannose-6-phosphate receptor. *Traffic* **4,** 26-35.

Hoflack, B. (1998). Mutant rab 7 causes the accumulation of cathepsin D and CI mannose 6-phosphate receptor in an early endocytic compartment. *J. Cell Biol.* **140,** 1075-1089.

Hoflack, B. and Kornfeld, S. (1985a). Lysosomal enzyme binding to mouse P388D_1 macrophage membranes lacking the 215 kDa mannose-6-phosphate receptor: Evidence for the

existence of a second mannose-6-phosphate receptor. *Proc. Natl. Acad. Sci. USA* **82,** 4428-4432.

Hoflack, B. and Kornfeld, S. (1985b). Purification and characterisation of a cation-dependent mannose 6-phosphate receptor from murine P388D1 macrophages and bovine liver. *J. Biol. Chem.* **260,** 12008-12014.

Honing, S., Griffith, J. M., Geuze, H. J. and Hunziker, W. (1996). The tyrosine-based lysosomal targeting signal in lamp-1 mediates sorting into Golgi-derived clathrin-coated vesicles. *EMBO J.* **15,** 5230-5239.

Honing, S. and Hunziker, W. (1995). Cytoplasmic determinants involved in direct lysosomal sorting, endocytosis and basolateral targeting of rat lgp120 (lamp-1) in MDCK cells. *J. Cell Biol.* **128,** 321-332.

Honing, S., Sandoval, I. V. and von Figura, K. (1998). A di-leucine-based motif in the cytoplasmic tail of LIMP-II and tyrosinase mediates selective binding of AP-3. *EMBO J.* **17,** 1304-1314.

Honing, S., Sosa, M., Hille-Rehfeld, A. and von Figura, K. (1997). The 46-kDa mannose 6-phosphate receptor contains multiple binding sites for clathrin adaptors. *J. Biol. Chem.* **272,** 19884-19890.

Howe, C. L., Granger, B. L., Green, S. A., Gabel, C. A., Helenius, A. and Mellman, I. (1988). Derived protein sequence, oligosaccharides, and membrane insertion of the 120 kDa lysosomal membrane glycoprotein (lgp120): Identification of a highly conserved family of lysosomal membrane glycoproteins. *Proc. Natl. Acad. Sci. USA* **85,** 7577-7581.

Hunziker, W. and Geuze, H. J. (1996). Intracellular trafficking of lysosomal membrane proteins. *Bioessays* **18,** 379-389.

Huynh, K. K., Eskelinen, E., Scott, C. C., Malevanets, A., Saftig, P. and Grinstein, S. (2007). LAMP proteins are required for fusion of lysosomes with phagosomes. *EMBO J.* **26,** 316-324.

Ihrke, G., Bruns, J. R., Luzio, J. P. and Weisz, O. A. (2001). Competing sorting signals guide endolyn along a novel route to lysosomes in MDCK cells. *EMBO J.* **20,** 6256-6264.

Ihrke, G., Gray, S. R. and Luzio, J. P. (2000). Endolyn is a mucin-like type 1 membrane protein targeted to lysosomes by its cytoplasmic tail. *Biochem J.* **345,** 287-296.

Ihrke, G., Kyttala, A., Russell, Mathew, R. G., Rous, B. A. and Luzio, J. P. (2004). Differential use of two AP-3-mediated pathways by lysosomal membrane proteins. *Traffic* **5,** 946-962.

Jadot, M., Canfield, W. M., Gregory, W. and Kornfeld, S. (1992). Characterization of the signal for rapid internalization of the bovine mannose 6-phosphate/insulin-like growth factor-II receptor. *J. Biol. Chem.* **267,** 11069-11077.

Janvier, K. and Bonifacino, J. S. (2005). Role of the endocytic machinery in the sorting of lysosome-associated membrane proteins. *Mol. Biol. Cell* **16,** 4231-4242.

Jimbow, K., Hara, H., Vinayagamoorthy, T., Luo, D., Dakour, J. Yamada, K., Dixon, W. and Chen, H. (1994). Molecular control of melanogenesis in malignant melanoma: Functional assessment of tyrosinase and lamp gene families by UV exposure and gene co-transfection, and

cloning of a cDNA encoding calnexin, a possible melanogenesis "chaperone". *J. Dermatol.* **21,** 894-906.

Jing, S. Q., Spencer, T., Miller, K., Hopkins, C. and Trowbridge, I. S. (1990). Role of the human transferrin receptor cytoplasmic domain in endocytosis: Localization of a specific signal sequence for internalization. *J. Cell Biol.* **110,** 283-294.

Johnson, K. F., Chan, W. and Kornfeld, S. (1990). Cation-dependent mannose 6-phosphate receptor contains two internalization signals in its cytoplasmic domain. *Proc. Natl. Acad. Sci. USA* **87,** 10010-10014.

Johnson, K. F. and Kornfeld, S. (1992a). The cytoplasmic tail of the mannose 6-phosphate/insulin-like growth factor-II receptor has two signals for lysosomal enzyme sorting in the Golgi. *J. Cell Biol.* **119,** 249-257.

Johnson, K. F. and Kornfeld, S. (1992b). A his-leu-leu sequence near the carboxyl terminus of the cytoplasmic domain of the cation-dependent mannose-6-phosphate receptor is necessary for the lysosomal enzyme sorting function. *J. Biol. Chem.* **267,** 17110-17115.

Jonas, A. J., Smith, M. L. and Schneider, J. A. (1982). ATP-dependent lysosomal cystine efflux is defective in cystinosis. *J. Biol. Chem.* **257,** 13185-13188.

Kanao, H., Enomoto, T., Kimura, T., Fujita, M., Nakashima, R., Ueda, Y., Ueno, Y., Miyatake, T., Yoshizaki, T., Buzard, G. S. et al. (2005). Overexpression of LAMP3/TSC403/DC-LAMP promotes metastasis in uterine cervical cancer. *Cancer Res.* **65,** 8640-8645.

Kannan, K., Divers, S. G., Lurie, A. A., Chervanic, R., Fukuda, M. and Holcombe, R. F. (1995). Cell surface expression of lysosome-associated membrane protein-2 (lamp2) and CD63 as markers of in vivo platelet activation in malignancy. *Eur. J. Haematol.* **55,** 145-151.

Kannan, K., Stewart, R. M., Bounds, W., Carlsson, S. R., Fukuda, M., Betzing, K. W. and Holcombe, R. F. (1996). Lysosome-associated membrane protein h-LAMP1 (CD107a) and h-LAMP2 (CD107b) are activation-dependent cell surface glycoproteins in human peripheral blood mononuclear cells which mediate cell adhesion to vascular endothelium. *Cell. Immunol.* **171,** 10-19.

Karlsson, K. and Carlsson, S. R. (1998). Sorting of lysosomal membrane glycoproteins LAMP-1 and LAMP-2 into vesicles distinct from mannose 6-phosphate Receptor/γ-adaptin vesicles at the trans-Golgi network. *J. Biol. Chem.* **273,** 18966-18973.

Kasper, D., Dittmer, F., von Figura, K. and Pohlmann, R. (1996). Neither type of mannose 6-phosphate receptor is sufficient for targeting of lysosomal enzymes along intracellular routes. *J. Cell Biol.* **134,** 615-623.

Kasuga, M., Kahn, R. C., Hedo, J. A., Van Obberghen, E. and Yamada, K. M. (1981). Insulin-induced receptor loss in cultured human lymphocytes is due to accelerated receptor degradation. *Proc. Natl. Acad. Sci. USA* **78,** 6917-6921.

Klumperman, J., Hille, A., Veenendaal, T., Oorschot, V., Stoorvogel, W., von Figura, K. and Geuze, H. J. (1993). Differences in the endosomal distributions of the two mannose 6-phosphate receptors. *J. Cell Biol.* **121,** 997-1010.

Klumperman, J., Kuliawat, R., Griffith, J. M., Geuze, H. J. and Arvan, P. (1998). Mannose 6-phosphate receptors are sorted from immature secretory granules via adaptor protein AP-1, clathrin, and syntaxin 6-positive vesicles. *J. Cell Biol.* **141,** 359-371.

Kobayashi, T., Beuchat, M., Lindsay, M., Frias, S., Palmiter, R. D., Sakuraba, H., Parton, R. G. and Gruenberg, J. (1999). Late enosomal membranes rich in lysobisphosphatidic acid regulate cholesterol transport. *Nature Cell Biol.* **1,** 113-118.

Koren, H. S., Handwerger, B. S. and Wunderlich, J. R. (1975). Identification of macrophage-like characteristics in a cultured murine tumor line. *J. Immunol.*

Kornfeld, S. (1987a). The interaction of phosphorylated oligosaccharides and lysosomal enzymes with bovine liver cation-dependent mannose 6-phosphate receptor. *J. Biol. Chem.* **262,** 123-129.

Kornfeld, S. (1987b). Studies of the biosynthesis of the cation dependent mannose 6-phosphate receptor in murine cell lines. *Arch. Biochem. Biophys.* **257,** 170-176.

Krise, J. P., Sincock, P. M., Orsel, J. G. and Pfeffer, S. R. (2000). Quantitative analysis of TIP47-receptor cytoplasmic domain interactions: Implications for endosome–to–trans-Golgi network trafficking. *J. Biol. Chem.* **275,** 25188-25193.

Kundra, R. and Kornfeld, S. (1999). Asparagine-linked oligosaccharides protect lamp-1 and lamp-2 from intracellular proteolysis. *J. Biol. Chem.* **274,** 31309-31046.

Kunzli, B. M., Berberat, P. O., Zhu, Z. W., Martignoni, M., Kleeff, J., Tempia-Caliera, A. A., Fukuda, M., Zimmermann, A., Friess, H. and Buchler, M. W. (2001). Influences of the

lysosomal associated membrane proteins (lamp-1, lamp-2) and mac-2 binding protein (mac-2-BP) on the prognosis of pancreatic carcinoma. *Am. Cancer Soc.* **94,** 228-239.

Laemmli, U. K. (1970). Cleavage of structural proteins during the assembly of the head of bacteriophage T4. *Nature* **227,** 680-685.

Le Borgne, R., Alconada, A., Bauer, U. and Hoflack, B. (1998). The mammalian AP-3 adaptor-like complex mediates the intracellular transport of lysosomal glycoproteins. *J. Biol. Chem.* **273,** 29451-29461.

Le Borgne, R., Griffiths, G. and Hoflack, B. (1996). Mannose 6-phosphate receptors and ADP-ribosylation factors cooperate for high affinity interaction of the AP-1 Golgi assembly proteins with membranes. *J. Biol. Chem.* **271,** 2162-2170.

Le Borgne, R. and Hoflack, B. (1997). Mannose 6-phosphate receptors regulate the formation of clathrin-coated vesicles in the TGN. *J. Cell Biol.* **137,** 335-345.

Le Borgne, R. and Hoflack, B. (1998). Protein transport from the secretory to the endocytic pathway in mammalian cells. *Biochim. Biophys. Acta* **1404,** 195-209.

Le Borgne, R., Schmidt, A., Mauxion, F., Griffiths, G. and Hoflack, B. (1993). Binding of AP-1 Golgi adaptors to membranes requires phosphorylated cytoplasmic domains of the mannose 6-phosphate/Insulin-like growth factor II receptor. *J. Biol. Chem.* **268,** 22552-22556.

Lee, N., Wang, W. and Fukuda, M. (1990). Granulocytic differentiation of HL-60 cells is associated with increase of poly-N-acetyllactosamine in asn-linked oligosaccharides attached to human lysosomal membrane glycoproteins. *J. Biol. Chem.* **265,** 20476-20487.

Lehmann, L. E., Eberler, W., Krull, S., Prill, V., Schmidt, B., Sander, C., von Figura, K. and Peters, C. (1992). The internalization signal in the cytoplasmic tail of lysosomal acid phosphatase consists of the hexapeptide PGYRHV. *EMBO J.* **11,** 4391-4399.

Lewis, V., Green, S. A., Marsh, M. and Vihko, P. (1985). Glycoproteins of the lysosomal membrane. *J. Cell Biol.* **100,** 1839-1847.

Li, M., Distler, J. J. and Jourdian, G. W. (1990). The aggregation and dissociation properties of a low molecular weight mannose 6-phosphate receptor from bovine testis. *Arch. Biochem. Biophys.* **283,** 150-157.

Lippencott-Schwartz, J. and Fambrough, D. M. (1986). Lysosomal membrane dynamics: Structure and interorganellar movement of a major lysosomal membrane glycoprotein. *J. Cell Biol.* **102,** 1593-1605.

Lippencott-Schwartz, J. and Fambrough, D. M. (1987). Cycling of the integral membrane glycoprotein, LEP 100 between plasma membrane and lysosomes: Kinetic and morphological analysis. *Cell* **49,** 669-677.

Lobel, P., Fujimoto, K., Ye, R. D., Griffiths, G. and Kornfeld, S. (1989). Mutations in the cytoplasmic domain of the 275 kd mannose 6-phosphate receptor differentially alter lysosomal enzyme sorting and endocytosis. *Cell* **57,** 787-796.

Lobel, P., Dahms, N. M. and Kornfeld, S. (1988). Cloning and sequence analysis of the cation-independent mannose 6-phosphate receptor. *The Journal of biological chemistry* **263,** 2563-2570.

Lodish, H. F., Kong, N., Snider, M. and Strous, Ger J. A. M. (1983). Hepatoma secretory proteins migrate from rough endoplasmic reticulum to Golgi at characteristic rates. *Nature* **304,** 80-83.

Ludwig, T., Griffiths, G. and Hoflack, B. (1991). Distribution of newly synthesized lysosomal enzymes in the endocytic pathway of normal rat kidney cells. *J. Cell Biol.* **115,** 1561-1572.

Luzio, J. P., Pryor, P. R. and Bright, N. A. (2007). Lysosomes: Fusion and function. *Nat. Rev. Mol. Cell Biol.* **8,** 622-632.

Majeski, A. E. and Dice, J. F. (2004). Mechanisms of chaperone-mediated autophagy. *Internatl. J. Bioch. Cell Biol.* **36,** 2435-2444.

Majlessi, L., Combaluzier, B., Albrecht, I., Garcia, J. E., Nouze, C., Pieters, J. and Leclerc, C. (2007). Inhibition of phagosome maturation by mycobacteria does not interfere with presentation of mycobacterial antigens by MHC molecules. *J. Immunol.* **179,** 1825-1833.

Mane, S. M., Marzella, L., Bainton, D. F., Holt, V. K., Ying, C., Hildreth, J. E. and August, J. T. (1989). Purification and characterisation of human lysosomal membrane glycoproteins. *Arch. Biochem. Biophys.* **268,** 360-378.

Marks, M. S., Woodruff, L., Ohno, H. and Bonifacino, J. S. (1996). Protein targeting by tyrosine- and di-leucine-based signals: Evidence for distinct saturable components. *J. Cell Biol.* **135,** 341-354.

Marsh, M., Schmid, S., Kern, H., Harms, E., Male, P., Mellman, I. and Helenius, A. (1987). Rapid analytical and preparative isolation of functional endosomes by free flow electrophoresis. *J. Cell Biol.* **104,** 875-886.

Mathews, P. M., Martinie, J. B. and Fambrough, D. M. (1992). The pathway and targeting signal for delivery of the integral membrane glycoprotein LEP100 to lysosomes. *J. Cell Biol.* **118,** 1027-1040.

Mattei, M. G., Matterson, J., Chen, J. W., Williams, M. A. and Fukuda, M. (1990). Two human lysosomal membrane glycoproteins, h-lamp-1 and h-lamp-2, are encoded by genes localized to chromosome 13q34 and chromosome Xq24-25, respectively. *J. Biol. Chem.* **265,** 7548-7551.

Mauxion, F., Le Borgne, R., Munier-Lehmann, H. and Hoflack, B. (1996). A casein kinase II phosphorylation site in the cytoplasmic domain of the cation-dependent mannose 6-phosphate receptor determines the high affinity interaction of the AP-1 Golgi assembly proteins with membranes. *J. Biol. Chem.* **271,** 2171-2178.

McNeil, P. L. (2002). Repairing a torn cell surface: Make way, lysosomes to the rescue. *J. Cell Sci.* **115,** 873-879.

Medigeshi, G. R. and Schu, P. (2003). Characterization of the *in vitro* retrograde transport of MPR46. *J. Biol. Chem.* **4,** 802-811.

Mellman, I. S., Plutner, H., Steinman, R. M., Unkeless, J. C. and Cohn, Z. A. (1983). Internalization and degradation of macrophage Fc receptors during receptor-mediated phagocytosis. *J. Cell Biol.* **96,** 887-895.

Mellman, I. and Plutner, H. (1984). Internalization and degradation of macrophage Fc receptors bound to polyvalent immune complexes. *J. Cell Biol.* **98,** 1170-1177.

Meresse, S. and Hoflack, B. (1993). Phosphorylation of the cation-independent mannose 6-phosphate receptor is closely associated with its exit from the trans-Golgi network. *J. Cell Biol.* **120,** 67-75.

Meril, C. R., Goldman, D. and Van Keuren, Margaret L. (1984). Gel protein stains: Silver stain. *Methods Enzymol.* **104,** 441-447.

Merion, M., Schlesinger, P., Brooks, R. M., Moehring, J. M., Moehring, T. J. and Sly, W. S. (1983). Defective acidification of endosomes in chinese hamster ovary cell mutants "cross-resistant" to toxins and viruses. *Proc. Natl. Acad. Sci. USA* **80,** 5315-5319.

Meyer, C., Zizioli, D., Lausmann, S., Eskelinen, E., Hamann, J., Saftig, P., von Figura, K. and Schu, P. (2000). μ1A-adaptin-deficient mice: Lethality, loss of AP-1 binding and rerouting of mannose 6-phosphate receptors. *EMBO J.* **19,** 2193-2203.

Mukherjee, S., Gnosh, R. N. and Maxfield, F. R. (1997). Endocytosis. *Physiol. Rev.* **77,** 759-803.

Mu, F-T., Callaghan, J. M., Steele-Mortimer, O., Stenmark, H., Parton, R. G., Campbell, P. L., McCluskey, J., Yeo, J-P., Tock, E. P. C. and Toh, B-H. (1995). EEA1, an early endosome-associated protein. EEA1 is a conserved alpha-helical peripheral membrane protein flanked by cysteine "fingers" and contains a calmodulin-binding IQ motif. *J. Biol. Chem.* **270,** 13503-13511.

Mullins, C. (2005). Biogenesis of cellular organelles. Springer. p 33.

Mullins, C. and Bonifacino, J. S. (2001). The molecular machinery for lysosome biogenesis. *Bioessays* **23,** 333-343.

Nabi, I. R., Le Bivic, A., Fambrough, D. M. and Rodriguez-Boulan, E. (1991). An endogenous MDCK lysosomal membrane glycoprotein is targeted basolaterally before delivery to lysosomes. *J. Cell Biol.* **115,** 1573-1584.

Nair, P., Rohrer, J. and Schaub, B. E. (2003). Characterisation of the endosomal sorting signal of the cation-dependent mannose 6-phosphate receptor. *J. Biol. Chem.* **278,** 24753-24758.

Neiss, W. F. (1984). A coat of glycoconjugates on the inner surface of the lysosomal membrane in the rat kidney. *Histochem. Cell Biol.* **80,** 603-608.

Nicoziani, P., Vilhardt, F., Llorente, A., Hilout, L., Courtoy, J., Sandvig, K. and van Deurs, B. (2000). Role for dynamin in late endosome dynamics and trafficking of the cation-independent mannose 6-phosphate receptor. *Mol. Biol. Cell* **11,** 481-495.

Nishino, I., Fu, J., Tanji, K., Yamada, T., Shimojo, S., Koori, T., Mora, M., Riggs, J. E., Oh, S. J., Koga, Y. et al. (2000). Primary LAMP-2 deficiency causes X-linked vacuolar cardiomyopathy and myopathy (Danon disease). *Nature* **406,** 906-909.

Obermuller, S., Kiecke, C., von Figura, K. and Honing, S. (2002). The tyrosine motifs of lamp 1 and LAP determine their direct and indirect targeting to lysosomes. *J. Cell Sci.* **115,** 185-194.

Ogata, S. and Fukuda, M. (1994). Lysosomal targeting of LIMP II membrane glycoprotein requires a novel leu-ile motif at a particular position in its cytoplasmic tail. *J. Biol. Chem.* **269,** 5210-5217.

Ohkuma, S. and Poole, B. (1978). Fluorescence probe measurement of the intralysosomal pH in living cells and the perturbation of pH by various agents. *Proc. Natl. Acad. Sci. USA* **75,** 3327-3331.

Ohno, H., Fournier, M., Poy, G. and Bonifacino, J. S. (1996). Structural determinants of interaction of tyrosine-based sorting signals with the adaptor medium chains. *J. Biol. Chem.* **271,** 29009-29015.

Ohno, H., Stewart, J., Fournier, M., Bosshart, H., Rhee, I., Miyatake, S., Takashi, S., Gallusser, A., Kirchhausen, T. and Bonifacino, J. S. (1995). Interaction of tyrosine-based sorting signals with clathrin-associated proteins. *Science* **269,** 1872-1874.

Olson, L. J., Hancock, M. K., Dix, D., Kim, J. P. and Dahms, N. M. (1999). Mutational analysis of the binding site residues of the bovine cation-dependent mannose 6-phosphate receptor. *J. Biol. Chem.* **274,** 36905-36911.

Olson, L. J., Zhang, J., Dahms, N. M. and Kim, J. P. (2002). Twists and turns of the cation-dependent mannose 6-phosphate receptor (ligand-bound versus ligand-free receptor). *J. Biol. Chem.* **277,** 10156-10161.

Olson, L., Zhang, J., Lee, Y. C., Dahms, N. M. and Kim, J. P. (1999). Structural basis for recognition of phosphorylated high mannose oligosaccharides by the cation-dependent mannose 6-phosphate receptor. *J. Biol. Chem.* **274,** 29889-29896.

Ooi, C. E., Dell'Angelica, E. C. and Bonifacino, J. S. (1998). ADP-ribosylation factor 1 (ARF1) regulates recruitment of the AP-3 adaptor complex to membranes. *J. Cell Biol.* **142,** 391-402.

Orsel, J. G., Sincock, P. M., Krise, J. P. and Pfeffer, S. R. (2000). Recognition of the 300-kDa mannose 6-phosphate receptor cytoplasmic domain by 47-kDa tail-interacting protein. *Proc. Natl. Acad. Sci. USA* **97,** 9047-9051.

Oshima, A., Nolan, C. M., Kyle, J. W., Grubb, J. H. and Sly, W. S. (1988). The human cation-independent mannose 6-phosphate receptor cloning and sequence of the full-length cDNA and expression of functional receptor in COS cells. *J. Biol. Chem.* **263,** 2553-2562.

Pain, R. H. (1963). The molecular weights of the peptide chains of gamma-globulin. *Biochem. J.* **88,** 234-239.

Pak, Y., Glowacka, W. K., Bruce, M. C., Pham, N. and Rotin, D. (2006). Transport of LAPTM5 to lysosomes requires association with the ubiquitin ligase Nedd4, but not LAPTM5 ubiquitination. *J. Cell Biol.* **175,** 631-645.

Pearse, B. M. (1988). Receptors compete for adaptors found in plasma membrane coated pits. *EMBO J.* **7,** 3331-3336.

Peden, A. A., Oorschot, V., Hesser, B. A., Austin, C. D. and Scheller, R. H. (2004). Localization of the AP-3 adaptor complex defines a novel endosomal exit site for lysosomal membrane proteins. *J. Cell Biol.* **164,** 1065-1076.

Peters, C., Braun, M., Weber, B., Wendland, M., Schmidt, B., Pohlmann, R., Waheed, A. and von Figura, K. (1990). Targeting of a lysosomal membrane protein: A tyrosine-containing endocytosis signal in the cytoplasmic tail of lysosomal acid phosphatase is necessary and sufficient for targeting to lysosomes. *EMBO J.* **9,** 3497-3506.

Peters, C. and von Figura, K. (1994). Minireview: Biogenesis of lysosomal membranes. *FEBS Letters* **346,** 108-114.

Peters, P. J., Borst, J., Oorschot, V., Fukuda, M., Krahenbuhl, O., Tschopp, J., Slot, J. W. and Geuze, H. J. (1991). Cytotoxic T lymphocyte granules are secretory lysosomes, containing both perforin and granzymes. *J. Exp. Med.* **173,** 1099-1109.

Peterson, G. L. (1979). Review of the folin phenol protein quantitation method of lowry. *Anal. Biochem.* **100,** 201-220.

Pohlman, R., Waheed, A., Hasilik, A. and von Figura, K. (1982). Synthesis of phosphorylated recognition marker in lysosomal enzymes is located in the *cis* part of Golgi apparatus. *J. Biol. Chem.* **257,** 5323-5325.

Pryor, P. R., Mullock, B. M., Bright, N. A., Gray, S. R. and Luzio, J. P. (2000). Lysosome biogenesis requires rab 9 function and receptor recycling from endosome to the TGN. *J. Cell Biol.* **149,** 1053-1062.

Pryor, P. R., Mullock, B. M., Piper, R. C., Goldberg, D. E., Gabel, C. A. and Kornfeld, S. (1983). Studies of the biosynthesis of the mannose 6-phosphate receptor in receptor-positive and -deficient cell lines. *J. Cell Biol.* **97,** 1700-1706.

Puertollano, R., Aguilar, R. C., Gorshkova, I., Crouch, R. J. and Bonifacino, J. S. (2001). Sorting of mannose 6-phosphate receptors mediated by GGAs. *Science* **292,** 1712-1716.

Raposo, G., Tenza, D., Murphy, D. M., Berson, J. F. and Marks, M. S. (2001). Distinct protein sorting and localization to premelanosomes, melanosomes, and lysosomes in pigmented melanocytic cells. *J. Cell Biol.* **152,** 809-823.

Reaves, B. J., Bright, N. A., Mullock, B. M. and Luzio, J. P. (1996). The effect of wortmannin on the localisation of lysosomal type I integral membrane glycoproteins suggests a role for phosphoinositide-3-kinase activity in regulating membrane traffic late in the endocytic pathway. *J. Cell Sci.* **109,** 749-762.

Reddy, S. T., Chai, W., Childs, R. A., Page, J. D., Feizi, T. and Dahms, N. M. (2004). Identification of a low affinity mannose 6-phosphate-binding site in domain 5 of the cation-independent mannose 6-phosphate receptor. *J. Biol. Chem.* **279,** 38658-38667.

Reddy, S. T., Kumar, S. N., Haas, A. L. and Dahms, N. M. (2003). Biochemical and functional properties of the full-length cation-dependent mannose-6-phosphate receptor expressed in pichia pastoris. *Biochem. Biophys. Res. Commun.* **309,** 643-651.

Renlund, M., Aula, P., Raivio, K. O., Autio, S., Sainio, K., Rapola, J. and Koskela, S. (1983). Salla disease: A new lysosomal storage disorder with disturbed sialic acid metabolism. *Neurology* **33,** 57-66.

Rijnboutt, S. (1992). Identification of subcellular compartments involved in biosynthetic processing of cathepsin D. *J. Biol. Chem.* **267,** 15665-15672.

Robbins, A. R., Oliver, C., Bateman, J. L., Krag, S. S., Galloway, C. J. and Mellman, I. (1984). A single mutation in chinese hamster ovary cells impairs both Golgi and endosomal functions. *J. Cell Biol.* **99,** 1296-1308.

Robbins, A. R., Peng, S., S. and Marshall, J. L. (1983). Mutant chinese hamster ovary cells pleiotropically defective in receptor-mediated endocytosis. *J. Cell Biol.* **96,** 1064-1071.

Rohrer, J., Schweizer, A. and Johnson, K. F. (1995). A determinant in the cytoplasmic tail of the cation-dependent mannose 6-phosphate receptor prevents trafficking to lysosomes. *J. Cell Biol.* **130,** 1297-1306.

Rohrer, J., Schweizer, A., Russell, D. and Kornfeld, S. (1996). The targeting of Lamp1 to lysosomes is dependent on the spacing of its cytoplasmic tail tyrosine sorting motif relative to the membrane. *J. Cell Biol.* **132,** 565-576.

Rous, B. A., Reaves, B. J., Ihrke, G., Briggs, John A. G., Gray, S. R., Stephens, D. J., Banting, G. and Luzio, J. P. (2002). Role of adaptor complex AP-3 in targeting wild-type and mutated CD63 to lysosomes. *Mol. Biol. Cell* **13,** 1071-1082.

Runquist, E. A. and Havel, R. J. (1991). Acid hydrolases in early and late endosome fractions from rat liver. *J. Biol. Chem.* **266,** 22557-22563.

Sahagian, G. G., Distler, J. and Jourdian, G. W. (1981). Characterization of a membrane-associated receptor from bovine liver that binds phosphomannosyl residues of bovine testicular beta-galactosidase. *Proc. Natl. Acad. Sci.* **78,** 4289-4293.

Sahagian, G. G. and Neufeld, E. F. (1983). Biosynthesis and turnover of the mannose 6-phosphate receptor in cultured chinese hamster ovary cells. *J. Biol. Chem.* **258,** 7121-7128.

Saitoh, O., Wang, W., Lotan, R. and Fukuda, M. (1992). Differential glycosylation and cell surface expression of lysosomal membrane glycoproteins in sublines of a human colon cancer exhibiting distinct metastatic potentials. *J. Biol. Chem.* **267,** 5700-5711.

Sandoval, I. V., Arredondo, J. J., Alcalde, J., Noriega, A. G., Vandekerckhove, J., Jimenez, M. A. and Rico, M. (1994). The residues leu(ile)475-ile(leu, val, ala)476, contained in the extended carboxyl cytoplasmic tail, are critical for targeting of the resident lysosomal membrane protein LIMP II to lysosomes. *J. Biol. Chem.* **269,** 6622-6631.

Sarafian, V., Jadot, M., Foidart, J., Letesson, J. and Van Den Brule, Frederic. (1998). Expression of lamp-1 and lamp-2 and their interactions with galectin-3 in human tumor cells. *Int. J. Cancer* **75,** 105-111.

Sawada, R., Jardine, K. A. and Fukuda, M. (1993). The genes of major lysosomal membrane glycoproteins, lamp-1 and lamp-2. 5'-Flanking sequence of lamp-2 gene and comparison of exon organization in two genes. *J. Biol. Chem.* **268,** 9014-9022.

Schweizer, A., Kornfeld, S. and Rohrer, J. (1996). Cysteine^{34} of the cytoplasmic tail of the cation-dependent mannose 6-phosphate receptor is reversibly palmitoylated and required for normal trafficking and lysosomal enzyme sortting. *J. Cell Biol.* **132,** 577-584.

Schweizer, A., Kornfeld, S. and Rohrer, J. (1997). Proper sorting of the cation-dependent mannose 6-phosphate receptor in endosomes depends on a pair of aromatic amino acids in its cytoplasmic tail. *Proc. Natl. Acad. Sci. USA* **94,** 14471-14476.

Silverstein, S. C. (1977). Endocytic uptake of particles by mononuclear phagocytes and the penetration of obligate intracellular parasites. *Am. J. Trop. Med. Hyg.* **26,** 161-169.

Simpson, F., Bright, N. A., West, M. A., Newman, L. S., Darnell, R. B. and Robinson, M. S. (1996). A novel adaptor-related protein complex. *J. Cell Biol.* **133,** 749-760.

Simpson, F., Peden, A. A., Christopoulou, L. and Robinson, M. S. (1997). Characterization of the adaptor-related protein complex, AP-3. *J. Cell Biol.* **137,** 835-845.

Sosa, M., Schmidt, B., von Figura, K. and Hille-Rehfeld, A. (1993). *In vitro* binding of plasma membrane-coated vesicle adaptors to the cytoplasmic domain of lysosomal acid phosphatase. *J. Biol. Chem.* **268,** 12537-12543.

Starcevic, M., Nazarian, R. and Dell'Angelica, E. C. (2002). The molecular machinery for the biogenesis of lysosome-related organelles: Lessons from Hermansky-Pudlak syndrome. *Cell Devel. Biol.* **13,** 271-278.

Stein, M., Braulke, T., Krentler, C., Hasilik, A. and von Figura, K. (1987a). 46 kDa mannose 6-phosphate-specific receptor: Biosynthesis, processing, subcellular location and topology. *Biol. Chem. Hoppe-Seyler* **368,** 937-947.

Stein, M., Zijderhand-Bleekemolen, J. E., Geuze, H., Hasilik, A. and von Figura, K. (1987b). Mr 46,000 mannose 6-phosphate specific receptor: Its role in targeting of lysosomal enzymes. *EMBO J.* **6,** 2677-2681.

Steinman, R. M., Mellman, I. S., Muller, W. A. and Cohn, Z. A. (1983). Endocytosis and the recycling of plasma membrane. *J. Cell Biol.* **96,** 1-27.

Stenbeck, G. (2002). Formation and function of the ruffled border in osteoclasts. *Seminars in Cell & Developmental Biology* **13,** 285-292.

Stockli, J. and Rohrer, J. (2004). The palmitoyltransferase of the cation-dependent mannose 6-phosphate receptor cycles between the plasma membrane and endosomes. *Mol. Biol. Cell* **15,** 2617-2626.

Stoorvogel, W. (1998). Analysis of the endocytic system by using horseradish peroxidase. *Trends Cell Biol.* **8,** 503-505.

Storch, S. and Braulke, T. (2001). Multiple C-terminal motifs of the 46-kDa mannose 6-phosphate receptor tail contribute to efficient binding of medium chains of AP-2 and AP-3. *J. Biol. Chem.* **276,** 4298-4303.

Sun, G., Zhao, H., Kalyanaraman, B. and Dahms, N. M. (2005). Identification of residues essential for carbohydrate recognition and cation dependence of the 46-kDa mannose 6-phophate receptor. *Glycobiology* **15,** 1136-1149.

Tagawa, K., Maruyama, K. and Ishiura, S. (1992). Amyloid beta/A4 precursor protein (APP) processing in lysosomes. *Ann. N. Y. Acad. Sci.* **674,** 129-137.

Tanaka, Y., Guhde, G., Suter, A., Eskelinen, E., Hartmann, D., Lullman-Rauch, R., Janssen, Paul M. L., Blanz, J., von Figura, K. and Saftig, P. (2000). Accumulation of autophagic vacuoles and cardiomyopathy in LAMP-2-deficient mice. *Nature* **406,** 902-906.

Tanaka, Y., Harada, R., Himeno, M. and Kato, K. (1990a). Biosythesis processing, and intracellular transport of lysosomal acid phosphatase in rat hepatocytes. *J. Biochem. (Tokyo)* **108,** 278-286.

Tanaka, Y., Yano, S., Okada, K., Ishikawa, T., Himeno, M. and Kato, K. (1990b). Lysosomal acid phosphatase is transported via endosomes to lysosomes. *Biochem. Biophys. Res. Commun.* **166,** 1176-1182.

Thilo, L. and de Chastellier, C. (1995). Phagocytic processing of the macrophage endoparasite, mycobacterium avium, in comparison to phagosomes which contain bacillus subtilis or latex beads. *Eur. J. Cell Biol.* **68,** 167-182.

Thilo, L., Stroud, E. and Haylett, T. (1995). Maturation of early endosomes and vesicular traffic to lysosomes in relation to membrane cycling. *J. Cell Sci.* **108,** 1791-1803.

Umeda, A., Fujita, H., Kuronita, T., Hirosako, K., Himeno, M. and Tanaka, Y. (2003). Distribution and trafficking of MPR300 is normal in cells with cholesterol accumulated in late endocytic compartments: Evidence for early endosome-to-TGN trafficking of MPR300. *J. Lipid Res.* **44,** 1821-1832.

Urbe, S., Tooze, S. A. and Barr, F. A. (1997). Formation of secretory vesicles in the biosynthetic pathway. *Biochim. Biophys. Acta* **1358,** 6-22.

Vaes, G. (1966). Subcellular localisation of glycosidases in lysosomes. *Methods Enzymol.* **8**, 509-514.

Vega, M. A., Rodriguez, F., Segui, B., Cales, C., Alcade, J. and Sandoval, I. V. (1991). Targeting of lysosomal integral membrane protein LIMP II. *J. Biol. Chem.* **266,** 16269-16272.

Vladutiu, G. D. and Rattazzi, M. C. (1978). Excretion-reuptake route of beta-hexosaminidase in normal and I-cell disease cultured fibroblasts. *J. Clin. Invest.* **63,** 595-601.

von Figura, K., Gieselmann, V. and Hasilik, A. (1984). Antibody to mannose 6-phosphate specific receptor induces receptor deficiency in human fibroblasts. *EMBO J.* **3,** 1281-1286.

von Figura, K. and Hille-Rehfeld, A. (1994). Proteolytic processing of cathepsin D in prelysosomal organelles. *J. Cell Biol.* **64,** 7-14.

von Figura, K. and Weber, E. (1978). An alternative hypothesis of cellular transport of lysosomal enzymes in fibroblasts. Effect of inhibitors of lysosomal enzyme endocytosis on intra- and extra-cellular lysosomal enzyme activities. *Biochem. J.* **176,** 943-950.

Waguri, S., Dewitte, F., Le Borgne, R., Rouille, Y., Uchiyama, Y., Dubremetz, J. and Hoflack, B. (2003). Visualization of TGN to endosome trafficking through fluorescently labelled MPR and AP-1 in living cells. *Mol. Biol. Cell* **14,** 142-155.

Waheed, A., Gottschalk, S., Hille-Rehfeld, A., Krentler, C., Pohlmann, R., Braulke, T., Hauser, H., Geuze, H. J. and von Figura, K. (1988). Human lysosomal acid phosphatase is transported as a transmembrane protein to lysosomes in transfected baby hamster kidney cells. *EMBO J.* **7,** 2351-2358.

Wan, L., Molloy, S. S., Thomas, L., Liu, G., Xiang, Y., Rybak, S. L. and Thomas, G. (1998). PACS-1 defines a novel gene family of cytosolic sorting proteins required for trans-Golgi network localization. *Cell* **94,** 205-216.

Williams, M. A. and Fukuda, M. (1990). Accumulation of membrane glycoproteins in lysosomes requires a tyrosine residue at a particular position in the cytoplasmic tail. *J. Cell Biol.* **111,** 955-966.

Williamson, A. R. and Askonas, B. A. (1968). Differential reduction of interchain disulphide bonds of mouse immunoglobulin G. *Biochem. J.* **107,** 823-838.

Willingham, M. C., Pastan, I. H. and Sahagian, G. G. (1983). Ultrastructural immunocytochemical localization of the phosphomannosyl receptor in chinese hamster ovary (CHO) cells. *J. Histochem. Cytochem.* **31,** 1-11.

Yeo, K. T., Parent, J. B., Yeo, T. K. and Olden, K. (1985). Variability in transport rates of secretory glycoproteins through the endoplasmic reticulum and Golgi in human hepatoma cells. *J. Biol. Chem.* **260,** 7896-7902.

Zhang, M., Dwyer, N. K., Love, D. C., Cooney, A., Comly, M., Neufeld, E., Pentchev, P. G., Blanchette-Mackie, J. E. and Hanover, J. A. (2001). Cessation of rapid late endosomal tubulovesicular trafficking in niemann-pick type C1 disease. *Proc. Natl. Acad. Sci. USA* **98,** 4466-4471.

Zhang, Y. and Dahms, N. M. (1993). Site-directed removal of N-glycosylation sites in the bovine cation-dependent M-P-R: Effects on ligand binding, intracellular targeting and association with binding immunoglobulin protein (bip). *J. Biochem.* **295,** 841-848.

Zhdankina, O., Strand, N. L., Redmond, J. M. and Boman, A. L. (2001). Yeast GGA proteins interact with GTP-bound Arf and facilitate transport through the Golgi. *Yeast* **18,** 1-18.

Zhou, D., Li, P., Lin, Y., Lott, J., Hislop, A., Canaday, D., Brutkiewicz, R. and Blum, J. (2005). Lamp-2a facilitates MHC class II presentation of cytoplasmic antigens. *Immunity* **22,** 571-581.

Zhu, Y., Doray, B., Poussu, A., Lehto, V. and Kornfeld, S. (2001). Binding of GGA2 to the lysosomal enzyme sorting motif of the mannose 6-phosphate receptor. *Science* **292,** 1716-1718.

Zhu, Y., Traub, L. M. and Kornfeld, S. (1998). ADP-ribosylation factor 1 transiently activates high-affinity adaptor protein complex AP-1 binding sites on Golgi membranes. *Mol. Biol. Cell* **9,** 1323-1337.

Zhu, Y., Traub, L. M. and Kornfeld, S. (1999). High-affinity binding of the AP-1 adaptor complex to trans-Golgi network membranes devoid of mannose 6-phosphate receptors. *J. Biol. Chem.* **10,** 537-549.